

Swansea University E-Theses

DNA printing on polymer substrates: Towards cost-effective medical diagnostic devices.

Ren, Ruobo

How to cite:

Ren, Ruobo (2011) *DNA printing on polymer substrates: Towards cost-effective medical diagnostic devices..* thesis, Swansea University.

<http://cronfa.swan.ac.uk/Record/cronfa43015>

Use policy:

This item is brought to you by Swansea University. Any person downloading material is agreeing to abide by the terms of the repository licence: copies of full text items may be used or reproduced in any format or medium, without prior permission for personal research or study, educational or non-commercial purposes only. The copyright for any work remains with the original author unless otherwise specified. The full-text must not be sold in any format or medium without the formal permission of the copyright holder. Permission for multiple reproductions should be obtained from the original author.

Authors are personally responsible for adhering to copyright and publisher restrictions when uploading content to the repository.

Please link to the metadata record in the Swansea University repository, Cronfa (link given in the citation reference above.)

<http://www.swansea.ac.uk/library/researchsupport/ris-support/>



Swansea University Prifysgol Abertawe

DNA Printing on Polymer Substrates: Towards Cost-effective Medical Diagnostic Devices

By
Ruobo Ren
B.Eng, M.Phil

**Thesis submitted to the University of Wales in fulfilment of
the requirements for the Degree of Doctor of Philosophy**

Swansea University

2011

ProQuest Number: 10821405

All rights reserved

INFORMATION TO ALL USERS

The quality of this reproduction is dependent upon the quality of the copy submitted.

In the unlikely event that the author did not send a complete manuscript and there are missing pages, these will be noted. Also, if material had to be removed, a note will indicate the deletion.



ProQuest 10821405

Published by ProQuest LLC (2018). Copyright of the Dissertation is held by the Author.

All rights reserved.

This work is protected against unauthorized copying under Title 17, United States Code
Microform Edition © ProQuest LLC.

ProQuest LLC.
789 East Eisenhower Parkway
P.O. Box 1346
Ann Arbor, MI 48106 – 1346



Summary

DNA for sensing has a diversity of life science applications. The aim of this work was to explore the printing DNA onto a flexible substrate. DNA printing has a diversity of life science applications. DNA can be printed onto rigid substrates at high resolution. Printing is a candidate process for volume manufacturing. This required identification of substrate and any surface treatment to ensure wetting and adhesion. Printing also involves matching the ink with printing process characteristics and for the purpose of sensing, it requires the formulation of an ink that can be printed and demonstrates suitable hybridisation characteristics. Each of these aspects was addressed within this thesis.

Measurement techniques and their robustness were established as a first step. The next stage focused on determining a suitable substrate and surface treatment for immobilisation of DNA. This was followed by an exploration of printing processes, which include ink jet as a reference and flexography and gravure as candidates for volume printing. This work was carried out on a bench top printed, while providing a path for volume printing. The third research strand was concerned with the hybridisation of DNA formulated within an ink. A CCP (Corona treated top coated BOPP) substrate was found to enable good immobilisation of DNA. It needed to be corona treated to enhance the covalent bonding mechanism. Inkjet printing was successful in applying out, however, within the range of process parameters explored, neither flexography nor gravure successfully printed DNA. Further work is needed to develop them so they successfully print and could be used for volume production. An appropriate hybridisation method for DNA deposited within an ink formulation was established.

Declarations and Statements

This work has not previously been accepted in substance for any degree and is not being concurrently submitted in candidature for any degree.

Signed (Candidate)

Date 6 Mar 2012

Statement 1

This thesis is a result of my own investigations, except where otherwise stated. Other sources are acknowledged giving explicit references. A bibliography is appended at the end of the thesis.

Signed (Candidate)

Date 6 Mar 2012

Statement 2

I hereby give consent for my thesis, if accepted, to be available for photocopying and for inter-library loan, and for the title and the summary to be made available to outside organisations.

Signed (Candidate)

Date 6 Mar 2012

Contents

Summary	I
Declarations and Statements	II
Contents	III
Acknowledgements.....	X
List of Tables	XI
List of Figures.....	XII
Abbreviation	XVII
Chapter 1 Introduction.....	1
1.1 DNA structure and function	1
1.1.1 DNA structure	2
1.1.2 DNA double helix	5
1.1.3 DNA functions	8
1.1.4 DNA variants and choice	8
1.2 Overview of printing methods	9
1.2.1 Flexography	11
1.2.2 Gravure.....	12
1.2.3 Ink Jet Technology.....	13
1.2.4 Printing Biomolecules.....	15
1.2.4.1 Contact printing techniques	17
1.2.4.1.1 Pin printing.....	18
1.2.4.1.2 Pin design	18
1.2.4.1.3 Pin printing system.....	24
1.2.4.2 Microstamping	24
1.2.4.3 Non-contact printing techniques	26
1.2.4.3.1 Inkjet printing of biomolecules	26
1.2.5 Printing of biosensors.....	28

1.2.6 Sensing elements.....	31
1.2.7 DNA as a sensor.....	34
1.2.8 Immobilisation techniques	34
1.2.9 Surface modification	43
1.2.10 DNA Microarray	46
Chapter 2 Materials and Methods.....	49
2.1 DNA choice and preparation.....	49
2.1.1 DNA choice.....	49
2.1.2 Pipetting techniques	49
2.1.3 DNA preparation.....	49
2.1.4 Quantification of DNA.....	51
2.1.5 Molecular structures of oligonucleotides and oligonucleotides with NH ₂ and Cy5	53
2.2 General solvent preparation	55
2.2.1 Surfactant	55
2.2.2 Buffer	58
2.3 Substrate preparation.....	60
2.4 Measurement and analysis of the printed image	61
2.4.1 Scanning the FI signals of the ODN	61
2.4.2 Analysis of the FI signals images.....	65
2.4.2.1 Analysis by the GeneTAC integrator microarray analysis software..	65
2.4.2.2 Analysis by Image J software	67
2.5 Oligonucleotides ink characterisation	70
2.5.1 Rheological measurements.....	70
2.5.1.1 Introduction.....	70
2.5.2 Surface Energy Measurement	72
2.6 Printing technology	73

2.6.1 Ink Jet Print	73
2.6.2 Flexography print	75
2.6.3 Gravure print	77
2.6.4 Process capability	77
2.7 Closure	77
Chapter 3 Immobilising the ODN Ink on a Flexible Substrate	79
3.1 Introduction	79
3.2 Materials	79
3.2.1 ODN	79
3.2.2 Polymer substrates	83
3.3 Methods	85
3.3.1 Immobilisation reaction chamber	85
3.3.2 Substrate handling	86
3.3.3 Manual printing techniques	86
3.3.4 Rinsing techniques	87
3.4 Results and discussion in the characterisation of the probe 1 ink on the substrates	88
3.4.1 Characterisation of the probe 1 in the optimal concentration on the substrates	88
3.4.2 Rinsing time investigations	89
3.4.3 The immobilisation reaction conditions investigations of the probe 1 ink on the substrates	91
3.5 Results and discussion in the characterisation of the different substrates to immobilize the probe 1 ink	91
3.5.1 The FI average signals analysis of the different substrates by depositing the probe 1 ink	91
3.5.2 The FTIR analysis of the surface of the CCP to immobilise the probe 1 ink	94

3.6 Results and discussion in the characterisation of the immobilisation mechanisms between the probe ODN ink and the CCP.....	95
3.6.1 Characterisation of the time of the immobilisation of the probe ODN ink on the CCP	96
3.6.2 The FI average signals comparison of the immobilisation of the probe 1 ink, probe 2 ink and Cy5 ink on the CCP	97
3.7 Closure	98

Chapter 4 The Production of the DNA Sensor by Conventional Printing

Technologies	99
4.1 Introduction	99
4.2 Materials.....	99
4.3 The surface characteristics of the CCP	100
4.3.1 The surface energy characteristics of the CCP	100
4.3.2 The roughness characteristics of the CCP.....	105
4.4 Rheological characteristics of the ODN ink.....	106
4.4.1 Surface tension of CTAB with series concentrations	107
4.4.2 Viscosity of ODN ink modification	108
4.5 The characterisation of the inkjet printing technology of the probe 1 ink for the DNA biosensor production	111
4.5.1 Materials.....	111
4.5.1.1 Substrates	111
4.5.2 Methods.....	112
4.5.2.1 The Fluorescent Image analyse measurement.....	112
4.5.2.2 Settings.....	112
4.5.2.3 Pattern Design	113
4.5.3 Results and discussion	113
4.5.3.1 Inkjet Printing Resolution Control.....	113
4.5.3.2 Pattern printing.....	115

4.5.3.3 The Immobilisation investigate of the inkjet pattern printing.....	116
4.6 Characterisation of the flexography printing technology for the probe 1 Ink	121
4.6.1 Materials.....	121
4.6.1.1 Substrates	121
4.6.1.2 Plate.....	121
4.6.1.3 Anilox rolls	122
4.6.2 Methods.....	123
4.6.3 Results and discussion	124
4.6.3.1 Dot pattern printing.....	124
4.6.3.2 Line pattern printing.....	128
4.7 Characterisation of the gravure printing technology of the probe 1 for the DNA sensor production	130
4.7.1 Materials.....	130
4.7.2 Methods.....	130
4.7.3 Results and discussion	131
4.8 Closure	132
Chapter 5 Hybridisation Study of Immobilised ODN on the CCP	133
5.1 Introduction.....	133
5.2 Materials.....	139
5.2.1 The preparation of immobilised and hybridised ODN ink for hybridisation	139
5.2.2 Preparation of the hybridisation buffer	140
5.2.3 Preparation of the washing buffer	140
5.3 Methods.....	141
5.3.1 Hybridisation chamber design	142
5.3.2 Substrates preparation	142
5.3.3 The characteristics of the hybridisation parameters.....	143
5.3.4 The hybridisation experiments procedures	145

5.4 Results and discussion of the hybridisation effects with the different washing buffers	145
5.4.1 Characterisation of the hybridisation effects on the hybridisation of the immobilised probe 3 on CCP with the different hybridisation duration	146
5.4.2 Characterisation of the hybridisation effects with thermal preconditioning of the hybridisation of probe 3	148
5.5 Results and discussion of the characterisation of the washing effects of the hybridisation of the probe 3 immobilised on the CCP by washing with the different washing buffers	149
5.5.1 Investigation of the washing effects by washing with the TNT buffer, Water, Tris Buffer, NaCl and SSC buffer	150
5.5.2 Investigation of the washing effects by washing with the Church buffer	151
5.5.3 Investigation of the washing effects by washing with the SDS (1%) aqueous solution	152
5.5.4 Investigation of the washing effects by washing with the sodium phosphate buffer	153
5.6 Results and discussion of the hybridisation stringent effects with the suitable hybridisation and washing buffers	154
5.6.1 Characterisation of the hybridisation stringent effects on the hybridisation of the probe 3 immobilized on the CCP by washing with the sodium phosphate buffer	154
5.6.2 Characterisation of the hybridisation stringent effects of the probe 3 immobilised on the CCP by washing with the sodium phosphate buffer as the washing buffer in detailed analysis	157
5.6.3 The reasons of the obscured hybridisation results	161
5.7 Closure	161
Chapter 6 Conclusions and Future Work.....	162
6.1 Conclusions	162
6.2 Recommended future work	163
Appendix A Supplement for Chapter 4	165

A.1 CTAB viscosity determination.....	165
A.2 Dimatix printer settings for depositing the probe 1 ink	168
Appendix B Survival Analysis of the Probe 1 Ink Sheared by Ink jetting	169
B.1 Introduction	169
B.1.1 Inkjet printing the DNA	169
B.1.2 PAGE (Polyacrylamide Gel Electrophoresis)	169
B.2 Material.....	170
B.3 Methods	170
B.3.2 PAGE.....	171
B.3.3 Analysis methods by the gel electrophoresis	171
B.4 Results and discussion in the PAGE analysis of the inkjet printed probe 1 Ink	172
Appendix C Supplement for Chapter 5	174
C.1 Hybridisation experiments	174
C.3 Bio-Rad iCycler PCR (Polymerase Chain Reaction) Machine	175
Glossary.....	176
Reference.....	177

Acknowledgements

There are many people who I would like to thank for their help and support both during the researching and writing-up of this thesis.

First of all, I would like to thank Prof Tim Claypole and Prof David T Gethin for allowing me to undertake my PhD studies with them. Their help, support, guidance and enthusiasm proved invaluable throughout the course of my PhD and provided me with many skills and experiences that I will take forward into the rest of my career. Many thanks must also go past to members of the WCPC group namely, Dr Eifion Jewell, Dr David Bould, Dr John Cherry, Dr Masood Yousef, Mr Frank Jachim, Dr Libby Pearson, Mr Joel Trinder, Mr Boyle Foong, and present namely Dr Chris Philips, Dr Simon Hamblyn, Dr Davide Deganello, Dr Tatyana Korochkina, Dr Dave Beynon, Mr Glyn Davies, Mrs Christine Hammett. Special thanks also go to Dr Woan Yi Soo and Dr George Vlahaba whose friendship and advice helped me to succeed through the course of my PhD.

My research would also not have been possible without many collaborators whom I worked with during my research. In light of this, I would like to thank Dr Chris Wright (College of Engineering) and Dr Steven Conlan (Institute of Life Science).

I am also grateful to Dr Chris Philips (WCPC) for handling with the surface data of printing materials and Dr Deya Gonzalez (Institute of Life Science) for the DNA samples supply and PAGE protocols.

I would also like to thank Dr Ricardo Del Sol Abascal (Institute of Life Science) for the guidance on the procedure of running the GeneTAC LSIV fluorescent laser scanner. The special thanks for Dr Chao Li for his helps on PCR buffer supply.

Finally, I would like to thank my family for their continued love and support, which was also crucial to me succeeding in my PhD research.

List of Tables

Table 1.1 Characteristics of high volume printing technologies	15
Table 1.2 Microarray printing techniques	15
Table 2.1 Oligonucleotides sequences for immobilisation and hybridisation	50
Table 2.2 Specification of NanoDrop ND-1000	53
Table 2.3 Malvern Bohlin Gemini rheometer specifications	72
Table 3.1 Surface modification to bind modified and unmodified DNA.....	81
Table 3.2 Plastics used as the ODN substrates in this Chapter.....	84
Table 4.1 Different scales proposed on the basis of estimates of the acid-base ratio for the reference liquid water in literatures	103
Table 4.2 Settings used for contact angle measurement	104
Table 4.3 The CCP surface energy calculation parameters	105
Table 4.4 The surface roughness of the CCP	106
Table 4.5 IGT F1 anilox rolls-specified volumes and line rulings	123
Table 4.6 The IGT F1 settings for the different anilox rolls.....	124
Table 5.1 Controlling the stringency of ODN hybridisations	136
Table A.1 viscosity symbols of different concentration CTAB.....	167

List of Figures

Figure 1.1 The structure of a nucleotide	3
Figure 1.2 A Short DNA polynucleotide showing the structure of the phosphodiester bond.....	4
Figure 1.3 The polymerization reaction that results in synthesis of a DNA polynucleotide	4
Figure 1.4 The double helix structure of DNA	5
Figure 1.5 Computer-generated images of B-DNA (left), A-DNA (center) and Z-DNA (right).....	7
Figure 1.6 Different types of DNA	9
Figure 1.7 Overview of printing technology.....	10
Figure 1.8 Flexography (the principle of process) and flexographic printing unit (schematic diagram)	11
Figure 1.9 Gravure printing (Schematic diagram)	12
Figure 1.10 A schematic diagram of the inkjet technology processes	13
Figure 1.11 Drop on demand inkjet/piezo inkjet	13
Figure 1.12 Printing pins.....	19
Figure 1.13 Solid pin printing process	19
Figure 1.14 Scanning Electron Microscope (SEM) pictures of solid pin etched textures	20
Figure 1.15 Split pin printing process	21
Figure 1.16 Two-part printing system comprising a pin with a supply section and a holding section	22
Figure 1.17 Schematic of a drafting pen	23
Figure 1.18 Loading of doped Si pins.....	23
Figure 1.19 System for microarray printing	24
Figure 1.20 Microstamping process.....	25
Figure 1.21 Schematic layout of a (bio) sensor.....	29
Figure 1.22 Possible bioreceptor molecules and molecular assemblies for biosensor applications; their requirements for structural integrity and signals generated	33
Figure 2.1 The NanoDrop ND-1000 Spectrophotometer microvolume sample retention system	52

Figure 2.2 Cy5 phosphoramidite before and after the deprotection of Cy5.....	54
Figure 2.3 Chemical structure of 3AC7	54
Figure 2.4 Different chemical structure of CTAB	56
Figure 2.5 Controls 1-PMT 2-laser GeneTAC LS IV scanner	61
Figure 2.6 The fluorescent images comparison of the probe 1 on the PS with the different PMT gain and black parameters	63
Figure 2.7 The FI (Fluorescent Intensity) signals of the probe 1 ink ($30 \times 10^{-2} \mu\text{M}$) on the PS and line query across the spots to show the conditions of the probe 1 ink on the PS	64
Figure 2.8 The fluorescent images of the control and immobilized probe 1 ink ($30 \times 10^{-2} \mu\text{M}$) on the CCP	66
Figure 2.9 The FI signals of the probe 1 ink and background on the CCP	67
Figure 2.10 The FI plot signals (analysed by Image J) of the ODN ink	68
Figure 2.11 The FI data signals (analysed by Image J) of the ODN ink	69
Figure 2.12 The comparason of the FI signals of the same fluorescent image analysed by both analysing softwares	70
Figure 2.13 Bohlin Gemini 200 HR Nano Rheometer.....	71
Figure 2.14 Fibro DAT 1100 tester.....	73
Figure 2.15 Dimatix materials printer (DMP-2800 series) and cartridge-style printhead.....	75
Figure 2.16 IGT F1 printability tester	76
Figure 2.17 IGT G1 printability tester	77
Figure 3.1 Immobilisation of DNA to solid surfaces.....	82
Figure 3.2 Schematic of a simple immobilisation reaction chamber design.....	86
Figure 3.3 The model shape of the substrate to print ODN ink on	86
Figure 3.4 The FI average signals analysis of the dilution series ($30 \times 10^{-1-12} \mu\text{M}$) for probe 1 printed on PS.....	89
Figure 3.5 The rinsing times comparison of the immobilisation of the probe 1 ink on the PS by TNT buffer and autoclaved water.....	90
Figure 3.6 The fluorescent images of the experiments of the probe 1 ink ($30 \times 10^{-2} \mu\text{M}$) on the PS	92
Figure 3.7 The FI average signals analysis of the immobilisation experiments of the probe1 ink ($30 \times 10^{-2} \mu\text{M}$) on the different substrates.....	93

Figure 3.8 The FI average images of immobilisation reaction of the probe 1 ink ($30 \times 10^{-2} \mu\text{M}$) on the CCP	93
Figure 3.9 The FTIR analysis comparisons of the CCP and the other substrates with the similar chemical functional groups	95
Figure 3.10 The FI average signals analysis of the immobilisation experiments of the probe 1 ink ($30 \times 10^{-2} \mu\text{M}$) on the CCP over the hourly immobilisation time (1-5 hours)	96
Figure 3.11 The FI average signals comparison of the immobilisation of the immobilized probe 2 ink ($30 \times 10^{-2} \mu\text{M}$), immobilized probe1 ink ($30 \times 10^{-2} \mu\text{M}$), control Cy5 ink and immobilized Cy5 ink	97
Figure 4.1 Surface tension on the dilution series of CTAB	107
Figure 4.2 The viscosity of the autoclaved water	108
Figure 4.3 The viscosity of the typical concentrations of CTAB aqueous solutions (0.01mM - green, 0.1mM - red and 0.8mM - blue mM).....	109
Figure 4.4 The viscosity of the probe 1 ink ($30 \times 10^{-2} \mu\text{M}$)	109
Figure 4.5 The viscosities of different concentration of glycerol in 0.1mM CTAB aqueous solutions	110
Figure 4.6 The zoom in flourescent image of the inkjet pattern printing probe 1 ink on the CCP of words 'CNH'	112
Figure 4.7 The FI signals analysis of the inkjet printing with the series of drop spacing.....	114
Figure 4.8 The Fluorescent Image and analysis of the Inkjet pattern printing of the probe 1 ink without washing of the word (WCPC)	115
Figure 4.9 The FI signals analysis of the inkjet printing the probe 1 ink in the series of drop spacing pattern.....	117
Figure 4.10 The FI signals analysis of the inkjet words pattern printing the probe 1 ink on the CCP	118
Figure 4.11.The FI signals analysis of the inkjet complex pattern printing the probe 1 ink on the CCP	120
Figure 4.12 The photo image of the dots and line pattern printing form of IGT FI printability tester to print the probe 1 ink	122
Figure 4.13 The fluorescent images and FI signals analysis of the large area pattern printing of the Probe 1 ink on the CCP before and after washing with TNT buffer and autoclaved water.....	125

Figure 4.14 The fluorescent image of the flexography dots pattern printed Probe 1 ink on the CCP before and after washing with TNT buffer and autoclaved water..	127
Figure 4.15 The fluorescent image and the FI analysis of the flexography line pattern printing of the probe 1 ink on the CCP	128
Figure 4.16 The fluorescent image and the FI analysis of the flexography line pattern printing of the probe 1 ink on the CCP (area 156).....	129
Figure 4.17 The volume and area characterisation with the different patches on the IGT G1 printing disc	130
Figure 4.18 The fluorescent image and analysis of the coating roll gravure printing of the probe 1 ink on the CCP without washing.....	131
Figure 5.1 A Schematic of the principles of hybridisation	133
Figure 5.2 The CCP substrate shape for the hybridisation experiment.....	143
Figure 5.3 The hybridisation effects with the range of the hybridisation duration by washing with the PCR buffer	147
Figure 5.4 The hybridisation effects of the target 1 hybridizing experiments on the preconditioning probe 3 by washing with the PCR buffer.....	149
Figure 5.5 The washing effects of the target 1 by washing with the TNT buffer, Water, Tris buffer, NaCl and SSC buffer.....	151
Figure 5.6 The washing effects of the target 1 by washing with the church buffer .	152
Figure 5.7 The washing effects of the target 1 by washing with the SDS (1%) buffer	153
Figure 5.8 The washing effects of the target 1 by washing with the sodium phosphate buffer	154
Figure 5.9.The fluorescent images analysis of the hybridisation effects of the target 1 by washing with the sodium phosphate buffer.....	156
Figure 5.10 The hybridisation stringent effects of the target 1 hybridizing on probe 3 by washing with the sodium phosphate buffer.....	156
Figure 5.11 The hybridisation effects analysis of the target 1 by washing with the sodium phosphate buffer (area 304).....	159
Figure A.1 Viscosity of the series concentration of CTAB	166
Figure A.2 Viscosity of the series concentration of CTAB in the large scale	167
Figure B.1 PAGE cassette with comb and glass plates.....	170
Figure B.2 UV ChemiDoc XRS+	172

Figure B.3 The fluorescent images of the PAGE (polyacrylamide gel electrophoresis) with the inkjet printed probe 1 ink and the original probe 1 ink.....	172
Figure C.1 Hybridisation Oven	174
Figure C.2 Bio-Rad iCycler PCR.....	175

Abbreviation

CTAB	Cetyl Trimethyl Ammonium Bromide
DNA	DeoxyriboNucleic Acid
BP	Base Pair
EDTA	EthyleneDiamine TetraAcetic acid
PCR	Polymerase Chain Reaction
RNA	RiboNucleic Acid
SSC	Saline Sodium Citrate
UV	Ultra-Violet
PAGE	Polyacrylamide Gel Electrophoresis
TBE	Tris/Borate/EDTA buffer
APS	Ammonium Persulf
TEMED	Tetramethylethylenediamine
ODN	Oligodeoxyribonucleotide
PS	Polystyrene
PDMS	Polydimethylsiloxane
TNT	10mM Tris-HCl, 150mM NaCl and 0.05% Tween 20
PMT	Photomultiplier Tube

Chapter 1 Introduction

The purpose of this chapter is to present the background of this project together with a critical review of the literature that is directly relevant. This project aims to demonstrate the ability to print DNA (deoxyribosenucleic acid) that will have direct relevance in the biomedical field adopting biomedical sensing as a potential application. Consequently, the review will address the relevant essential aspects of DNA, printing technologies and the principles of sensor devices. The chapter will be concluded by identifying the knowledge gaps that exist in the printability of DNA as a route to achieving low cost biosensor technology. Printing DNA in an economic way will offer cost effective array diagnostic devices and provide the chance of economic tool for bio mark of food goods. The clinical, veterinary, medico-legal, environmental and the food industry can be involved into areas of application [Zhai et al, 1997]. Many existing biosensors for clinical applications are commercialised. Measuring analytes such as DNA targets or specific hormones or proteins as the extending the field of disposable biosensors has not yet been achieved. The difficulty in detecting the binding events of DNA or immunological reactions is limit to such disposable biosensor development [Murphy 2006].

To quick, convenient and economic detection of genetic and infectious disease, DNA biosensor, based on nucleic acid recognition processes, is being advanced swiftly [Christopoulos 1999, Zhai et al. 1997] to the detection of DNA injury and reactions [Palecek et al, 1998]. Contrary to enzyme or antibodies, DNA sensible layers can be manufactured and reused for various applications easily [Wang 2000]. Compared to enzyme biosensors and immunosensors, there is still a scarcity of DNA biosensors available in the market and under research and development. Unlike enzymes or antibodies, DNA forms biological recognition layers easily synthesizable, highly stable and reusable after simple thermal melting of the DNA duplex [Mikkelsen 1996]. Within this work, deposition, immobilisation and hybridisation will be investigated and consequently the following review will attempt to relate the existing literature to these requirements and how these can be combined to facilitate deposition through volume printing technologies.

1.1 DNA structure and function

DNA was first separated by the Swiss physician Friedrich Miescher who identified a fine entity in the virus of removed surgical plaster in 1869. He called it "nuclein" by its location in the nuclei of cells [Dahm 2008]. In 1919, the base, sugar and phosphate nucleotide units were explored by Phoebus Levene [Levene 1919]. DNA's character in heredity was certified in 1952, when Alfred Hershey and Martha Chase in the Hershey–Chase experiment clarified that DNA was the genetic matter of the T2 phage [Hershey and Chase 1952]. In 1953, James D. Watson and Francis Crick claimed the first accurate double-helix description of DNA structure [Watson and Crick 1953].

Nucleic acids serve as genetic elements of living creatures because they are required in the maintenance, displacement and expression of genetic information. They include all the fundamental information involved in the formation of an individual or organism and determine the physical suitability of an individual to living. Furthermore, some nucleic acids act like enzymes and coenzymes. DNA shows structural polymorphism, it forms several kinds depending on certain conditions. The Human Genome Project (HGP) was accomplished in 2003. It is valuable for researching fields of numerous sicknesses whose initiators are unfamiliar. It may also make improvement of both new therapeutics and diagnostics.

Nucleic acid structure deal with the structure of nucleic acids such as DNA and RNA. It is often categorised into four different grades: the primary structure is its covalent structure and nucleotide arrangement; the secondary structure describes the area of regular conformation of the chain, stabilised by regular, repeating interactions such as double helix of DNA; the tertiary structure is how DNA is stored in a restricted space to create the chromosomes; the quaternary structure is the more superior-level composition of DNA in chromatin or the interactions between individual RNA units in the ribosome or spliceosome [Rastogi and Dwivedi 2007, Boddunan 2009-10].

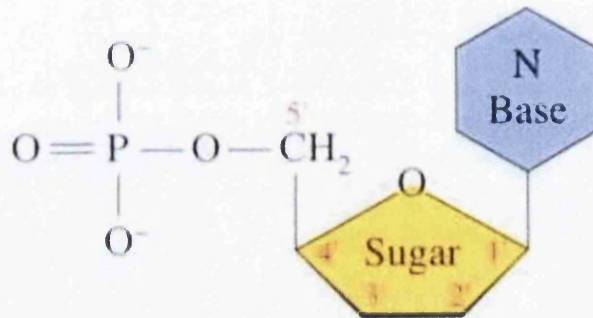
1.1.1 DNA structure

DNA is a polymer with linear, straight chains. Its monomeric subunits comprise four nucleotides. Each nucleotide has three components (**Figure 1.1**)

The primary structure shows the stability of the double helix by the stacking forces between the ODN (Oligodeoxyribonucleotide) bases to give the primary structure.

The primary structure also shows the phosphate group giving the negative charge of the ODN (oligonucleotides). This will provide a route to immobilize on a suitable substrate.

(A) A nucleotide



(B) The four bases in DNA

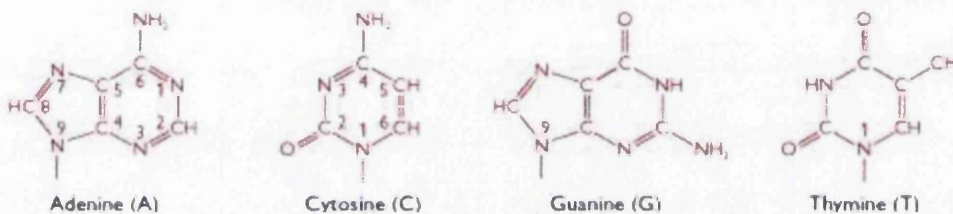


Figure 1.1 The structure of a nucleotide [A: Review of the Universe 2008. B: Brown 2002]

(A) The general structure of a deoxyribonucleotide, the type of nucleotide discovered in DNA. (B) The four bases that occur in deoxyribonucleotides.

Firstly, 2'-deoxyribose is a pentose sugar, derivative of ribose, in which the hydroxyl (-OH) group connected to the 2'-carbon of ribose has been replaced by a hydrogen (-H). Secondly, a nitrogenous base, one of four bases called as C (cytosine), T (thymine) (single-ring pyrimidines), A (adenine) or G (guanine) (double-ring purines). The base is attached to the 1'-carbon of the sugar by a β -N-glycosidic bond to nitrogen at the 1' of the pyrimidine or the 9' of the purine. Thirdly, a phosphate group has one, two or three bonded phosphate units, stuck to the 5'-carbon of the sugar.

A nucleoside combines the sugar and base. A nucleotide is made up of a nucleoside plus the phosphates. To synthesise DNA, only the nucleoside triphosphates act as substrates shown in **Figure 1.2**.

Note that the two ends of the polynucleotide are chemically distinct

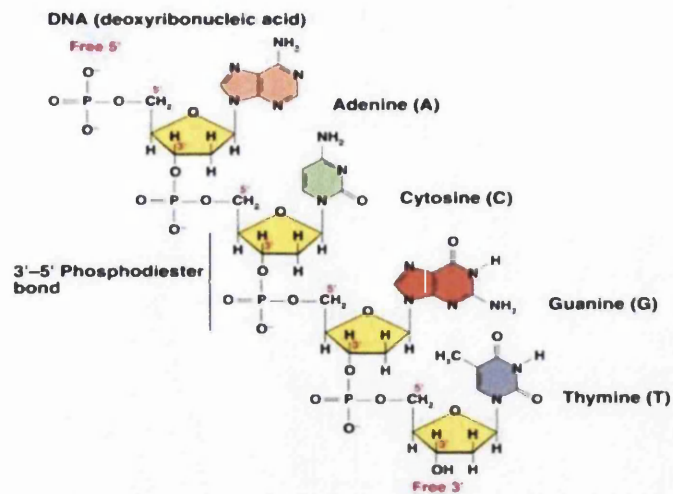


Figure 1.2 A Short DNA polynucleotide showing the structure of the phosphodiester bond. [SMU 2012]

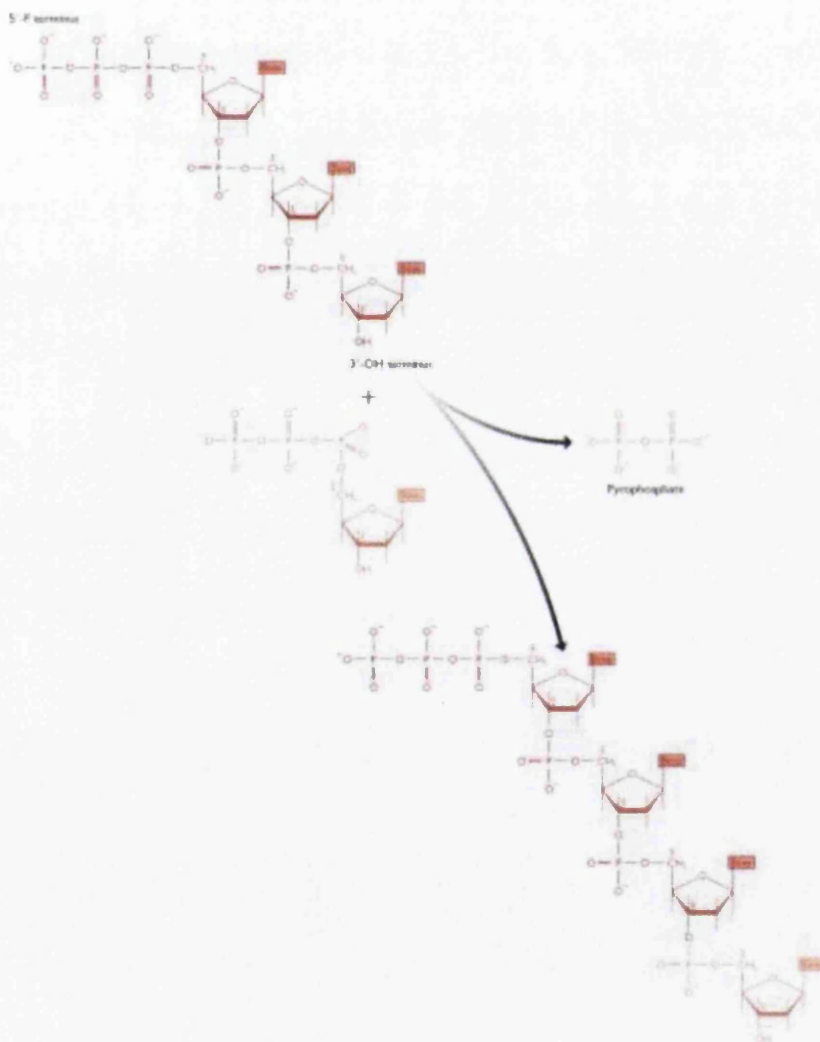


Figure 1.3 The polymerization reaction that results in synthesis of a DNA polynucleotide [Brown 2002]

DNA synthesis direction occurs in the 5' to 3'. In a polynucleotide, phosphodiester bonds between 5'- and 3'- carbons link separate nucleotides (**Figure 1.2**). The polymerization reaction (**Figure 1.3**) includes reduction of the two outer phosphates (the β - and γ -phosphates) from one nucleotide and substitute of the hydroxyl group connected to the 3'-carbon of the second nucleotides. DNA synthesis from 5' to 3' can be done by all natural DNA polymerase enzymes.

Then the secondary structure is entailed as follows.

1.1.2 DNA double helix

The DNA double helix was the most important breakthrough in biology during the 20th century.

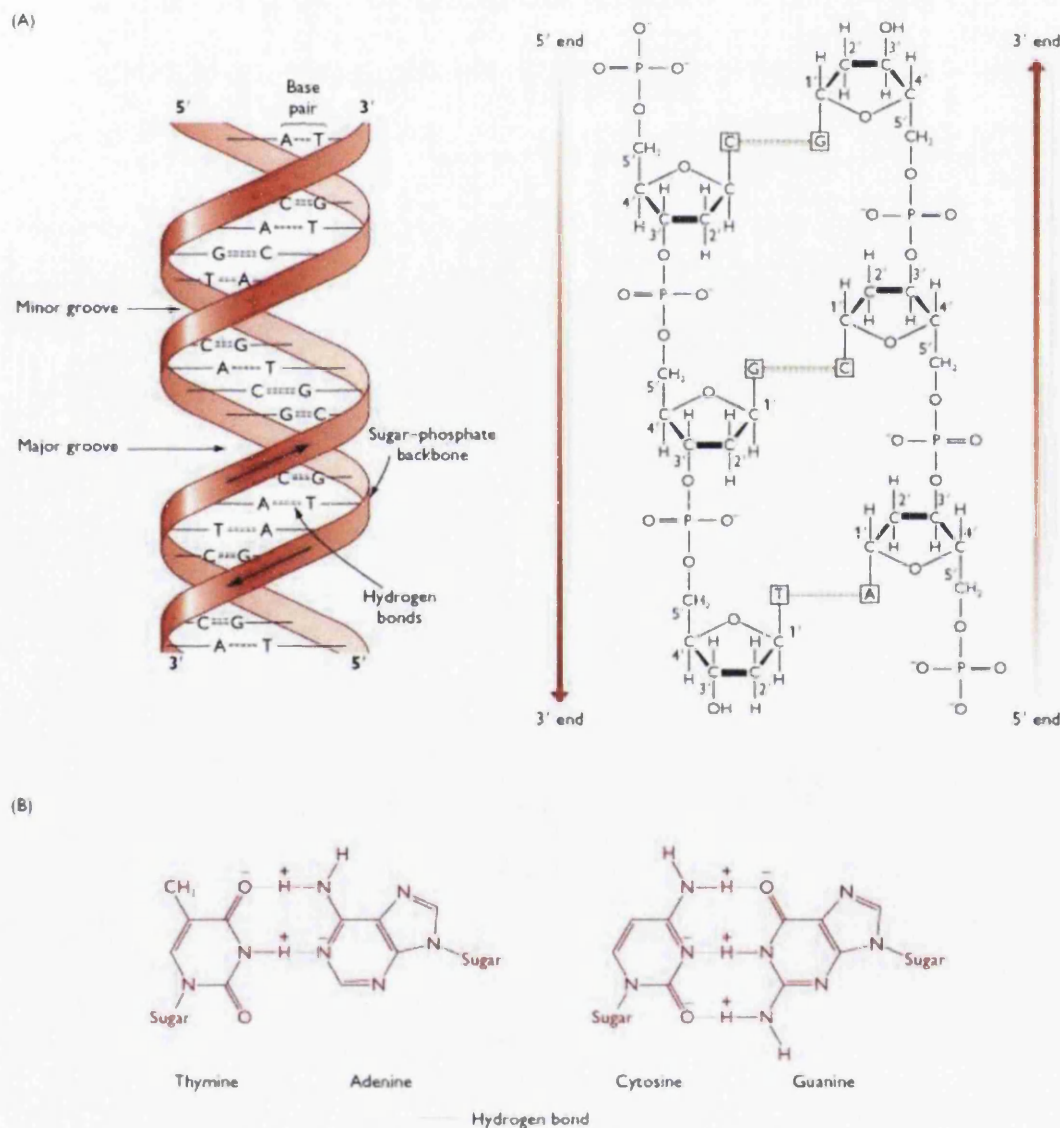


Figure 1.4 The double helix structure of DNA [Brown 2002]

The structures in part (A) are redrafted from [Turner et al. 1997] (left) and [Strachan and Read 1999] (right).

Figure 1.4A shows two illustrations of the double helix. On the left, the structure is presented with the sugar-phosphate ‘backbones’ of each polynucleotide charted as a red ribbon with the base pairs in black. On the right, the chemical structure for three base pairs is shown. **Figure 1.4 B** shows T and A base pairs together with C and G base pairs. The bases are depicted graphically using solid lines, with the hydrogen bonding displayed by dotted counterparts. Note that the G-C base pair has three hydrogen bonds while the A-T base pair has just two.

The double helix is right-handed. The two strands operate in opposite directions (**Figure 1.4A**). The helix is stabilised by two kinds of chemical interaction.

Firstly, hydrogen bonds between A and T or between C and G compose the base pairing between the two strands (**Figure 1.4 B**). This pairing is particularly relevant in hybridisation and this is an aspect that will be explored in Chapter 5 within this thesis. Hydrogen bonds are fragile electrostatic attractions between an electronegative atom (such as oxygen or nitrogen) and a hydrogen atom connected to a second electronegative atom. They are longer than covalent bonds and are much weaker. Secondly, base-stacking or π - π interactions comprises hydrophobic interactions between connected base pairs and creates immobility to the double helix once the double helix strands have been formed by the first kind of interaction above. The water-like hydrogen-bonded structure takes hydrophobic units into the internal itema of a substance and directs these hydrophobic interactions to occur [Brown 2002].

Two DNA polynucleotides are held together by both of the above interactions, but the first interaction is the dominant contributor. Cellular DNA polymerases apply the scheme to systhesise the template-dependent DNA [Brown 2002].

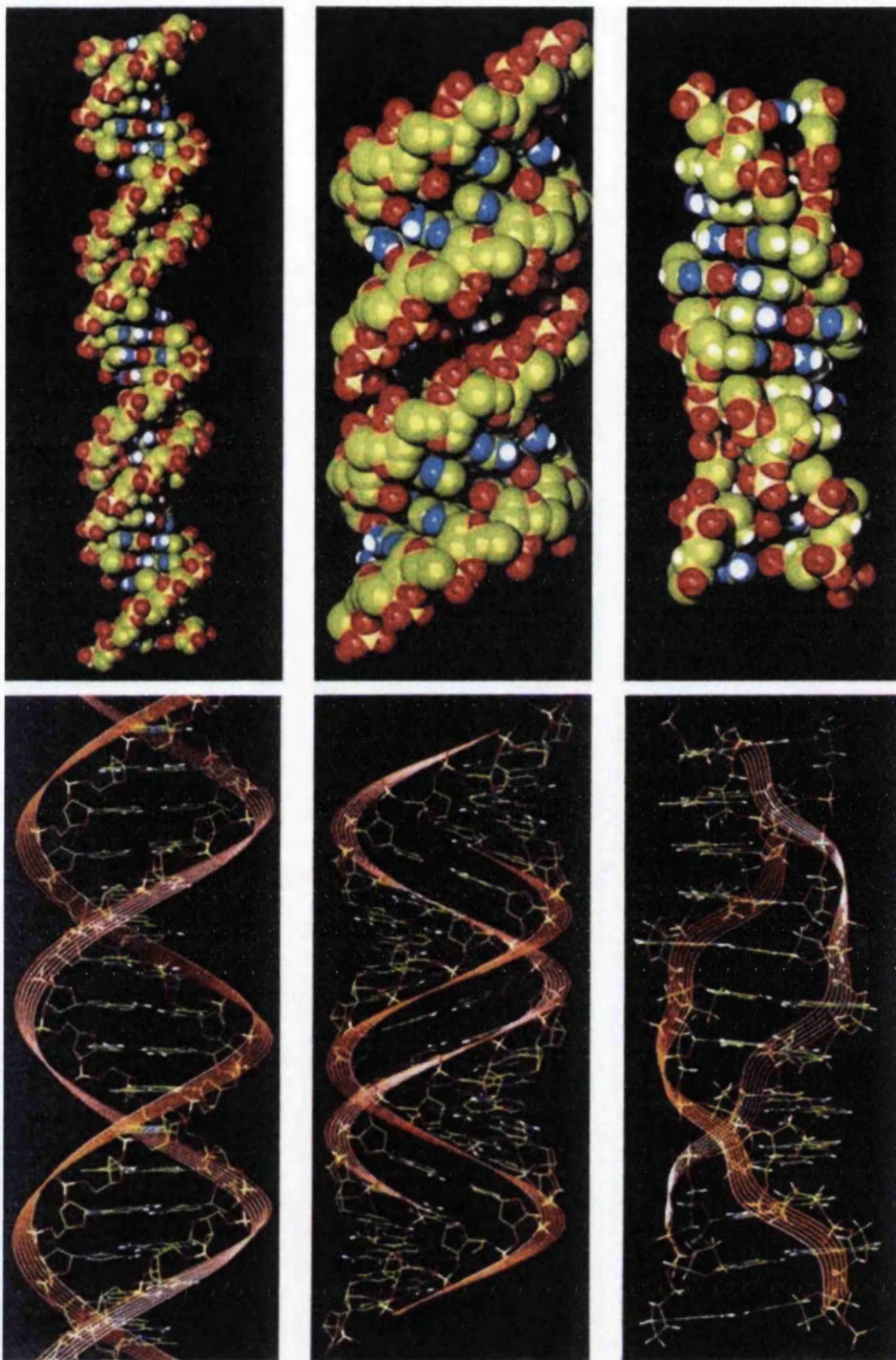


Figure 1.5 Computer-generated images of B-DNA (left), A-DNA (center) and Z-DNA (right) [Kendrew 1994]

The structural flexibility of the DNA double helix leads to the DNA tertiary structure.

The double helix first proposed by Watson and Crick in **Figure 1.4 A** is named the B-form of DNA. Its characteristic features remain in its dimensions. It is thought to be the essential DNA form in living cells, but it is not totally uniform. The small changes in the relative positions of the atoms in the nucleotide achieve different conformations. Most common conformational adjustment includes rotation around the β -N-glycosidic bond, altering the orientation of the base relative to the sugar, and rotation around the bond between the 3' - and 4' -carbons. This leads to a number of DNA forms as shown in **Figure 1.5**, notably A-form B-form and Z-DNA as a left handed form [Brown 2002].

1.1.3 DNA functions

DNA is the genetic substance of all living systems. It contains all the information required for the construction of a creature or organism. DNA imparts the characteristic elements of the living creature like colour of the skin and eye, height, intelligence, ability to metabolise particular material, ability to withstand stress, susceptibility to disease and inability to produce or synthesize certain materials. All the above phenotype characteristics of living organisms are exactly related to functions of proteins. Therefore, DNA is the origin of information for the production of all cellular proteins. The segment of DNA that contains information for a protein is known as a gene. DNA is transmitted from parent to offspring and hence DNA passes from one generation to another in a given species. Moreover, DNA provides information inherited by daughter cells from parent cells. In general terms, the amount of DNA in mammalian cell is 1000 times more than bacteria types of DNA molecules. Also bacteria contain more DNA than viruses. The amount of DNA in any given species or cell is consistent and is not influenced by nutritional or metabolic states. The DNA tertiary and quaternary structures are described in the variants [Rao 2006].

1.1.4 DNA variants and choice

Although DNA may be used to identify cell uniquely, there are many types of DNA, notably: A, B and Z DNA (glycosidic bonds are in the syn conformation in **Figure 1.5**); Nucleosome DNA; Mitochondrial DNA; Bacterial DNA in **Figure 1.6 (a)**; Viral DNA in **Figure 1.6 (b)**; Plasmid DNA in **Figure 1.6 (c)**.

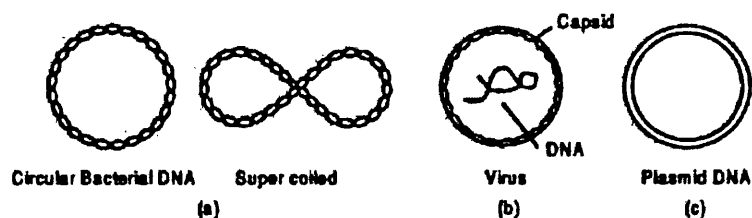


Figure 1.6 Different types of DNA [Rao 2006]

(a) Bacterial DNA (b) Virus (c) Plasmid

Bacteria such as *E. coli* includes a single molecule of double stranded DNA shown in **Figure 1.6 (a)**. Viruses are intensively tiny particles in **Figure 1.6 (b)**.

From the DNA structures (as above), the short length ODN that builds the DNA long molecules plays the key role to understand best the DNA functionality. Thus the short length ODN has been the choice for DNA sensor to understand the applications in the molecular biology field like gene expression, gene sequences etc. To make a DNA sensor, the ODN' modification for immobilisation and visibility has been linked with the amino motif and fluorescent tag. To make a DNA sensor, the ODN printability can be analysed by considering the viscosity and surface tension. The adjustment of viscosity and surface tension cannot be allowed if the adjustment affects the immobilisation of ODN on the substrate surface. Also for investigating the DNA sensibility, the structures of ODN must remain the flexible and intact to enable hybridisation. The hybridisation is the way to know the efficiency of immobilized ODN functionality.

1.2 Overview of printing methods

Printing offers a way for the volume manufacture of discrete biosensors and arrays at appropriate scales, e.g. in well plates. Different processes may be applied to different parts of a biosensor. For example conducting elements may be delivered by traditional methods, whereas the transduction and biomolecular recognition elements may be deposited by inkjet, pin or drop coating.

An overview of high volume printing technologies is given in **Figure 1.7**. A distinction is made between technologies requiring a master for conventional contact printing and so called non-impact printing (NIP) technologies which do not require an image carrier.

Current printing technologies are dependent on an asset of inventions. The innovations made in the engineering sciences, information technology, physics, and chemistry have given their helps on the advancement of printing technologies. In recent years it is computer and information technology that had the most lasting influence on the printing industry and technologies, and this direction is keeping going [Kipphan 2001].

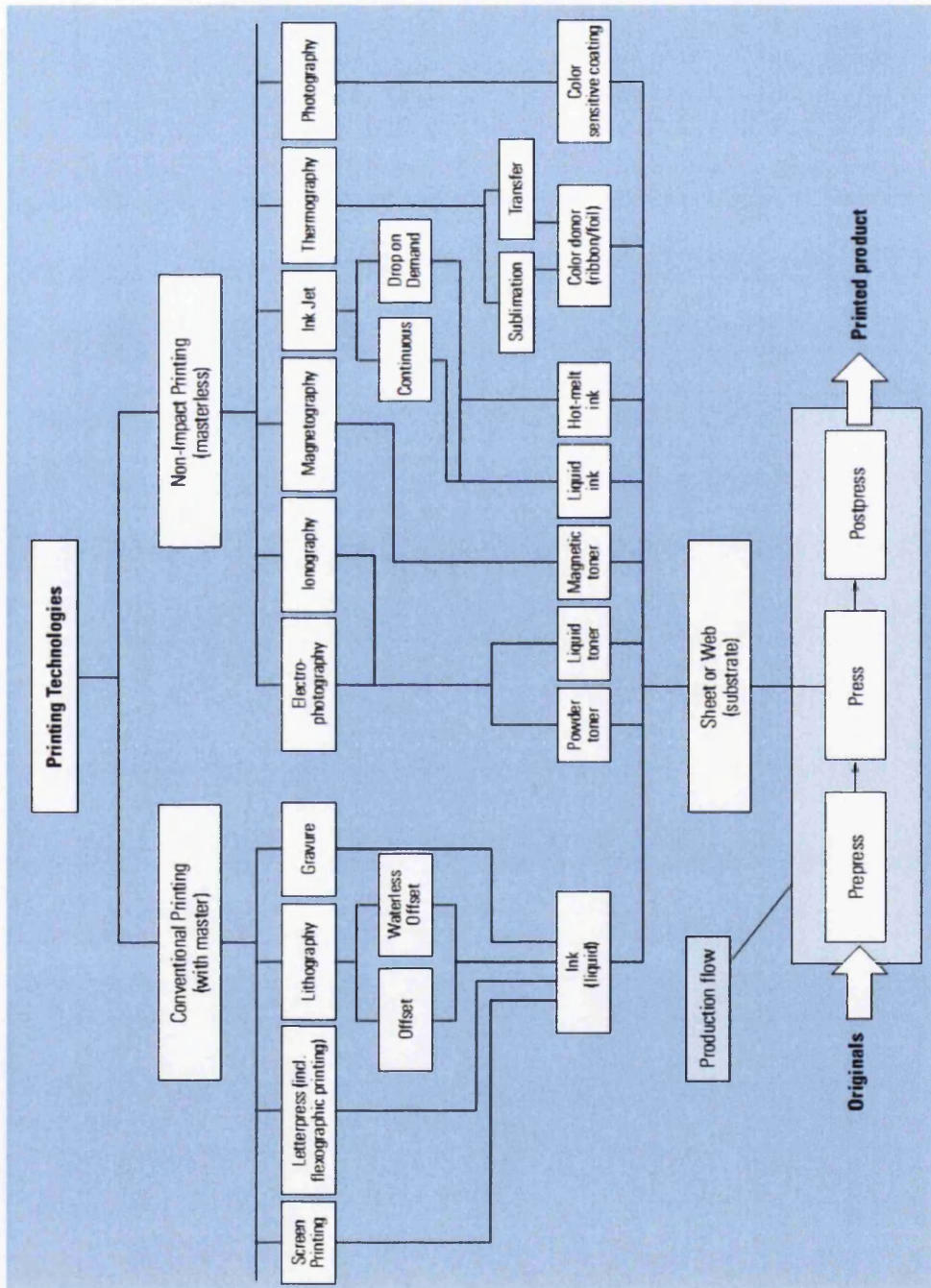


Figure 1.7 Overview of printing technology [Kipphan 2001]

Printing technologies with an image carrier include technologies such as lithography (offset), gravure, letterpress (equivalent to flexography) and screen printing. The electrophotography and ink jet are the most familiar NIP technologies [Kipphan 2001].

The printing processes that are specific for biomaterials will be discussed later in section **1.2.5**.

Printing is a technology that has the potential to be used as a means of volume manufacturing of a standard product at low cost in an efficient and repeatable manner.

Printing is a reproduction process in which ink is applied to a printing substrate in order to transmit information (images, graphics, text) in a repeatable form using an image-carrying medium [Kipphan 2001]. The following sections will overview processes that are candidates for DNA printing where a focus is on the stress that is applied to the DNA when incorporated into an ink. This will include conventional processes and processes that have been developed for printing biomolecular systems.

1.2.1 Flexography

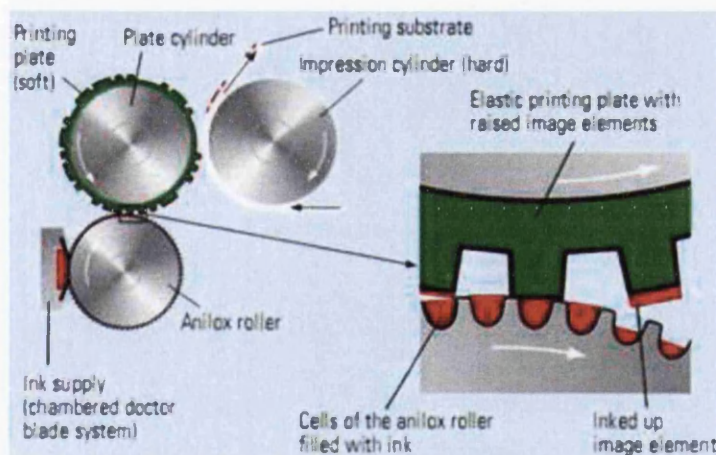


Figure 1.8 Flexography (the principle of process) and flexographic printing unit (schematic diagram) [Kipphan 2001]

Flexography is a printing technology by means of which printing can be done on very thin, flexible, and solid films, virtually all papers, thick cardboard, rough-surfaced packaging materials, and fabrics.

The resilience of the flexographic printing plate in conjunction with low viscosity ink makes it possible, in particular, to print on a non-absorbent and rough substrate. Moreover, flexography is particularly suitable for printing on flexible materials such as plastic film [Kipphan 2001].

The printing technology requires only a slight contact pressure to enable reliable ink transfer from printing plate to substrate. This contact pressure must, however, be exerted as evenly as possible on all printing locations along the contact area and during the pass of the entire print length. Eccentricities in the cylindrical form and radial deviations can be compensated by setting a somewhat higher pressure. The satisfactory preliminary requirements for even print-out of the entire print image are met if a contact pressure can be maintained with only slight fluctuations [Kipphan 2001].

1.2.2 Gravure

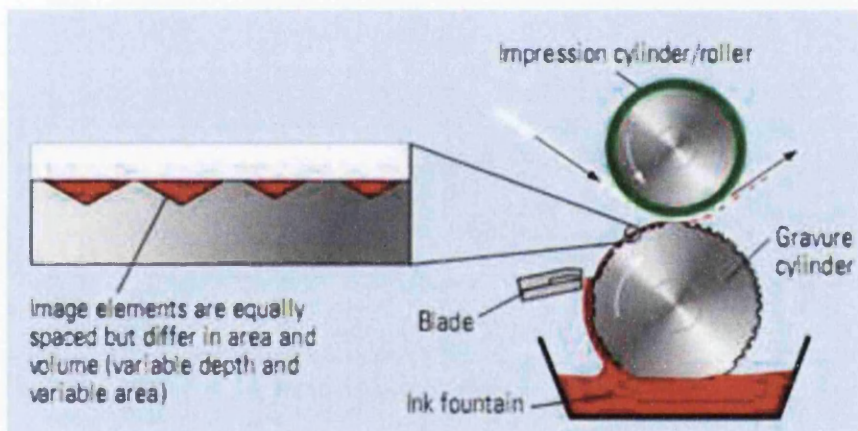


Figure1.9 Gravure printing (Schematic diagram) [Kipphan 2001]

The distinctive feature of gravure printing technology is the fact that the image elements are engraved into the surface of the cylinder. The non-image areas are at a constant, original level. Prior to printing, the entire printing plate (non-printing and printing elements) is inked and flooded with ink. Ink is removed from the non-image (by a wiper or blade) before printing, so that ink remains only in the cells. The ink is transferred from the cells to the printing substrate by a high printing pressure and the adhesive forces between printing substrate and ink [Kipphan 2001].

In biosensor applications, flexography and gravure can be used for depositing the layers that comprise the electronic component of the sensor element. There is benefit in exploring their application in depositing the bio recognition element as this will provide an integrated route for sensor manufacture.

In well plate type applications, the ability to image DNA onto a surface to conduct analyte measurement is also attractive. These sensor applications will be discussed more fully in section 1.2.4.

1.2.3 Ink Jet Technology

This is a printing technology, which does not require a stable, physical, fixed image carrier and can, in principle, generate a different printed page print per print [Kipphan 2001] and there are two variants as shown in **Figure 1.10**.

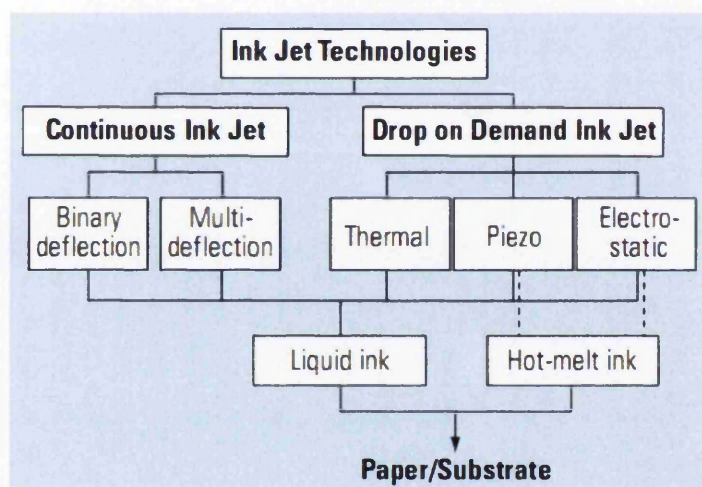


Figure 1.10 A schematic diagram of the inkjet technology processe [Kipphan 2001]

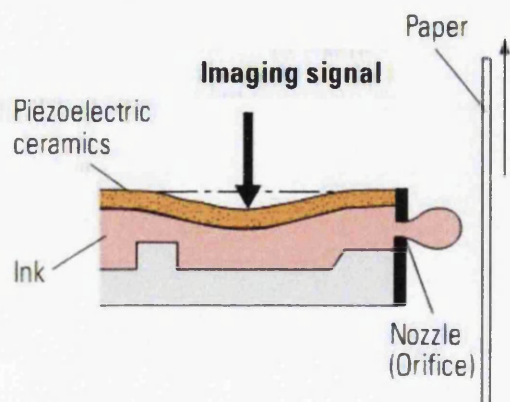


Figure 1.11 Drop on demand inkjet/piezo inkjet [Kipphan 2001]

Ink jet is a non-impact printing technology that does not require an intermediate carrier for the image information and is therefore a computer to print technology. In the inkjet process, the ink can be transferred directly onto the paper. Inkjet technologies can be classified as continuous ink jet and drop on demand ink jet. The ink used for ink jet printing is usually liquid. The ink is sprayed onto the substrate where it solidifies after impact [Kipphan 2001].

The more important “drop on demand” technologies are thermal ink jet and piezo inkjet printing. Thermal ink jet (also known as “bubble jet”) generates the drops by heating and localised vaporisation of the liquid in a jet chamber. With piezo ink jet the ink drop is formed and catapulted out of the nozzle by mechanically deforming the jet chamber, an action resulting from an electronic signal and the piezoelectric properties of the chamber wall, **Figure 1.11**. Due to the physical components and principles, the possible droplet frequencies are lower with thermal droplet generation than with piezo technology [Kipphan 2001].

In conclusion, the characteristics of these printing processes can be summarised as set out in **Table 1.1**. This lists typical resolution, deposition thickness and rheology range of the working fluids to which the ink is subjected. The stress levels are difficult to quantify as they arise from shear and extensional mechanisms and is influenced directly by speed and film thickness. The stress levels are likely to have an impact on survival of DNA and the fluid properties must be compatible with that required by the biomolecule.

Table 1.1 Characteristics of high volume printing technologies

	Screen	Gravure	Offset Lithography	Flexography	Pad	Inkjet
Finest track and gap	75-75 μm	100-100 μm	75-50 μm	50-50 μm	45 μm track	10 μm
Cured film thickness	40 nm to 50 μm	Up to 9 μm	Up to 3 μm	Up to 9 μm	Up to 8 μm	Up to 8 μm
Speed	4000 copies/hr	1000 m/min	600 m/min	200 m/min	2000 stroke/hr	1 m/min
Ink dynamic viscosity	10^{-2} Pa·s-paste	0.05-0.2 Pa·s	40-100 Pa·s	0.05-0.5 Pa·s	0.05-0.2 Pa·s	0.005-0.02 Pa·s

1.2.4 Printing Biomolecules

Printing techniques have also been developed specifically for printing very fine features and for handling bimolecular inks and these are presented and discussed in the following sections. These can also be classed as contact and non-contact as set out in **Table 1.2**. These have application in the manufacture of microarray devices, but they may also be used in larger scale applications.

Table 1.2 Microarray printing techniques [Barbulovic-Nad et al. 2006]

Contact		Non-contact	
Serial	Parallel	Serial	Parallel
Solid/Split Contact pins	Microstamps	Dynamic Controlled Pins	Photochemical Printing Electro-Printing
Nano-Tips		Laser Writing	Inkjet/Nozzle Printing Electrospray Deposition

All microarray fabrication techniques target the same objective: efficient deposition of uniform, dense arrays of small droplets of probe molecules. This review analyzes the capabilities and limitations of conventional and emerging technologies for microarray fabrication [Morozov 2005].

An ideal printing system should be capable of creating uniform, dense arrays of small droplets using a minimum volume of fluid, while preventing solution contamination and bimolecular damage. Furthermore, the system should be inexpensive, reliable, and durable. None of the existing methods fulfils all of these criteria. Contact printing with solid and split pins is currently the most prevalent system used in industry and research laboratories. Overall, this technology imparts reproducible results with little required maintenance; however, this form of contact printing is slow, expensive, and at times suffers from problems of contamination. Contact pin printing is plagued by several problems that have led to the development of competing technologies. The main limitations for split pin printing include low speed, the requirement of pre-printing, pin clogging, tip deformation, and droplet uniformity. Precise control of the pin motion would eliminate the need for pin tapping to deposit fluid, thereby improving droplet uniformity and increasing pin life. Clogging is a very serious problem for split pins and can lead to poor performance and contamination. Recent pin designs have relied on alternative materials to metals, such as silicon, ceramics, and polymers. These new materials have allowed engineers to evaluate a wide range of geometries and material characteristics. Elastomeric polymers such as PDMS (Poly(dimethylsiloxane)) are used to mould microstamps that are also capable of parallel contact printing. Microstamping is an inexpensive and efficient printing technique compared to contact pin printing and is well-suited for high-throughput microarray fabrication. However, an improvement in the control of printed sample volumes is necessary for wide-spread use of this technique. In addition to new materials and fabrication technologies, new surface treatment methods are being explored to increase control over wetting phenomena. For example, electrowetting, which enhances capillary forces by controlling the surface tension in an electrostatic field, is being used to drive fluids through nozzles. Besides microscale methods, nanoscale techniques, based on atomic force

microscopy, are being investigated for printing high density arrays at a submicron scale.

Completely different approaches are being developed for non-contact printing. Of these methods, inkjet technology shows great promise for reducing the cost of microarray fabrication. Unfortunately, the printing inaccuracies which are often acceptable in document printing cause unacceptable problems for biochip microarray fabrication. Splashing and satellite droplets cause contamination and irregular spot sizes. Another method, electrospray deposition, suffers from similar drawbacks, with the additional disadvantage of negative effects of electric fields on certain types of biomolecules. Photo-chemical non-contact printing, which enables very efficient high-throughput microarray fabrication, can lead to biomolecular denaturation as well. In summary, there are a variety of new technologies that hold promise for faster, more efficient, less expensive microarray fabrication. In order for competing technologies to be viable in the long term, microarray quality (e.g., spot uniformity and size) must also be evaluated alongside throughput and cost considerations. Although no single one of these new methods has yet supplanted the conventional method of contact pin printing, the continued development of new materials and micromachining techniques may soon lead to an alternative technology, making the technique of biomolecular microarray analysis even more accessible to the scientific community.

1.2.4.1 Contact printing techniques

Contact printing methods are used to form arrays by means of direct contact between the printing device and the substrate. As shown in **Table 1.2**, contact printing technologies employ solid pins, split pins, nano-tips, and microstamps. One of the first approaches used for microarray fabrication was contact printing with a single pin, which evolved into methods relying on an array of pins. While pin printing is a serial deposition method, microstamps are used for depositing a large number of proteins or DNA molecules in a parallel fashion. Nano-tip printing is the most recent technology based on Scanning Probe Microscopy (SPM) and yields arrays with submicron spots.

1.2.4.1.1 Pin printing

Spot uniformity is primarily determined by the sample viscosity, pin contact area, pin surface properties, substrate surface properties, and substrate planarity. Additional factors include pin velocity, the precision of robotic controls, and environmental control of humidity, temperature, and contamination. A high pin velocity (>2 cm/s) can induce high inertial forces that drive large sample volumes out of the pin, making the size of spots very large [Rose 2000]. However, inertia typically does not play a large role in pin printing. Pin printing is governed by the surface tension of the solution, and the wettability of the solution on the substrate. Maintaining a high, stable humidity prevents the sample from evaporating from the wells and pin channels. Temperature affects the sample viscosity and therefore, the dispensed volume. Contamination and dust must be controlled if high-quality arrays are to be produced with minimal risk of split pin clogging.

1.2.4.1.2 Pin design

The first microarrays were fabricated by contact printing with pins [Schena 1995, Shalon 1996, University of Stanford 2005]. This technique continues to be widely used for most non-commercial microarray fabrication. A key feature of this method is the pin design. **Figure 1.12** depicts designs that are currently used for microarray contact printing. The simplest design (**Figure 1.12 (a)**) is a solid pin. The first solid pins had convex tips while the solid pins used today have flat tips with a precisely controlled diameter or concave tips for more efficient printing [Mace 2000]. Other designs (**Figure 1.12 (b)–(e)**) incorporate splits (or “gaps”) with various shapes, and diameters ranging from 60 μm to 200 μm . The most complex design (**Figure 1.12 (e)**) [University of Stanford 2005] has a screw to adjust the gap distance. Pins are more difficult to manufacture as the pin diameter shrinks. The most commonly used contact printing tips used today are “Ink stamps,” developed by TeleChem International, Inc., Sunnyvale, CA [TeleChem International Inc 2005].

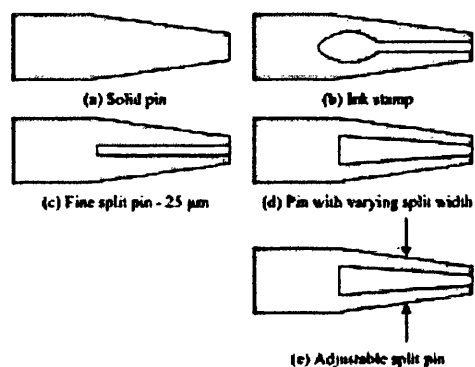


Figure 1.12 Printing pins [Barbulovic-Nad et al. 2006]

(a) Schematic of solid pin. (b) Schematic of ink-stamp. (c, d, e) Schematics of different split pins

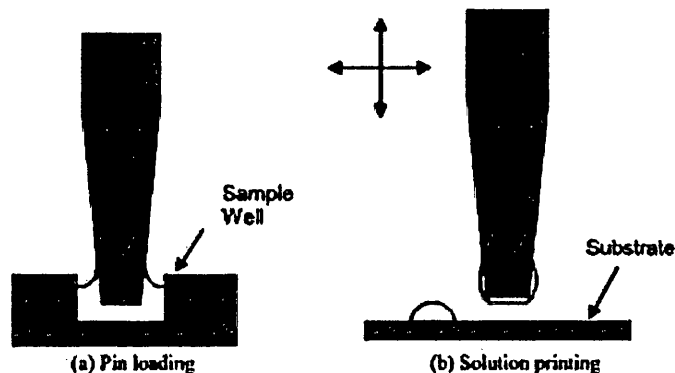


Figure 1.13 Solid pin printing process [Barbulovic-Nad et al. 2006]

(a) Solid pin is loaded with solution from well plate by capillary force action. (b) Spot printing with a single load

In operation, the pin is dipped into a reservoir to load the sample as shown in **Figure 1.13** and the pin then touches the substrate surface to deposit the sample. A single sample load is usually sufficient for printing a few spots. If more than a few spots are needed, the pin must be repeatedly moved between the array and the microplate, which slows the process considerably. Therefore, solid pins are usually used for low-density arrays. However, there are a number of key advantages to this system. For highly viscous solutions, which may clog small orifices, solid pin deposition is the only effective method [Weibel 2002]. They can be cleaned more easily. The simple design enables robust and reliable printing. The construction of solid pins is not

trivial. They are commonly manufactured from metals, such as stainless steel, tungsten, and titanium. There are a number of fabrication limitations when using conventional mechanical machining techniques. During machining, a pin experiences stresses that leave it vulnerable to corrosion and deformation [Weibel 2002]. More importantly, mechanical fabrication processes are not capable of forming uniform surfaces, which are essential for uniform drop printing. Machining creates burrs, grinding marks, and polish lines that have a significant effect on the pin surface area and adhesive properties. In addition, these processes often leave residual surface impurities and contaminants. Compared to conventional mechanical machining, an alternative, electrochemical micromachining, allows for greater control of tip shape and surface characteristics [Weibel 2002]. Much of the innovation in solid pin designs has been to develop different tip shapes to improve spot uniformity. For example, Weibel [Weibel 2002] used electrochemical techniques to develop several different tip shapes and surface textures. A particularly interesting design had a very smooth, hydrophobic surface along the side, with an etched, hydrophilic surface on the tip as shown in **Figure 1.14**. The spot volume was controlled by texturing the pin differently along the length of the pin. Ito et al [2004] developed a complex tip shape capable of forming uniform spots of various diameters. A unique modification of the solid pin design is the pin and ring spotter [Mace 2000]. Mace et al. [Mace 2000] also demonstrated that this printing device can produce droplets with consistent diameters. Unfortunately, this system requires significant modification of conventional microarray robotic systems, which limits its utility for widespread immediate use.

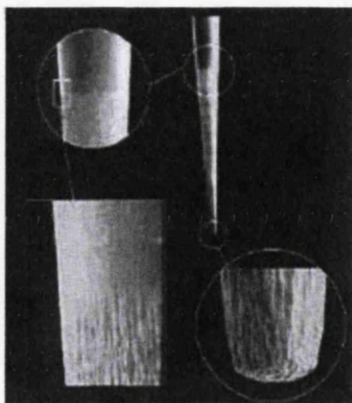


Figure 1.14 Scanning Electron Microscope (SEM) pictures of solid pin etched textures [Barbulovic-Nad et al. 2006]

“Zonal texturing” increases surface area, which affects spot size and density without changing pin size [Weibel 2002].

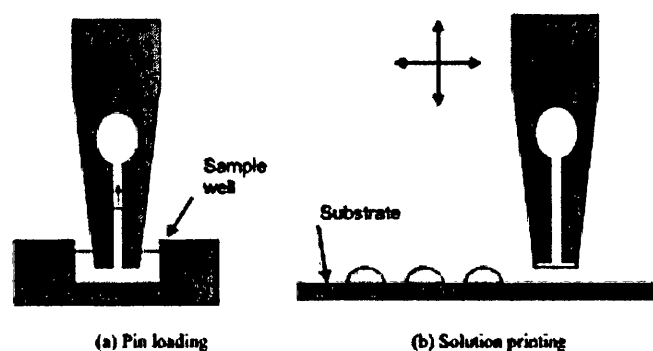


Figure 1.15 Split pin printing process [Barbulovic-Nad et al. 2006]

(a) Split pin (ink stamp) is loaded with solution from well plate by capillary force action. (b) Multiple spot printing with a single load

Split pins are the most commonly used printing devices in DNA microarray production. The main advantage of this method over using solid pins is the ability to print many spots serially without having to recharge the pin, providing higher throughput. During spot deposition, the tapping force can cause the pin tip to deform; thus, the choice of pin materials is important. Split pins are more prone to deformation than solid pins due to the tip structure. Split pins are commonly constructed from stainless steel, tungsten, or titanium [Weibel, 2002] by Electric Discharge Machining (EDM). Differences between pin materials have been reported [University of Stanford 2005]. Titanium is more difficult to machine, which leads to poor slot geometry fidelity, while tungsten carbide is susceptible to shattering, especially at the tip. Ceramics are also used for pin manufacturing. Ceramics provide robustness so that the tip is less susceptible to damage caused by tapping forces. Rose et al [Rose 2003] patented a split pin printing system consisting of a ceramic tip coated with a hydrophobic film. George et al. [George et al. 2001] reported increased consistency in spot morphology printed by ceramic microcapillaries when compared to spots printed by standard stainless steel split pins. In addition to tip deformation, another shortcoming of split pin technology is clogging by dust particles or contaminants, making it unsuitable for printing high viscosity solutions, such as proteins. However, as reported, [University of Stanford 2005] wide slits suffer from spot size irreproducibility. Tip size is often a compromise between spotting accuracy

and susceptibility to clogging. Ito and Tachibana [Ito and Tachibana 2004] developed a variation on the split pin design, shown in **Figure 16**. The split pin spots reproducible volumes onto a water-absorbing substrate, such as a nylon membrane. This design is developed for printing onto a water-absorbing substrate, making it of questionable value for printing onto standard glass slides. An interesting method for printing biomolecule samples, which resembles split pin printing, was developed by Sheehan et al. [Sheehan 2003] utilising the principles of a drafting pen as shown in **Figure 1.17** which can deposit spots with diameters ranging from 100 μm to 600 μm . In this system, an array of pens is mounted on a translation stage, enabling simultaneous deposition of tens of spots of DNA solution onto the substrate. This device is simple to implement and relatively inexpensive. Additionally, the spotting solution can be stored in the pen for multiple uses.

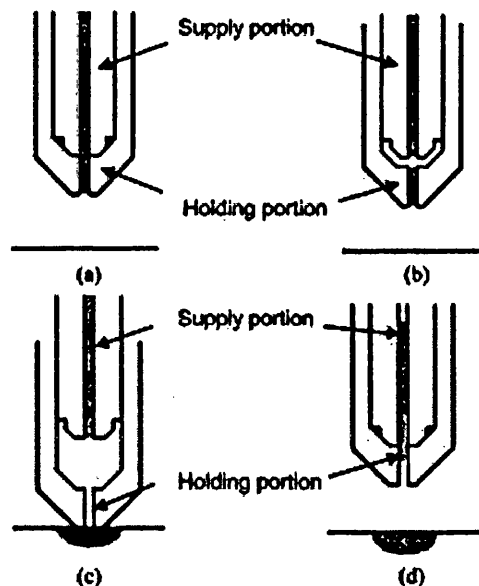


Figure 1.16 Two-part printing system comprising a pin with a supply section and a holding section [Ito and Tachibana 2004]

(a) Two parts touch, such that the holding portion is filled with solution from the supply portion. (b) Two parts separate. (c) Pin delivers solution from the holding portion by physical contact. (d) Supply portion delivers new solution load to the holding portion by capillary force action

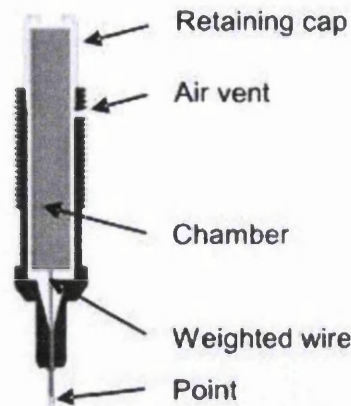


Figure 1.17 Schematic of a drafting pen [Sheehan 2003]

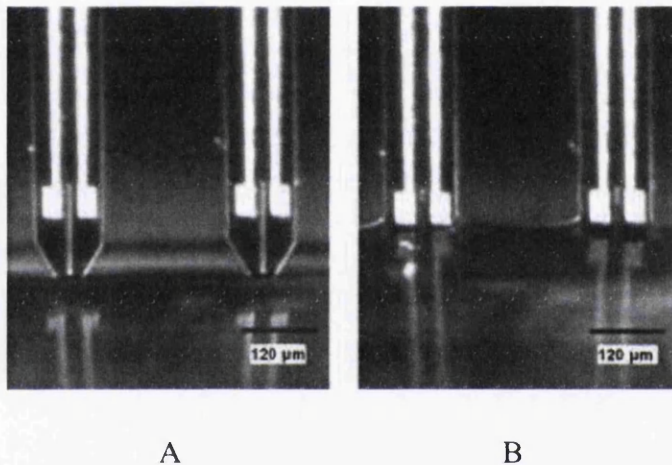


Figure 1.18 Loading of doped Si pins [Leichle et al. 2005]

(A) No voltage is applied. (B) After applying 30 V

Recently, silicon pins have been developed as an alternative to conventional metal pins. Silicon presents several advantages over metal, including cost effectively, light weight, reproducibility, parallel fabrication, smaller features, and robust material properties. These properties improved performance and durability. However, micromachined silicon pin technology has not yet been widely adopted because these pins occasionally cause fractures in substrate coating, yielding undesirable, doughnut-shaped spots [Martinsky and Haje 2000]. Furthermore, pin clogging, pin sliding (i.e. movement in the horizontal direction) and the need for preprinting are problematic for pins formed from silicon and metal alike. But silicon shows promise for printing systems relying on disposable, low-cost devices.

1.2.4.1.3 Pin printing system

Figure 1.19 shows an example of a microarray printing system. There are usually 16, 64, or 96 pins in one pinhead [Rose 2000]. The usual pin spacing of 4.5 mm or 9 mm is determined by the commercial microplate configuration—384 or 96 wells respectively. As described, the pins are dipped into the wells, and the solution is held by surface tension on the outside of solid pins or driven into the slit/channel in split pins by capillary forces. Dipping split pins in a larger sample volume results in spot inconsistency in the first few spots due to the draining of the excess sample solution from the pin sidewalls; therefore, preprinting is necessary until uniform printing is achieved [Rose 2000]. The typical substrates for microarray printing are microscope slides. Prior to spotting, the slides are treated with poly-lysine, amino silanes or amino-reactive silanes that enable DNA or protein to bind to the surface and prevent the sample from being washed away during the hybridisation process. In addition, the dispensed sample spot spreads less if the surface is hydrophobic, allowing higher

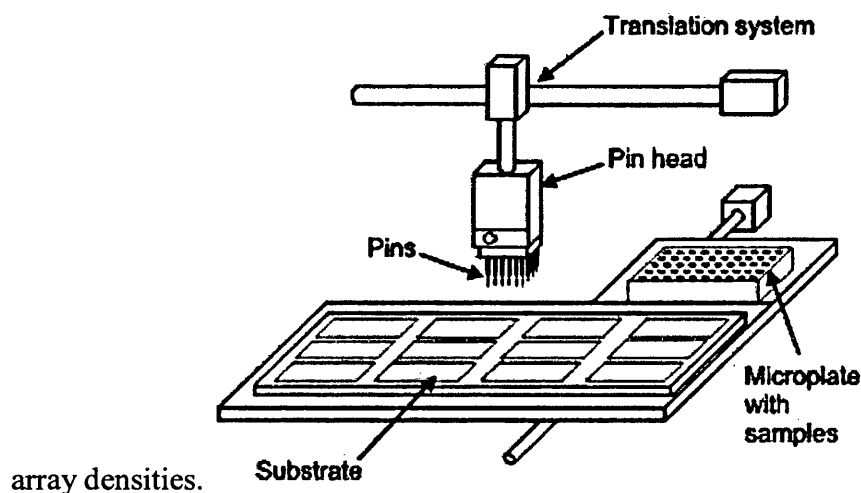


Figure 1.19 System for microarray printing [Ito and Tachibana 2004]

Print head mounted on translation system carries printing devices (pins) from the source microplate to the substrate, where it deposits sample.

1.2.4.2 Microstamping

Pin printing is an inherently serial technique in which a single pin or groups of pins are iteratively loaded for spotting. An alternative to pin printing is microstamping. With microstamps, hundreds of spots are printed in parallel, enabling high-throughput microarray fabrication. The microstamping process, depicted in **Figure 1.19**, is simple and inexpensive and can be readily conducted in a laboratory. A

sample is first adsorbed on the patterned surface of a stamp and then transferred to a substrate by physical contact. In order to obtain good contact, microstamps are generally made from elastomeric materials, such as poly (dimethylsiloxane) (PDMS), which conform to surface roughness under an applied load.

Microstamping has the capacity to form arrays with very high resolution (e.g., inter-spot spacing of 100 nm) [Bernard et al. 1998, Renault et al. 2003]. The low elastic modulus of the commonly used PDMS (e.g., Sylgard 184, Dow Corning) limits the production of arrays with spots smaller than 100 nm [Odom et al. 2002]. Stamp tips smaller than 100 nm buckle and deform under stamping forces. Based on the design by Schmid and Michel, Odom et al. developed stamps capable of forming even smaller spots using two layer devices [Schmid and Michel 2000, Odom 2002]. These stamps were formed from a stiff layer made of a “hard” PDMS and a flexible layer made of conventional PDMS. Some disadvantages for microstamping are related to the sample volumes transferred. In microstamping, the amount of sample transferred from the stamp to the substrate is not well controlled and depends on both surface and sample properties. Additionally, for the same amount of printed sample, microstamping requires larger initial sample volumes, as only a small amount of solution in a well is adsorbed onto the stamp surface, and only a small fraction of the adsorbed solution is transferred from the stamp to the substrate, due to strong non-specific adsorption to the hydrophobic stamp material. Likewise, if microstamps are to be reused, the washing process is more tedious than for pins because of non-specific adsorption [Morozov 2005].

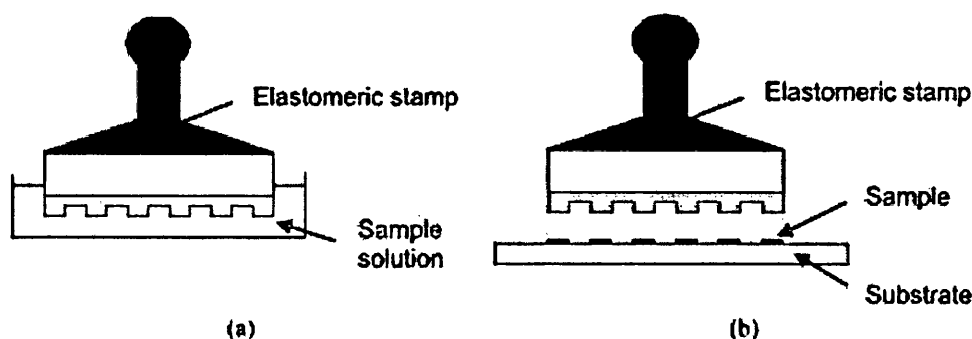


Figure 1.20 Microstamping process [Ito and Tachibana 2004]

(a) Stamp inking in a sample solution well. (b) Transferring sample to the substrate by physical contact between the elastomeric stamp and the substrate

Essentially they show the capability to print small volumes very precisely in small arrays. The processes are costly and hence the microarrays are expensive and not accessible for routine health monitoring and management.

In comparing the pin and micro-stamping technologies there are close similarities with gravure and flexography respectively. The pin could be considered analogous to a single cell gravure print; flexography shares similarities with the PDMS stamp. However, gravure and flexography offer the opportunity for a continuous (volume) printing of DNA, rather than a print run that is governed by the capacity of the pin or stamp. Screen and offset both require a high viscosity ink. DNA is not a high viscosity liquid.

1.2.4.3 Non-contact printing techniques

There are two main advantages to non-contact printing: reduced contamination and higher throughput. By keeping the printing device and the substrate separated at all times, the likelihood of contamination is greatly reduced. Hence, the need to constantly clean the printing device between uses is eliminated. Furthermore, in the absence of experience of volume contact printing in this application, non-contact printing methods are currently considered to hold the greatest potential for increasing microarray fabrication throughput. Many non-contact methods deposit solutions in parallel, allowing entire arrays to be produced simultaneously.

1.2.4.3.1 Inkjet printing of biomolecules

The principles of inkjet have already been discussed in section 1.2.3. In order to reduce the cost of printing biomolecules, attempts have been made to use ink-jet printing technology. In most cases, commercially available printers are modified to dispense a biomolecule solution instead of ink [Allain et al. 2001]. These printers are often one or two orders of magnitude cheaper than robotic pin printing systems and use thermal or piezo activation as described in section 1.2.3. Inkjet printing technology is attractive as it is inexpensive and delivers small droplets with reproducible volumes. Unfortunately, there are four significant drawbacks. Firstly, commercial printers are not designed to print on glass slides. Thus, microarrays can only be spotted onto flexible membranes such as cellulose, nylon, and nitrocellulose [Allain et al. 2004]. Although these membranes are compatible with inkjet printers, droplet smearing and contamination often occur. Secondly, inkjet nozzles have a

tendency to produce undesirable satellite droplets that contaminate surrounding spots and thus, reduce printing resolution [Tseng et al. 2002]. Thirdly, it is difficult to completely flush printing nozzles before a new solution is loaded [Allain et al. 2004]. This problem is more serious in piezoelectric printers since the nozzle is separated from the ink reservoir and all linking channels must be flushed clean. Fourthly, the droplets experience high shear rates while passing through the nozzle and impacting the substrate surface. Under these shear rates there is a risk of denaturing biomolecules in the solution. Allain et al summarised a number of studies that demonstrated that DNA can be spotted with inkjet printers and remain intact; however, proteins are more fragile and may be more sensitive to the extreme conditions of inkjet printing [Allain et al. 2004]. Okamoto et al. have fabricated microarrays with bubble jet technology, and report that DNA solutions can be used without damage [Okamoto et al. 2000]. Furthermore, they suggest that the elevated temperature of solutions spotted with inkjet printers may enhance DNA reaction times, and is a notable advantage [Okamoto et al. 2000]. Efforts have been made to modify inkjet printers to make them more suitable for microarray printing. For example, Tseng et al. [2002] proposed a novel thermal inkjet nozzle that eliminates satellite droplets and improves the speed and control of droplet deposition. The new device was a modification of a commercial thermal inkjet printer, with an additional resistive heater. This heater is used to form a second vapour bubble, which eliminates satellite droplets by pinching off or “tail trimming” the exiting droplet. Other printing systems use existing inkjet printing technology, modified with new dispensing mechanisms to overcome the limitations of commercial inkjet printers. The most common configuration for these types of spotters is a deposition head with a large number of top loaded reservoirs that each feeds to a separate nozzle. Using this configuration, many droplets of different solutions can be dispensed simultaneously. Inkjet printing has also found an application in generating microarrays of *in situ* synthesized oligonucleotides which is typically performed by photochemical means. Instead of using light to direct synthesis, jets of reagents for DNA synthesis are delivered to microscopic spots on a substrate. Different piezoelectric jets fabricated in glass, silicon or ceramics are employed to synthesize DNA arrays [Butler 2001, Hughes 2001], and solvents that have low volatility, high surface tension and high viscosity are preferable to alleviate evaporation and mixing of adjacent sites. An

alternative to prevent mixing is to create pre-printing regions between synthesis sites [Butler 2001].

Electrospray deposition (ESD): as with inkjet printing, electrospray deposition (ESD) is a technique borrowed from an existing application and applied to microarray fabrication. ESD is most commonly used to deposit thin films of polymers, semiconductive ceramics, and radioactive sources. [Morozov and Morozova 1999] In recent years, there have been a variety of studies using this technique to deposit biological solutions [Avseenko et al, 2001, 2002, Kim et al, 2005, Moerman et al. 2001, Morozov and Morozova 1999, 2002].

1.2.5 Printing of biosensors

Sensors are devices that respond to physical or chemical stimuli and produce detectable signals [Tsien 1993, Czarnik 1995, Iqbal et al, 2000, Ligler and Taitt 2002, Wilson 2005]. Sensors used for detection of chemical or biological environments are important largely because people are much less sensitive to the chemical or biological environment than to the physical environment (e.g., light, pressure, temperature, or humidity). However appropriate chemical or biological compositions are tightly linked to the quality of life. Therefore, the development of highly sensitive and selective sensors to recognize important analysts has long been a focus of research for many areas, including environmental monitoring and medical diagnostics [Liu et al. 2009].

A chemical sensor is defined as a device which responds to a particular analyte in a selective way through a chemical reaction and can be used for the qualitative or quantitative determination of the analyte. Such a sensor is concerned with detecting and measuring a specific chemical substance or set of chemicals [Catterall 1997].

Biosensors are a sub-set of chemical sensors, but are often treated as a topic in their own right. A biosensor by definition is an analytical device that combines the specificity of biological sensing element with a transducer to produce a signal proportional to target analyte concentration [Vadgama and Grump 1992], see **Figure 1.21**. The key difference is that the recognition element is biological in nature [Eggins, 2002]. This signal can result from a change in proton concentration, release or uptake of gases such as ammonia or oxygen, light emission, absorption or reflectance, heat emission, mass change, etc. The signal is

converted by a transducer into a measurable response such as current, potential, temperature change, absorption of light, or mass increase through electrochemical, thermal, optical, or piezoelectric means. The signal may be further amplified, processed, or stored for later analysis. In principle, any receptor may be combined with any suitable transducer to produce an operational biosensor [Vadgama and Grump 1992].

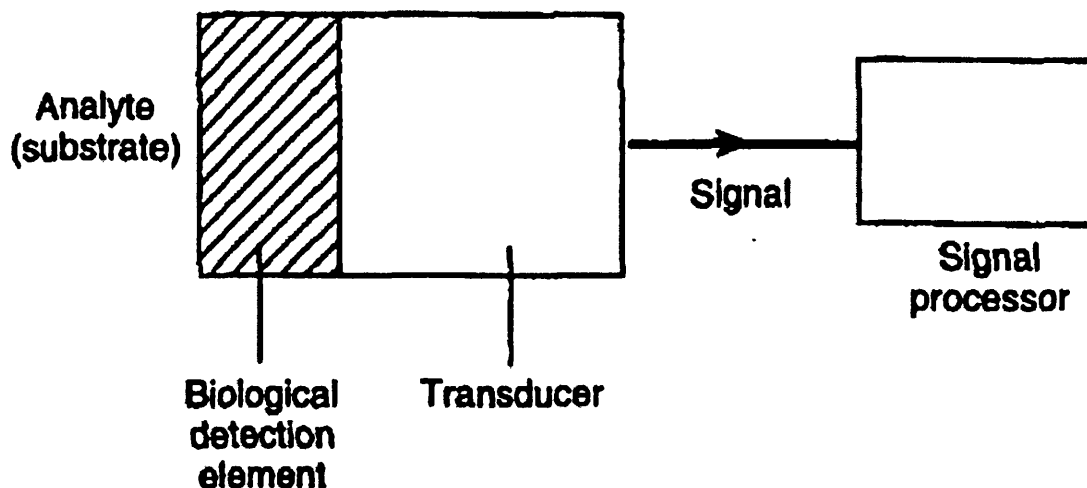


Figure 1.21 Schematic layout of a (bio) sensor [Eggins 1996]

Recognition elements are the key component of any sensor device. They impart the selectivity that enables the sensor to respond selectively to a particular analyte or group of analytes, thus avoiding interferences from other substances [Eggins 2002].

The target recognition element can be any chemical or biological entity such as small organic molecules, peptides, proteins, nucleic acids, carbohydrates, or even whole cells. Ideally, this element should have high affinity (low detection limit), high specificity (low interference), wide dynamic range, fast response time, long shelf life, and good generality for detecting a broad range of analytes with the same class of recognition element. Antibodies are protein-based binding molecules that have long been used for target recognition because they meet most of the above criteria. Signal transduction elements are responsible for converting molecular recognition events into physically detectable signals such as fluorescence, colour, electrochemical signals, or magnetic resonance image changes [Liu et al. 2009]. For example, single-stranded DNAs or RNAs can bind to their complementary strands with high

specificity and are useful for nucleic acid detection [Liu et al. 2009] and this may be detected through fluorescence.

Analytical methods in chemistry have mainly been based on photometric transducers, as in spectroscopic and colorimetric methods. However, most sensors have been developed around electrochemical transducer, because of simplicity of construction and cost.

Electrochemical transducers can be subdivided into the following four main types [Eggins 2002].

- (i) Potentiometric. These involve the measurement of the emf (potential) of a cell at zero current. The emf is proportional to the logarithm of the concentration of the substance being determined.
- (ii) Voltammetric. An increasing (decreasing) potential is applied to the cell until oxidation (reduction) of the substance to be analysed occurs and there is a sharp rise (fall) in the current to give a peak current. The height of the peak current is directly proportional to the concentration of the electroactive material.
- (iii) Conductometric. Most reactions involve a change in the composition of the solution. This will normally result in a change in the electrical conductivity of the solution, which can be measured electrically.
- (iv) FET-based sensors. Miniaturisation can sometimes be achieved by constructing one of the above types of electrochemical transducers on a silicon-chip-based field-effect transistor. This method has mainly been used with potentiometric sensors, but could also be used with voltammetric or conductometric sensors.

Optical transducers have taken a new lease of life with the development of fibre optics, thus allowing greater flexibility and miniaturisation. The techniques used include absorption spectroscopy, fluorescence spectroscopy, luminescence spectroscopy, internal reflection spectroscopy, surface plasmon spectroscopy and light scattering.

The performance of a biosensor is a critical requirement for the quality of information that it may be used to gather. The following are factors that require consideration.

- (i) Selectivity. Sensitivity range. This usually needs to be sub-millimolar, but in special cases can go down to the femtomolar (10^{-15}M) range.
- (ii) Accuracy. This needs to be better than $\pm 5\%$.
- (iii) Nature of solution. Conditions such as pH, temperature and ionic strength must be considered.
- (iv) Response time. This is usually much longer (30s or more) with biosensors than with chemical sensors.
- (v) Recovery time. This is the time that elapses before the sensor is ready to analyse the next sample-it must not be more than a few minutes.
- (vi) The working lifetime is usually determined by the stability of the selective material. For biological materials this can be as short as a few days, although it is often several months or more. [Eggins 2002]
- (vii) Linearity of response. The linearity of the transducer is an expression of the extent to which the actual measured curve of a sensor departs from the ideal curve.
- (viii) Reproducibility. Reproducibility refers to the ability of an entire experiment or study to be reproduced, or by someone else working independently.

1.2.6 Sensing elements

A sensor can recognise an analyte in various ways. The recognition should ideally be specific for that analyte alone, although sometimes it is just selective, i.e. it responds to the required analyte more than to other species. In this case, there may be interferences from other species if they are present in too high a concentration. [Eggins 2002]

There are a number of modes of sensing including the following: ionic, molecular and biological and these are explained fully in [Eggins 2002].

Biological systems provide the major selective elements used in biosensors. There are two types of biosensors, depending on the nature of the recognition event. Bioaffinity devices rely on the selective binding of the target analyte to a surface-confined ligand partner (e.g. antibody, oligonucleotide). In contrast, in biocatalytic devices, an immobilised enzyme is used for recognising the target substrate. For example, sensor strips with immobilised glucose oxidase have been widely used for personal monitoring of diabetes.

These must be substances that can attach themselves to one particular substrate, but not to others. Four main groups of materials can achieve this, notably Enzymes, Antibodies, Nucleic acids and Receptors.

Enzymes have been the most widely used bioreceptor molecules in biosensor applications, with antibodies and proteins receptor molecules increasingly incorporated in biosensors. This specificity of a biosensor comes from the specificity of the bioreceptor molecule used. An enzyme is a good example. It has a three-dimensional structure that fits only a particular substrate. An enzyme is a protein synthesised in the cell from amino acids according to the codings written in DNA. Enzymes act as catalysts for biochemical reactions occurring in the cell. To maintain high enzyme activity, the temperature and pH of the environment have to be maintained at suitable levels for each enzyme [Wilson 2005].

In principle, any biomolecule and molecular assembly that has the capability of recognizing a target analyte can be used as a bioreceptor. In fact, membrane slices or whole cells have been used in biosensor. **Figure 1.22** summarises possible bioreceptors that can be utilised in a biosensor [Wilson 2005].

	Biolayer Type	Main needs for structural integrity	Typical signal generated
Complexity hierarchy	End of Organ (e.g., Olfactory)	Intact tissue architecture	Action potential
	Tissue	Nutrient/O ₂ supply	Metabolic end product
	Whole cell		
	Cell organelle (e.g., mitochondrion)	Osmotic/pH stability	Product of electron chain
	Biomembrane (e.g., receptor)	Mechanic protection	Released contents
	Enzyme	pH/electrolyte stability	Reaction product
	Antibody	pH stability	Antigen uptake/mass change
	Ionophore	Adequate retention	EMF/absorbance change (chromionphore)

Figure 1.22 Possible bioreceptor molecules and molecular assemblies for biosensor applications; their requirements for structural integrity and signals generated [Wilson 2005]

One major requirement for a biosensor is that the bioreceptor is immobilised in the vicinity of the transducer. The immobilisation is done either by physical entrapment or chemical attachment. Chemical attachment often involves covalent bonding to the transducer surface by suitable reagents. A comprehensive treatment of immobilisation is available in Hermanson (1996). It is to be noted that only minute quantities of bioreceptor molecules are needed, and they may be used repeatedly for measurements [Wilson 2005]. The covalent binding causes numbers of molecules concentration to denatured.

Deoxyribonucleic acids (DNA) are arguably the most important of all biomolecules. The unique complementary structure of DNA between the base pairs adenine/thymine and cytosine/guanine has been the basis for genetic analysis over the last few decades. The ability of a single stranded DNA (ssDNA) molecule to 'seek out', or hybridise to, its complementary strand in a sample is the foundation of DNA based detection systems. There is a great potential market for simple, cheap, rapid, and quantitative detection of specific genes.

DNA sequence detection is currently a routine procedure using DNA chip microarrays. This class of tools allows researchers to measure global genome mRNA expression levels [Brown and Botsten 1999, Wu et al. 2001] and to characterize single nucleotide polymorphisms (SNPs) within individual organisms and within populations [Wang et al. 1998, Syvanen 2001]. However, sample size and numerous preparative steps prevent microarrays from easily assessing tissue-specific or cell-specific polynucleotide sequences, or providing real-time results [Meldrum, 2000; Wang 2000, Eberwine et al. 2001, Gut 2001]. These constraints also preclude rapid detection of trace DNA or RNA levels that are diagnostic of bacterial food contamination, genetically modified organisms, or the presence of biological warfare agents. Alternative technologies are in development that addresses these issues by combining DNA with signal transducers.

1.2.7 DNA as a sensor

The DNA techniques, including hybridisation, amplification, and recombination, are all based on the double helix structure of the DNA. Nucleic acid hybridisation is the underlying principle of DNA biosensors.

Like other biosensors, DNA sensors are usually in the form of electrodes, chips, and crystals; hence, hybridisation on a sensory surface is a solid-phase reaction. Solution hybridisation is more rapid than hybridisation on solid-supports, but unless the assay is homogeneous, a separation step is required before final detection [Tenover 1988, Walker and Dougan 1989]. Solid phase or filter hybridisation is the longest established and the most often used [Wolcott 1992]. The kinetics of nucleic acid hybridisation at a solid substrate-solution interface are still not well understood because there is a dearth of suitable methods for the continuous measurement of the hybridisation process. The process is also difficult to predict from theoretical considerations, partly because the exact concentration of the immobilized nucleic acid and its availability for hybridisation are unknown [Maniatis et al. 1989]. Furthermore, the actual mechanism of strand association in solid-support hybridisation remains obscure. The kinetics and mechanism of nucleic acid single strand hybridisation concentration have been widely studied only in cases where both strands are in free solution [Hames and Higgins 1985]. The nature of the hybridisation reaction on solid surfaces has been assumed to approximate closely to that of hybridisation in solution. However, the rate of solid-phase hybridisation is only about a tenth to a hundredth of that in solution [Bunemann 1982]. Although not systematically examined, it has been suggested that efficient hybridisation to DNA attached to solid supports can be impeded by several related phenomena. For example, the immobilized DNA molecules may link to solid surface at several points along the DNA chain, hence some of the attached DNA may not be accessible for hybridisation in 1 mM cisplatin and 6 mM transplatin solutions [Su 1995].

1.2.8 Immobilisation techniques

The selective element must be connected to the transducer. This presents particular problems if the former is biological in nature. Five classes of methods of connection have evolved, as follows: [Eggins 2002]

- (i) Absorption. This is the simplest approach and involves minimal preparation. However, the bonding is weak and this method is only suitable for exploratory work over a short time-span.
- (ii) Microencapsulation. This was the method used in the early biosensors. In this technique, the biomaterial is held in place behind a membrane, thus giving close contact between the biomaterial and the transducer. Such a method is adaptable, does not interfere with the reliability of the enzyme, and limits contamination and biodegradation. It is also stable towards changes in temperature, pH, ionic strength and chemical composition. However, such systems may be permeable to some materials, e.g. small molecules, including gases, and electrons.
- (iii) Entrapment. Here, the biomaterial is mixed with a monomer solution, which is then to a gel, thus trapping the material. Unfortunately, this can cause barriers to the diffusion of substrate, thus slowing the reaction. It can also result in loss of bioactivity through pores in the gel-this effect can be counteracted however, by cross-linking. The most commonly used gel is polyacrylamide, although starch, nylon and silastic gels have also been used. Conducting polymers, such as polypyrroles, are particularly useful with electrodes.
- (iv) Cross-linking. In this method, the biomaterial is chemically bonded to solid supports or to another supporting material, such as a gel. Bifunctional reagents, such as glutaraldehyde, can be used in such techniques. Again, there is some diffusion limitation and there can also be damage to the biomaterial. In addition, the mechanical strength of the system is poor. However, it can be a method used for stabilising absorbed biomaterials.
- (v) Covalent bonding. This approach involves a carefully designed bond between a functional group in the biomaterial and the support matrix. Nucleophilic groups in the amino acids of the biomaterials, which are not essential for the catalytic action of, say, an enzyme, are suitable in this respect. The reaction must work under conditions of low temperature, low ionic strength, and neutral pH, and in this way the enzyme will not be lost from the biosensor device when using this technique.

Overall, the lifetime of the biosensor is greatly enhanced by proper immobilisation. Typical lifetimes for the same biosensor, in which different methods of immobilisation are used, are as follows: [Eggins 2002]:

Adsorption: 1 day, membrane entrapment: 1 week, physical entrapment: 3-4 weeks, covalent entrapment: 4-14 months

Adsorption:

Many substances adsorb enzymes on their surface, e.g. alumina, charcoal, clay, cellulose, kaolin, silica gel, glass and collagen. No reagents are required, there is no clean-up step and there is less disruption to the enzymes.

Adsorption can roughly be divided into two forms, namely physical adsorption (physisorption) and chemical adsorption (chemisorptions). Physisorption is usually weak and occurs via the formation of van der Waals bonds, occasionally including hydrogen bonds or charge-transfer forces. Chemisorption is much stronger and involves the formation of covalent bonds.

Adsorbed biomaterial is very susceptible to changes in pH, temperature, ionic strength and the substrate. However, this approach has proved to be satisfactory for short-term investigations.

Microencapsulation

In this method, an inert membrane is used to trap the biomaterial onto the transducer. This was the technique originally used to develop the first glucose biosensor on the oxygen electrode. [Eggins 2002]

The advantages of this approach are as follows:

- (i) There is close attachment between the biomaterial and the transducer.
- (ii) It is very adaptable, and also very reliable.
- (iii) The reliability of the biomaterial (enzyme) is maintained as follows:
 - (a) A high degree of specificity is achieved;
 - (b) There is good stability to changes in temperature, pH, ionic strength, E^0 and substrate concentration;
 - (c) It can act as an inbuilt device to limit contamination and biodegradation;
 - (d) If used with a patient, infection can be avoided.
- (iv) There is always the option to bond the biological component to the sensor via molecules that conduct electrons, such as polypyrrole.

Entrapment [Eggins 2002]

In this approach, a polymeric gel is prepared in a solution containing the biomaterial. The enzyme is thus trapped within the gel matrix. The most commonly used polymer is polyacrylamide, which is prepared by the copolymerization of acrylamide with N, N'-methylenebisacrylamide. Polymerization can be effected by UV irradiation in the presence of vitamin B₁ as a photosensitizer. Other materials which have been used include starch gels, nylon, silastic gels and conducting polymers (such as polypyrrole).

The problems encountered with this method include the following:

- (i) Thick barriers are created, thus inhibiting the diffusion of the substrate, which slows down the reaction, and hence the response time of the sensor.
- (ii) There is loss of enzyme activity through the pores in the gel, although this may be overcome by cross-linking, e.g. with glutaraldehyde.

Cross-linking

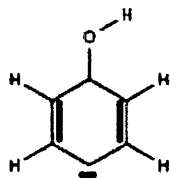
This approach uses bifunctional agents to bind the biomaterial to solid supports, and has proven to be a useful method for stabilising adsorbed enzymes. It does, however, have the following disadvantage: [Eggins, 2002]

- (i) Damage is caused to the enzyme by changing the functional conformation of the enzyme.
- (ii) Diffusion of the substrate is limited.
- (iii) There is poor rigidity (mechanical strength)

Covalent bonding

Some functional groups, which are not essential for the catalytic activity of an enzyme, can be covalently bonded to the support matrix (transducer or membrane).

This method uses nucleophilic groups for coupling, such as -NH₂, -CO₂H, -OH,



-C₆H₄OH

and -SH, as well as imidazole [Eggins 2002].

The particular advantage of this method is that the enzyme will not be released during use. In order to protect the active site, the reaction is often carried out in the presence of the substrate [Eggins 2002].

In practice, it is unusual for only one of the methods described above to be used at a time, robust stability is essential for a commercial sensor, combined with reproducibility to match the performance required for the particular application. Cost is likely to be less important in the immobilisation of a biological component than in other aspects, such as the performance of the transducer and the read-out. The covalent-bonding approach would be the most suitably robust method, followed by microencapsulation (depending on the biomaterial being used). However, if the sensor is to be disposable, the latter could be screen-printed and entrapment in a polymer matrix might then prove suitable [Eggins 2002].

Hybridisation biosensors rely on the immobilisation of a single-strand DNA probe onto the transducer surface. The duplex formation can be detected following the association of an appropriate hybridisation indicator or through other changes acquired from the binding event [Wang 2000].

The environment of the immobilized probes at the solid surface depends upon the mode of immobilisation and can differ from that experienced in the bulk solution. Depending upon the nature of the physical transducer, various schemes can be used for attaching the DNA probe to the surface. These include the use of thiolated DNA for self-assembly onto gold transducers (gold electrodes or gold-coated piezoelectric crystals), covalent linkage to the gold surface via functional alkanethiol-based monolayers, the use of biotylated DNA for complex formation with a surface-confined avidin or strepavidin, covalent (carbodiimide) coupling to functional groups on carbon electrodes, or a simple absorption onto carbon surfaces. As in solution-based hybridisation assays, conditions for interfacial hybridisation events (e.g. ionic strength, temperature, presence of accelerators) have to be optimized. Chemical and thermally-induced dehybridisation of the resulting duplex is often used for regenerating the interface [Eggins 2002].

DNA dendrimers can be used for imparting higher sensitivity onto DNA biosensors. These tree-like superstructures possess numerous single-stranded arms that can hybridize to their complementary DNA sequence. A greatly increased hybridisation capacity and hence a substantially amplified response is achieved by immobilizing these dendritic nucleic acids onto the physical transducer [Wang et al. 1998].

So this work suggests that covalent bonding is the common immobilisation method for biological material but the adsorption, micro capsulation, encampment and cross linking are also alternative immobilisation methods for such materials with advantages such as convenience, speed and cost.

The existing immobilisation chemistry is too slow to use with volume printing techniques. It requires modified DNA, with inferred additional costs and restricts selection of DNA for the sensor. A simpler immobilisation technique is needed.

There are papers [Nikiforov and Rogers 1995, Nikiforov et al. 1994a] that have illustrated ways to attach ODN (oligodeoxyribonucleotide) onto PS (Polystyrene).

It is in general thought that short, single-stranded ODN molecules are attached only very weakly to this kind of solid phase [Nikiforov et al. 1994a]. The data from this investigation suggest that the attachment of the ODN needs the existence of salt reagents. The attachment is very inefficient in salt-free aqueous solutions. Moreover, in the presence of Tween 20, no attachment happens. This is possibly due to an "inactivation" of the plate surface by the preferential absorbance of this surfactant compound. Also, no binding can be obtained if the plate is washed with a solution with Tween 20 before the immobilisation experiment, even though the immobilisation solution does not contain the surfactants. The use of 250 mM NaCl in the immobilisation experiment led to little change in signal in the subsequent hybridisation assay [Nikiforov et al. 1994a].

Two alternative methods need only the incubation of DNA molecules on the plate either with salt-containing solutions or in the presence of cationic detergents [Nikiforov and Rogers 1995]. These methods enabled the non-covalent, passive adsorption of ODN probes to the PS surface. They showed results indicating that these two classes of reagents improve the ODN attachment with different mechanisms, and also suggested that the latter class of compounds was better than

the former in functional examinations. The first type comprise compounds like NaCl and TMAC, which act best when applied at relatively high concentrations, generally higher than 50 mM, and best at 250 to 500 mM. Comparatively short, unmodified ODN can be efficiently attached onto the surface of hydrophilic PS plates simply by incubation in a solution with 50 mM NaCl. All of these data indicate that the attachment is non-covalent binding. So the ODN are possibly attached by a combination of hydrophobic and ionic bonds to the PS surface. The requirement for the existence of ~50 mM salt to obtain binding appears to support this, because hydrophobic forces are stronger at higher salt concentrations. It is also possible that the existence of a salt (enhanced ionic strength of the solution) reduces electrostatic repulsion between the phosphates groups of the ODN backbone and negatively charged groups on the PS surface. Whatever the exact mechanism of attachment, ODN molecules are immobilized to the surface with sufficient stability and are not removed by a relatively short (1 hr) treatment with 0.1 M NaOH. Furthermore, concentrations at 1 M can be used without any noticeable effect on the attachment. ODN attachment by incubation with NaCl-containing solutions has also been reported in other articles [Balaguer et al. 1993, Cros et al. 1994]. The hydrophobic interactions between the ODN molecule and hydrophobic sections at the PS surface are increased to a degree that immobilizes the DNA.

The mechanism of immobilisation which combines reagents can be considered as linking a positively charged 'head' and a relatively hydrophobic 'tail'. These are the typical properties of cationic surfactants for which the immobilising mechanism, is possibly much different. Reagents of this kind are the cationic surfactants CTAB, ODL-HCl (octyldimethylamine hydrochloride), and EDC (1-ethyl-3-(3-dimethylaminopropyl) carbodiimide hydrochloride). Cationic surfactant-induced ODN binding, has been described following investigation carried out by Pontius and Berg [Pontius and Berg 1991] and Bromberg and Klibanov [Bromberg and Klibanov 1994]. The first describes the accelerating effect of cationic surfactant on the rate of hybridisation of complementary DNA molecules, while the second one indicates that DNA can be solubilized in hydrophobic organic solvents in the presence of cationic surfactant. Both of these effects are discussed by the authors suggesting the cationic surfactants significantly change the hydrophobic characters of the DNA strands. The mechanism of binding in the presence of EDC or cationic surfactants is probably

very similar to the mechanism of delivery of DNA and proteins through an organic phase in the presence of surfactants that has been explained recently [Bromberg and Klibanov 1994]. Chemicals of a similar structure, but with a negatively charged 'head' (e.g., SDS) fail completely as ODN attachment compounds, similar to non-ionic surfactants [Nikiforov et al. 1994a]. The number of surfactant molecules that are connected with each ODN molecule will be based on the ODN length, but should be apparently higher than one in the case of a 25 bases ODN. These chemicals can be applied for ODN attachment at very low concentrations, (at 0.03 mM for CTAB), but a lower hybridisation result is achieved when they are used at higher concentrations. When CTAB is used at 0.03 mM for the immobilisation of a 25 bases ODN at 0.2 μ M, there are 6 CTAB molecules present for each phosphodiester bond. Likewise, EDC and ODA-HCl resist the immobilisation when applied at higher concentration (approx. 300-500 mM). The CMC of CTAB, (a very good surfactant), is very small, whereas EDC and ODA-HCl, (which are very poor surfactants), make micelles and resist the attachment only at comparatively high concentrations [Nikiforov and Rogers 1995]. One of these papers shows that the hybridisation effect is working only when the cationic surfactants are applied at concentrations smaller than their CMC [Bromberg and Klibanov 1994]. It shows that the surfactant-enabled transfer through liquid membranes should be a rather common situation, effective if the bio polyelectrolyte and surfactants have opposite charges (and the surfactant's concentration is less than the CMC) [Bromberg and Klibanov 1994]. If the concentration of the surfactant molecules is higher than their CMC (Critical Micelle Concentration) described in 2.2.1, then micelles will be made. They have suggested previously that no ODN immobilisation to Immulon 4 plates can be made when CTAB is used at concentrations higher than its CMC [Nikiforov et al. 1994a]. The data collected by them strongly indicate that this chemical for ODN attachment to Immulon 4 or similar plates does not include the formation of covalent interactions between the ODN and the plate surface. Although ODN might still interact electrostatically with the surfactant molecules, the micelles have a hydrophobic core that is completely covered by a polar surface; therefore, no hydrophobic force with the plate surface will appear and there will be no ODN attachment. The connections with compounds carrying a hydrophobic group to supply the ODN will direct its attachment to the plate surface by hydrophobic interactions. The different resisting concentrations discovered for the different chemicals mirror the widely different

concentrations at which these compounds will make micelles. For many different commercially available 96 well plates, their suitability for ODN attachment was promoted for a more hydrophilic surface while the hydrophobic surface was found to be unsuitable. They investigated many different commercially available 96-well plates for their suitability for ODN immobilisation. Examples of suitable plates include Immulon 4 (Dynatech), Maxisorp (Nunc), and Immuno Ware (Pierce). No immobilisation could be achieved on Immulon 1 (Dynatech) and Polysorp (Nunc) plates. All investigations explained below have been tested with Immulon 4 plates [Nikiforov et al. 1994a].

The attached ODN needs to join efficiently in the hybridisation experiment. Even if shorter ODN can also be attached, a length of ~12 bases was required to hybridize efficiently to the single-stranded PCR templates. Thus, it is very likely that parts of the attached compounds are inaccessible to hybridisation because they are included into the reaction with the PS surface [Nikiforov et al. 1994a]. They examined selected cationic surfactants for their ability to initiate DNA hybridisation. CTAB is hypothesized to immobilize along the nucleic acid molecule with one CTAB compound linked per DNA phosphate. Unlike polypeptides, cationic surfactant cannot make amphipathic α -helices or other specific secondary structures, ruling out the possibility that such motifs are needed for hybridisation reaction [Pontius and Berg 1991]. Their current data indicated that the simple cationic surfactant dodecyl trimethyl ammonium bromide (DTAB) and CTAB can increase the kinetics of hybridisation of complementary DNA molecules >10⁴-fold when compared with reactions run in the absence of surfactant and that, under optimised conditions, CTAB-mediated hybridisation is >2000-fold faster than experiment in 1 M NaCl at 68°C. Hybridisation is sequence specific, since the kinetics and extent of the reaction are not resisted by the existence of up to a 10⁶-fold excess of non-complementary molecules. Furthermore, CTAB helped hybridisation to occur well above the melting temperature of the duplex DNA, suggesting that this surfactant has DNA helix-stabilizing characteristics [Pontius and Berg 1991].

This is motivated with reference to the works of above. These works point to two basic immobilisation mechanisms and identify PS as a most suitable candidate material while excluding CCP from their list. Thus the mechanism of immobilisation onto CCP requires further investigation as this represents a substrate that can be used

for volume production of devices that exploit immobilized DNA. This will be explored fully in Chapter 3.

To characterise modified polymer surface properties, the type of analytical devices used must be suited to the prospected property the modification, the specificity needed and the available resources. Not only must the quantity and activity of the attached bioactive material be analysed, but the surface chemistry must be evaluated after each step in the modification in order to validate the proposed mechanism by which the bioactive material was covalently immobilised [Goddard and Hotchkiss 2007].

1.2.9 Surface modification

Many surface modification methods have been explored to assist wetting, adhesion, and printing of polymer surfaces by offering a variety of polar groups, with little attention to functional group specificity. But, when surface modification is a precursor to attaching a bioactive compound, these techniques must be tailored to supply a specific functional group. Techniques, which modify surface properties by offering random, non-specific groups or by coating the surface, are less useful in bioconjugation to polymer surfaces [Goddard and Hotchkiss 2007]. There are four techniques in surface modification.

The first technique uses wet chemical. A material is treated with liquid reagents to form reactive functional groups on the surface. This classical way to surface dedication does not need specialized device and thus can be used in most laboratories. It is also more capable of infiltrating porous three-dimensional substrates than plasma and other energy source surface modification techniques [Liu and Ma, 2004], and allows for *in situ* surface functionalization of microfluidic equipment. However, these wet chemical methods are non-specific, forming a range of oxygen-containing functional groups. In addition, those which target amendment of polymer side chains depend on side chain surface arrangement. So the degree of surface functionalization may not be repeatable between polymers of different molecular weight, crystallinity, or tacticity. These wet chemical methods also produce harmful chemical waste and can cause to uncommon surface etching [Desai and Singh 2004]. Several these techniques also need extended treatment in concentrated destructive solutions. For

these reasons, while useful in the laboratory atmosphere, these wet chemical processes may not be proper for larger scale, industrial field.

Second, it is silane monolayers. The immobilisation of organosilanes to surfaces was originally explored as a way to combine an organic polymer to an inorganic substrate, for example to introduce binding between glass and polymers in the advance of glass-reinforced polymers (fiberglass) [Plueddemann 1991]. The unique orientation of silanes on a surface has been largely investigated by Whitesides, and has been dubbed a self-assembled monolayer (SAM) because of the ability to self-organize onto an suitably functionalized surface as an ordered, single molecular layer [Yan et al. 2004, Whitesides and Laibinis 1990, Xia et al. 1996]. Because of their almost crystalline combination, SAMs introduce the potential for more determined surface functionalization than conventional wet chemical or ionized gas functionalization techniques [Whitesides and Laibinis 1990]. But, the siloxane binding can be hydrolyzed at high temperatures or alkaline pH [Xia et al. 1996, Wasserman et al. 1989]. Although investigation on surface adjustment using silane monolayers continues to focus primarily on inorganic substrates, this is certain to be an emerging field for polymer surface modification.

Third, it is ionized gas treatments. This is classified further into plasma, corona discharge, flame treatment and UV irradiation. For plasma, it is a high energy state of substance, where a gas is partially ionized into charged fragments, electrons, and neutral molecules [Dinklage et al. 2005]. Plasma can provide adjustment of the top nanometer of a polymer surface without using solvents or inducing chemical waste and with less damage and hardening of the material than many wet chemical treatments [Desai and Singh 2004, Chan et al. 1996, Lane and Hourston 1993, Ozdemir et al. 1999]. The property of functionalization imparted can be varied by selection of plasma gas (Ar, N₂, O₂, H₂O, CO₂ and NH₃) and operating parameters (pressure, power, time, gas flow rate) [Lane and Hourston, 1993]. Plasma can be used as a precursor to other surface modification techniques, for example, plasma activation with ultraviolet (UV) graft polymerization [Cen et al. 2004] or plasma activation with silanization [Long et al. 2006, Prissanaroon et al. 2005]. However, with the exception of a recent development of an atmospheric plasma system [Shenton and Stevens 2001], plasma generation needs a vacuum to empty the

chamber of latent gases, which shows complications for continuous operation in a large scale industrial setting [Inagaki 1996]. Also, results are difficult to duplicate between laboratories as there are a lot of parameters involved to optimise conditions, including time, temperature, power, gas composition/flow/ pressure, orientation of reactor and distance of substrate from plasma source [Chan et al. 1996]. It should be noted that in addition to the monomers and gases intentionally introduced to the plasma chamber, latent chemicals from prior users may be present thus posing a risk of contamination. So the plasma chamber should be fully cleaned, for example by oxygen plasma, before introducing polymers for surface modification. For corona discharge, it is a simple, cost effective, continuous process in which an electrically induced stream of ionized air bombards the polymer surface. It is commercially used to increase printability and binding to inert polymers [Lane and Hourston 1993] by introducing surface oxidation products [Desai and Singh 2004, Briggs et al. 2003]. However, this result in a broad range of oxygenated groups and therefore may be less useful as a technique to introduce specific functionalities for bioconjugation. Contamination may also be an issue and variations in local temperature and humidity can affect consistency of treatment because it does not operate under a vacuum, [Desai and Singh 2004]. Finally, it has been reported that surface polar groups on corona treated polyolefins are particularly changeable. Materials should therefore be used quickly after treatment [Ozdemir et al. 1999]. For flame treatment, such as corona discharge, flame treatment is a non-specific surface functionalization method that bombards the polymer surface with ionized air, generating a broad spectrum of surface oxidation products to the top several monolayers [Desai and Singh 2004, Lane and Hourston 1993]. In this method, the reactive oxygen is generated by burning an oxygen rich gas mixture. Flame treatment has been shown to impart hydroxyl, aldehyde, and carboxylic acid functionalities to poly (ethylene) and is utilized to enhance printability, wettability, and adhesion [Briggs et al. 2003]. Although fundamentally simple and inexpensive, flame treatment can reduce optical clarity to polymers, and there are many parameters (including flame temperature, contact time and composition) that must be accurately controlled to keep consistent treatment and to avoid burning [Ozdemir et al. 1999].

Fourth, it is UV irradiation. When contact to UV light, polymer surfaces produce reactive sites which can become functional groups touching gas or can be applied to

initiate UV-induced graft polymerization. This technique differs from ionized gas treatments by corresponding to the depth of surface reactivity by varying wavelength and thus absorption coefficient [Chan et al. 1996]. But UV treatment can influence the optical properties of the polymer and UV light can be blocked by fragments, which may affect treatment consistency.

1.2.10 DNA Microarray

DNA microarrays offer high throughput analysis of gene expression which has application in mutation analysis, drug discovery, diagnostics, and other applications [Goddard and Hotchkiss 2007]. Because the term DNA microarray was coined in publications from the laboratory of DeRisi et al. [DeRisi et al. 1996] and Schena et al. [Schena et al. 1995], this technique evolved from a very specialised method that is only available to few people [Bowtell 1999, Cheung et al. 1999, DeRisi et al. 1997, Lashkari et al. 1997] to a common tool with many different applications that became important in microbiology [Dharmadi and Gonzalez 2004]. There are several other types of microarrays, such as protein microarrays, but the DNA microarray is by far the most widespread. The essence of microarray technology is the parallel hybridisation of a mixture of labelled nucleic acids known as target, with thousands of individual nucleic acid species called probes, which can be identified by their spatial position in a single experiment. The definitions of terms of probe and target are used as the different in Chapter 3 because the probe ODN is used for investigation of the ODN immobilisation on the polymer substrates. So the probe ODN in Chapter 3 is target ODN in Chapter 5. In Chapter 5, the terms of the probe and target are the same as the meanings shown above. Whereas the probes are immobilized on a solid support, the targets are applied as a solution onto the array for hybridisation after fluorescent labeling [Brown and Botstein 1999]. This nomenclature will be used in this work, but it is notable that the terms probe and target sometimes got mixed up in literature, but the definition used in this review was given in a special issue of nature genetics [Phimister 1999] and is now commonly agreed upon.

Microarrays were developed from Southern blots [Southern 1975, 2001], colony filters [Nguyen et al. 1995], to dot blots [Kafatos et al. 1979]. “DNA macroarrays” or “filter arrays” were made through miniaturisation by using robotic devices for spotting thousands of probes on a nylon membrane. This number was already enough

to probe each gene of a bacterial genome. The targets were labelled radioactively [Granjeaud et al. 1999], thereby allowing only one hybridisation at a time. The disadvantage of the so-called one-channel experiments is that the variance of each single array affects the final expression ratios. This problem was solved by two-channel experiments in which two mRNA populations are labelled with different fluorescent dyes and are hybridized simultaneously on one array. Glass slides are commonly used as support because of their low background fluorescence [Schena et al. 1995, 1996]. Moreover, the rigid glass slides allow much higher probe density than the flexible membranes of macroarrays, thereby reducing the amount of target required. Additionally, glass allows covalent linkage of DNA to the surface and is inert to high ionic strength washing and high temperature. After microarray fabrication, the most important issue in microarray-based analysis is probe–target hybridisation. Conceptually, microarray hybridisation and detection are quite similar to the traditional membrane-based hybridisation (Eisen and Brown 1999). Before hybridisation, the free functional groups (e.g., amine) on the slide should be blocked or inactivated to eliminate nonspecific binding. Nonspecific binding causes high background and depletion of probes. In addition, the unbound DNA on the slides can be washed away during the prehybridisation process. Removal of unbound DNA in prehybridisation is important, because any DNA that washes from the surface during hybridisation competes with DNA bound to the slide. Since the rate of hybridisation in solution is much greater than that on surfaces, the presence of unbound probe DNA can lead to a dramatic decrease in the measured signals obtained from microarrays. After prehybridisation, the microarray is hybridized with fluorescently labelled target DNA or RNA for a period of time. The unbound material is washed away. Regardless of the hybridisation format, the hybridisation solution should be mixed well so that the labelled targets are evenly distributed on the array surface to obtain optimal target–probe interactions across the entire microarray. The wash solutions should be uniformly distributed to eliminate unbound probes, remove nonspecific hybridisation and minimize background signal.

1.3 Research Challenges

The preceding review has highlighted the pertinent previous work that focuses on the deposition of DNA including the techniques that have been developed around pin

technologies. The consequent DNA sensor devices are costly to manufacture and are therefore not used as extensively in diagnosis. Printing offers an alternative manufacturing process and the aim of this thesis is to explore this possibility. Building on the review, the following three key questions are concerned.

The deposition of DNA on a flexible substrate – this will facilitate a sheet to sheet extending to reel to reel deposition by printing. This will require immobilisation of DNA (formulated as an ink) onto a substrate. The research in this area will be described in Chapter 3.

DNA can also be deposited by ink jet technologies, for volume manufacturing of sensors, other printing techniques need to be explored. This includes the flexographic and gravure processes. The survival of DNA is a crucial requirement and consequently this will be explored within the research and the work is described in Chapter 4.

The application of DNA in a sensor technology will require a hybridisation process. To date, DNA hybridisation has focused on complementary DNA materials that have not been formulated within an ink. For implementation in a printing process the hybridisation of a DNA ink is an important consideration and the research on this topic is described in Chapter 5.

The work in Chapter 2 is concerned with application of methods that will underpin the three key research challenges.

Chapter 2 Materials and Methods

The purpose of this chapter is to explain the methods and materials used within this research programme. This includes the choice of materials as well as the procedures that were adopted and the impact on the statistical robustness of the results. To achieve an understanding of the deposition of DNA requires a number of experiments to be undertaken to characterise the DNA for deposition as well as its immobilisation, hybridisation and survival. Principally, this required the measurement of pH, concentration, fluorescent signals, surface tension, viscosity and various buffer washing.

2.1 DNA choice and preparation

2.1.1 DNA choice

The 25 bases oligonucleotide sequences were chosen from the Gene title 'cytochrome P450, family 19, subfamily A, polypeptide 1' with the Gene Symbol CYP19A1. This gene was chosen because the gene CYP19A1, located on chromosome 15q21.1, encodes the aromatase enzyme. Aromatase is an enzyme that is responsible for a key step in the biosynthesis of Estrogens. Because Estrogens promotes certain cancers and other diseases, aromatase inhibitors are frequently used to treat those diseases [Toda 1993]. These oligonucleotides (ODN) were purchased from Sigma-Genosys (Poole, UK).

2.1.2 Pipetting techniques

Preparation of solutions by mixing is a crucially important process to ensure results are repeatable and this starts with ensuring control over the volumes being mixed. Gilson Pipettes with 0.5-10 μ l (P10), 2-20 μ l (P20), 20-100 μ l (P100) and 200-1000 μ l (P1000) capacity were used for transferring of sample and solvents depending on the volumes being handled. All pipette tips and glassware was sterilized to remove nuclease contamination using an autoclave.

2.1.3 DNA preparation

Table 2.1 Oligonucleotides sequences for immobilisation and hybridisation

Name	Oligonucleotides sequences (5'-3') modified and non- modified	Gene categories	Application in project
5'- ?ssDNA [3AC7]	5'- ?CCTCCCTCAAAGCTACTA AACATGA[3AC7]* (desalted), 31.5 nmol	Aromatase (antisense)	Immobilisation Hybridisation
5'- ?ssDNA	5'- ?CCTCCCTCAAAGCTACTA AACATGA (desalted), 15.6 nmol	Aromatase (antisense)	
5'- ssDNA	5'- TCATGTTTAGTAGCTTTGA GGGAGG (desalted), 104.5 nmol	The complimentary oligonucleotide above	Immobilisation

*The 5' refers to the 5 prime end which is the start of an oligo sequence when placing an order, the 3' being the end of the sequence. ? is a Cy5 modification and [3AC7] was 3' amino C7 modification. (All purchased from Sigma-Genosys), ss refers to single strand.

There is distribution of 117 blast hits on the sequence with the risks to get fake signals to the hybridisation experiments.

The original oligonucleotides are supplied in a near solid form from Sigma-Genosys. They are mixed with autoclaved nuclease free water to the stock concentration which was determined by measuring absorbance at 257 nm using the NanoDrop spectrophotometer. Some of this stock was stored in about 20 aliquot for the experiments. All the stock of oligonucleotides was stored at -80 °C. The aliquots were stored at -20 °C. When doing the experiments, the aliquot were taken out from the freezer then left at laboratory temperature (typically 20°C) for 10 minutes. They were centrifuged for a few seconds to ensure the ODN fully collected at the bottom of the tube. After carefully open tube, they were diluted with autoclaved water to the

concentration desired to rehydrate for 2 minutes and mixed using a Vortex Genie mixer for 15 seconds at 3200rpm after mixing the tube by hand for a minute. Then re-centrifuge the solution and aliquot and/or store the ODN. The concentration was again determined using the NanoDrop and adjusted by dilution with the autoclaved water to be the same concentration for the experiments.

2.1.4 Quantification of DNA

Two requirements for printing of DNA are to establish its presence and whether processing has caused any damage reflected in its survival. These need to be measured and spectrophotometry may be adapted for this purpose.

In this work, substrate choice will be an important consideration and spectrophotometry will also be used to explore and understand the presence and immobilisation of DNA onto this substrate. In the hybridisation study, the engagement between the DNA pairs needs to be explored, leading to the optimised parameter investigations for hybridisation.

DNA concentration measurement in connection with printing is to understand whether the DNA can survive the stresses that are imposed during the processing steps. Thus, concentration measurement is required in preparing the DNA as an ink and following its deposition.

In the liquid ink phase, concentration was measured using a Thermo Scientific NanoDropTM 1000 Spectrophotometer that is capable of measuring 1µl samples with high accuracy and reproducibility. It was chosen since it is capable of measuring the full spectrum (220nm-750nm). The NanoDrop 1000 Spectrophotometer also has the capability to measure highly concentrated samples without dilution (50 × higher concentrations than the samples measured by a standard cuvette spectrophotometer). For nucleic acid quantification, the Beer-Lambert equation is modified to use an extinction coefficient with units of ng-cm/ml. Using this extinction coefficient gives a manipulated equation:

$$c = (A \times e) / b$$

Where c is the nucleic acid concentration in ng/µl, A is the absorbance in AU, e is the wavelength-dependent extinction coefficient in ng-cm/µl and b is the path length

in cm. The generally accepted extinction coefficient, ϵ , for single-stranded DNA is 33 ng-cm/ul.

The sequence for using the Nandrop is shown in **Figure 2.1** and in conducting the experiments the technique shown was followed consistently.

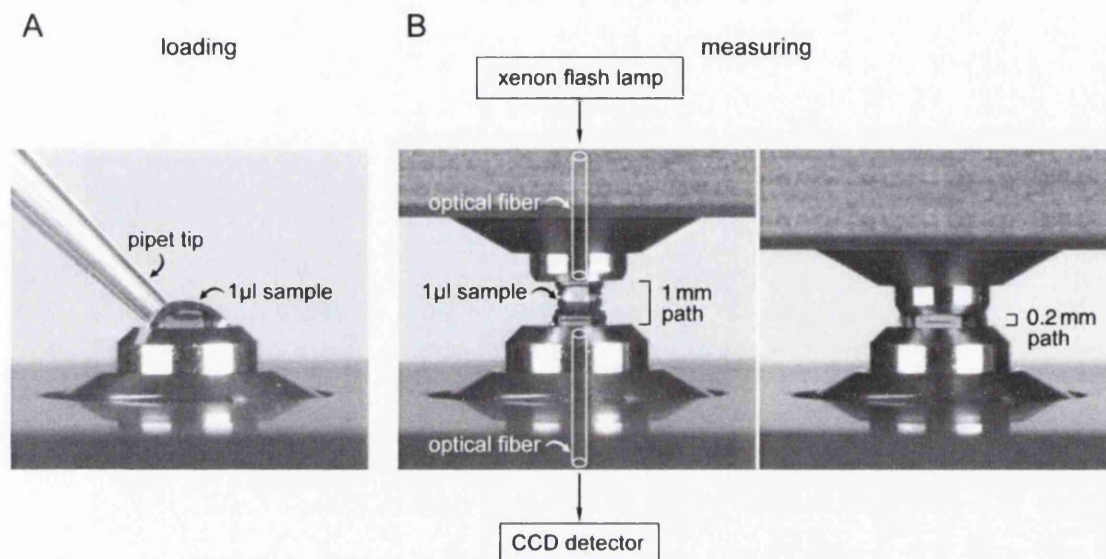


Figure 2.1 The NanoDrop ND-1000 Spectrophotometer microvolume sample retention system

(A) A sample volume of 1 µl is dispensed onto the lower optical surface. (B) Once the instrument lever arm is lowered, the upper optical surface engages with the sample, forming a liquid column with the path length defined by the gap between the two optical surfaces. During each measurement, the sample is assessed at both a 1 mm and 0.2 mm path, providing a large dynamic range of nucleic acid detection.

The equipment specification is itemised in **Table 2.2** and repeated measurements on oligonucleotides diluted with autoclaved water gave results consistency within $\pm 2\%$. The upper and lower optical surfaces were cleaned completely using autoclaved water between sample characterisation.

Table 2.2 Specification of NanoDrop ND-1000

Detector type	2048-element linear silicon CCD array
Wavelength range	220-750 nm
Wavelength accuracy	1 nm
Wavelength resolution	3 nm (FWHM at Hg 546 nm)
Absorbance precision	0.003 absorbance (1mm path)
Absorbance accuracy	2% (at 0.76 absorbance at 257 nm)
Absorbance range	0.02-75 (10 mm equivalent absorbance)
Detection limit	2 ng/ μ l (dsDNA)
Maximum concentration	3700 ng/ μ l (dsDNA)
Measurement cycle time	10 seconds
Sample pedestal material of construction	303 stainless steel and quartz fibre

The ODN ink was specified to be the ODN diluted in the CTAB aqueous solutions that will be described in 2.2.1 with the different concentrations chosen depending on the experiment purpose. Where deviations occur, this will be explained in the relevant section. A serial method was used for making dilutions of the ODN to 0.1 μ M, 0.01 μ M, etc. to 10⁻¹² μ M in autoclaved water solution and this will be described in 3.4.1.

2.1.5 Molecular structures of oligonucleotides and oligonucleotides with NH₂ and Cy5

The structure of 25 bases oligonucleotides needs to be considered with respect to the mechanisms of immobilisation, including CTAB and the polymer surfaces together with (or without) the fluorescent dye (Cy5).

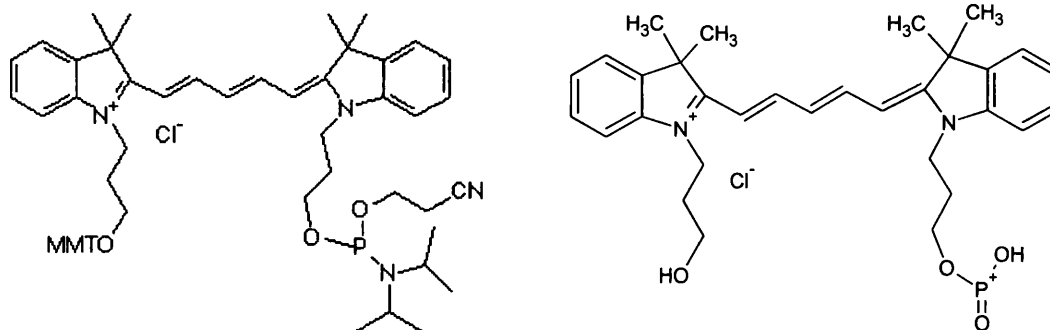


Figure 2.2 Cy5 phosphoramidite before and after the deprotection of Cy5

The Cy5 is a fluorescent dye of the cyanine dye family. It was synthesised with the reactive groups and covalent bonded to the ODN molecules. ODN labelling has been done using Cy5 for visualisation and quantification purposes for a wide variety of biological applications including comparative genomic hybridisation and in the gene microarray. This structure shows the functional group to link with ODN and possibly with others reagents. This structure illustrates the architecture that will be used to explain the ODN immobilisation mechanisms on the substrates that will be presented in Chapter 3.

Figure 2.3 shows the structure of the 3AC7 which the modified -NH₂ group on the ODN. The ODN with -NH₂ in Chapter 3 is the Probe 2. The ODN without -NH₂ is the Probe 1. The Probe 2 is used for investigating the different immobilisation mechanism of the ODN on the polymer substrate in Chapter 3. The probe 1 and probe 2 are the ODN with the Cy5 dye shown in **Figure 2.2**.

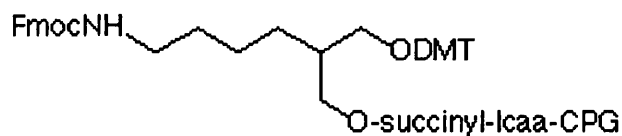
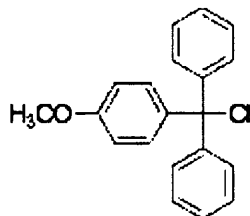
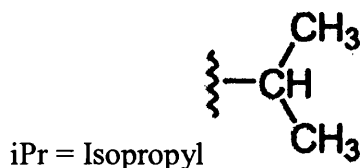


Figure 2.3 Chemical structure of 3AC7

CPG = Controlled Pore Glass

DMT = 4, 4'-Dimethoxytrityl

Fmoc = Fluorenylmethoxycarbonyl



MMT = 4-Monomethoxytrityl

C7 referred to the length of the branched carbon chain. Chain extension occurs by removal of the DMT group by acid, leaving an active -OH group.

Fmoc was the protecting group for the amino group, removed during ammonia cleavage.

Succinyl-lcca-cpg also was removed by ammonia, leaving a free -OH group.

This was the modification applied to the ODN by amino group which was chemically synthesized with the functional groups to covalently bond to the ODN molecules forming protective groups at both ends. This structure has been shown to illustrate the details of 3AC7 on the ODN molecules to support the further investigations on the ODN immobilisations mechanisms that will be presented in Chapter 3.

2.2 General solvent preparation

Most biological processes in the cell take place in a water-based environment. Water is an amphoteric substance; that is, it may serve as a proton donor (acid) or a proton acceptor (base). The autoclaved water was the basic solvent for the ODN because of its simplicity for making the ODN ink.

The experiments required many solvents such as CTAB to be the reagents of ODN immobilisation, TNT buffer for rinsing, various buffer for hybridisation and rinsing buffer for hybridisation experiments. Their preparations will be summarised in the following sections.

2.2.1 Surfactant

The preparation of these solvents and buffer solution is set out in the following paragraphs,

1mM Cetyl Trimethyl Ammonium Bromide (CTAB) ((C₁₆H₃₃) N (CH₃)₃Br, cetyltrimethylammonium bromide, hexadecyltrimethylammonium bromide or palmityltrimethylammonium bromide) aqueous solution was purchased from Sigma-Aldrich. Different concentrations were achieved through dilution using autoclaved water and this was used as the oligonucleotide solvent.

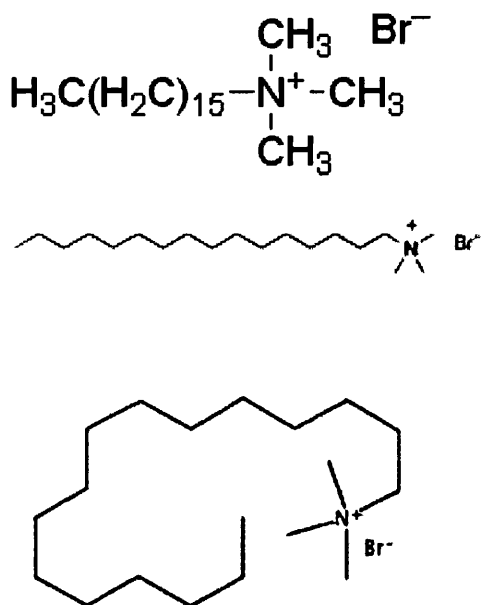


Figure 2.4 Different chemical structure of CTAB

The CTAB had two functions in this project. Firstly, it made the ODN ink to do the immobilisation reaction on the optimized substrate. Secondly, it adjusted the surface tension of the ODN ink for making the ink suite the printing technologies like inkjet, flexography and gravure printing while noting the limitation on concentration dilutions. These two functions of CTAB made the ODN ink need to balance the process of ODN immobilisation reaction on the substrate and the printability adjustment of surface tension and viscosity for the various printing technologies. Further discussion will be presented in Chapter 3 and Chapter 4.

With regard to ODN molecule immobilisation, the CTAB has a long chain structure that interacts with the ODN molecules in the aqueous form through their positively charged molecules. It was the one reagent that facilitated the ODN ink immobilisation reaction on the final substrate choice. The detail explanation and discussion will be set out in Chapter 3. Practically, the solvent is autoclaved water to

dissolve the ODN and CTAB. Their concentration is controlled by diluting with autoclaved water to the concentrations needed. Then, the required amount of ODN aqueous solution is mixed with the fixed concentration of CTAB

For adjusting the ODN ink surface tension, the CTAB is a surfactant to decrease the surface tension of the ODN ink to make it wet the various substrates.

The following presents a characterisation of the CTAB molecule. It is one of the components of the topical antiseptic cetrimide. The cetrimonium (or hexadecyltrimethylammonium) cation is an effective antiseptic agent against bacteria and fungi. It is a cationic surfactant. Its uses include providing a buffer solution for the extraction of DNA.

As any surfactant, it forms micelles in aqueous solutions. At 303 K (30 °C) it forms micelles with aggregation number 75-120 (depending on method of determination, usually average ~95) and degree of ionization α (fractional charge) 0.2 - 0.1 (from low to high concentration). The standard constant of Br^- counter ion binding to the micelle at 303 K (30 °C) is $K^\circ \approx 400$. This value is calculated from Br^- and CTA^+ ion selective electrode measurements and conductometry data by using literature data for micelle size ($r = \sim 3$ nm), extrapolated to the critical micelle concentration. However, it varies with total surfactant concentration so it is extrapolated to the point at which the concentration of micelles is zero). In colloidal and surface chemistry, the critical micelle concentration (CMC) is defined as the concentration of surfactants above which micelles form and almost all additional surfactants added to the system go to micelles [Mcnaught 1997].

The CMC is an important characteristic of a surfactant. Before reaching the CMC, the surface tension changes strongly with the concentration of the surfactant. After reaching the CMC, the surface tensions remains relatively constant or changes with a lower slope. The value of the CMC for a given dispersant in a given medium depends on temperature, pressure, and (sometimes strongly) on the presence and concentration of other surface active substances and electrolytes. Micelles only form above critical micelle temperature.

The CTAB aqueous solution in this project was made in the way as follows:

1mM CTAB can be diluted to 0.01, 0.05, 0.1, 0.15, 0.2, 0.4, 0.6, 0.8mM with autoclaved water using the Gilson Pipettes. For instance, for making 10ml 0.1mM CTAB solution, 100 μl of the original 1mM CTAB is mixed using the Vortex Genie

mixer in 10 ml autoclaved water. This was stabilized for one hour to defoam the solution and sterilized by using a Millex filter unit. The oligonucleotide was dissolved in 0.1mM CTAB to make different concentration oligonucleotide solutions in CTAB. The stock of original CTAB was stored in a centrifuge tube (50ml, sterilized polypropylene transport tube) at room temperature. The aliquots with the different concentration were stored in 5-10ml snap-cap centrifuge tubes.

2.2.2 Buffer

Biochemical processes occurring in cells and tissues depend on strict regulation of the hydrogen ion concentration. Biological pH is maintained at a constant value by natural buffers. When biological processes are studied *in vitro*, artificial media must be prepared that mimic the cell's natural environment. Because of the dependence of biochemical reactions on pH, the accurate determination of hydrogen ion concentration has always been of major interest.

Buffer ions are used to maintain solutions at constant pH values. The selection of a buffer for use in the investigation of biochemical processes is of critical importance.

Virtually all biochemical investigations must be carried out in buffered aqueous solutions. The natural environment of biomolecules and cellular organelles is under strict pH control. When these components are extracted from cells, they are most stable if maintained in their normal pH range of 6 to 8. An artificial buffer system is found to be the best substitute for the natural cell milieu. It should also be recognised that many biochemical processes (especially some enzyme processes) produce or consume hydrogen ions. The buffer system neutralizes these solutions and maintains a constant chemical environment.

Within this work, the main application of buffers will be in rinsing in Chapter 3, 4 and 5 and for hybridisation in Chapter 5. The buffer solutions concerned include TNT buffer which is used as the washing buffer in Chapter 3 and Chapter 4, in Chapter 5 the hybridisation buffer (Church buffer, SSC buffer and PCR buffer), the washing buffer (PCR buffer, TNT buffer, Tris buffer, SSC buffer, Church buffer, 1% SDS buffer and sodium phosphate buffer).

The TNT buffer as the washing buffer in Chapter 3 and Chapter 4 is described as followed. TNT, Tris HCl (Tris-hydroxymethyl) aminomethane hydrochloride,

$\text{H}_2\text{NC}(\text{CH}_2\text{OH})_3\cdot\text{HCl}$), Sodium Chloride and Tween 20, all of which were purchased from Sigma-Aldrich.

Tween 20 is a non-ionic detergent that which minimizes non-specific fluorescence background on the substrates [Redon, 2009]. It was part of the rinsing TNT buffer to offer the non-specific immobilisation of ODN ink on the substrates. The TNT buffer comprises 10mM Tris-HCl, pH 7.5, 150mM NaCl and 0.05% Tween 20. This was prepared by taking Tris-HCl powder (0.16g, measured on a digital balance scale with 0.1 gram accuracy) and dissolving it in autoclaved water (100ml) held in a Erlenmeyer flask or conical flask having 250ml capacity. This was mixed on a magnetic stirrer fitted with a 3cm stir bar running at 500-600 rpm for 4 hours. A similar measurement procedure was used for preparing the Sodium Chloride solution, but this was shaken manually. Mixing the Tris-HCl and NaCl solutions together was accomplished by using an Erlenmeyer flask having 1000ml capacity on the magnetic stirrer run at 500-600rpm for ten minutes. The Tween 20 (0.05ml of a viscous liquid) (measured by Gilson pipette in reverse mode) was added into the mixer solution and mixed for a further 30 minutes on the magnetic mixer. Adjustment of the pH to 7.5 was by adding NaOH and HCl together with autoclaved water to make 400ml total volume as a stock of washing buffer solution.

The PCR buffer was purchased from Promega (Southampton, UK) (1×PCR buffer diluted from 15× used for hybridisation buffer, preparation followed the procedure provided as a document with the product).

The Tris buffer (pH 7.6) recipe is described in [Maniatis et al. 1982].

The SSC (Saline Sodium Citrate) buffer (pH 7.0) was purchased from Promega (Southampton, UK) (1×SSC buffer diluted from 20× used for hybridisation buffer, preparation followed the procedure provided as a document with the product) and was also used as a washing buffer.

The Church buffer is (pH 7.2) preparation followed the protocol that is set out fully in [Church and Gilber 1984] with components purchased from Sigma-Aldrich.

The SDS (Sodium Dodecyl Sulfate) (1%, pH 7.2) is an anionic surfactant that is used in many cleaning and hygiene products. It is a highly effective surfactant and is used

in any task requiring the removal of oily stains and residues. Its recipe is described in [Kim 2002].

The Sodium phosphate buffer (pH 8.0) preparation followed the protocol described in [Institute of Molecular Development LLC 2001]. Both Na_2HPO_4 and NaH_2PO_4 were purchased from Sigma-Aldrich.

From the literature [Covington, 1985], pH is defined and measured in the traditional way. The electrode was removed from the storage solution rinsed with distilled water and dried gently. It was then immersed in the test solution and the pH recorded. The time of immersion was typically 2 minutes and the depth of immersion below 20 mm. The consistency of measurement was found to stay in the range of relative accuracy. The equipment used was a pH meter METTLER TOLEDO S-20K that has a pH measurement range from 0.00 to 14.00. Its resolution is 0.01 in pH and the relative accuracy is ± 0.01 .

A measurement of pH is susceptible to experimental errors. Some common problems are the sodium error, concentration effects and temperature effects. The sodium error is caused by the influence of glass combination electrodes. The sodium error can become quite significant at high pH values (e.g. pH 12.5), where 0.1 N Na^+ may decrease the measured pH by 0.4 to 0.5. Concentration and temperature effects reflect the solution property and have no impact on the measurement method and accuracy.

2.3 Substrate preparation

A range of substrates may be used for printing DNA, such as glass, silicon, gold coated surfaces and polymeric systems. In this work a range of uncoated and coated polymers were used as itemised in **Table 3.1**. The substrate surface needs to be nuclease free. This was achieved by washing in ethanol (70%, volume concentration) and autoclaved water to clear away all dust, then it was put in an UV chamber for 10 minutes to kill any possible nuclease remaining on the polymer surface. Any surface contamination will degrade the oligonucleotide with a consequent impact on immobilisation. Substrate sheets were then cut into small squares as this made it easier to print on with several spot immobilisation or hybridisation experiments to do

at the same time. Tweezers were used to handle the samples at the edge of substrates throughout to reduce the nuclease contaminations.

2.4 Measurement and analysis of the printed image

2.4.1 Scanning the FI signals of the ODN

The Oligonucleotides were labelled using the dye Cy5 which provides a fluorescent signal after they have been scanned using a laser beam with the wavelength at 633nm. Cy5 is excited maximally at 649 nm and emits maximally at 670 nm. The scanners actually use different laser emission wavelengths (typically 635 nm) and filter wavelengths (655-695 nm) to avoid background contamination. Cy5 labels were used for the detection because the selection of optimal operation conditions to reduce the substrates intrinsic fluorescence background is essential [Liu and Rauch 2003]. The FI was processed to show the difference of concentration of sample on the surface after binding on the polymers surface. The measurement was performed using a GeneTAC LS IV.

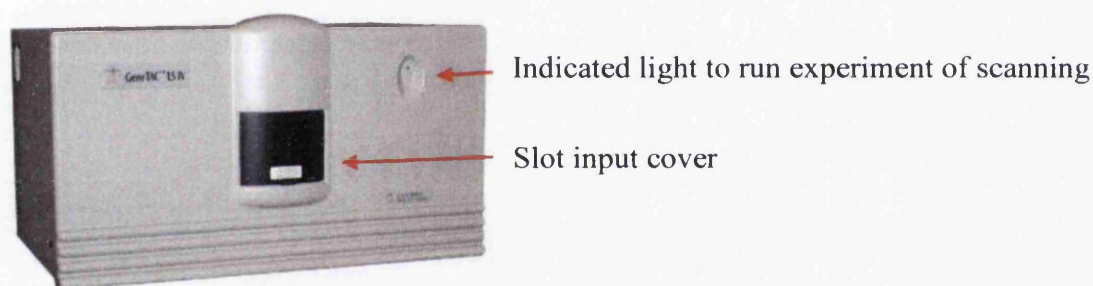


Figure 2.5 Controls 1-PMT 2-laser GeneTAC LS IV scanner

It combines a laser-beam source, dark-field imaging, sequential scanning, and photo multiplier tube (PMT) detection. In the dark-field approach, the laser beam is angled so that the backscattered light cannot reach the PMT, which improves the contrast and the signal sensitivity. The GeneTAC LS IV optical design uses a proprietary oblique illumination light path (dark-field illumination) so that excitation light does not enter the collection optics. Custom designed band-pass filter pairs block excitation with an efficiency greater than one in ten billion (OD10) for all wavelengths. This ensures that any light scattered from the surface of the biochip cannot be detected unless its wavelength has been changed by a fluorescence event. This gives the LS IV exceptional tolerance of sample thickness, flatness, roughness

and opacity. As a drawback, these technologies yield images that are dimmer than those projected in other scanners, so the images require longer exposure to the laser. However, the improved side-window PMT system compensates by preventing photo bleaching. In addition, the system has an increased focal depth of approximate 500 μ m. Thus, there is no variability resulting from uneven slide surfaces.

Lasers typically have 0.5% of high frequency output noise, and 0.5 – 1.0% long-term power stability noise. As a laser is swept across the sample, the amount of light deposited is varied by this amount. Unless the beam is concentrated into a sub-micron area to saturate the fluorophore, this will result in a corresponding variation in fluorescence output. To compensate for this, each pixel can be sampled many times by re-scanning the sample frame by frame or line by line. However the LSIV PMT is typically only run at 20-50% of full range. Fluorescent intensities (FI) were tested for the analysis of the ODN with Cy5 fluorescent dye.

All ODN on the polymer surface was freshly made and scanned once to make the fluorescent constant without photo bleaching and resist the contaminations by environment. The laser power in the GeneTAC LS IV was spread over a 20 μ m spot, and so the energy density experienced by the fluorophore was 300 times lower than a confocal system, but the dwell time was 20 times higher. This allows the GeneTAC LS IV to use much more powerful lasers without risking bleach damage or thermal degradation to the target molecule. The GeneTAC LS IV does not use confocal optics because they impede the ability to collect reproducible results. Slide thickness, flatness or placement does not affect the results on an LS IV as long as all spots fall within a 500 μ m depth range. Dust can accumulate on the charged surface of a biochip.

The fluorescent images taken from the GeneTAC LS IV Software Version 3.0 need adjustment of the PMT gain and black parameters to get the optimise image to scan and data to be saved for GeneTAC Integrator Microarray Analysis Software. The purpose of ODN fluorescent imaging in Chapter 3 is to prove the different fluorescent intensities of ODN on the same substrate before and after the washing process. So the different gain parameters must not affect the fluorescent data analysis when comparing the fluorescent data before and after the washing processing of

ODN on the same substrates. Settings on gain and black need be fixed to compare the different data after scanning. So the only comparable data shall be the spots on the same slides. If the sample has a high background signal, the dynamic range can be improved by increasing the Black value until the dimmest part of the sample is just above zero (dark purple/gray on the Spectral palette). Black values can also be set so the dimmest pixels fall below the data collection range. This produces good looking images, but because the data range is cropped, such images should not be used for quantification. General settings for getting the comparable and high repetitive data on the same substrates are set out next.

Imaging characteristics are field size (24.4×65.2 mm), resolution and zoom (100 μm), zoom (1.0) and distance (25%). With the setting parameters (Cy5 dye, red laser and 675BP filter. Gain 28.3, Black 0), the previewing scan will rapidly scan the whole slide area, with a resolution of 50 microns. Then with satisfactory scan parameters, most data will be collected with the same settings in case of the better images in the different settings. This will give the different FI comparison with Image J of the same images.

Figure 2.6 is an example of ODN image with different gain and black PMT parameters taken from the analysis software described in **2.4.2.1**.

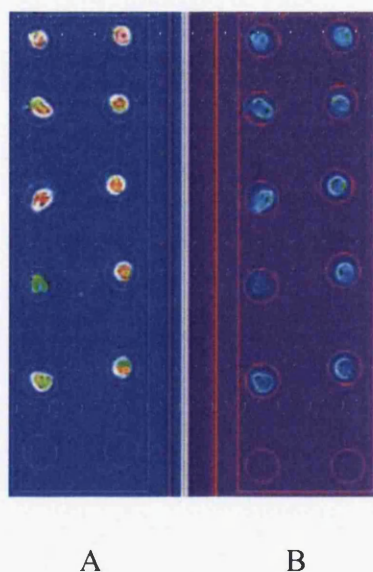


Figure 2.6 The fluorescent images comparison of the probe 1 on the PS with the different PMT gain and black parameters

(A) it was scanned with gain 30.3, black 0, (B) it was scanned with gain 25.7, black 0.

The image below shows an example of the original image of oligonucleotides on the PS (Polystyrene) obtained by the GeneTAC LS IV scanner. The probe 1 is described in 3.2.1.

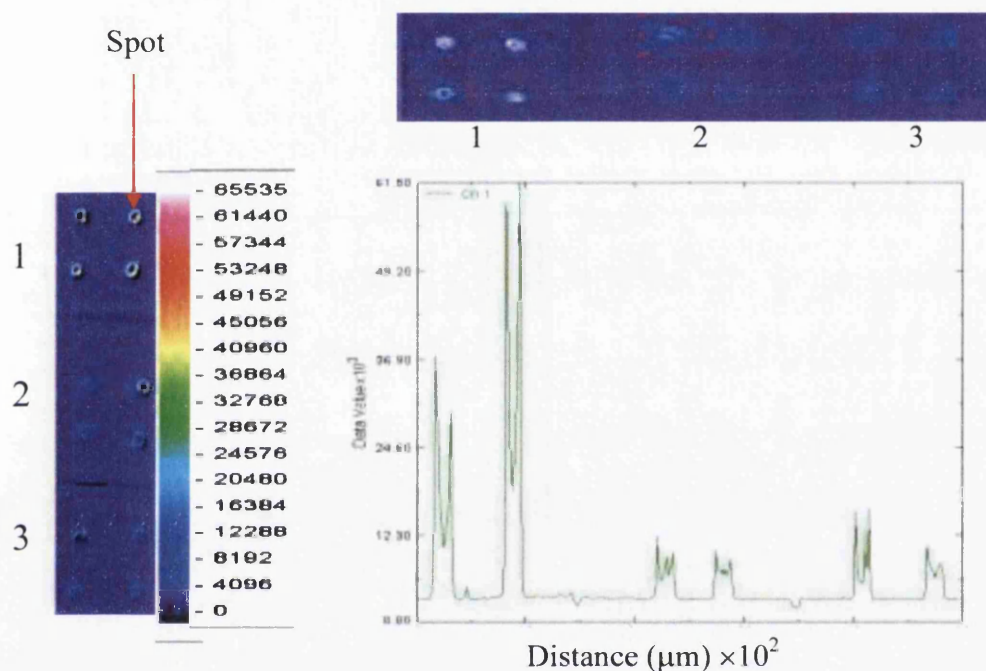


Figure 2.7 The FI (Fluorescent Intensity) signals of the probe 1 ink ($30 \times 10^{-2} \mu\text{M}$) on the PS and line query across the spots to show the conditions of the probe 1 ink on the PS

Figure 2.7 shows an image with analysis by the GeneTAC LS IV Software Version 3.0. It showed the fluorescent images and intensity values for the different spots of the control probe 2. The colour can be changed from the Cy5 red to the spectrum which showed the different saturated state of contours. The left image shows three pieces of the PS. The top picture shows the fluorescent image of the control probe 1. The spots on it illustrate the significant bright colours with the number on the right hand of it which showed the FI. The numbers are equal to the first two peaks on the line graph. The middle and lower pictures are the fluorescent images of the immobilized probe 1 which showed the lower FI signals with the same comparison of peaks in the line graph with the middle two peaks and right two peaks. This figure

shows that the analysis by this software cannot give the comparable data instead of the graph only which is weaker to analyse than the methods in 2.4.2.

2.4.2 Analysis of the FI signals images

Two analysis methods of fluorescent images were used in this project.

The ODN immobilisation pattern in Chapter 3 and Chapter 5 was determined by the pattern achievable from the GeneTAC Integrator Microarray Analysis Software (Version 3.3.0) that determines the spot size and distance between spots. The fluorescent images taken and analysed in Chapter 5 were processed by Image J [Abramoff, 2004]. In this work, Image J was used because it provides the flexible tools to do FI analysis for the different printed image patterns other than the spots.

2.4.2.1 Analysis by the GeneTAC integrator microarray analysis software

The GeneTAC Integrator Microarray Analysis Software (Version 3.3.0) for the image and data processing needs to be set up to establish the target average parameter settings to facilitate data comparison.

Given a grid of spots, the procedure to scan the spots using the GeneTAC LS IV is as follows with reference to the spot identification and size.

The spot diameter was selected at 4016 μm and the alignment tolerance: chosen was 1205 μm . The fluorescence intensities from each spot on the array were measured as “target average”, which was the sum of all pixels contained within the spot size.

The sample images of the non-rinsed ODN on the polymer surface after immobilisation showed four pieces of information as follows: the location of spots; the ODN fluorescent signal intensity; the background noise of the substrate and the concentration of oligonucleotides by the intensity of spots. **Figure 2.9** shows a typical example.



Figure 2.8 The fluorescent images of the control and immobilized probe 1 ink ($30 \times 10^{-2} \mu\text{M}$) on the CCP

The background fluorescent noise limits the substrate choice. The polymer substrate must be transparent to give the lowest background noise. Every spot on the polymer substrates surface shows one immobilisation experiment. So the fluorescent images of the different spots shows the comparisons of the immobilisation efficiencies in a statistical manner **Figure 2.8** shows 12 spots on the polymer substrates surfaces.

They were measured and the results treated statistically as shown in **Figure 2.9**. The immobilized and control probe definitions shown in **3.3.4**. Firstly, the FI signals are reported to the individual spots on each slide. Then the average FI is calculated to make the bar in **Figure 2.9**. The error bar shows the FI signals difference between the actual individual spots and average data. The FI signals in different individual spots show a little change which is caused by the manual deposition techniques shown in **3.3.3** and effects of the atmosphere of immobilisation reaction in the chamber. The error bars given are good enough to see the difference between the immobilized and control probe 1 on the CCP described in **Table 3.2**.

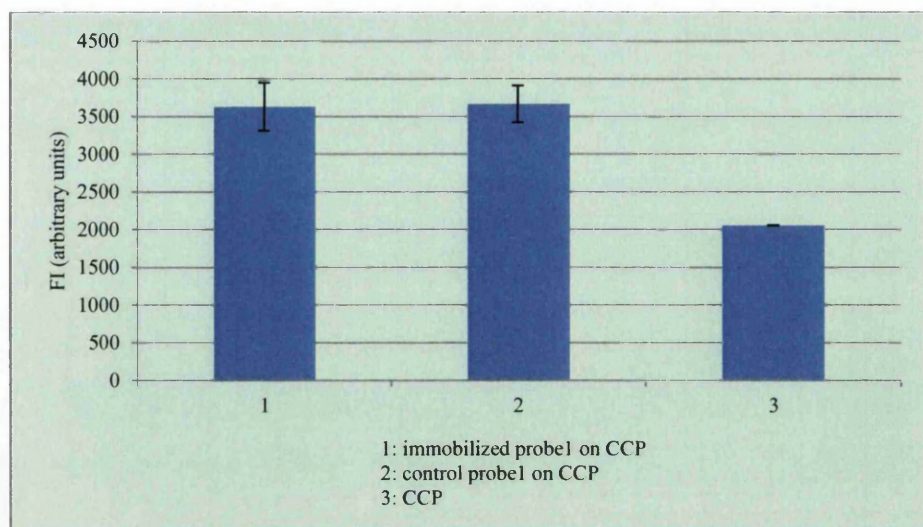


Figure 2.9 The FI signals of the probe 1 ink and background on the CCP

These data show the analysis of the depositing 12 probe 1 ink spots on the substrates with each spot relevant to one reaction. These are independent of the gain or black setting because the same ODN spots are analysed on the substrates. The error bars are the standard deviation.

2.4.2.2 Analysis by Image J software

The other analysed software was Image J (Image Processing and Analysis in Java) and is a public domain, Java-based image processing program developed at the National Institutes of Health [Collins 2007] and analyse the special pattern of printed fluorescent ODN. The Image J analysis could be applied to the different patterns of images rather than spots. The spots pattern images could be analysed by Image J, but the steps required to set up the areas to measure and analyse are less straight forward and the advantages of automation are preferred as set out in 2.4.2.1. The data of the FI mean of the CCP cannot be comparable because the scanning setting by GeneTAC LSIV described in 2.4.1 is adjusted to get the better fluorescent images. Then the dynamic range of the scanned fluorescent images changed with the settings to give the different data for the substrate FI mean. The analysis included the background signals. The FI signals vary depending on the area chosen so the analysis was conducted to compare the same experiments with the same size area on the CCP.

The samples of typical analysis by Image J are illustrated as follows in **Figure 2.10**.

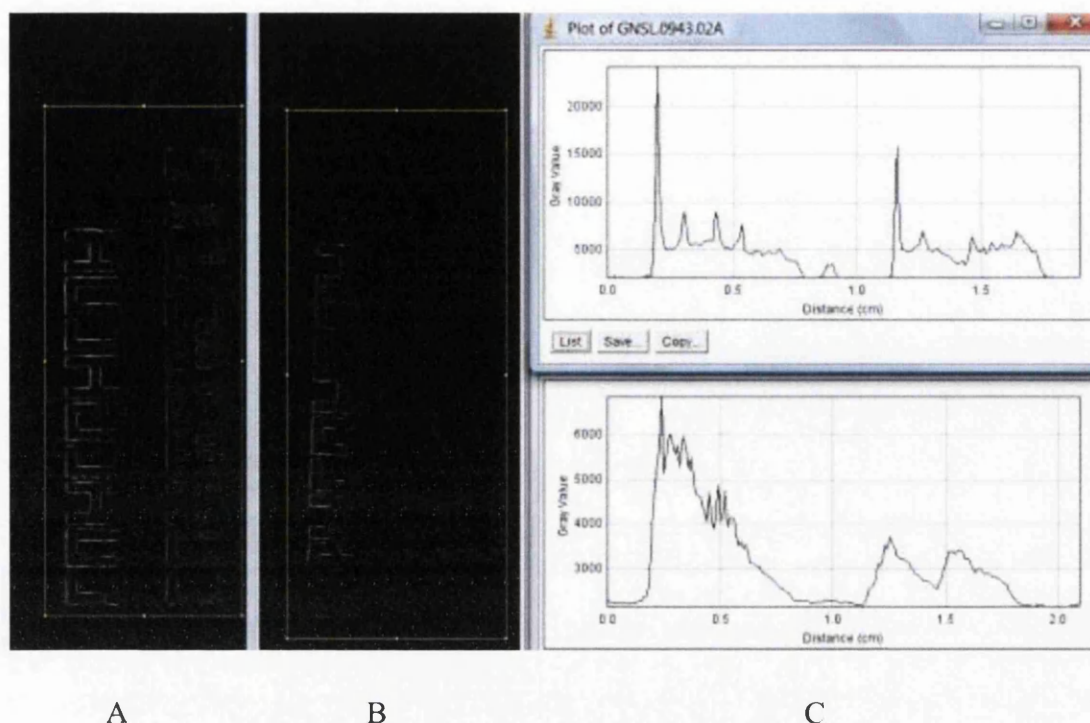


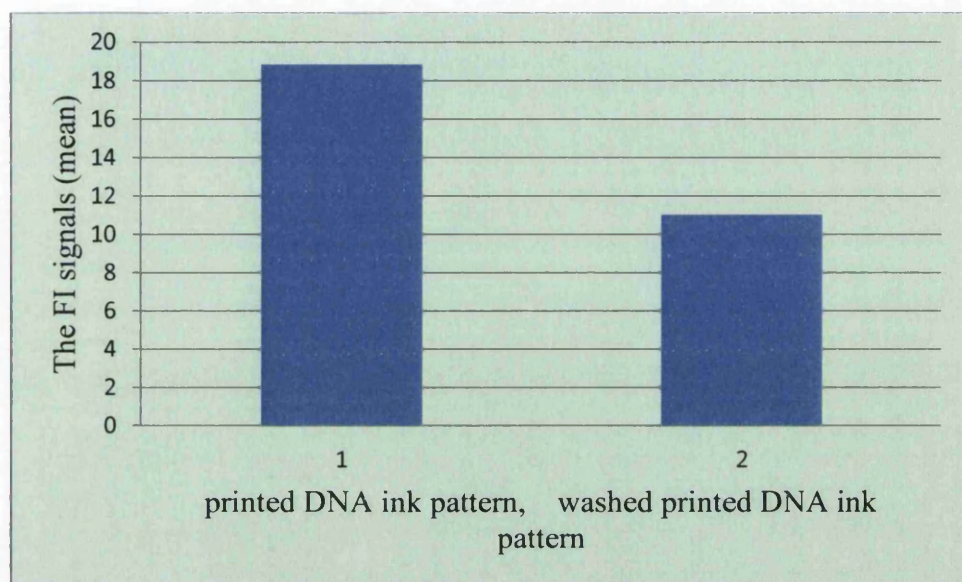
Figure 2.10 The FI plot signals (analysed by Image J) of the ODN ink

(A: the control ODN; B: the immobilized ODN) on the optimal substrate by inkjet printing

In **Figure 2.10**, the rectangle was chosen to pick the area to analyse. The Plot Profile could be chosen to analyse the image as a graph comparison. The quantitative comparison by the data of mean can also be extracted as shown in the **Figure 2.11**.

	Area	Mean	StdDev	Min	Max	IntDen	RawIntDen
1	6020	18.835	27.746	8	255	113388	113388
2	6020	11.037	6.912	8	127	66442	66442

A



B

Figure 2.11 The FI data signals (analysed by Image J) of the ODN ink

(A: the image of inkjet printed and washed pattern ODN and FI signals mean; B: the FI signals (mean) graph of A)

The Image J software can analyse the different pattern image but the GeneTAC Integrator Microarray Analysis Software (Version 3.3.0) is designed to analyze the DNA chip with a circle which is used to choose the different area of ODN spots. The Image J can be used to analyse the same image which GeneTAC Integrator Microarray Analysis Software (Version 3.3.0) can analysis not vice versa. The **Figure 2.12** shows the analysed results from both software.

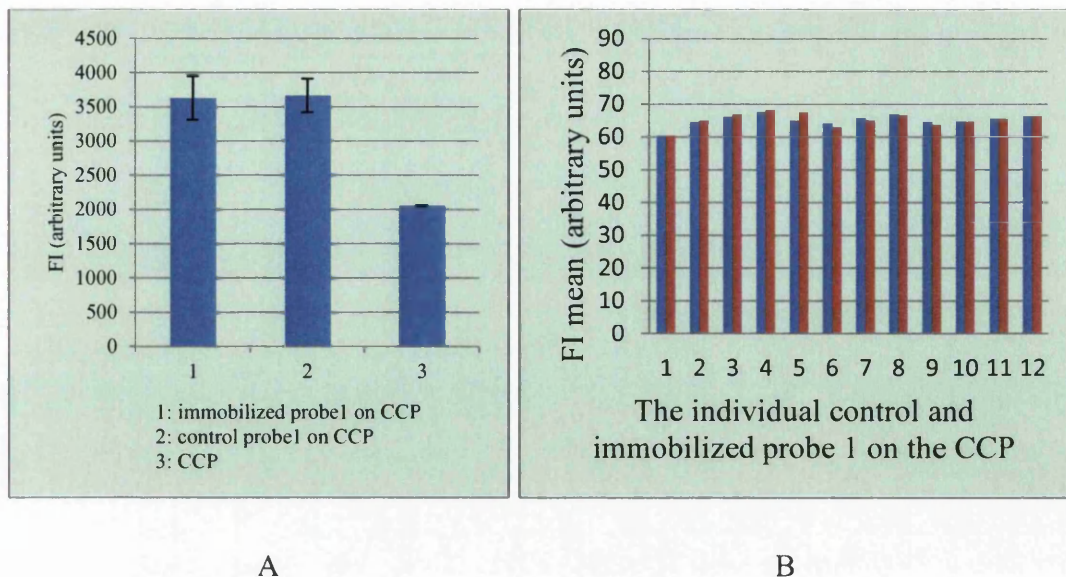


Figure 2.12 The comparison of the FI signals of the same fluorescent image analysed by both analysing softwares

A: the FI average analysed by GeneTAC Integrator Microarray Analysis Software (Version 3.3.0); B: the FI mean analysed by Image J software.

In **Figure 2.12 B**, the blue bars give the FI mean of control probe 1 on the CCP in **Figure 2.8 A** and the red bars show the FI mean of immobilized probe 1 on the CCP in **Figure 2.8 B**. The area size chosen to analysis is 506.

2.5 Oligonucleotides ink characterisation

The printing process needs the characteristics of the biological ink to make it printable with the current printing technology. This section describes the instrumentation used to measure the ink characteristics. The flow properties of the ink were measured using a rheometer and the relative surface tension of the inks was measured using a dynamic contact angle measurement instrument.

2.5.1 Rheological measurements

2.5.1.1 Introduction

The majority of polymeric fluids tend to fall into the non-Newtonian category. However, the ODN solutions in lower concentrations show Newtonian behaviour.



Figure 2.13 Bohlin Gemini 200 HR Nano Rheometer

The rheological characterisation of the DNA ink was conducted using a Bohlin Gemini HR Nano Rheometer as shown in **Figure 2.13**. It is a high performance, modular rheometer system designed to provide accurate rheological measurements on a wide variety of materials. Its adaptive control technology is optimized for both stress controlled and strain controlled operations in steady, dynamic and transient modes. For this work, the Bohlin rheometer enables the measurement and control of nano-torque levels to probe sensitive or weak material structures. In this case, the DNA is considered to be a low viscosity biopolymer ink, leading to a working torque range from 3 nNm to 200 mNm. The high resolution continuous torque mapping system designed into the Bohlin allows low torques to be set with high accuracy.

The specifications of this rheometer are itemised in **Table 2.3**.

Table 2.3 Malvern Bohlin Gemini rheometer specifications

Torque range	10 nNm – 200 mNm, controlled stress/rate viscometry. 3 nNm – 200 mNm, controlled stress/strain oscillation.
Torque resolution	Better than 1 nNm
Position resolution	50 nano radians
Frequency range	1 micro Hz to 150 Hz
Controlled speed rage	0.01 mili rad/sec – 600 rad/sec
Measurable speed range	10 nano rad/sec – 600 rad/sec
Normal force NI measurement range	0.001 N – 20 N
Step change in strain	< 10 ms
Temperature range	- 150°C – 550 °C

In conducting the test, the sample was loaded carefully on the centre of the lower plate and the gap was properly filled. A bubble could be formed when filling the DNA ink with the pipette. This was caused by the CTAB as surfactant in the DNA ink. This can be fixed by reduction of the air bubble by the pipette. Given its Newtonian nature, the loading of ink samples and tests was straight forward to complete and no special procedures are necessary to undertake this measurement.

2.5.2 Surface Energy Measurement

The relative surface tension of the DNA solution was measured using a Fibro DAT 1100 (Fibro System AB, Sweden) dynamic absorption and contact angle tester at ambient temperature,

Figure 2.14 The instrument consists of a syringe containing the test liquid, tubing through which the liquid is passed, a cannula through which the drop is delivered to the test chamber, a CCD camera to monitor the change in dot profile and a testing block to capture the drop after detachment.

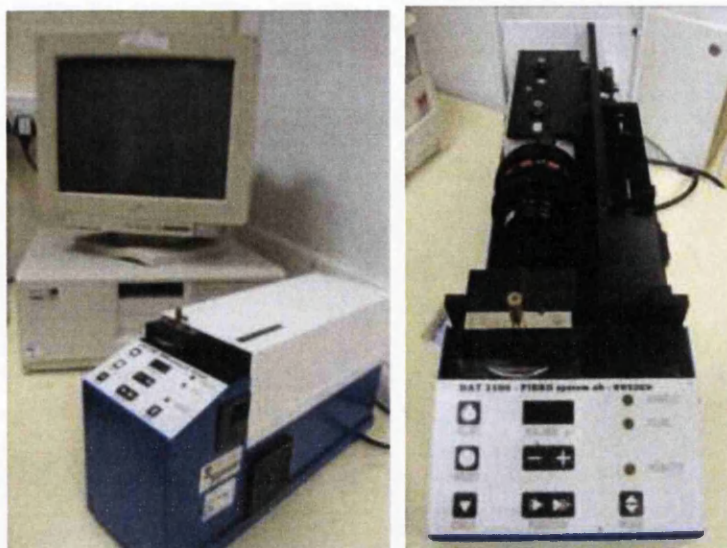


Figure 2.14 Fibro DAT 1100 tester

Prior to testing, the syringe and almost the whole of the tubing were filled up with the DNA ink and placed in the holder. Before the tubing was connected to the syringe, the air bubbles were removed by tapping. The pendant drop mode was the most widely used simple static method for measuring the interfacial tension and surface tension of a variety of fluids with established accuracy and reliability.

Another common method of surface tension measurement is sessile drop mode where a sitting drop is utilised instead of a hanging drop. However, in this work the pendant drop mode was used because it is more accurate than the sessile drop mode because the assumption of axial symmetry is easier to satisfy. The sessile drop mode is normally used when the test materials do not form a pendant drop readily.

2.6 Printing technology

The project will explore a range of printing technologies to deposit DNA onto a flexible substrate. This includes ink jet technology as well as flexography and rotogravure. The latter are attractive since they have the potential to manufacture medical devices at high volume and low cost.

2.6.1 Ink Jet Print

The inkjet printer used to print the aqueous DNA solutions was a Dimatix materials printer DMP-2800 series, **Figure 2.15**. This printer operates a drop-on-demand process where the print head is controlled by software to move to the desired position before jetting ink droplets. This high precision digital system is capable of depositing

micro-droplets of functional fluids, including nanoparticle-based metallic and organic materials, for printing feature sizes or line widths as small as 50 microns on any flat substrate, utilising a disposable piezo-inkjet cartridge. The jettable fluid viscosity range is 2 to 30mPa.s. Ideally, the fluid should have a viscosity of 10mPa.s and a surface tension of about 30mN/m (DMP-2800 Jettable Fluid Formulation Guidelines). The particles should not aggregate or settle.

One of the key features of this printer is that the characteristics of the drop as it is jetted out from the nozzle can be optimised via manipulation of the electronic pulses to the piezo-jetting device by the waveform editor and drop-watch camera system. In jetting, when a voltage is applied, the piezoelectric material changes shape or size, which generates a pressure pulse in the fluid forcing a droplet of ink from the nozzle. There is also a built-in cleaning station with a program editor that includes an automatic capping mechanism. Although the nozzle is made from a biocompatible material, the Ink is subjected to considerable stress in the jet head as the nozzle size is typically approximately 21.5 μm and the jetting velocity is typically 6-8 m/s.

The most unique feature of this table top printing system is its disposable cartridge-style printhead (DMC-11610) which allows users to fill with almost any type of jettable fluids and print instantly in the lab. This inkjet head cartridge can be heated up to 70°C, depending on the ink characteristics. Each cartridge reservoir has a maximum capacity of only 1.5 ml to minimise waste; while the minimum volume a cartridge can hold is about 0.2 ml. Under filling may not allow jet priming. Each cartridge has 16 nozzles linearly spaced at 254 microns with typical drop sizes of 1 and 10 picolitres,

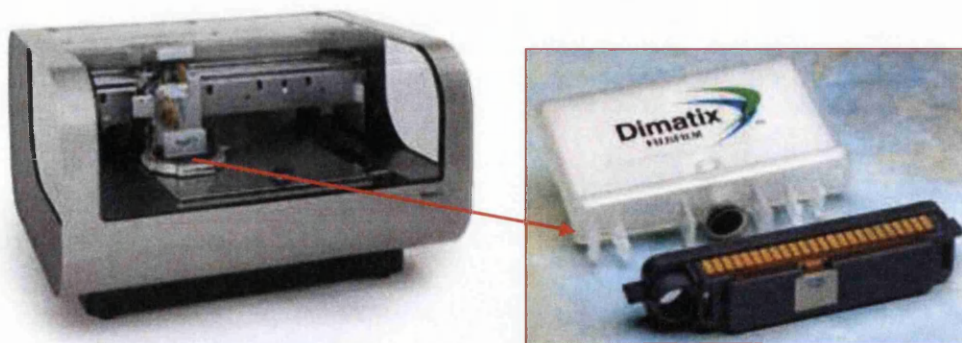


Figure 2.15 Dimatix materials printer (DMP-2800 series) and cartridge-style printhead

The DNA ink was transparent. So the way to understand the pattern of printing only was depending on the fluorescent scanner and location can be pre design with the pattern designer in the inkjet printer software.

The cartridge was autoclaved in the UV chamber as the immobilisation experiment for the polymer substrates. As discussed in Chapter 1, whether the DNA used in this work can be transferred using this process and survive the cycle is unknown and will be explored within this work.

2.6.2 Flexography print

Flexography was explored through the use of an IGT F1 bench top machine. The IGT F1 printability tester, **Figure 2.16** is designed to simulate the flexographic printing process. It was used in this investigation because only a small volume of ink was required to print images comparing to a full-scale printing press. The IGT F1 consists of a combined inking section with an anilox roll and doctor blade and a printing section with a plate cylinder and impression cylinder. A photopolymer plate is mounted to the plate cylinder using a double-sided tape.

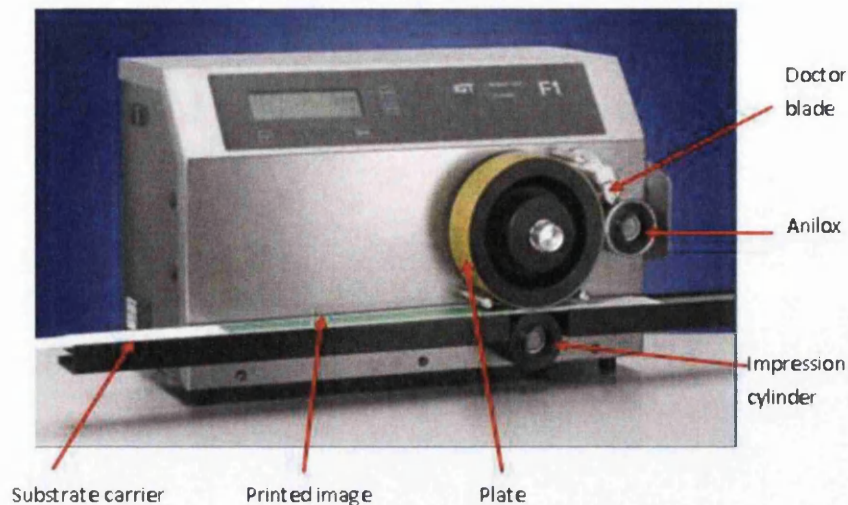


Figure 2.16 IGT F1 printability tester

When the IGT F1 was activated, the anilox and the substrate come into contact with the printing plate and the doctor blade contact the anilox. To produce a print, a volume of ink was applied to the nip between the doctor blade and the anilox using a pipette. The anilox force (between the anilox and plate) and printing force (between the plate and the substrate) were preset independently. The anilox was rotated a set number of times in contact with the plate to ensure that the anilox cells were well filled, therefore transferring a constant amount of ink to the plate surface for each trial. The reverse angle doctor blade removed the excess ink on the anilox to prevent excess inking of the plate. Then, the impression roll was engaged with the plate, bringing the substrate in contact with the plate surface. The rotation of the plate cylinder pulls the substrate carrier along the channel through the print nip, therefore transferring the ink from the printing plate to the substrate. The impression cylinder and anilox were both driven from the rolling contact with the substrate carrier and plate respectively. Ink is continuously transferred to the plate from the anilox. At the end of the print the impression cylinder and anilox were disengaged from the plate automatically. Within this cycle, the ink was subjected to a complex stress history that comprises shear and tensile stages.

2.6.3 Gravure print

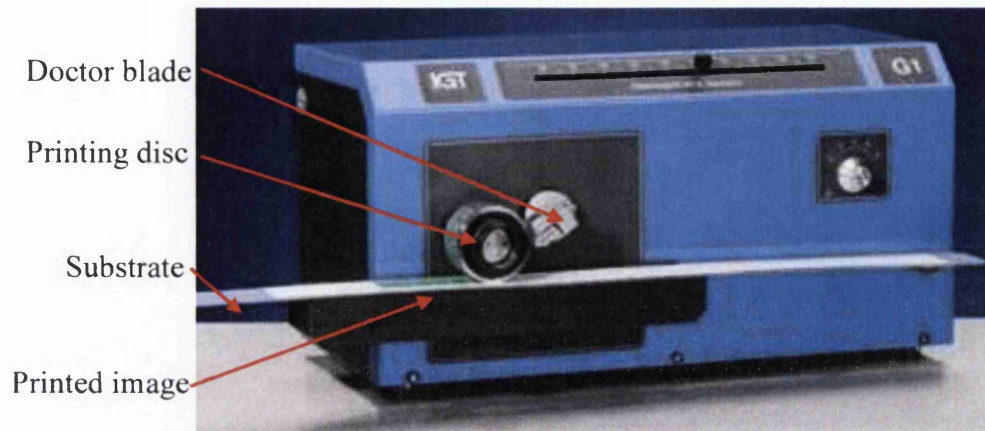


Figure 2.17 IGT G1 printability tester

This was similar and may respects to the flexography process, the difference being that the image was transferred from an engraved cylinder that holds the pattern.

The drops of ink are applied in the nip between the doctor blade and the printing form. The print system is now started: the surplus of ink is wiped off by the doctor blade and the printing ink is released from the cells of the printing disc and printed on the substrate. After two revolutions the doctor blade and the printing disc are lifted automatically. The substrate is removed for appraisal and the doctor blade and the printing disc are taken off for cleaning. In gravure printing the print quality is very much dependent upon the speed and the ink viscosity. Therefore the speed of the system is adjustable in five steps from 0.2 to 1.0 m/s. Two prints are automatically made to ensure that the cells of the printing form are consistently filled with ink on the second revolution. The second print is the most reproducible and used for further evaluation. The printing form can be lifted about 4 mm, so there is sufficient space for easy changing of the substrate and the printing disc. The printing force is selectable between 100 - 1000 N.

2.6.4 Process capability

Inkjet, flexography and gravure can be benchmarked according to their graphics printing capability and this is set out in **Table 1.1**.

2.7 Closure

The chapter has set out the DNA choice and how it may be formulated into the ink system. Measurement techniques to characterise the ink has been described as well as techniques to measure deposition with the GeneTAC LS IV and analyse with the GeneTAC integrator microarray analysis software and Image J. The statistical robustness of measurement has been explored and demonstrated and these measurement techniques will be used within the following chapters.

Chapter 3 Immobilising the ODN Ink on a Flexible Substrate

3.1 Introduction

The purpose of this chapter was to explore the ODN ink immobilisations on the substrates to give the foundation for DNA biosensor and array manufacture. So the combination of ODN ink to print with and the substrate were investigated here to establish the feasibility of transferring an ODN ink onto a flexible substrate while ensuring the survival of the DNA.

One of the first choices to make when fabricating DNA biosensor is which chemistry to use to immobilize the DNA to the solid support. Factors that influence the fabrication of DNA onto a surface are the immobilisation chemistry, spotting buffer choice, probe concentration and physical factors such as spotter type, pins used and environmental conditions.

This chapter showed the characteristics of the ODN ink delivered to the substrate using the pipette technologies and its attachment to different substrates.

The substrates were the polymer films described in **Table 3.2**. They are cheaper and easier to handle than glass slides. Nine types of polymers were tested to explore their suitability for the ODN ink immobilisations. The comparison of the FI of the ODN ink was analysed to show the suitability of substrates to immobilize DNA in a convenient, faster and economic way.

The immobilisation mechanisms between the ODN ink and the substrate were also investigated to establish the mechanisms that are present to facilitate this.

3.2 Materials

This section specified the materials used specifically in the immobilisation experiments in addition to those described in Chapter 2.

3.2.1 ODN

The ODN used in this chapter was the ODN with the fluorescent tag (Cy5). This was added to facilitate visibility after immobilisation and it was also used in the hybridisation target set out in Chapter 5. The Cy5 tag has no impact on the DNA itself, other than facilitating its visibility through fluorescence.

As described in Chapter 2, the ODN 5'-? ssDNA in this chapter as defined as probe1 and ODN 5'-? ssDNA-[3AC7] * in defined as a Probe 2. Probe 2 is the ODN with the amino modification on the 3' prime at the end of the ODN sequence.

Many immobilisation methods have already been developed by a number of other researchers as itemised and categorised according to chemistries in **Table 3.1**.

Table 3.1 Surface modification to bind modified and unmodified DNA

DNA modification	Substrate modification	References
None	Polylysine	[Chu et al. 1998]
	Amine	[Chiu et al. 2003]
	Epoxy	[Chiu et al. 2003]
	Diazonium ion	[Dolan et al. 2001]
	SU-8	[Schmid et al. in Press]
	Unmodified glass	[Call et al. 2001]
	Agarose film	[Dufva et al. 2004]
	Membrane	[Stillman and Tonkinson 2000]
Silanes	Unmodified glass	[Kumar et al. 2000]
Thiols (-SH)	Gold	[Csaki et al. 2001, Steel 1998]
	Mercaptosilanes	[Rogers et al. 1999]
	Maleimide	[Fixe et al. 2004a, Chrisey 1996]
	Iodoacetyl	[Chrisey et al. 1996]
Amines (-NH ₂)	Aldehydes	[Schena et al 1996, Fixe et al. 2004a, Berre et al. 2003]
	Epoxy	[Preininger et al. 2004]
	Isothiocyanate	[Beier and Hoheisel 1999, Benters et al. 2002]
Phosphates (PO ₃)	Aminated surfaces	[Zammatteo 2000]
Biotin	Avidin	[Sosnowski et al. 1997, Sabanayaga et al. 2000]

Binding DNA to a surface is a multistep process. In each step the surface is modified and the goal is to have a surface that can efficiently accept and bind the DNA probes

being spotted onto it. In most cases, the substrate is modified chemically to bind DNA (**Table 3.1**). Furthermore, the DNA is also modified with a functional group that specifically reacts with the functional group on the solid support. A linker can be used between the DNA and the modified solid support [Fixe et al. 2004a, Strother et al. 2000, Chrissey et al. 1996, Hong et al. 2005, Beier and Hoheisel 1999, Benters et al. 2002] to change the functional group extending from the surface to another functional group as described in **Figure 3.1**. A linker can also, if sufficiently long, function as a spacer to lift up the DNA probes from the surface making it more accessible for the incoming target which is used as the terms for the target 1 in Chapter 5 [Shchepinov et al. 1997].

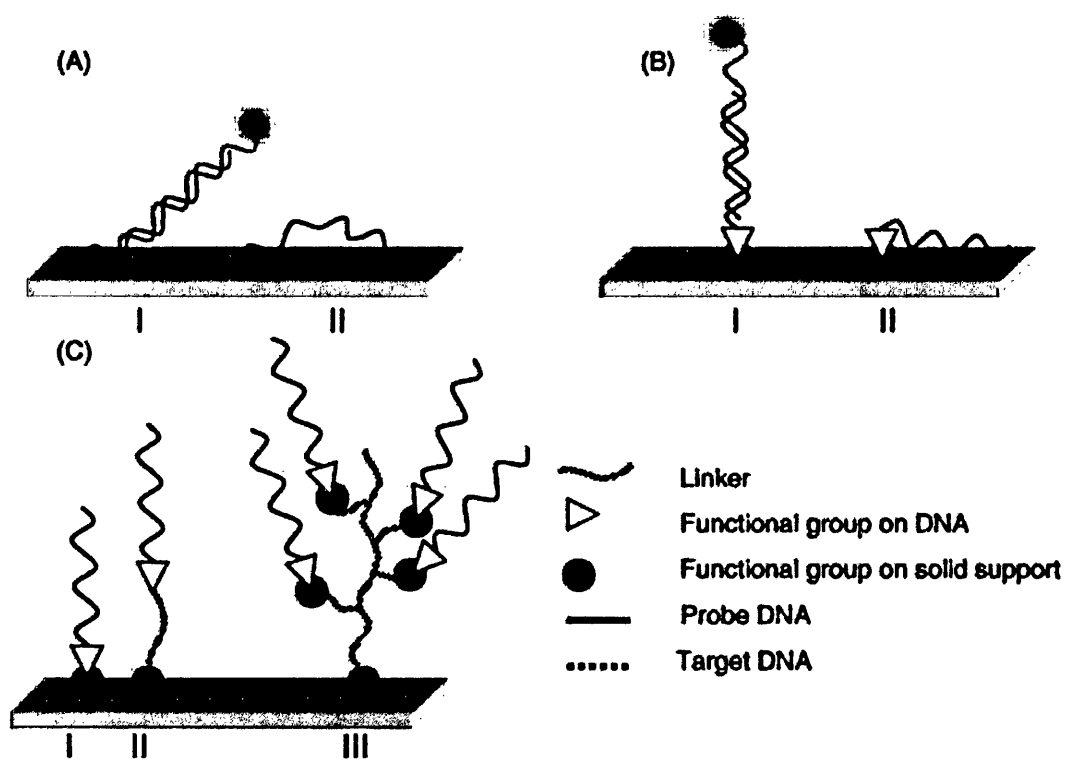


Figure 3.1 Immobilisation of DNA to solid surfaces.

(A: Unmodified DNA is randomly immobilised to surfaces meaning that some DNA strands can participate hybridisation (I) while other cannot (II); B: Immobilisation of DNA using end modifications (I) can also result in intra chain bonds (II); C: Molecular organisation of end modified probes directly immobilised to the active groups on the solid support (I) or displaced from the surface using a linker (II) or a dendrimeric linker (III)) [Dufva 2005]

Unmodified probes can be directly linked to unmodified glass but the interaction is not stable at high pH or high temperature suggesting that the DNA is not covalently bound to glass [Call et al. 2001]. Although typically constructed by immobilizing DNA on glass, silicon, or gold surfaces, there are cost and fabrication benefits to utilizing polymeric substrates [Goddard and Hotchkiss 2007].

They basically depend on the modification of ODN molecules and the substrates with the chemical functional groups like amines or thiols etc. with the special solvents to make stable covalent bonding. In this project, the requirement is for convenient, faster and economic ways to immobilize the ODN on the substrates and previous techniques are insufficient to achieve this. An innovative interesting way to immobilize the ODN on the substrate was discovered by adding the surfactant CTAB which was normally considered to decrease the surface tension of the ink to make it easier to print with the various printing technologies. This surfactant CTAB acted as not only the detergent to decrease the surface energy of the ODN ink but also the ODN ink immobilization reagent on the substrate. In this way immobilization can be cost effective, convenient and faster than any of the other covalent bonding reactions to make the ODN immobilization on the substrate. The details are set out in the following sections.

3.2.2 Polymer substrates

A range of polymer substrates were considered as candidate materials to print the ODN ink on. These were chosen upon the basis of the common types, the transparent property which gives lower fluorescent background when doing the fluorescent imaging measurement and availabilities. The list is set out in **Table 3.2**.

Table 3.2 Plastics used as the ODN substrates in this Chapter

Name [designation]	Description
PS	Polystyrene homopolymer, known as “crystal” polystyrene in the trade. Modified by the incorporation of elastomers, it is opaque white and biaxially oriented.
PC/PET1 (30/70) [1]	X4235 (fine matt/polished surfaces) 0.25 mm thickness polycarbonate/polyethylene terphthalate blend with 30 % polycarbonate and 70 % polyethylene terphthalate, manufactured by GE Structured Products and available as XYLEX™.
OHP [2]	Overhead Projector film (Polyethylene terephthalate)
PC/PET2 (50/50) [3]	X4236 (fine matt/polished surfaces) 0.25 mm thickness polycarbonate/polyethylene terphthalate blend with equal ratios of each component polymer, manufactured by GE Structured Products.
PC/PBT [4]	Bayfol® CR 6/2, (fine textured/very fine matt surfaces) 0.25 mm thickness polycarbonate/polybutylene terphthalate blend manufactured by Bayer.
PP [5]	Polypropylene, Rayoface™ C is Uncoated clear, high gloss film for facestock applications.
CP (Corona treated BOPP) [6]	Rayoface CPA is a high performance, clear, top coated, high gloss biaxially orientated polypropylene (BOPP) film for facestock applications, coated on one side with a proprietary aqueous dispersion and corona discharge treated on the reverse side.
CCP (Corona treated top coated BOPP) [7]	This is a high performance, clear, top coated, high gloss BOPP film for facestock applications, coated on one side with a proprietary aqueous dispersion and corona discharge treated on the same side.

3.3 Methods

The basic process of ODN ink immobilisation on the substrate is described as follows. Although it is a manual process, the aim is to explore the wetting and adhesion as a precursor to attempting printing trials.

The oligonucleotides with concentrations described 3.4.1 were diluted in aqueous CTAB (0.1mM) with the different concentrations. They were manually dropped on using the Gilson pipettes with the pattern designed in 2.4.2.1 and kept in the humidity chamber for immobilisation reactions for a range of times which was investigated as described in 3.6. Then the bottom side of the substrate surface with the printed ODN ink on it was adhered on a glass slide with a drop of water and the fluorescent scan carried out using the GeneTAC LS IV scanner as in 2.4.1 and analysis by the GeneTAC Integrator Microarray Analysis Software as in 2.4.2.1. This provided the original control data to test the immobilisation reactions. The ODN ink on the substrate was then washed using the TNT buffer and water several times and this was investigated in 3.4. Then they were dried in closed petri dishes with tissues to absorb the moisture. After this, the samples were scanned and analysed. Then these two sets of data (ODN ink on the substrates before and after rinsing) were compared statistically to establish the ODN ink immobilisation on the different substrates and used to discover the appropriate substrate on which to immobilize the ODN ink.

3.3.1 Immobilisation reaction chamber

The common type of chamber was not used for controlling the humidity. A simple chamber was designed to keep the humidity and temperature stable while minimising light bleaching of the ODN ink on the substrate surface and minimising room dust contamination during the immobilisation or hybridisation experiments. The impact of humidity level on immobilisation or hybridisation experiments was not included in the factors to influence the reactions. So a simple humidity chamber was constructed to facilitate the immobilisation and hybridisation experiments.

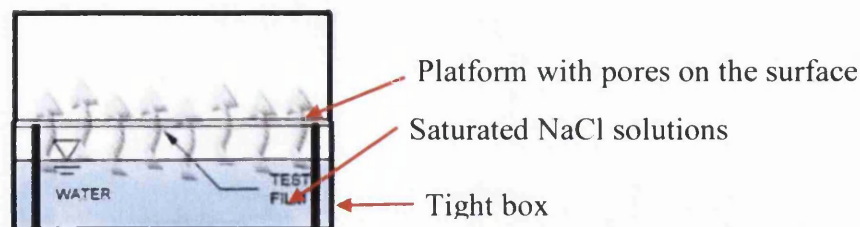


Figure 3.2 Schematic of a simple immobilisation reaction chamber design

This humidity chamber used a sealed air tight box. A saturated sodium chloride solution contained in the box and a perforated platform placed above it. The relative humidity level in this simple chamber is 75% below the platform as this is a known calibration for a hygrometer [Wexler and Hasegawa 1954].

3.3.2 Substrate handling

To facilitate substrate for the fluorescent scanning measurement, the polymer substrates sheets were cut to a size that was smaller than the microscope glass slide, typically 75 by 25 mm. When performing the fluorescent scanning measurement, this substrate with the ODN on it was fixed to a microscope glass slide by a droplet of water.



Figure 3.3 The model shape of the substrate to print ODN ink on

Also the substrate was designed so that the side on which the ODN was deposited could be identified easily and this was achieved by simply clipping off one corner,

Figure 3.3.

3.3.3 Manual printing techniques

The manual printing techniques were to use the pipettes to deposit the ODN pendant on the tips on the substrates. The process was as follows.

The ODN aqueous aliquots were thawed at room temperature and diluted using the CTAB aqueous solution to achieve different concentrations depending on the purpose of the experiments. Then they were mixed using the VORTEX-GENIE mixers for 10 seconds at 3200 rpm. The samples after mixing were stabilised for 10

minutes and the mini-centrifuge with 6000 rpm speed was used to make the samples splashed on the inside walls of tubes concentrated at the bottom of tube for better delivery during further experiments and for removing the bubbles of the solution in the tubes. Gilson Pipettes with 0.5-10 μ l (P10) and 20-100 μ l (P100) capacity were used for transferring the ODN ink and solvents to achieve the correct concentrations. The amount of the ODN ink was appropriate for deposition by the Gilson Pipette at 1 μ l, which was adjusted to this set volume before depositing the ODN ink on the substrate from 4 to 12 separate spots as according to the pattern shown in **Figure 2.7**. This was done by simply clicking the push-button to print the ODN on the substrate on the bench, but in a dark background. This printing process mechanism applies a low level of pressure to the ODN ink to push it out of the pipette tip on to the substrate. It is a precursor to an actual high volume printing technology such as inkjet. The deposition speed of pipetting the ODN ink on the substrates must be quick so that the previously deposited ODN ink at different locations on the substrate does not dry. So the maximum number of spots in one printing trial was 12 on the same substrate to reduce such evaporation causing the unstable ODN ink to be immobilized in air by dust contamination.

Furthermore, in depositing the 12 spots on the substrate there will be some time difference as it is a manual process. This provides an opportunity for differences in immobilisation to occur. However in the subsequent washing and measurement cycles, the same spot was measured and hence this removes any discrepancy that could occur through delay in deposition.

The immobilisation experiments checked the different polymer substrates to immobilize the ODN ink in CTAB aqueous solution by pipetting, rinsing with TNT buffer and scanning the fluorescent signals from the tag (Cy5) on the ODN. The optimized substrate surface was discovered to immobilize ODN ink with the promising advantages such as convenient, faster and economic. Also the exploration on the mechanism behind the data was figured out.

3.3.4 Rinsing techniques

On the completion of deposition, the printed surface needs to be subjected to a rinsing sequence (TNT buffer and autoclaved water) to get rid of the excess ODN on the substrate that has not been immobilized together with the CTAB. A TNT buffer

was used for the first rinsing by plunging the substrates in the liquid reservoir several times, and then they were transferred to the autoclaved water. This cycle was repeated several times the adequacy of which will be investigated experimentally in 3.4.2. TNT, water and CTAB were tested and produced no detectable fluorescent noise in the experiments. Highly charged bioactive compounds, such as ODN, can present problems during immobilisation-both with non-covalent adsorption, which can confound the results of bioactivity assays, and with electrostatic repulsion, which can hinder biomolecule immobilization. An alkaline wash can aid in removing non-covalently bound ODN [Tran et al. 2003], and including NaCl in the immobilization buffer can reduce the effects of electrostatic repulsion [Fuentes et al. 2004]. The ODN ink deposited on the substrate without rinsing was referred to as a control probe or immobilized probe and designated as Probe 1.

3.4 Results and discussion in the characterisation of the probe 1 ink on the substrates

The purpose of the work described in this section was to choose the optimal concentration to be used for probe 1 ink immobilization on the substrate and the rinsing times required after printing the probe 1 ink on the substrates,

3.4.1 Characterisation of the probe 1 in the optimal concentration on the substrates

Probe 1 aqueous dilutions were needed to obtain the optimal concentration for immobilisation on the substrate. The aqueous dilutions did not include any CTAB or other reagents.

The probe 1 dilution series was deposited on the same substrate following the procedure in 3.3.3. After overnight storage within the humidity chamber during which time the ODN is deposited onto the substrate, the samples were scanned by the GeneTAC LS IV scanner as described in 2.4.1 and analysed using the procedure described in 2.4.2.1 to give a FI index. The results are shown in **Figure 3.4**.

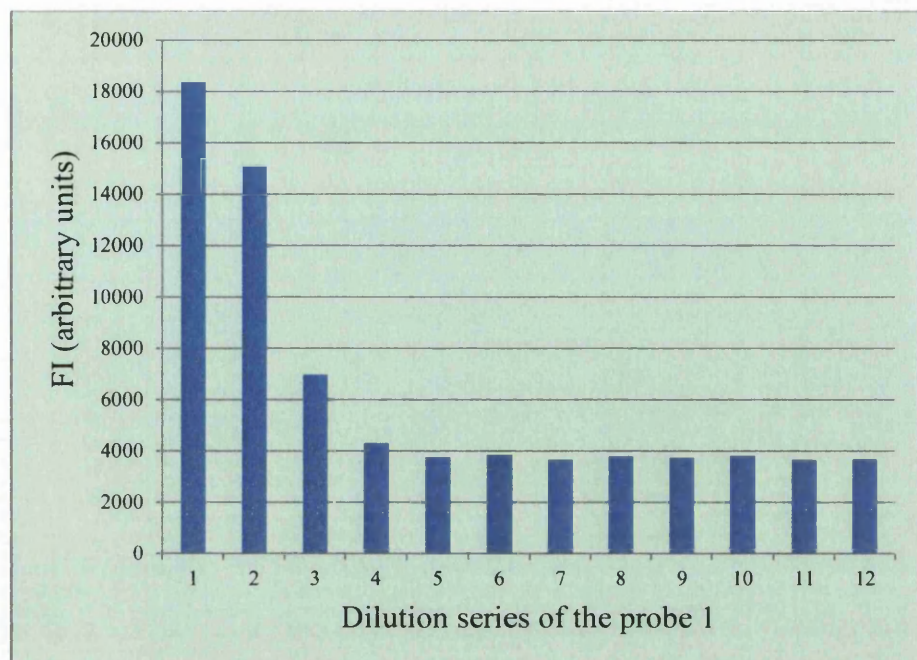


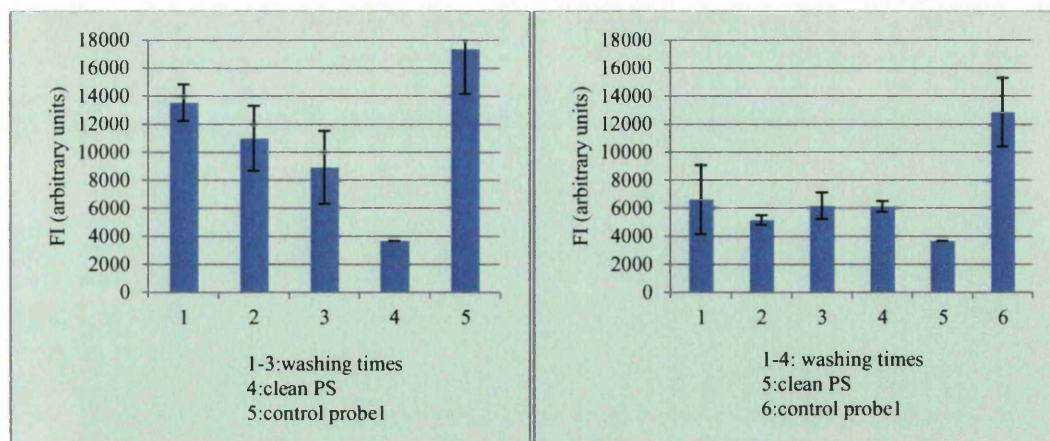
Figure 3.4 The FI average signals analysis of the dilution series (30×10^{-1} to 30×10^{-12} μM) for probe 1 printed on PS

This histogram shows the FI average from 30×10^{-1} to 30×10^{-12} μM . The probe 1 stock (the dilution solution with the original pack purchased) has a concentration of 30 μM , determined by the NanoDrop ND-1000 described in 2.1.4. The histogram in **Figure 3.4** shows general behaviour of the immobilisation of the probe 1 ink on the substrate by the non-covalent bonding expressed as a series concentration.

3.4.2 Rinsing time investigations

The probe 1 ink at 30×10^{-1} and 30×10^{-2} μM dilution was made of the probe 1 stock (30 μM) through the dilution by CTAB (0.1mM) aqueous solution, described in 2.1.3 and 2.2.1.

This probe 1 ink was deposited on the same substrate, the PS, following the procedure in 3.3.3. After overnight storage, the probe 1 ink on the substrate was scanned by the **GeneTAC LS IV** scanner as described in 2.4.1 to give the FI average signals of the control probe 1. The FI average signals of the control probe 1 on the same substrate, the PS, was analysed by the software described in 2.4.2.1. The FI average signals of the control probe 1 follows the same procedure as above and the results are shown in **Figure 3.5**.



A

B

Figure 3.5 The rinsing times comparison of the immobilisation of the probe 1 ink on the PS by TNT buffer and autoclaved water

(A: rinsing times experiment on the probe 1 ($30 \times 10^{-1} \mu\text{M}$) deposited on the PS; B: rinsing times experiment on the probe 1 ($30 \times 10^{-2} \mu\text{M}$) deposited on the PS)

The graph A in **Figure 3.5** shows that the FI average signal of the probe 1 ink ($30 \times 10^{-1} \mu\text{M}$) changes after the different rinsing times (1-3) by TNT buffer and autoclaved water. The rinsing techniques were described in 3.3.4. The graph B in **Figure 3.5** showed that the FI average of probe 1 ink at $30 \times 10^{-2} \mu\text{M}$ changes after the different rinsing times (1-4) by TNT buffer and autoclaved water, the rinsing techniques were described in 3.3.4. The last bar in both of the graphs illustrated the FI average signals of the control probe 1 on the PS.

The histograms in **Figure 3.5** show that the highest concentration of the probe 1 ink ($30 \times 10^{-1} \mu\text{M}$) on the substrate cannot be the optimal choice for the immobilisation of the probe 1 ink as the FI average index changes with washing sequence. A possible reason for this is that the probe 1 molecules are compacted together to stay on the top of the deposited drops far away from the surface of the substrates rather than at the substrate interface and so they are washed away. This condition was showed in **Figure 2.8**. The comparisons of the lower concentration with the higher concentrations showed the effect of rinsing on the immobilisation of the probe 1 ink on the substrates.

Also the rinsing experiments in **Figure 3.5** showed that the immobilisation of the probe 1 ink ($30 \times 10^{-1} \mu\text{M}$) on the substrate was not strong and most of the probe 1 ink with the non-covalent bonding on the substrate was rinsed off by the TNT buffer and autoclaved water. The probe 1 ink at $30 \times 10^{-2} \mu\text{M}$ showed a more constant FI average signal for different washing cycles and thus it was chosen as the optimal concentration for subsequent immobilisation experiments.

In future experiments, the rinsing times determined above will be adopted for the probe 1 ink immobilisation experiments on the other substrates.

3.4.3 The immobilisation reaction conditions investigations of the probe 1 ink on the substrates

Initial consideration included environmental factors such as temperature and humidity. An initial trial on temperature effects was carried out, but little effect was noted for the PS substrate. Consequently a detailed programme of work combining temperature and humidity was not pursued as this is very extensive in its own right. The identification of an appropriate substrate is the main focus, following which such a rigorous investigation on temperature/humidity remains as an option for future study. Consequently the substrate work was conducted using the simple humidity chamber to maintain sample cleanliness.

3.5 Results and discussion in the characterisation of the different substrates to immobilize the probe 1 ink

The section purpose was to discover a usable substrate from the list described in **Table 3.1** to immobilize the probe 1 ink.

3.5.1 The FI average signals analysis of the different substrates by depositing the probe 1 ink

The substrates were prepared by the method described in 3.3.2. The probe 1 ink ($30 \times 10^{-2} \mu\text{M}$) described in 3.4.2 was deposited on the substrates, following the procedure in 3.3.3. After overnight immobilisation, the probe 1 ink on the substrate was scanned by the **GeneTAC LS IV** scanner as described in 2.4.1 to give the FI average signals from the control probe 1 that was analysed using the software described in 2.4.2.1.

Following washing, the FI average signals from the immobilized probe 1 ink analysis followed the same procedure as described above. The result is shown in **Figure 3.5** and this includes the background signal from the substrate itself.



Figure 3.6 The fluorescent images of the experiments of the probe 1 ink ($30 \times 10^{-2} \mu\text{M}$) on the PS

(Top: the fluorescent images of the control probe 1; bottom: the fluorescent images of the immobilized probe 1)

The fluorescent noise from the background of the PS is seen to be significant when compared with the immobilised washed material. Thus, it is not clear if the ODN was immobilised, or whether it was washed away as part of the immobilisation test. The data may also be presented quantitatively as shown in **Figure 3.7** below. This figure includes the deposited ink (blue), the immobilised ink after washing (red) and the substrate signal (green). However, with regard to the data in **Figure 3.6** the PS was deleted from the candidate substrate list.

The substrates designated 1 to 7 in the list described in **Table 3.2** with the clear transparent property were tested using an identical procedure.

The comprehensive results from the immobilisations experiments for the probe 1 ink ($30 \times 10^{-2} \mu\text{M}$) on the substrates is shown in **Figure 3.7**.

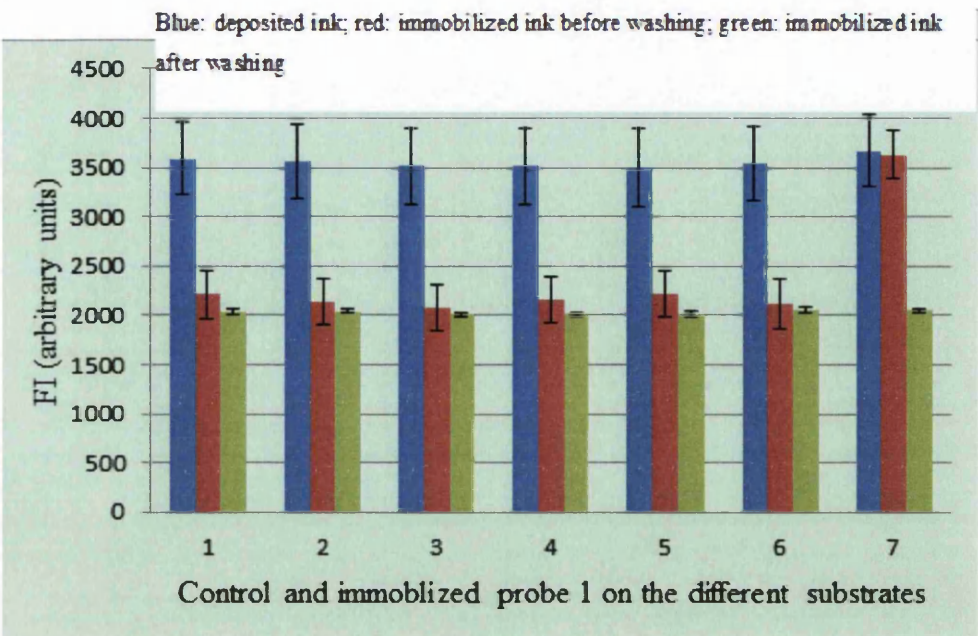


Figure 3.7 The FI average signals analysis of the immobilisation experiments of the probe1 ink ($30 \times 10^{-2} \mu\text{M}$) on the different substrates

This graph shows clearly the immobilisation effects of the probe 1 ink on the seven different candidate substrates, identifying the substrate 7 (CCP) to be suitable. The image from scans on this substrate type is shown in **Figure 3.8**. 1 to 7 is described in **Table 3.2**.



Figure 3.8 The FI average images of immobilisation reaction of the probe 1 ink ($30 \times 10^{-2} \mu\text{M}$) on the CCP

This graph showed that the optimal substrate, the CCP, was the promising substrate to immobilize the probe 1 ink on it. There was not a big change in the FI signals of the control probe 1 and immobilized probe 1 on this substrate. This indicated that the substrate could be used as the DNA sensor substrate to immobilize the ODN ink on it.

The following focus on further immobilisation experiments using probe 1 ink on the CCP. The purpose of these experiments was to gain a more complete understanding of the immobilisation mechanism together with exploration of washing cycle parameter settings.

3.5.2 The FTIR analysis of the surface of the CCP to immobilise the probe 1 ink

Fourier transform infrared spectroscopy (FTIR) uses infrared radiation to determine the chemical functionalities present in a sample. When an infrared (IR) beam hits a sample, chemical bonds stretch, contract, and bend, causing it to absorb IR radiation in a defined wavenumber. In attenuated total reflectance (ATR) FTIR, the incident IR beam first passes through a ZnSe, Ge, or diamond crystal, improving the surface sensitivity of the technique. The resulting plot is of absorbance (or transmittance) versus wavenumber. Sampling depth is dependent on the infrared transmitting crystal used to internally reflect the incident IR beam as well as the refractive index of the sample, and is on the order of microns [Desai and Singh 2004]. Although ATR-FTIR has a relatively deep sampling depth, it does not require ultra-high vacuum conditions, as do XPS and ToFSIMS, and an analysis can therefore be conducted in less than ten minutes [Hsu 1997]. ATR-FTIR can also be used to monitor migration of functional groups to the polymer bulk [Rasmussen et al. 1977].

FTIR was used as a technique for exploring the immobilisation of ODN onto the CCP substrate. This was chosen because it identifies the chemical function group on the substrate surface.

The surface chemical function of the CCP as the appropriate substrate was unknown in the data available from commercial sources. This comprised four tests. The first used a plain PP as a base stock material (PP uncoated), the second is coated with an acrylic material (PP coated) and the third is a corona treatment of the PP coated surface in which the corona treatment has a direct impact as it further promotes adhesion by surface modification. The latest may be compared with the surface properties of an acrylic adhesive that was available in the research laboratory.

The **Figure 3.9** shows the comparable spectrum graphs for the different substrate surfaces. The closer match between the corona treated coated PP surface and the

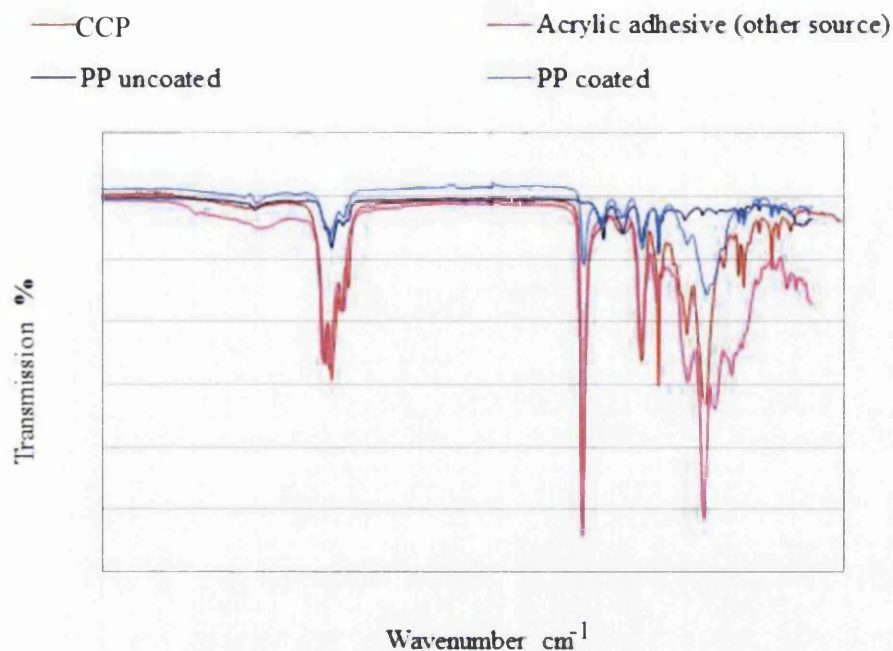


Figure 3.9 The FTIR analysis comparisons of the CCP and the other substrates with the similar chemical functional groups

The CCP (surface 1.1 in **Figure 3.8**) is a BOPP that has been coated with an acrylic. The corona treatment was done after coating from the commercial information of the product. There is distinct absorption for both surfaces at 1730 indicative of a C=O bond.

In the next Chapter, the surface chemistry of CCP will be explored to establish why it is the best performing.

3.6 Results and discussion in the characterisation of the immobilisation mechanisms between the probe ODN ink and the CCP

It was understand the immobilisation mechanism of the probe 1 ink on the CCP by comparing the immobilisation of the probe 2 ODN ink and the Cy5 dye ink in 0.1mM CTAB. The time of the immobilisation of the probe ODN ink on the CCP was optimised.

3.6.1 Characterisation of the time of the immobilisation of the probe ODN ink on the CCP

The probe 1 ink ($30 \times 10^{-2} \mu\text{M}$) or probe 2 ink ($30 \times 10^{-2} \mu\text{M}$) was deposited on the CCP, following the procedure in 3.4.2. In the maximum 5 hours period, one CCP with the probe 1 ink or probe 2 ink on it was scanned by the **GeneTAC LS IV** scanner as described in 2.4.1 to give the FI signals of the probe 1 or probe 2. The FI signals of the probe 1 or probe 2 on the CCP was analysed by the software described in 2.4.2.1. The FI signals of the immobilized probe 1 or probe 2 was followed the same procedure as above but the time of the immobilisation experiments was tested hourly up to 5 hours. The results are shown in **Figure 3.10**.

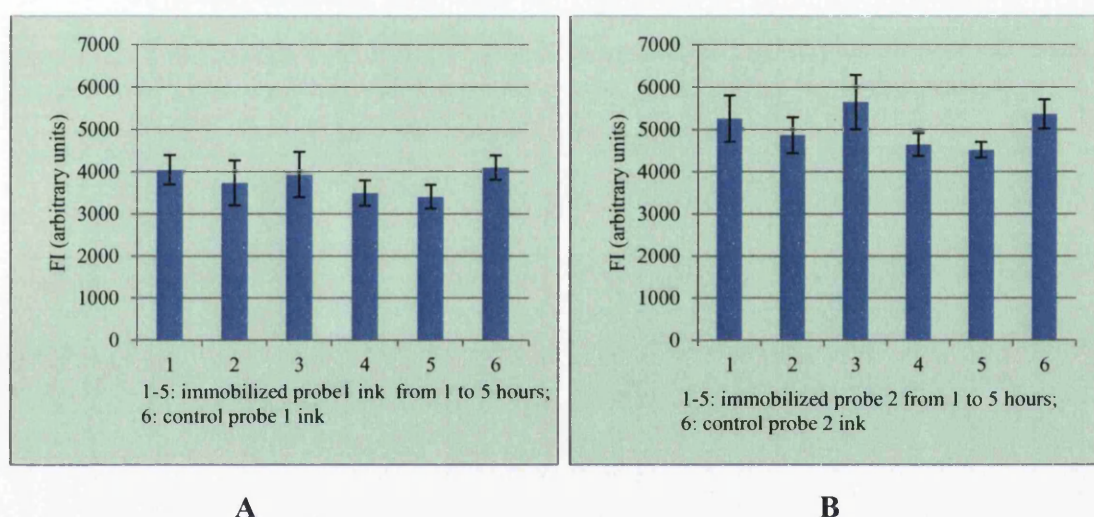


Figure 3.10 The FI average signals analysis of the immobilisation experiments of the probe 1 ink ($30 \times 10^{-2} \mu\text{M}$) on the CCP over the hourly immobilisation time (1-5 hours)

(A: the FI average signals of the immobilisation of the probe 1 ink on the CCP; B: the FI average signals of the immobilisation of the probe 2 ink on the CCP)

This graph showed that the time of the immobilisation of the probe 1 ink and probe 2 ink could be shortened to one hour only from the overnight to achieve the same immobilisation effect of the probe 1 ink or the probe 2 ink. Also, the significant difference of the immobilisation effects of the probe 1 ink and probe 2 ink was not to illustrate that the amino group modification could not help the immobilisation of the ODN molecules on the CCP. The probe 2 was not chosen as the ODN ink to do the

printing because the probe 2 which is ODN modified with the amine group increases costs between 100 and 300% [Dufva 2005].

3.6.2 The FI average signals comparison of the immobilisation of the probe 1 ink, probe 2 ink and Cy5 ink on the CCP

The purpose of this section was to understand further about the immobilisation mechanisms of the probe 1 ink and probe 2 ink on the CCP. The Cy5 as the fluorescent dye of the probe 1 ink and probe 2 ink would be the first suspected molecule involving the immobilisation experiments. So the pure Cy5 aqueous solution (0.6 ml) purchased from BIO-RAD as the iCycler iQ Calibrator Dye Solution Set was used as the Cy5 ink to dilute in the CTAB aqueous solution (0.1mM) with the concentration of the Cy5 aqueous solution adjusted by the same FI average signals as the immobilized probe 1. The probe 1 ink ($30 \times 10^{-2} \mu\text{M}$) and probe 2 ink ($30 \times 10^{-2} \mu\text{M}$) were made through the process described in 3.4.2.

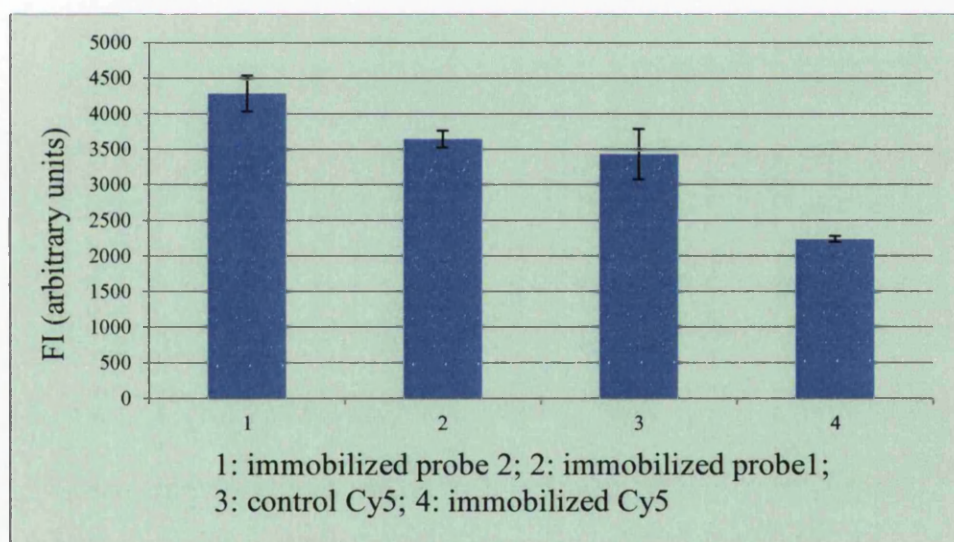


Figure 3.11 The FI average signals comparison of the immobilisation of the immobilized probe 2 ink ($30 \times 10^{-2} \mu\text{M}$), immobilized probe 1 ink ($30 \times 10^{-2} \mu\text{M}$), control Cy5 ink and immobilized Cy5 ink

This graph showed that the FI average signals of the immobilized probe 2 and the immobilized probe 1 were not the same as the immobilized Cy5. So the Cy5 ink did not show the good immobilisation on the CCP. This illustrated that the immobilisation mechanisms of the probe 1 ink and probe 2 ink on the CCP was

reacted on the ODN molecules themselves instead of the other modifications of like amine groups or Cy5 dye.

So these data above and mechanism proposed in other peers' papers illustrate that the possible immobilisation happened by the complex forms between ODN and CTAB and the CCP surface functional group. The different point here from the literatures is that the CCP instead of PS. So the binding of the ODN on the CCP will not follow the mechanism with non-covalent bonding but the different way with some parts involved in covalent bonding because the CCP is the polymer substrate with more polar charge functional group on the top surface after corona treatment described in 1.2.7 and polar functional group acrylic modification on the surface as showed in **Figure 3.9**.

3.7 Closure

In this Chapter, a series of ODN concentrations was tested to obtain the suitable concentration for immobilizing the ODN. The washing cycle was tested to decide the suitable way. The different polymer substrates were tested to discover the suitable substrate for immobilizing the ODN. The suitable polymer substrate was tested and investigated to understand the surface character by FTIR technique. The immobilisation mechanisms were investigated with experiments on the different ODN probe1 and probe 2 and the dye Cy5. The possible immobilisation mechanism of the ODN ink on the CCP was proposed to direct the further experiments on printing experiment in next chapter and hybridisation experiment in Chapter 5. The key findings in this Chapter are as follows: The suitable polymer substrate CCP was discovered and tested to immobilize ODN. The immobilisation method was developed with the CTAB aqueous solution (0.1mM) as the ODN ink. The concentration of the ODN immobilized on the CCP was tested and decided with the suitable concentration ($30 \times 10^{-2} \mu\text{M}$). The next Chapter will investigate the printability of the ODN ink on the CCP by inkjet, flexography and gravure printing technology.

Chapter 4 The Production of the DNA Sensor by Conventional Printing Technologies

4.1 Introduction

The choice of printing process for a functional product is determined by ink rheology, feature geometry and manufacturing volume. The purpose of this chapter is to explore printing options for DNA, starting with ink jet, but including the volumeprinting technologies of flexography and gravure. Ink rheology includes the parameters of viscosity and surface tension, which need to be established to be compatible with the substrate properties to facilitate wetting and finally immobilisation. For DNA, adjustment of rheology is difficult as the additives used must not affect the DNA itself, or its immobilisation and curing behaviour. The additive Glycerol was chosen because of its known biocompatibility [Bailey et al. 1991, Yazdani and Gonzalez 2007]. For the ODN ink identified in Chapter 3, this needs to be characterised with regard to printing process choice.

Surface tension and viscosity are the main considerations to achieve delivery on the substrate followed by immobilisation and the factors that affect this part of the process. Survival of the printing stage is vital if DNA is to be used for applications in sensing.

Therefore, on completion of a print, the target was washed and scanned using the procedures developed within this project and described in 3.3.4, 2.4.1 and 2.4.2.1.

Thus, the main consideration in this chapter is the development of an ink formulation and its linkage with the printing processes.

4.2 Materials

The choice of ink and substrate has been discussed in Chapter 3 and the probe 1 ink and CCP substrate has been determined from this work. The properties of this ink, (including modification) and the substrate properties need to be evaluated for the purpose of deposition by printing. Glycerol is a candidate ink rheology modifier. Glycerol is a colourless, odourless, viscous liquid purchased from Promega, Southampton. Gilson Pipettes were used to measure the different volumes of Glycerol to dilute in the calculated volume of 0.1 mM CTAB aqueous solution to

make the different volume concentration of Glycerol - CTAB solution: 90%, 80%, 70%, 60% and 50%.

For most ink to form a good print, it must have good adhesion to the substrate.

A number of mechanisms have been identified [Kipphan 2001]. Firstly, the ink anchors mechanically to the substrate surface by penetrating into pores and encasing paper fibres. This may require some positive pressure that is generated in the contact between the image carrier and substrate surface as it passes through the press in a contact printing process. Such pressure may be generated by impact of the ink droplet on the substrate in the case of non-contact printing technology, such as ink jet. The ink must wet the substrate and this is determined through the liquid surface tension together with the components of substrate surface energy. The second mechanism is penetration through capillary action where the surface is open. Thirdly, in the case of extremely smooth surfaces, the ink may be adhered by means of chemical bonding between the ink and substrate. The CCP was corona treated to introduce the oxidation products on the surface to increase the adherent force to the ODN ink described in 1.2.7 [Desai and Singh 2004, Briggs et al. 2003].

4.3 The surface characteristics of the CCP

The surface characteristics of the CCP, surface energy and roughness, were tested to gain a better understanding of the printability of the ODN ink. Surface roughness is relevant because it is essential that the deposited ink covers the substrate completely and furthermore it may provide physical anchorage for the deposited ink. The area of deposited ODN ink can affect the forces to immobilize the ODN on the CCP because the more ODN ink is in contact with the CCP surface functional group, the more bonds can be formed to immobilize the ODN ink on the CCP. The surface roughness shows a 3D state which will physically anchor the ODN ink to the CCP surface.

4.3.1 The surface energy characteristics of the CCP

The surface energy of the CCP was tested by the methods described in 2.5.2. The surface energy is important in determining substrate wetting and hence the likelihood of image transfers with later immobilisation. In this work, wetting will be restricted to a static still presents several research challenges [Blake and Shikhmurzaev 2002, 2004, Eggers and Evans 2004].

The surface free energy of a solid substrate is typically characterised through the analysis of contact angle of a drop resting over the solid surface. The contact angle is related to the key thermodynamic parameters of the surface by the Young equation [Young 1805]:

$$\gamma_{lv}\cos\theta = \gamma_{sv} - \gamma_{sl}$$

While the surface energy of the liquid/vapour interface can be experimentally calculated, the surface energies related to the solid are estimated based on theoretical considerations. These can be classified within two major fields, namely microscopic and macroscopic, often in discussion one with each other [Siboni et al. 2004, Kwok 1999].

A macroscopic approach for surface energy determination is based on the equation of state as proposed by Neumann [Neumann and Spelt 1996] and Kwok [Kwok 1999]

Microscopic approaches were originally proposed by Fowkes [Fowkes 1962] and Owens and Wendt [Owens and Wendt 1969]. They are based into splitting of surface free energy into two components:

$$\gamma = \gamma^p + \gamma^d$$

The component γ^d is called “dispersive” component, with and is associated to the van der Waals electrodynamic forces such as the Keesom force, Debye force and London dispersion force. The interactions based on hydrogen bonds constitute the second component of the equation, the “polar” component γ^p .

The currently dominant microscopic approach is the Lifshitz–van der Waals acid-base approach, or vOGT, developed by Van Oss et al. [Oss et al. 1988]. Here, the polar component is defined in function as an acid-base model or electron-acceptor/electron-donor. Hence, the surface free energy is expressed as:

$$\gamma = \gamma^{LW} + \gamma^{AB}$$

$$\gamma^{AB} = 2\sqrt{\gamma^+\gamma^-}$$



Where γ^{LW} is the “dispersive” component, while the “polar” component γ^{AB} is composed by the acidic component γ^+ and the basic component γ^-

The work of adhesion of a liquid phase onto a solid substrate can be expressed as [Oss et al. 1988]:

$$W^{Adh} = \gamma_l (1 + \cos \theta)$$

$$= 2 \left(\sqrt{\gamma_l^{LW} \gamma_s^{LW}} + \sqrt{\gamma_l^+ \gamma_s^-} + \sqrt{\gamma_l^- \gamma_s^+} \right)$$

with θ being the static contact angle of the liquid on the solid substrate and the solid, and with $\gamma_l^{LW}, \gamma_l^-, \gamma_l^+, \gamma_s^{LW}, \gamma_s^-, \gamma_s^+$ being the vOGT dispersive, basic and acidic components of the liquid and of the solid respectively.

For most liquids, values of the dispersive and polar components of the liquids are present in the literature. While the values for the component γ_d and the component γ^{AB} are well known and accepted, the ratio between the acid and basic component are still the object of research and discussions: different scales have been proposed on the base of estimates of the acid-base ratio for the reference liquid water [Oss et al. 1988, Volpe and Siboni 2001, Lee 2001]. This is shown in **Table 4.1**. Lee [2001] claimed that intermolecular interactions are primarily dominated by dispersion, d, hydrogen bonding, h, and secondarily affected by orientation, o, and induction, i. Generally, the polarization component, p, represents both i and o interactions. Fowkes suggested that the acid–base component, γ^{ab} , of the surface tension should consist of both h and p interactions. However, VCG proposed that the acid–base components, γ^{ab} , result solely from hydrogen bonding, γ^h , that is equivalent to $2(\gamma^+ \gamma^-)^{1/2}$, where γ^+ and γ^- are the two hydrogen bonding parameters. VCG defined γ^{LW} as the Lifshitz-van der Waals component consisting of d, o and i contributions, thus, surface tension, γ , equals $\gamma^{ab}(\text{VCG}) + \gamma^{LW}$. Both Fowkes and VCG assumed that the polar interactions for a liquid on a low energy surface are negligible. Lee treats the specific acid-base interaction to be hydrogen bonding. In addition, we also take into account the nonspecific polarization, p, interaction in terms of the equilibrium spreading pressure, π_e , resulting from the adsorption of a liquid vapor on the polymer surface. Thus, our unified approach uses the dispersion component, γ^d , of Fowkes, the hydrogen bonding, h, of VCG and the polarization, p, in terms of π_e . The

difference between the initial (theoretical) and equilibrium (experimental) surface tensions is π_e , and others have observed that π_e on some polymers is substantial. The determination of several initial surface tensions of polymers by considering the effect of polarization is discussed.

Table 4.1 Different scales proposed on the basis of estimates of the acid-base ratio for the reference liquid water in literatures

Dispersive	Polar	Acid	Base	Ratio	Author(year)
72.8	21.8	25.5	25.5	1:1	Van Oss [Oss, et al 1988]
		48.5	11.16	4:1	Della Volpe [Volpe and Siboni 2001]
		34.2	19.0	2:1	H. Lee [Lee 2001]

The three components of the surface free energy of the solid substrate are the typical unknown to be determined. This can be achieved by analyzing a set of three known liquids; from the measurement of their contact angle, a set of three non-linear equations in three unknown is determined:

$$\gamma_{l,i} (1 + \cos \theta_i) = 2 \left(\sqrt{\gamma_{l,i}^{LW} \gamma_{s,i}^{LW}} + \sqrt{\gamma_{l,i}^+ \gamma_{s,i}^-} + \sqrt{\gamma_{l,i}^- \gamma_{s,i}^+} \right) \quad i = 1, 2, 3$$

This set of equations can be made linear into the form:

$$Ax=B$$

with

$$A = \begin{pmatrix} \sqrt{\gamma_1^{LW}} & \sqrt{\gamma_1^+} & \sqrt{\gamma_1^-} \\ \sqrt{\gamma_2^{LW}} & \sqrt{\gamma_2^+} & \sqrt{\gamma_2^-} \\ \sqrt{\gamma_3^{LW}} & \sqrt{\gamma_3^+} & \sqrt{\gamma_3^-} \end{pmatrix},$$

$$b = \begin{pmatrix} \gamma_1(1 + \cos\theta_1)/2 \\ \gamma_2(1 + \cos\theta_2)/2 \\ \gamma_3(1 + \cos\theta_3)/2 \end{pmatrix},$$

$$x = \begin{pmatrix} \sqrt{\gamma_3^{LW}} \\ \sqrt{\gamma_3^-} \\ \sqrt{\gamma_3^+} \end{pmatrix}.$$

From the solution of this set of equation the components can be derived.

In order to improve the quality and reliability of the calculation, Van Oss define the importance of using three distinctive fluids, one primary dispersive, one acid and one basic. Mathematically this need can be quantified as this set of equations is typically strongly ill-conditioned; this can be controlled by choosing a liquid triplet with the lowest possible value of the condition number, a coefficient which expresses ill-conditioning in a quantitative way [Volpe at al. 2004]. A corrected acid-base scale has been proposed by Della Volpe [Volpe and Siboni 2000, Volpe and Siboni 2001].

Three standard liquids have been used as itemised in **Table 4.2**. This table also includes the settings that were recommended and used on the Fibro DAT in determining the components for the CCP substrate.

Table 4.2 Settings used for contact angle measurement

Parameter	Water	Ethylene Glycol	Diiodomethane
Drop size (μl)	4	3	2
Stroke pulse	9	9	8
Cannula tip position	360	360	410
Substrate position	100	100	100
Pump delay (s)	0	0	5

The steady state contact angles measured from using these liquids on the CCP substrates are itemised in **Table 4.3**, from which the surface properties of the CCP substrate have been evaluated and are also shown in **Table 4.3**. The tension in the table means the surface tension of the different liquids.

Table 4.3 The CCP surface energy calculation parameters

	surface tension	dispersive	p+	p-	contact angle
Water	72.8	26.5	48.5	11.16	74.10
Diiodomethane	50.8	50.8	0	0	47.40
Ethylene glycol	48	33.9	0.97	51.6	62.70

The CCP surface energy is calculated with the above formula, $Ax=B$ to get 34.3mN/m.

4.3.2 The roughness characteristics of the CCP

The surface topography of CCP is required to determine its roughness. This is important in contact printing as it determines the extent to which asperities are covered by the ink. The topography was measured using a WYKO NT 2000 white light interferometer [WYKO NT 2000 noncontact optical profiler (Veeco Instruments, Woodbury, NY, USA)] and the signals analysed using the WYKO vision 32 software. The operational details of the interferometer are set out in [Yesille et al. 2005, Harasaki et al. 2000]. The WYKO NT 2000 can be operated in two scanning modes, phase shifting interferometry (PSI) or vertical scanning interferometry (VSI). PSI, however, is only suitable for the measurement of very smooth surfaces as only a small measurement range is possible. VSI, however has an operating range of approximately 500 μm making it suitable for the measurement of flexographic printing plates. In this work, the VSI mode was used throughout. A 20 \times magnification lens was used and the system calibrated on at least a daily basis. In this way, the WYKO vision 32 software was then used to analyse the measurements. Measurement on the CCP substrate is shown in **Table 4.4**.

Table 4.4 The surface roughness of the CCP

measurement number	Rq (nm)	Ra (nm)
1	210.9	155.32
2	121.4	84.75
3	119.58	86.68
4	146.66	93.7
5	111.38	81.84
6	117.99	84.83
Average	123.402	86.36
Deviation	13.54039	4.453689

Table 4.4 shows that the CCP surface was very smooth with no local peaks and valleys. This confirms CCP to be a good surface on which to print with any candidate process.

From the surface energy described in 4.3.1 and roughness analysis described in 4.3.2, this the evidence of CCP performs better than the other substrates discovered in 3.5.1. This is due to the special chemical function group, acrylic, which gives more polar charge molecules to the CTAB linked with ODN and the corona treated surface after it has been coated with acrylic molecules gives more oxygen molecules with the polar charges increasing the surface energy. So the CCP can attach the ODN in the CTAB aqueous solution better than the other substrates in **Table 3.2**. The coating on the other films could be an option for future work.

4.4 Rheological characteristics of the ODN ink

The rheological properties of additives that include surfactants (CTAB) viscosity modifiers (Glycerol) and their impact on the DNA used in this work were explored.

4.4.1 Surface tension of CTAB with series concentrations

The surface tension was measured by the procedure described in 2.5.2. The aqueous CTAB solution was made through the method described in 2.2.1. CTAB is a cationic detergent having a CMC of about 0.9 mM which is measured by the electrical conductivity of an ionic surfactant solution of the surfactant solution with the increasing surfactant concentration [Naorem and Devi 2006]. The CMC value can be determined by the change in the physicochemical properties (i) the UV-vis spectrum of benzoylacetone, (ii) the fluorescence emission spectrum of pyrene monomers, and (iii) the electrical conductivity of an ionic surfactant solution of the surfactant solution with the increasing surfactant concentration [Roessler 1979; Furton and Norelus 1993; Rujimethabhas and Wilairat 1978; Worley and Myers 1992]. The CMC can be affected by many variables [Myers, 1991], temperature and pressure being of relatively minor importance. It decreases with increasing hydrocarbon chain-length of the apolar groups, and for ionic surfactants it also depends on the nature and concentration of counterions in solution. The UV-vis spectrum of benzoylacetone is satisfactory for the determination of CMC of anionic, cationic, or nonionic surfactant under any experimental conditions of electrolyte or nonelectrolyte concentration. The fluorescence method is the most versatile and precise. The electrical conductance method, obviously, can only be applied to ionic surfactants. Added electrolytes decrease the CMC, and the effect increases with decreasing charge density of the counterion [Domínguez et al. 1997]. From **Figure 4.1** the dilution point at which there is no change in the surface energy is 0.1 mM. This surface tension agrees with that at the CMC as set out in other publications [Naorem and Devi 2006, Svitova and Wetherbee 2003].

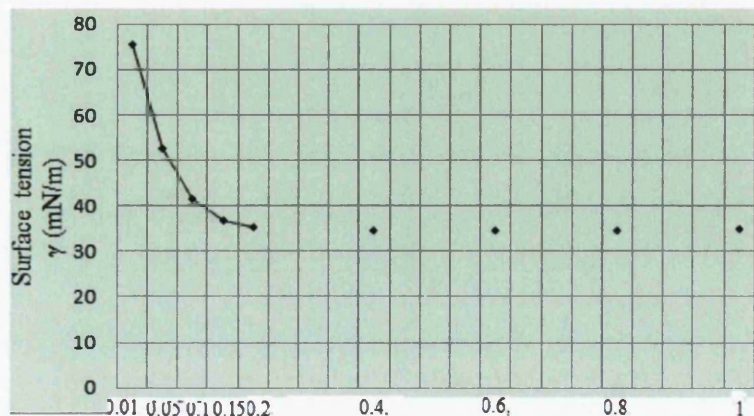


Figure 4.1 Surface tension on the dilution series of CTAB

(1-9: 0.01 mM, 0.05 mM, 0.1 mM, 0.15 mM, 0.2 mM, 0.4 mM, 0.6 mM, 0.8 mM and 1 mM CTAB)

This graph shows the surface tension of the CTAB aqueous solution to behave as a surfactant. The optimal concentration of the CTAB aqueous solution to be used with the DNA for printing will be 0.1mM beyond which no further changes in surface tension occur. This information on surface tension will also be used to understand the surface tension and rheology characteristics of the ODN ink at different dilutions using CTAB. This may also be used as the basis to choose a suitable printing technology to produce the DNA sensor.

4.4.2 Viscosity of ODN ink modification

The impact of the CTAB as a viscosity modifier needs to be established and this was done in conjunction with tests on the ODN ink. The Bohlin Gemini 200 HR Nano Rheometer was used for the viscosity test as described in 2.5.1.1. In the pre-conditioning stage, a shear stress of 0.04808 Pa was applied for 10 seconds, the test then proceeds in controlled stress mode for 900 seconds duration.

The following graphs (**Figures 4.2 and 4.3**) show the viscosity of the solvent components of the probe 1 ink (autoclaved water and the CTAB aqueous solutions) with the dilutions series described in 2.2.1. The autoclaved water was loaded following the procedure described in 2.5.1.1. The extra data are shown in **Appendix A.1**.

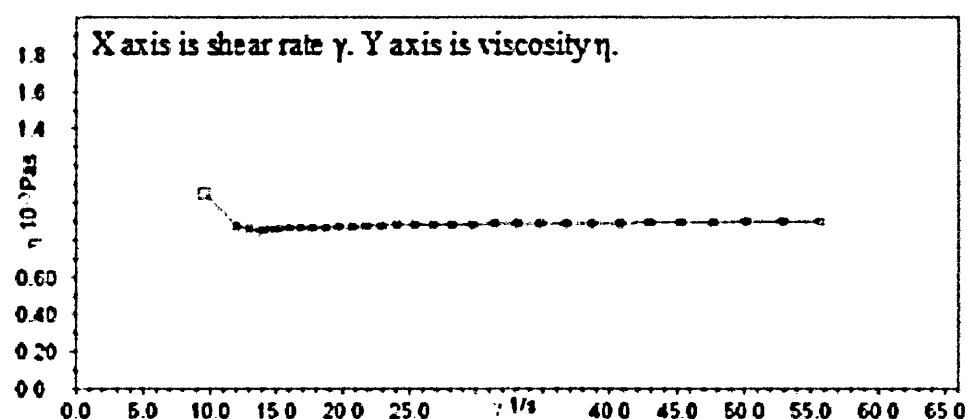


Figure 4.2 The viscosity of the autoclaved water

The graph shows the constant viscosity of autoclaved water which is typical of a Newtonian fluid and this is as reported in the literature [Kirby, 2010] and so confirms the measurement procedure is appropriate.

The effect of including CTAB at various concentrations was also explored, the results from which are shown in Figure 4.3. These show little change in the viscosity of CTAB aqueous solution at different shear rates confirming that the liquid is Newtonian. When changing the concentration of CTAB there are step changes in the viscosity level.

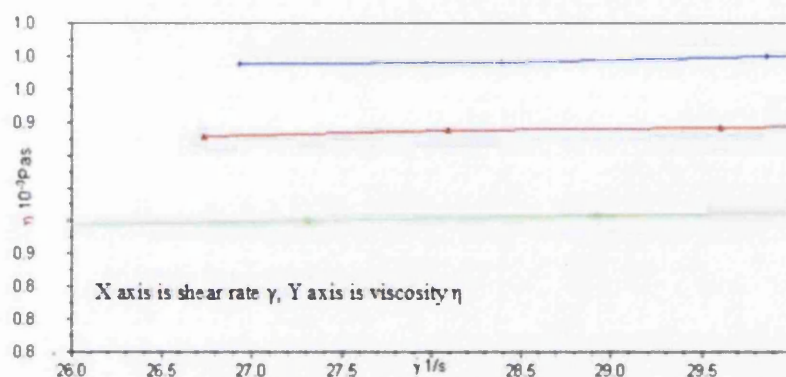


Figure 4.3 The viscosity of the typical concentrations of CTAB aqueous solutions (0.01mM - green, 0.1mM - red and 0.8mM - blue mM)

Figure 4.4 shows the ODN ink viscosity that includes the CTAB solution at 0.01.mM concentration. The response is similar to that for the CTAB solution as shown in Figure 4.3. This also shows that the ODN ink behaves as a Newtonian fluid and that its rheological response is determined by that of CTAB. A similar test was used for the other probe ink components as follows.

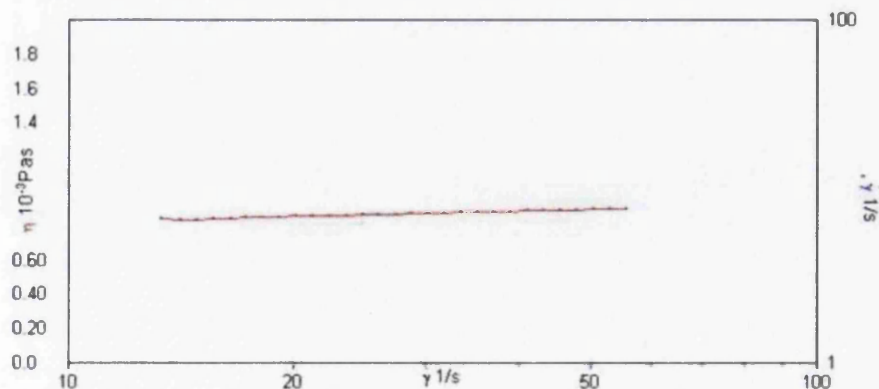


Figure 4.4 The viscosity of the probe 1 ink ($30 \times 10^{-2} \mu\text{M}$)

Rheology modification is required to make the ink compatible with the requirements of the printing process as set out in Section 4.2. For this purpose, Glycerol is a candidate additive and its impact on the ink viscosity is explored below. As CTAB determines the basic viscosity of the ink system, DNA will not be included in the solution. The results for a number of Glycerol additions are shown in **Figure 4.5**. Flexography and gravure printing need the viscosity of the ink in the range of 0.05-0.5 Pa·s and 0.05-0.2 Pa·s [Kipphan, 2001]. Glycerol was added at concentrations of 90%, 80%, 70%, 60% and 50% v/v to modify the viscosity and to establish if it can be used to make the ink printable using the contact printing methods of flexography or gravure.

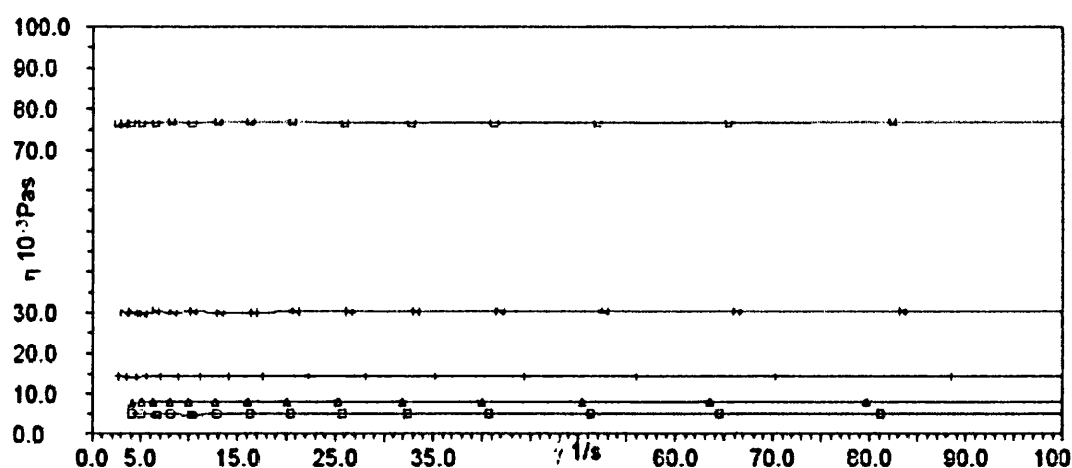


Figure 4.5 The viscosities of different concentration of glycerol in 0.1mM CTAB aqueous solutions

(lines from top to the bottom in the graph shows the concentration of glycerol at 90%, 80%, 70%, 60% and 50% v/v)

Adapting a solvent or chemical system to ensure compatibility with the ink-jet printing can be done for a wide variety of applications. In many cases, alternative synthetic approaches with solvent systems that are much more compatible with ink-jet delivery have already been reported in the literature. Adding co-solvents to the reagent that overcome the limitations of a particular reagent is also possible. In either case, care must be taken to ensure that the change in a chemical reagent or solvent does not adversely affect the yield of the desired reaction. The Glycerol increased the viscosity of the Probe 1 ink to make it possible to print using flexography or screen which has the higher viscosity requirements. However, the immobilisation of Probe 1

ink was another critical requirement for making a DNA sensor. This immobilisation reaction needs the curing of Probe 1 ink on the substrate CCP. The Glycerol modified Probe 1 ink deposited on the substrate CCP was difficult to cure on the surface of the CCP and prevented good immobilisation. Also there is strong fluorescent noise from the Glycerol solution when using the GeneTAC LSIV to scan the Probe 1 ink with the Glycerol addition. So the Glycerol was not applied in printing the Probe 1 ink. The problems on the curing are due to the high boiling point of Glycerol to resist the proper immobilisation of the ODN on the CCP.

All the substrates were cured in the chamber described in 3.3.1. The inkjet printing substrate was cut to the glass slide shape before printing, the flexography and gravure printed substrates were cut to the glass slide shape after printing.

4.5 The characterisation of the inkjet printing technology of the probe 1 ink for the DNA biosensor production

This part of the work was carried out to establish if the Probe 1 liquid could be formulated as an ink and to print it with an inkjet printer with appropriate settings.

4.5.1 Materials

This section describes the substrate and ink to be used in the inkjet printing process. The inkjet printing was done using a Dimatix material printer (DMP-2800 series) described in 2.6.1.

4.5.1.1 Substrates

The CCP was used for inkjet printing the probe 1 ink described in chapter 1.

For the purpose of handling, the substrates were cut as described in 3.3.2. The thickness of the substrate was measured by the Vernier Calliper to be 59 μm and as part of the procedure the printer was set to account for this thickness. The platen temperature was chosen to be ambient and the substrate was placed to register with the origin in the reference frame for the printer. After printing, the substrates were adhered on the glass slide with the water drop and scanned by the GeneTAC LS IV scanner as described in 2.4.1 and analysed using the procedure described in 2.4.2.2 to give a FI index.

4.5.2 Methods

This section describes the image design and analysis and the inkjet printing settings

4.5.2.1 The Fluorescent Image analyse measurement

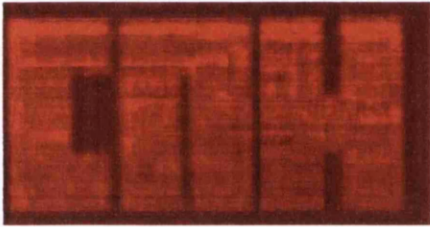


Figure 4.6 The zoom in fluorescent image of the inkjet pattern printing probe 1 ink on the CCP of words 'CNH'

The image in **Figure 4.6** has been designed as a novelty to show the inkjet pattern printing technique. The image shows the ability to print a feature pattern that comprises very many dots instead of a simple dot pattern and thus will indicate the success or failure of the head to deliver the ink over many pulse cycles. The Probe 1 ink surface tension and viscosity were out of the normal range of ink to be deposited by inkjet printing where appropriate values (viscosity in 10-12 centipoise at jetting temperature with the jettable range at 2-30 centipoise, surface tension in 28-33 mN/m at jetting temperature). However despite these concerns, attempts were made to deposit the probe 1 ink by ink jet printing, the most likely problem being one of blocking nozzles and hence incomplete feature deposition. Furthermore, the Drop Watcher and Fiducial Camera tools could not be specified because of the Probe 1 ink rheology property and the excitation wave form was restricted to default settings with single pulse waveform controls at duration scaler 1, overall width 11.520 μsec with 3.584 μsec at the individual segment controls at level 27% and slew rate 1.00 and each nozzle firing voltage is 16.

4.5.2.2 Settings

Nozzle to target distance represents a key process setting as the drop must form in this distance as well as travel to the target substrate in a controlled manner. The system automatically adjusts the height of the cartridge to 1.0 mm above the CCP, so the correct measure of CCP thickness must be entered. If this is smaller than the actual thickness this may cause the carriage to crash into or drag across the CCP. The

effective diameter of the nozzle is 21.5 μm and maximum operating frequency is 20 kHz – these are default settings. The expected position repeatability is ± 25 microns.

Also the printer was operated without performing a cleaning cycle, thus minimising the likelihood of a nozzle blockage. The extra settings are described in **Appendix A.2**.

4.5.2.3 Pattern Design

The Pattern Editor was used to design the image, part of which is shown in Figure 4.12 for which a pattern of drops can be deposited to achieve it. Droplet spacing is one printer setting that was explored in this work. Spacing can be adjusted from 5 to 254 microns. This achieved through changing the combination settings of spatial distance by adjusting the parameters in the software to change the X direction and printing grid angle by adjusting the cartridge angle. Small spacing will lead to thick local deposits whereas the converse is true for large grid spacing. Further features were added to deposit the text CNH, MNC, WCPC and ILS. Subsequent to deposition, these were washed as described in 3.4.2 and fluorescent analysis measurement carried out as described in 2.4.2.2.

4.5.3 Results and discussion

4.5.3.1 Inkjet Printing Resolution Control

Results from a typical printed image are shown in **Figure 4.7**. This figure shows areas that are printed at a range of droplet spacing, from 5 to 254 microns achieved with the Probe 1 ink even though this formulation does not fulfil the normal properties of an ink jet ink in terms of surface tension and viscosity parameters.

Figure 4.13A shows part of the image at the drop spacing of 254 μm , 230 μm , 205 μm , 180 μm , ..., 55 μm , 30 μm , 5 μm with 25 μm as the individual distance to differ the different drop spacing.

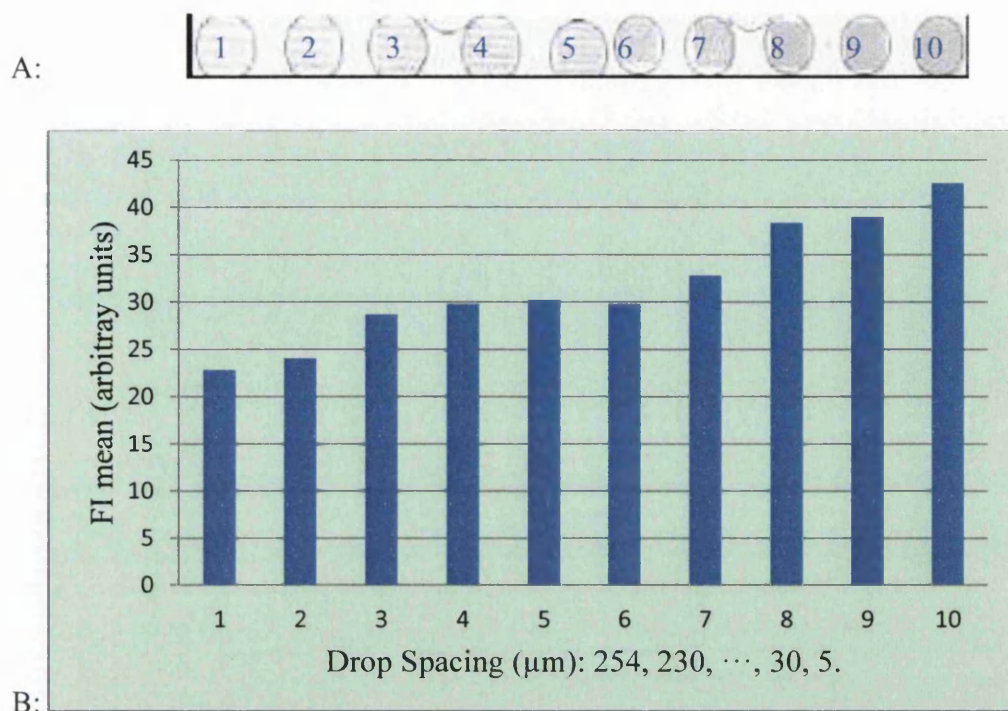


Figure 4.7 The FI signals analysis of the inkjet printing with the series of drop spacing

(A: the fluorescent images of the inkjet printing the Probe 1 ink on the CCP; B: the FI signals (mean) analysis by Image J following the procedure in 2.4.2.2)

Figure 4.7 shows the fluorescent image of the inkjet printing at different drop spacing. The solid image later was obtained from the drop spacing at 5 μm. The higher drop spacing leads to a lower resolution of the printed images and also a lower FI signal is collected. The FI profile against drop spacing does not seem to be linear and becomes flat at spacing 180, 155 and 130 μm illustrate that the inkjet printing with the ODN ink is not smooth printing but the ODN ink got stuck during delivering the ODN ink through the nozzle of the cartridge or the dot spreading mechanism. Also the drop at spacing 254 μm shows that the largest spacing with the 90 degree of cartridge angle which the 16 nozzles in a single row is located on to the X direction which the cartridge printing direction. The 4 rows of printing lines image in the blue number 1 of **Figure 4.7 A** shows that the printed probe 1 ink by the 16 nozzles adjusted in an angle vertical to the X direction but the only 4 nozzles working as the distance of the each row at about 1mm ($4 \times 254 \mu\text{m} = 1\text{mm}$). Other nozzles could be

blocked or made up to one spots with the distance 1mm nozzles before attaching the CCP. But the X direction printed spots cannot see the significant distance of spots because the spacing in X direction is handled by the motor software instead of the fixed distance between the nozzles. Following this study, the subsequent pattern printing in this section used the 5 microns drop spacing to print the Probe 1 ink on the CCP. Drop size repeatability is within 3.5% untuned and about 0.5% tuned. Generally, a 40 μm spot can be produced with a 10 pl drop which is nominal drop size. Patterns that are to be jetted are resolved into 5 μm pixels. This means that the smallest increment between one drop and the next can be 5 microns which is equivalent to 5080 dpi. At this spacing you will get drop overlap on the substrate because most spots will be at least 40 microns in diameter. The stages use 1 μm encoders.

4.5.3.2 Pattern printing

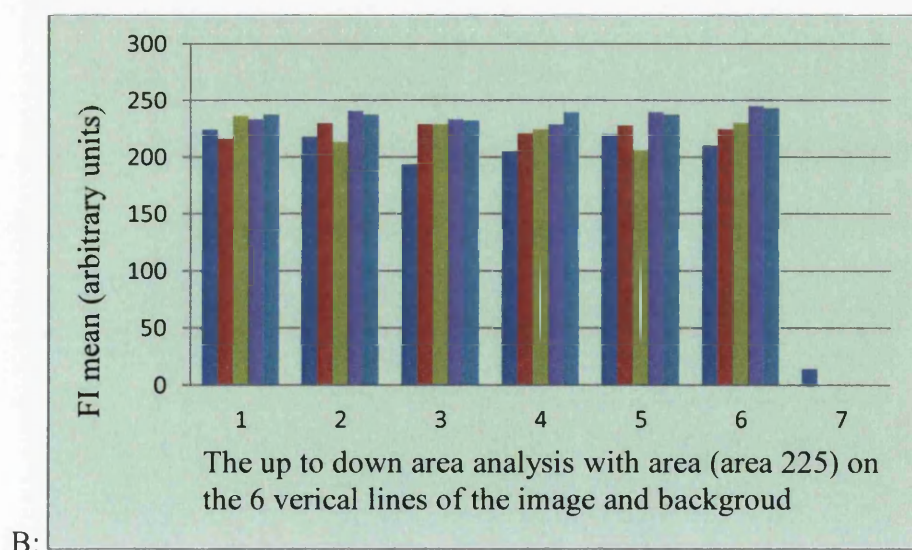
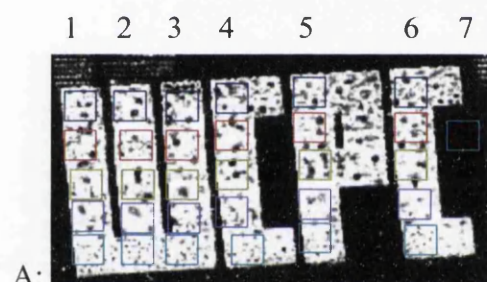


Figure 4.8 The Fluorescent Image and analysis of the Inkjet pattern printing of the probe 1 ink without washing of the word (WCPC)

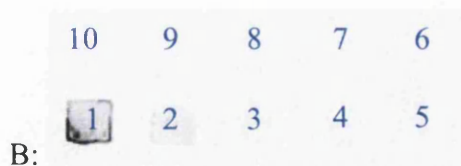
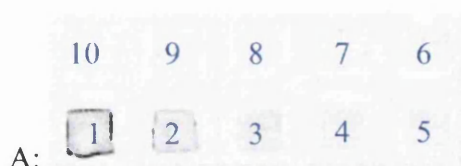
This image in **Figure 4.8 A** shows that the oligonucleotides can be printed finely with the drop spacing at 5 microns with the Probe 1 ink achieving a good image with no unprinted area confirming that the ink could be deposited without nozzle blocking.

The histogram in **Figure 4.8 B** shows a detailed quantitative analysis of this image by sections. Column 1 is on the leftmost part of the image and column 6 on the right. Within each column, the individual histogram bars reflect the FI from top to bottom – corresponding to the sequence in which the image was printed. The short bar (designated 7) is the background FI. The different colours squares in **Figure 4.8 A** which show the areas analysed by Image J correspond to the different colour bars in the **Figure 4.8 B**. This illustrates that there is more probe 1 ink coming out at the end of printing than the beginning. The different FI signals in the different areas of the line images show that the inkjet printing of the probe 1 ink is not uniform all the time. This is because the surface tension and viscosity of the probe 1 ink is not in the range of the appropriate ink value described in 4.5.2.1 and the probe 1 ink supply is caused by this limit to affect the uniformity of printing over the time.

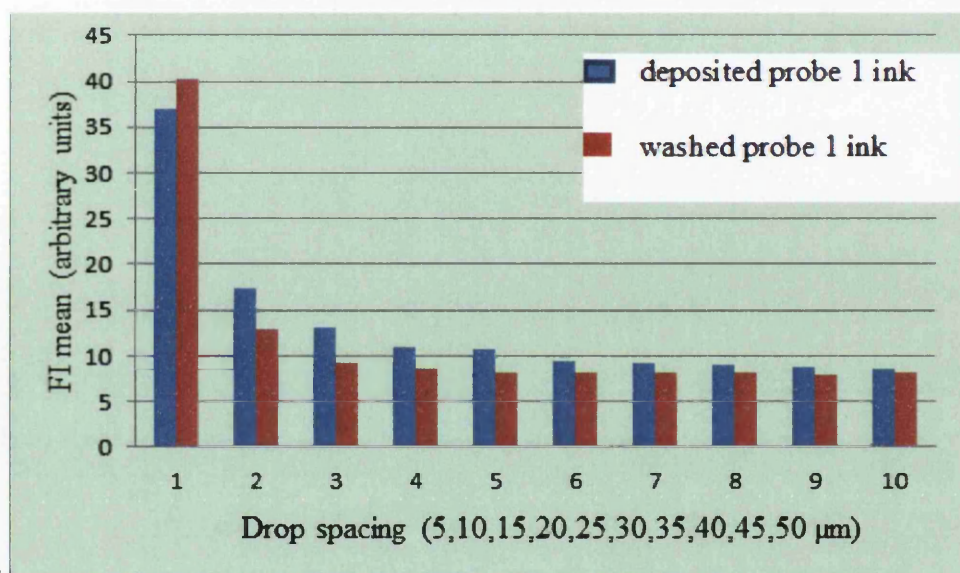
4.5.3.3 The Immobilisation investigate of the inkjet pattern printing

This section describes the effect of rinsing on immobilisation after inkjet printing the probe 1 ink on the CCP. The inkjet-printed probe 1 ink on the CCP is taken in the immobilisation reaction chamber described in 3.3.1 for one hour then the steps in 3.3 are followed to get the fluorescent images using the GeneTAC LSIV described in 2.4.1 and analysed by Image J described in 2.4.2.2.

The **Figure 4.9** shows the immobilisation of Probe 1 ink on the CCP by inkjet printing with the series of drop spacing (5, 10, 15, 20, 25, 30, 35, 40, 45, 50 μm) followed by rinsing with the TNT buffer and autoclaved water. The reason of taking this investigation is to test more details about the smooth printing image on 8, 9 and 10 taken from **Figure 4.7**



Blue bar: deposited probe 1 ink; red bar: immobilised probe 1 ink after washing by TNT buffer



C:

Figure 4.9 The FI signals analysis of the inkjet printing the probe 1 ink in the series of drop spacing pattern

(A: not washed; B: washed by TNT buffer and autoclaved water; C: the FI signals analysis of A and B)

Figure 4.9 shows the fluorescent image from inkjet printing the probe 1 ink on the CCP with the series drop spacing resolution. The FI measurement by Image J compares the images in the series of the drop spacing in the order 1 to 10 where the blue bars correspond to the condition where no washing has taken place.

In **Figure 4.9**, the rinsing did not change the FI signals too much and still shows the good immobilisation of the Probe 1 ink on the CCP after inkjet printing. The slightly

higher FI signal at a drop spacing of 5 μm after rinsing was due to migration of the ink within the rinsing liquid, gathering at the corner when drying.

This experiment shows that the different spacing images are printed by inkjet and the following printing pattern is done by the same spacing setting with 5 μm . They will show the printability and immobilisation effects of the words patterns.

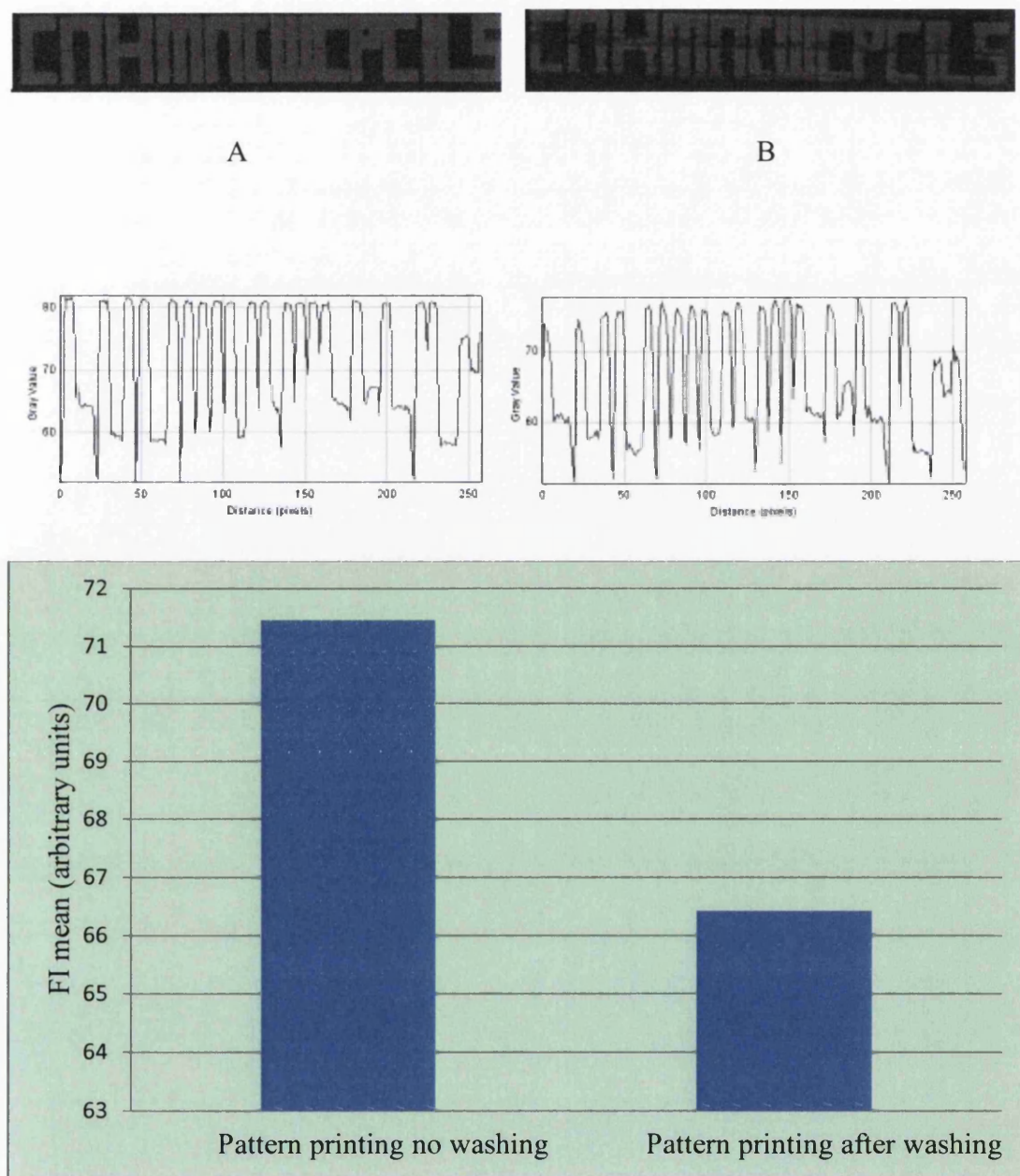
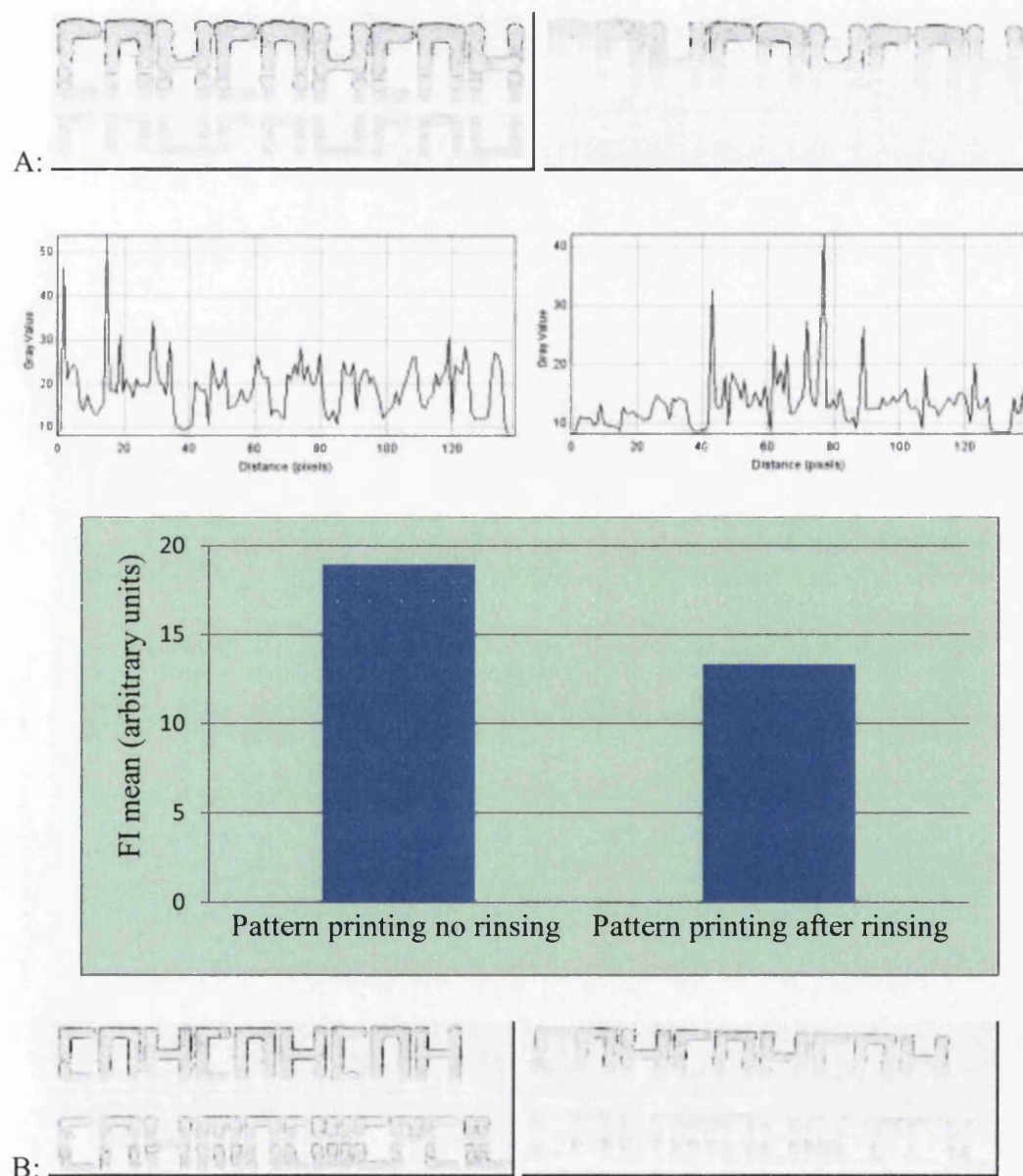


Figure 4.10 The FI signals analysis of the inkjet words pattern printing the probe 1 ink on the CCP

(A: The FI signals analysis of the inkjet pattern printing the Probe 1 ink on the CCP before rinsing with the words (CNH, MNC, WCPC and ILS); B: The same but after rinsing with TNT buffer and water)

This graph showed that the fluorescent images of the the probe 1 ink by inkjet pattern printing on the CCP to investigate the immobilisation of the inkjet-printed probe1 ink on the CCP through rinsing with TNT buffer and autoclaved water described in 3.4.2.

The Plot of Fluorescent Image could show the detailed comparison of the FI signals with the positions of the patterns.



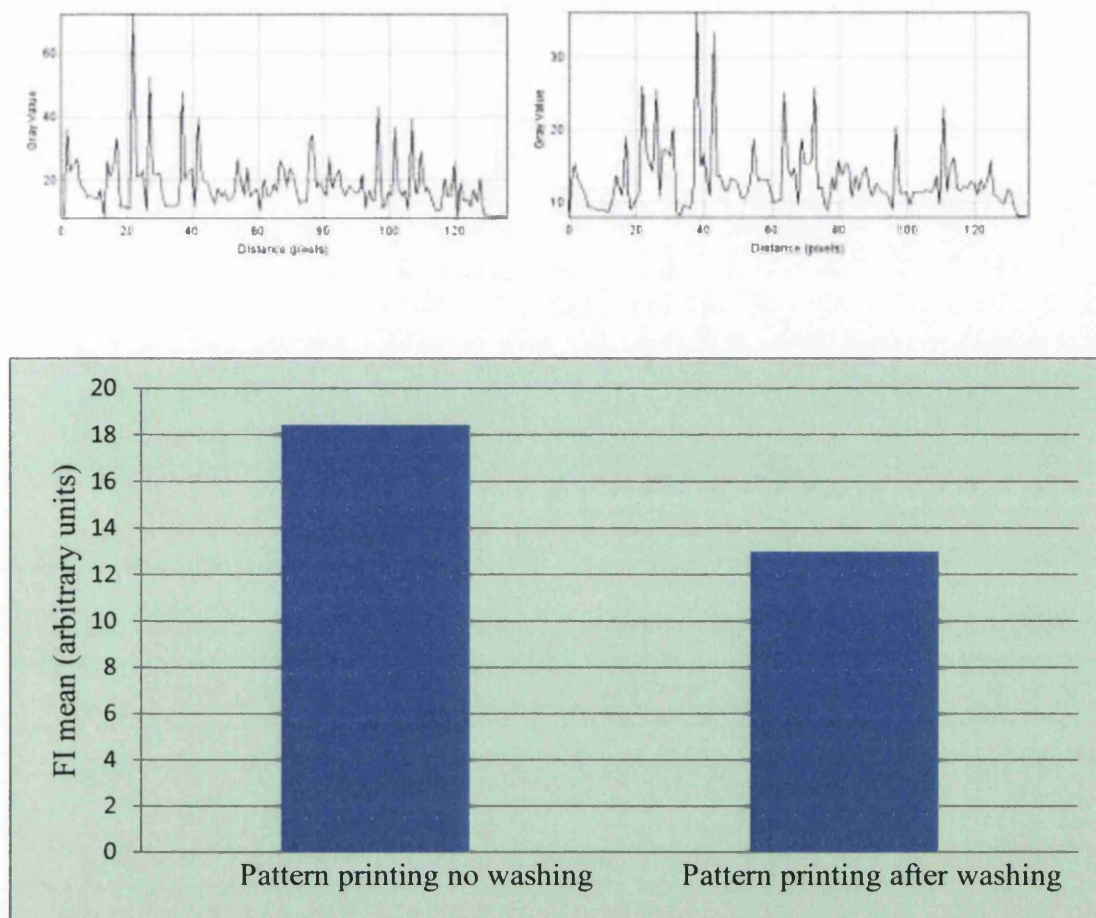


Figure 4.11.The FI signals analysis of the inkjet complex pattern printing the probe 1 ink on the CCP

(A: words pattern printing with the left (no washing) and the right (washing); B: the other kind of complex pattern printing with the left (no washing) and the right (washing))

The **Figure 4.11** showed that the FI signals analysis with the inkjet 2 complex pattern printing the Probe 1 ink on the CCP. The left of the fluorescent images of A and B shows the no washing images vice versa to the right. The plot graphs show the position FI signals analysis on the fluorescent images. The bars graph showed the FI signals analysis with the whole pattern to compare with.

These graphs in **Figure 4.11** showed that the inkjet printing could not affect the immobilization too much even though the pattern becomes complex. The vital control conditions in the inkjet printability of the probe 1 ink are the ink surface tensions and viscosity to make the smooth printing actions. From above experiments on the immobilisation investigations, it can be seen that the immobilisation of the

probe 1 ink inkjet printed on the CCP is affected by printing with inkjet rather than manual printing technique. There is lower immobilisation than the manually printing. This could be caused by the shearing force of nozzles to the probe 1 ink to affect the large scale block of probe ink immobilized on the CCP. This could illustrate some bits of the immobilisation mechanism on the forces of molecular attractions favourite on the large scale rather than small scale of molecules groups. The immobilisation effect of the large block probe 1 ink (1 μ l) deposited in the way described in Chapter 3 is better than the inkjet printing probe 1 ink nominal volume (10 pl (picoliter)) because the attached probe 1 ink layer between the droplet from the pipette and the CCP is protected by the big droplet from the evaporation after manual printing in Chapter 3 and the higher concentration of the probe 1 ink on the CCP surface caused by the evaporation when drying in the humidity chamber. The inkjet printing probe 1 ink on the CCP is easier to dry out before it is moved to the humidity and less concentration can be achieved with less amount ink on the CCP.

4.6 Characterisation of the flexography printing technology for the probe 1 Ink

This technique may be used to print the DNA at a higher speed and in large format.

4.6.1 Materials

4.6.1.1 Substrates

The CCP was cut to the size of the substrate carrier that measures (200 mm long by 50mm wide and fixed using a plastic sticking tape at each end of the carrier. The CCP was washed with ethanol aqueous solution (70% v/v) and autoclaved water to sterilise the surface of the CCP as the print was done in an open laboratory environment. Because the printed areas that will be measured are away from the substrate fixing, this is not likely to introduce any contamination issues.

4.6.1.2 Plate

The printing form pattern designed for printing the features is shown in Figure 4.18 below, comprising large solid areas and lines.



Figure 4.12 The photo image of the dots and line pattern printing form of IGT FI printability tester to print the probe 1 ink

This plate was sterilized using Ethanol aqueous solution (70% v/v) and autoclaved water. This siloxane photopolymer printing form does not degrade the DNA [Naydenova et al. 2009, Quick and Anseth 2003] and the ceramic anilox roll does not kill the DNA [Ramakrishna et al. 2001].

From the calculation converting load to engagement in the peer thesis [Hamblyn 2004], the contact engagement width (calculated to get 5.433mm) under 10 N printing forces between the printing form and the substrate is taken as the model to calculate the dots and lines area pressure held under the printing force. The dots patterns with the protection squares at the right edge of the photopolymer plate (dot size at 100 μm with the screen ruling 100 lpi at 3% coverage) shows the difference pressures by the different areas of protection squares at the both side of the printed dots patterns.

4.6.1.3 Anilox rolls

Three anilox rolls were used (402-407, 402-411, 402-419) and their engraving characteristics are summarised in **Table 4.5**. They have ceramic, laser engraved surfaces.

Table 4.5 IGT F1 anilox rolls-specified volumes and line rulings

Anilox Roll	Volume (cm ³ /m ²)	Line Ruling (lpi)
402-419	2.7	600
402-409	8	350
402-411	12	300

4.6.2 Methods

The anilox roles were sterilised by washing with ethanol aqueous solution (70% v/v) and autoclaved water before loading the Probe 1 ink. The Probe 1 ink was applied on the anilox rolls using a disposable pipette. The anilox roll (402-419) can be covered by only one drop of the Probe 1 ink (about 40 µl). The others can be covered by six drops of the Probe 1 ink (about 240 µl). After printing using the IGT F1 printability tester described in 2.6.2, the Probe 1 ink printed on the CCP was taken in the immobilisation reaction chamber described in 3.3.1 for an hour and then scanned by GeneTAC LSIV described in 2.4.1 and the images analysed using Image J as described in 2.4.2.2. This printing experiment was done using the model ink of CTAB aqueous solution (0.1mM) with the similar viscosity and surface tension as the Probe 1 ink. The printing force between the anilox roll and the printing form was tested from 10 to 500N with 50 N as the step. The printing force between the printing form and the substrate was also tested from 10 to 500N with 50 N as the step. The printing speed was tested from 0.2 to 1.5m/s. The experiments were done by using the highest speed 1.5 m/s first then adjusting the printing force and anilox force in order to get a print. The combination of printing force and speed to give a successful print may be summarized as suitable setting as follows. The load settings applied on the printability tester are itemised in Table 4.6.

Table 4.6 The IGT F1 settings for the different anilox rolls

	Printing Force between the anilox roll and the printing form: 150 N Printing Force between the printing form and the substrate: 150 N Printing Speed: 1.00 m/s	Printing Force between the anilox roll and the printing form: 200 N Printing Force between the printing form and the substrate: 250 N Printing Speed: 1.5 m/s
Anilox Roll (402-419)	Bad	Good
Anilox Roll (402-409)	Bad	Bad
Anilox Roll (402-411)	Bad	Bad

Loading the model ink of aqueous CTAB solution (0.1mM) on the anilox roll was difficult to control the ink stabilizing on the edge of nip between anilox roll and blade by the ink flowed away from the edge. The way to handle this was to drop the ink only on the top of anilox roll instead of in the nip and keep the ink droplets separate on the top of the anilox roll. The probe 1 ink is loaded in this way too. The results of printing the model ink can be seen by the naked eyes through the reflection of light on the ink images on the CCP and this need to be done quickly before evaporation of ink on the CCP takes place. The probe 1 ink printed on the CCP must be kept in a dark box and cut to fit the glass slide before analysis by the GeneTAC LSIV. The entire test for the probe 1 ink must be done in a dark environment that is kept as clean as possible by elimination of ventilation to maintain a quiescent environment.

4.6.3 Results and discussion

4.6.3.1 Dot pattern printing

These results illustrate the printed image and immobilisation effects of the Probe 1 ink as a line pattern resolution printing. In the following figure, the anilox roll (402-419) is used with the printing force between the anilox roll and printing form (200 N),

the printing force between the printing form and the substrate (250 N) and the printing speed at 1.5 m/s.

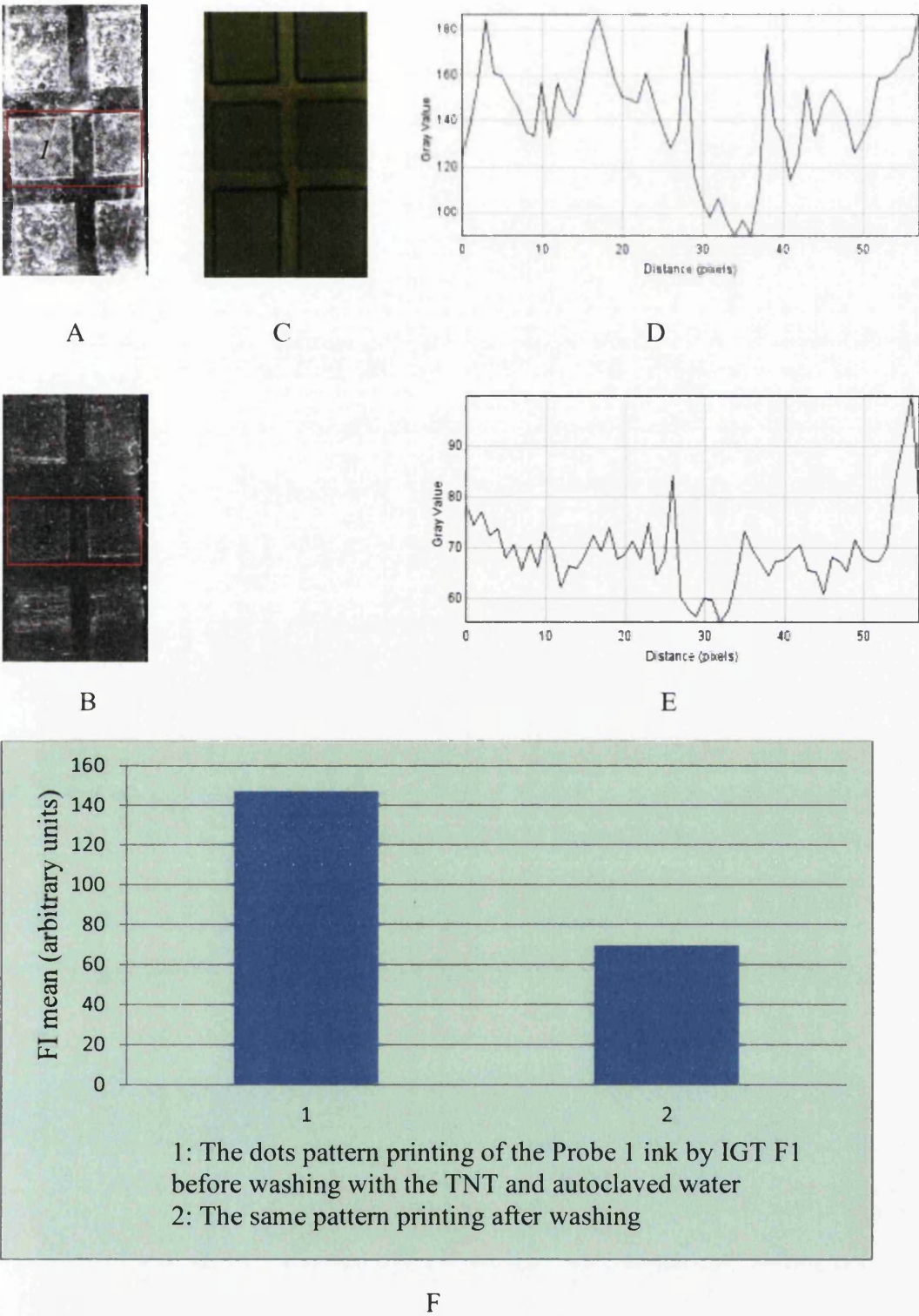


Figure 4.13 The fluorescent images and FI signals analysis of the large area pattern printing of the Probe 1 ink on the CCP before and after washing with TNT buffer and autoclaved water

Figure 4.13 comprises five components. **Figure 4.13 A, B:** The fluorescent image of the flexography dots pattern printing of the Probe 1 ink on the CCP before and after washing with TNT buffer and autoclaved water; **C:** The corresponding dots pattern area on the plate; **D, E:** The plot profile by Image J of the dots pattern printing before and after washing with TNT and autoclaved; **F:** The FI signals comparison of the dots pattern printing of the Probe 1 ink before and after washing with TNT and autoclaved water.

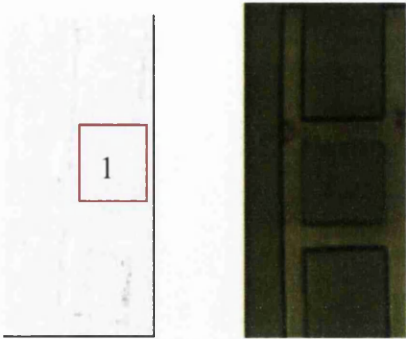
From **Figure 4.13 A**, the image shows that the dot pattern printing cannot get full coverage with the resolutions of dots in 100 lpi at 3% covering of dots (100 μm) (this dots pattern is designed for this photopolymer printing form) with the different pressure between the printing form and the substrate because the different size area holds the printing force.

This graph shows the immobilisation of the dot pattern on the CCP highlighting a poor performance. This may be attributed to failure of transfer or that the immobilisation is impaired due to the interaction between the ink and substrate.

Image transfer conditions were determined through a visual evaluation and process settings established to ensure success as set out in Section 4.6.2. The bond at the substrate is determined by potential covalent bonds forces and these are weaker than the bond between the DNA molecules and also with the Cy5. Consequently, it may be hypothesised that the failure of immobilisation is a consequence of the stresses that are generated within the nip contact. These stress effectively overcomes the immobilisation forces allowing the DNA to be washed away. This is in contrast with the ink jet deposition where the liquid may be subjected to high shear stress in the ink jet nozzle, but lower pressure when it impacts with the substrate. Nip pressure can be estimated to be $2.78 \times 10^6 \text{ Pa}$ for line pattern printing and $1.05 \times 10^6 \text{ Pa}$ for dots pattern printing and the shear stress in the ink jet nozzle to be 152Pa. However, the resilience of the DNA to stress application has not been systematically explored at this time and therefore no clear conclusion about the immobilisation failure may be drawn.

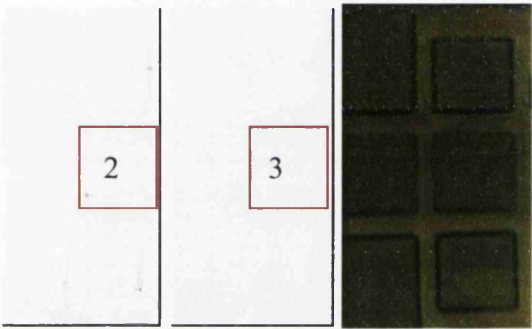
The survival tests are done for the inkjet-printed probe 1 ink through the PAGE described in Appendix B. The probe 1 ink can survive after inkjet printing with the

settings described in 4.5.2.2. This survival tests cannot be done for the flexography printing.



A

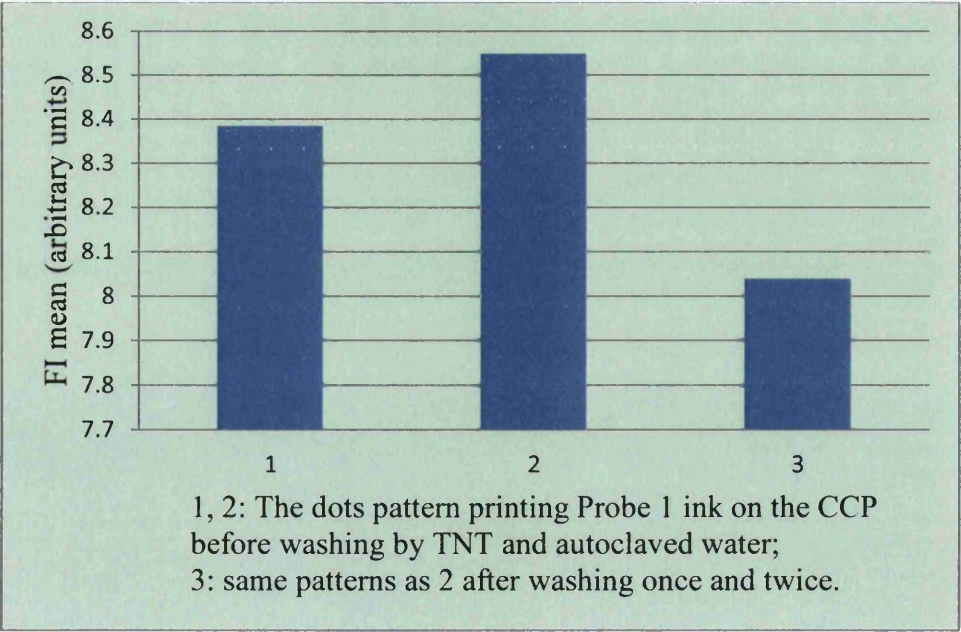
B



C

D

E



F

Figure 4.14 The fluorescent image of the flexography dots pattern printed Probe 1 ink on the CCP before and after washing with TNT buffer and autoclaved water

(A, C: The fluorescent images of the dots pattern printing of the Probe 1 ink on the CCP before washing; D: The fluorescent images of the dots pattern printing of the Probe 1 ink on the CCP after washing by TNT buffer and autoclaved water; F: The FI signals analysis by Image J of the sample B and C with the red areas illustrated on A, C and D; B, E: The correspondence areas of the dots pattern on the plate. The dots pattern is the 100 lpi at 3% coverage with dot size at 100 μm under the different pressing pressure between the printing form and the substrate because the different size area holds the printing force.

From the results above, the flexography printing of the Probe 1 by IGT F1 can be used as the printing technique to print but the fluorescent images and analysis shows that the printing effects are not as good as inkjet printing by DMP-2800 inkjet printer. The line pattern is broken and dots pattern is misting after printing. So the inkjet printing can be used as the current Probe 1 ink printing technique. The flexography printing technique needs better ink with the viscosity and surface tension improvement because the current ink is a poorly formulated one. Or the less tolerance printing technique is flexography printing than the inkjet printing for the current Probe 1 ink.

4.6.3.2 Line pattern printing

These results illustrate the existence and fluorescent images of the probe 1 ink on the CCP. In the following figure, the printing setting that were used comprise anilox roll (402-419) with anilox force (200N), printing force (250N) and printing speed (1.5m/s).

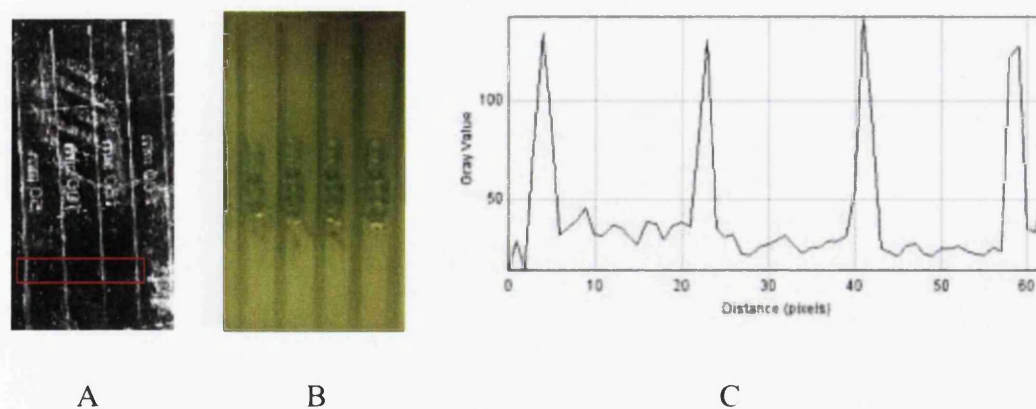


Figure 4.15 The fluorescent image and the FI analysis of the flexography line pattern printing of the probe 1 ink on the CCP

Figure 4.15 comprises three elements. A: the fluorescent images of the flexography line pattern printed probe1 on the CCP in 50 μ m, 100 μ m, 150 μ m and 200 μ m line width on the plate line pattern; B: the corresponding line pattern area on the plate; C: the analysis by Image J with the plot profile across the red area of the line pattern (see A).

This graph shows that the flexography line pattern printing of the probe 1 ink can be done but the relevant the noise over the plate and inconstant line is requiring solving in the future.

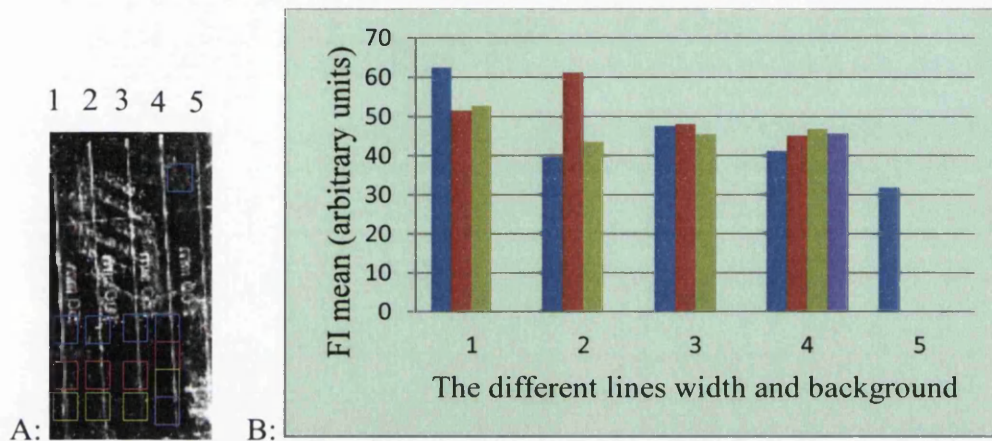


Figure 4.16 The fluorescent image and the FI analysis of the flexography line pattern printing of the probe 1 ink on the CCP (area 156)

This graph shows that the line pattern printing of probe 1 ink on the CCP gives an irregular line width for the different line widths. The colour shows the different area chosen to be analysed by Image J. The number shows the different line pattern printing with the number 5 indicated the background. The number 1 shows the line with the width of 50 μ m, the number 2 shows the line with the width of 100 μ m, the number 3 shows the line with the width of 150 μ m and the number 4 shows the line with the width of 200 μ m. From the comparison from the **Figure 4.16** A and B, the best one is the line width of 200 μ m. Also the image is affected by the background signal. The high background is caused by the splitting of the probe 1 ink on the plate roll, when printing, transferring to the CCP. Also, the real printed line width is much greater than the original printing form from 50 to 200 μ m due to the spreading of probe 1 ink under the pressure by the printing force between the printing form and the CCP.

4.7 Characterisation of the gravure printing technology of the probe 1 for the DNA sensor production

It is to test the dots pattern printing of the Probe 1 ink by IGT G1 printability tester. The fluorescent image is taken by GeneTAC LSIV described in 2.4.1 and analysis by Image J described in 2.4.2.2.

4.7.1 Materials

The Probe 1 ink ($30 \times 10^{-2} \mu\text{M}$) in the aqueous CTAB (0.1 mM) was used. The substrate is the CCP which is handled by the procedure described in 4.6.1.1. The printing disc (402-153) is used in the printing process and its engraving characteristic is described in Figure 4.17. The printing disc is copper engraved, chromium plated with the risk of the chromium plated anilox roll killing the DNA by degrade the DNA structure with small parts with or without Cy5 [Snow 1993]. The disc and the substrate CCP were washed by ethanol aqueous solution (70% v/v) and autoclaved water to sterilize before loading the Probe 1 ink. The substrate is cut by 210 mm long and 40 mm wide and fixed using a plastic sticking tape at each end of the carrier. The image was printed using the IGT G1 printability tester described in 2.6.3.

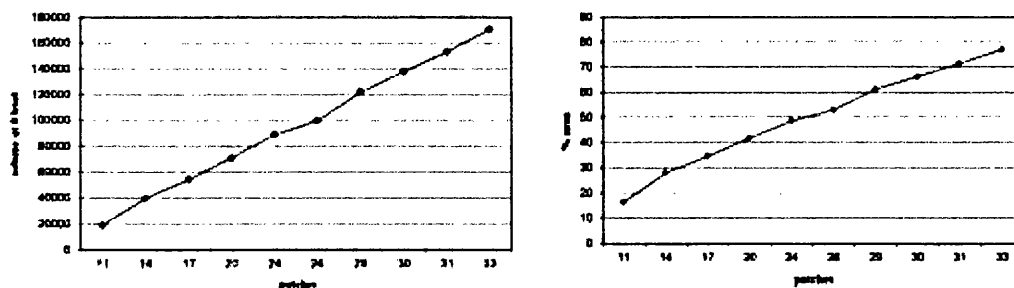


Figure 4.17 The volume and area characterisation with the different patches on the IGT G1 printing disc

4.7.2 Methods

With the similar steps as the IGT F1 described in 4.6.2 to discover the suitable settings for the printing force and printing speed, the model ink (aqueous CTAB at 0.1 mM solution) was used to test the suitable settings. The analysis of the printing results is done by looking at the light reflection of the printed model ink on the CCP. The printing speed (0.2-1 m/s) was set to the largest one first. Then, the printing force (100-1000 N) was adjusted to find the suitable level. The suitable printing

speed was found to be 0.6 and 0.8 m/s with the printing force at 1000 N to get the acceptable printed images of the gravure roll cells on the CCP. Six drops of the Probe 1 ink (240 μ l) was loaded on the printing disc using a disposable pipette to cover the printing disc for the printing process.

The way to face the difficulties is similar as flexography printing described in 4.6.2.

4.7.3 Results and discussion

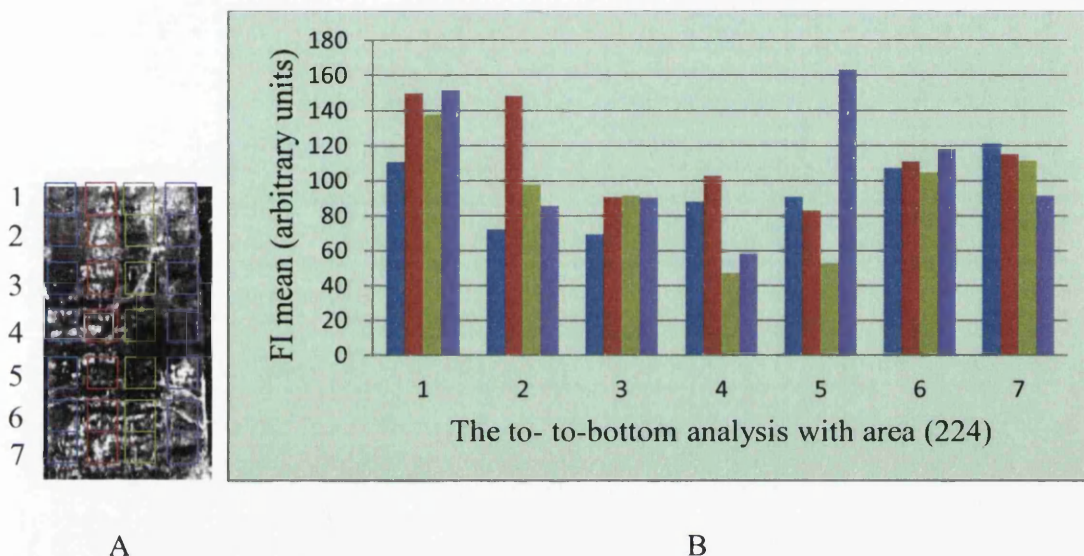


Figure 4.18 The fluorescent image and analysis of the coating roll gravure printing of the probe 1 ink on the CCP without washing.

The image in A shows that the IGT G1 can print the Probe 1 ink on the CCP with the cells of a coating roll as the print pattern. The different colour area in **Figure 4.18A** links to the relevant bar in **Figure 4.18B**. The areas have been analysed by Image J. The results show that the coating roll printing images with the different patches of volumes. The different volume shows that the different screen ruling to cover the unit area. The graph in B shows that the FI signals analysis by Image J with the area (224) to measure the image from top to bottom gives the irregular gravure printing of the Probe 1 ink on the CCP. The image in **Figure 4.18A** shows the printed image of the gravure coating roll at the patch 30, 31 and 33 for the first three patches when running the printing process. The printed images for patch 30 are illustrated in the areas chosen by 1 and 2 in **Figure 4.18A**. The printed images for patch 31 are illustrated in the areas chosen by 3 and 4 in **Figure 4.18A**. The printed images for

patch 33 are illustrated in the area chosen by 5, 6 and 7 in **Figure 4.18A**. More Probe 1 ink is spread at the bottom of printing run and less ink is left in the middle of the image. This shows that the gravure printing gives better images for the patch 33 screen ruling.

4.8 Closure

In the work described in this chapter, the surface tension of CTAB with the series concentration range and viscosity of the probe 1 ink ($30 \times 10^{-2} \mu\text{M}$) and CTAB with the series concentration range and water are tested. The surface energy of the CCP is calculated by the contact angles measurement with the three reagents. The inkjet and flexography and gravure printing of the probe 1 ink are tested. The ink jet spacing $5 \mu\text{m}$ gives overlapping drops which ensure a complete coverage of the surface. It is probable that washing then removes the surplus, confirming that this requires further work, for example measuring the quantity ink jetted and comparing this to the volume on the substrate surface. This is beyond the scope of the thesis. The key finding in this chapter is that the viscosity and surface tension of probe 1 ink allow this ink to be printed by inkjet printing technology with the more suitable results than flexography and gravure printing even though the viscosity modification ingredient (Glycerol) is added to increase the viscosity for making probe 1 ink suitable for the flexography and gravure printing. Printing with inkjet has been demonstrated successfully. For contact printing, the ink needs to be modified in terms of viscosity. However, adding glycerol makes it non-viable. Thus the surface tension and viscosity of the probe 1 ink cannot be modified by the common chemicals because any changes of those characters will affect the immobilisation on the CCP. It requires further ink development to facilitate successful transfer by either flexography or gravure. In next chapter, the suitable protocols for hybridisation experiments are investigated to understand the bioactivity of the ODN ink immobilized on the CCP.

Chapter 5 Hybridisation Study of Immobilised ODN on the CCP

5.1 Introduction

A printable DNA biosensor may be developed from the immobilisation of ODN on the CCP substrate. The purpose of this chapter was to explore the hybridisation characteristics of the immobilized ODN on the CCP described in Chapter 3.

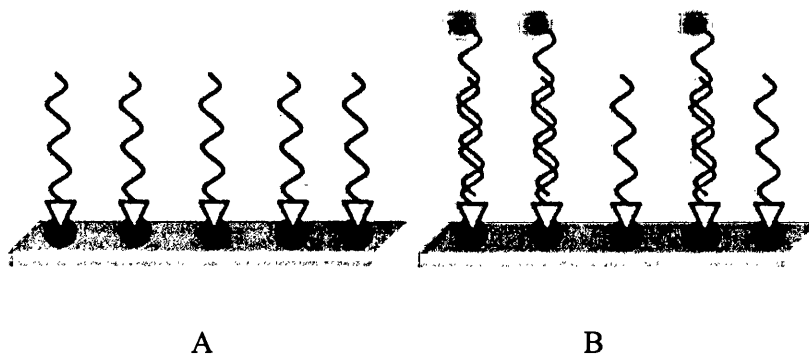


Figure 5.1 A Schematic of the principles of hybridisation [Dufva 2005]

Nucleic acid hybridisation describes a range of techniques in which single-stranded nucleic acids are incubated under conditions of temperature and ionic strength that favour pairing of complementary bases and duplex formation. The techniques are powerful and have had a major impact on knowledge of gene structure and information flow in the cell [Anderson 1999]. The main five types of hybridisation used today are solution hybridisation, filter hybridisation, the polymerase chain reaction (a specialized form of solution hybridisation), *in situ* hybridisation and hybridisation to 'chips' (a specialized form of hybridisation on a solid surface) [Anderson 1999].

In solution hybridisation, the reacting species (denatured, single strands of nucleic acid) are free in solution and are incubated under conditions that favour hybrid formation. Solution hybridisation is the stranded method for studies which determine the numbers of copies of sequences and their relatedness. Competing reactions occurring at the same time make it very difficult to interpret results. The problem can

be overcome by immobilizing one of the reacting species and this is the basis of filter hybridisation [Anderson 1999].

In filter hybridisation, single-stranded DNA or RNA is bound to an inert surface and is hybridized to a nucleic acid-the probe-added in solution. The main disadvantage of filter hybridisation is that it is much slower than solution hybridisation and the times required for hybrid formation to go to completion are often impossible to attain. Thus, it is a less useful technique than solution hybridisation for analysing rare sequences.

The technique of Southern blotting is named after its inventor, Ed Southern [Southern, 1975]. Northern blotting is similar to Southern blots except that the nucleic acid being analysed is RNA instead of DNA [Davis 1980]. In dot blots, DNA or RNA in solution is spotted on to filters and allowed to dry. For slot blots, the procedure is similar except that the nucleic acid is applied through a slot-shaped template. Dot blots are faster to set up than Southern or Northern blots. However, dot blots give no information on the size and number of different sequences contributing to the hybridisation signal. Dot blots are well-suited to analysis of many samples at once and have the added advantage that it is easy to prepare replicate filters [Anderson 1999].

In situ hybridisation is a powerful method used to locate nucleic acid sequences in histological and cytological preparations of tissues, organelles, cells and chromosomes [Leitch et al, 1994]. The polymerase chain reaction (PCR) is a procedure for generating large amounts of a specific DNA target in an enzymatic reaction [Saiki et al, 1985].

DNA chips consist of large numbers of oligonucleotides or cloned DNA sequences attached to a small surface in such a way that each sequence has a known position. Many thousands of sequences can be immobilized on a surface smaller than a microscope slide. Hybridisation usually takes place using probes labelled with fluorescent dyes. After hybridisation, the position of hybrids is detected automatically by a computer-controlled reader. Applications include sequencing and detecting mutations. The procedure is well-suited to automation, but the equipment required is specialised and is expensive. So this technique may currently be beyond the resources of many laboratories [Anderson 1999].

Hybridisation strategy: hybrids containing oligonucleotides are much less stable than hybrids of long nucleic acids. This is reflected in lower melting temperatures. The instability of the hybrids is one of the more important factors to be considered when designing oligonucleotide hybridizations. Hybridization and washing conditions are significantly different from those used with long probes. In factors affecting the hybridization of ODN and stability of hybrids, melting temperature T_m of ODN hybrids is defined as the temperature at which 50% of the hybrids have dissociated. At T_m , there is equilibrium between the dissociation and association of the hybrid. Mismatches substantially reduce the thermal stability of ODN hybrids particularly for shorter ODN [Wallace et al, 1979].

Rate of hybridization: single ODN probes hybridize rapidly to their targets [Anderson 1999].

Salt concentration: although the stability of ODN hybrids depends on the concentration of salt [Wetmur and Davidson, 1968], salt concentration is not generally used to control stringency of hybridisation. Hybridisations are usually carried out in either $6 \times \text{SSC}$ or $6 \times \text{SSPE}$. The salt concentration of washing may be reduced to $2 \times \text{SSC}$ or $2 \times \text{SSPE}$ [Anderson 1999].

Time period for hybridisation: because hybrids containing ODN are unstable even when they are perfectly matched, hybridisation times are usually kept to a minimum. This is not a problem when using single ODN probes because the rate of hybridisation is rapid. However, the actual rate of hybridisation on filters is about 3-4 times slower than the calculated rate from the pseudo-first order kinetics [Anderson, 1999]. With mixtures of ODN, the complexity of the pool is high and at an overall probe concentration of 20 ng ml^{-1} , each ODN will be present at a much lower concentration than in the above example. So incubation time has to be extended – perhaps for 1-2 days [Sambrook et al, 1989].

Washing: hybrids containing ODN may be unstable even at $T_m - 10^\circ\text{C}$. If an ODN dissociates from its complement during washing, dissociation is essentially irreversible. So, to minimise dissociation of hybrids, washing times are kept short – sometimes only to a few minutes [Anderson 1999].

Control of stringency: in practice the specificity is usually controlled by manipulating the temperature of hybridisation and the temperature, salt concentration and time of washing described in **Table 5.1**.

Table 5.1 Controlling the stringency of ODN hybridisations [Anderson 1999]

	Hybridisation	Washing
High stringency	Incubation temperature close to T_m High salt concentration ($6 \times$ SSC)	Incubation temperature close to T_m Low salt concentration ($2 \times$ SSC)
Low stringency	Incubation temperature 10°C or more below T_m High salt concentration ($6 \times$ SSC)	Incubation temperature 10°C or more below T_m High salt concentration ($6 \times$ SSC)

Optimising conditions: it is the most important for ODN hybridisations that pilot experiments are first carried out to check and optimize the selected conditions. Slight changes in hybridisation and washing conditions can have a major effect on which hybrids form and which are allowed to persist. An initial set of conditions were chosen that were estimated to be appropriate for the proposed experiment. Hybridisation is carried out and the result monitored. A further series of hybridisation is carried in which one variable is altered. The process of optimizing one variable at a time is continued until the hybridisation signal is no longer improved [Anderson 1999].

The main disadvantage in their use is that hybrids containing ODN are much less stable than hybrids containing longer nucleic acids. So great care must be taken to optimize hybridisation and washing conditions [Anderson 1999].

Washing: filters are washed extensively after hybridisation. This serves to remove both unreacted probe in solution and probe which binds loosely and non-specifically to the filter. Washing also dissociate unwanted, mismatched hybrids. Washing solutions contain salt and a detergent, usually SDS, but do not contain formamide or other denaturing agents. Manipulation of the salt concentration and temperature of

washing are important means of controlling stringency, which determines which hybrids are allowed to persist [Anderson 1999].

In most hybridisation the rate-limiting event is nucleation [Anderson 1999].

From the rate of reaction formula, the reaction conditions affect the rate of duplex formation and thus the time for which incubation must be carried out in order that the reaction goes to completion. The main variables that affect the rate of formation of duplexes are temperature, salt concentration and fragment length [Anderson 1999].

Temperature: hybridisation is often carried out at an incubation temperature (T_i) that is 20-25°C below the T_m in order to achieve the maximum rate of hybridisation. The midpoint of the increasing temperature to denaturing DNA in the simplest ways until the hydrogen bonds and stacking forces have been broken is defined as the melting temperature (T_m). The T_m of a nucleic acid is a measure of its stability.

Oligonucleotide hybrids are too short to contain both single and double-stranded regions. Their T_m is the temperature at which 50% of the molecules have dissociated into single-strands. At the T_m there is equilibrium between single-strands and duplexes [Anderson 1999].

At low ionic strength, the rate of DNA:DNA hybridisation is very low, but increases markedly as the salt concentration increases up to about 1.2 M NaCl when the rate becomes constant [Wetmur and Davidson, 1968].

Other factors: Changes in pH can alter the ionization state of bases, sugars and phosphates. Within the pH range 5-9 the hybridisation rate is essentially independent of pH [Wetmur and Davidson, 1968]. There is an effect of base composition on the rate of hybridisation, but the effect is small and is usually ignored. Increase in viscosity decreases the rate of reaction and the effect can be quite large [Wetmur and Davidson, 1968]. In practice, standard and unknown DNAs are incubated under precisely the same conditions so that viscosity affects both equally [Anderson 1999].

The difference between T_m and T_i is called the criterion. To detect distantly related sequences, conditions must be made favourable for mismatched hybrids to form. This means that the incubation temperature must be reduced considerably. These conditions are said to be relaxed, open or of low stringency. It should be noted that under conditions which permit poorly matched sequences to form, the rate of

hybridisation is less than that for perfectly matched hybrids and this needs to be taken into consideration when planning the total time of incubation. That is the reason the hybridisation temperature is chosen to make the low stringency hybridisation because there are more chances to find the proper hybridisation buffers and washing buffers. Through the mismatched probe 4, described in 5.2.1, which can be used in this purpose to check the level of stringency conditions at this temperature [Anderson 1999].

The following procedure of doing the hybridisation experiment in this chapter is led by the procedure above because the immobilisation mechanisms of the probe 1 ink on the CCP is not clearly recognized before and the basic technique of hybridisation procedure followed by the filter hybridisation will give the basic insights on the hybridisation protocol for this special immobilized probe 1 ink on the CCP.

The theoretical basis and purpose of hybridisation has been reported in the literature and is well established (Marmus 1962, Ederg 1985). Hybridisation required complementary sequences and the success is influenced principally by temperature, time, and ionic strength and physical spacing. So does buffer choice impact on the ionic strength.

The purpose of the hybridisation study was to understand the functionalities of the ODN immobilized on the substrate. Thus, the purpose of this chapter was to find a suitable protocol to do the hybridisation of the Probe 3 ink on the CCP determining a good buffer to facilitate hybridisation and a good buffer to perform washing. The optimal buffer is one that enables both hybridisation and washing. From the list of candidate buffers, the first step is to identify the buffer for hybridisation following which the list of candidate buffers may be explored to identify the appropriate washing system.

One of the more useful properties of the ODN probes is that they can discriminate between target sequences that differ by as little as a single nucleotide. The main disadvantage in their use is that hybrids containing oligonucleotides are much less stable than hybrids containing longer nucleic acids. Consequently, great care must be taken to optimise hybridisation and washing conditions.

The occurrence of hybridisation between the target 1 and probe 3 (described in 5.2.1) will be demonstrated in this Chapter. Selection of the washing buffer will be determined from the experiments presented in 5.5. To accomplish this, the ODN with the fluorescent tag (Cy5) was used as this is the only tag whose signal which can be seen after scanning by GeneTAC LSIV when hybridisation happens and when it is washed by the suitable washing buffer.

5.2 Materials

The purpose of this section is to present the preparation of the ODN ink that will be immobilized on the CCP substrate, the ODN ink for hybridisation, the hybridisation buffer and the washing buffer.

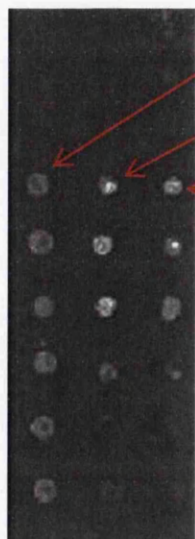
5.2.1 The preparation of immobilised and hybridised ODN ink for hybridisation

As explained in the opening remark, an ODN ink was prepared for immobilisation on the CCP substrate. This differs from the ODN ink used in the immobilisation investigation described in Chapter 3 because it does not have a fluorescent tag and furthermore is the complement of the ODN used in Chapter 3.

However, the procedure used for immobilisation onto the substrate was identical to that described in Chapter 3. This immobilisation method will be referred to as probe 3 in this chapter.

Probe 3 was the complete complimentary ODN to the target 1 (referred to as probe 1 in Chapter 3). The sequence is as follows:

5'-TCATGTTTAGTAGCTTTGAGGGAGG-3'



Control probe used as the probe 1 in Chapter 3

Target 1 used as probe 1 in Chapter 3 on the probe 3
which complimentary to the target 1

Target 1 used as probe 1 in Chapter 3 on the probe
34 which not complimentary to the target 1

The schematic graph taken from **Figure 5.9** to illustrate the probe 1, probe 2, probe 3 and probe 4.

There is no fluorescent tag (Cy5) in probe 3. So the fluorescent signals can only be detected when the ODN ink used in Chapter 3 was successfully hybridized to probe 3 on the CCP as this contains the Cy5 fluorescent tag. The T_m is 65.2 °C.

The hybridisation effect of the probe 3 was tested by comparing the FI signals of the washed spots from the hybridized probe 3 with a fourth probe (designated Probe 4) that uses an ODN that has a completely different sequence that is not complementary. The ODN ink for probe 4 was deposited on the same CCP substrate.

Probes 3 and 4 were printed in columns on the same CCP substrate to facilitate side by side comparison and to allow a measure of statistical robustness. The left column in **Figure 5.2** represents the control probe the middle column represents probe 3 and the rightmost column represents probe 4. Probe 4 is used only in the experiments described in 5.6.

5.2.2 Preparation of the hybridisation buffer

A hybridisation buffer was used as the media to support the formation of the hydrogen bonding between the probe immobilized on the CCP (probe 3) and the ODN ink (probe 1) in the hybridisation buffer. It served to make better contacts with the two complimentary ODN molecules, which were activated and stabilised in a double helix structure. The buffers used for the immobilisation experiments for the ODN probe 1 have been described in **Chapter 3**. The current focus is the hybridisation process. In these hybridisation experiments, three types of hybridisation buffer were explored as follows: Church buffer, SSC buffer and PCR (Polymerase Chain Reaction) buffer described in 2.2.2.

The requirement for the hybridisation buffers was to increase the hybridisation rate between probes 1 and 3. The current set of hybridisation buffers was chosen because they are common simple types for DNA hybridisation.

5.2.3 Preparation of the washing buffer

A washing buffer was used to remove the non-hybridized probe 1 ink from the CCP after the hybridisation experiments following the procedure that will be described in 5.3.4 and further it must not affect the immobilized probe 3. In these hybridisation

experiments, nine washing buffers were explored: the PCR buffer, TNT buffer, sterilized H₂O, Tris buffer, 500mM NaCl aqueous solution, SSC buffer, Church buffer, 1% SDS and the sodium phosphate buffer. They were all autoclaved before use to kill enzymes that have the potential to damage the oligonucleotides. The candidates were chosen on the basis of common simple washing buffers.

PCR buffer, TNT buffer, Tris buffer, SSC buffer, Church buffers, 1% SDS and sodium phosphate buffer were applied using the procedure described in 2.2.2.

Autoclave water was used for general washing. The NaCl (500 mM) was chosen mainly for reducing electrostatic repulsion [Fuentes, 2004].

Tris buffer, NaCl aqueous solution and water are used as the washing buffer because they are the components of TNT buffer which give the possible washing effects signals in details. 1% SDS and sodium phosphate buffer are used as the washing buffer because they are the components of Church buffer which give the possible washing effects signals in details.

The appropriate hybridisation and washing buffers were chosen based on the following procedure in which there were 3 candidate hybridisation buffers and 9 candidate washing buffers. The suitable hybridisation buffer was found by using the same buffer for hybridisation and washing experiments. Using a single buffer is appropriate without considering the other factors affecting the hybridisation experiments, then the only factor affecting the hybridisation experiments for a single candidate buffer when washing will be the buffer concentration when washing the hybridized ODN on the CCP. Then the main concerned factors affecting the other candidate buffers chosen for hybridisation of the ODN on the CCP will be the temperature and the pH described in 5.3.3.

5.3 Methods

The purpose of this section is to describe the hybridisation chamber, the CCP shape design, the characterisation of the parameters of hybridisation and the procedure for the hybridisation experiments. In conducting the experiments, following immobilisation of the ODN compliment on the substrate it was immersed in the hybridisation buffer by depositing the hybridisation buffer that carries the target 1.

Following deposition of the ODN ink, it was washed with the washing buffer to remove any free material.

Because the tagged ODN are free to attach to the surface in traditional filter hybridisation experiment, then the surface needs to be blocked to prevent this occurrence. After nucleic acid has been firmly bound, the filter is ready for pre-hybridisation. Pre-hybridisation serves two purposes: it equilibrates the filter with solution and it blocks sites at which the probe could bind non-specifically. During hybridisation, the labelled probe is incubated with the target sequences under conditions which allow the desired hybrids to form [Anderson 1999].

However in this work, this pre-hybridisation is not a consideration because the target 1 cannot attach to the CCP without the CTAB aqueous solution. The unique immobilisation chemistry as set out in Chapter 3 does not need to modify the surface of the substrate and ODN to show the efficiency of hybridisation after immobilisation.

The control probe 1, probe 3 and probe 4 were exposed in a similar manner as they were all deposited onto the same substrate as shown in **Figure 5.2**.

5.3.1 Hybridisation chamber design

Hybridisation needs to be conducted within a controlled environment having constant temperature and humidity levels. For this purpose, an air tight box with a small platform inside to hold a glass slide with the CCP was designed. It contained a volume of saturated NaCl solution to keep the humidity constant. This was described fully in **3.3.1**. The immobilisation reaction chamber was placed in a constant temperature hybridisation oven as described in **Appendix C.1**.

5.3.2 Substrates preparation

The substrate used was the CCP described in Chapter 3. The CCP was cut to the shape and size as 75×25 mm illustrated in **Figure 5.2**. Because the CCP was transparent, the location of the probe 3 or probe 4 (circular areas in **Figure 5.2**) immobilized on the CCP was defined by the same pattern drawn on a paper sheet as a template. This was placed underneath the CCP so that the target 1 was deposited by a pipette instead of the traditional use of a cover slide which needs a larger volume of

buffer solution to avoid mismatch. The hybridisation experimental procedure will be described in 5.3.4.

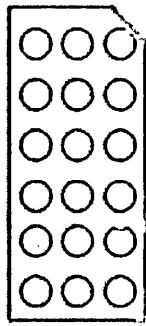


Figure 5.2 The CCP substrate shape for the hybridisation experiment

5.3.3 The characteristics of the hybridisation parameters

This section describes the hybridisation experiment parameters which concern the hybridisation of the immobilized probe 3 on the CCP.

The hybridisation parameters concerned in this chapter are the hybridisation and washing buffer temperature, the pH in the hybridisation experiments, the target 1 concentration and the duration of hybridisation.

The hybridization temperature is 47.5 °C (T_m of target 1 is 65.2 °C). The pH of the hybridization buffer lies in the range 6.5-7.5.

In the hybridization experiment, the target 1 concentration used was $90 \times 10^{-2} \mu\text{M}$. This is from the following discussion.

Sequences present at higher concentration reassociate faster than those present at lower concentration. This is the basis of reassociation kinetics (the rate at which denatured DNA becomes double-stranded) which is used to determine if DNA samples contain sequences that are repeated relative to others. This approach allows the number of copies of repeated sequences, their size and how they intersperse with unique sequences to be determined. The size of the genome can also be deduced. Repeated and single copy sequences can be isolated [Anderson 1999].

In the solution hybridisation, two complementary strands of DNA are incubated under appropriate conditions. The rate of reaction as measured by the disappearance

of single strands (into double-stranded DNA), is described by the equation [Anderson 1999]:

$$\frac{-dC}{dt} = kC \times C = kC^2 \quad (5.1)$$

Where C is the concentration in nucleotides of the single strand (mole/l), t is the time (seconds) and k is the rate constant for a second order reaction ($1 \text{ s}^{-1} \text{ mol}^{-1}$). Equation 5.1 shows that the rate of reassociation is dependent on the following: the concentration of DNA. The higher the concentration of DNA, the faster the reaction proceeds. This is because at higher concentrations of DNA there are more copies of the complementary strands than at lower concentrations and therefore collisions and nucleation events occur more frequently. In the reaction conditions, the rate constant, k , is affected by variables such as temperature, salt concentration and DNA fragment site. To allow results from different laboratories to be compared, rates of reaction are usually expressed under standard conditions. Correction factors are applied if necessary. It can be shown that the concentration of DNA remaining single-stranded, C , at time t , is related to the total concentration of DNA, C_0 , by the equation [Anderson 1999]:

$$\frac{C}{C_0} = \frac{1}{1+kC_0t} \quad (5.2)$$

When the reaction is half complete, at time, $t_{1/2}$

$$\frac{C}{C_0} = \frac{1}{2}$$

And $C_0 t_{1/2} = \frac{1}{k}$

Thus, $C_0 t_{1/2}$ is inversely proportional to the rate constant and is a measure of the rate of reaction [Anderson 1999].

Because a higher concentration of the target 1 than that of the probe 3 immobilized on the CCP can improve the hybridisation effects, the target 1 concentration is 3 times that of probe 3 or probe 4 concentrations ($30 \times 10^{-2} \mu\text{M}$) immobilized on the CCP as described in 3.4.

The duration of hybridisation of the probe 3 immobilized on the CCP was from 15 minutes to 72 hours. This was evaluated to get an appropriate hybridisation time. From the literature, the successful hybridisation for the long strand DNA requires a duration from 1 hour to 15 hours [Anderson 1999] and this has been used to guide the duration of the experiments reported in this chapter.

5.3.4 The hybridisation experiments procedures

This section is to explain the procedure for the hybridisation experiments after immobilizing probe 3 on the CCP as described in 3.3.3. The immobilized probe 3 on the CCP was prepared freshly and the pre-conditioning experiments described in 5.3.3 were carried out depending on the experiment purpose. The target 1 (30 μM) was mixed with the hybridisation buffers to make the target 1 solution ($90 \times 10^{-2} \mu\text{M}$) as described in 3.3.3 but without any CTAB. This was then pipetted (1 μl) on probe 3 or probe 4 immobilized on the CCP. The complete system was then transferred onto a glass slide and adhered using water and transferred to the platform in the humidity chamber in the hybridisation oven with the pre-set hybridisation temperature. After overnight hybridisation, this was taken out of the humidity chamber and scanned using a GeneTAC LSIV described in 2.4.1. The FI signals images were analysed by Image J software as described in 2.4.2.2. After washing and drying, the system was scanned again and the FI signals before and after washing, were compared to obtain the hybridisation effects. The FI mean signals from the control probe 1 (refers to target 1) were used as the blank reference to the hybridisation experiment and buffer washing effects.

The Image J analysis software was used to measure the FI mean of the target 1 hybridized on probe 3 or probe 4 and to compare with the control probe 1. The data compares the washing effects and hybridisation trends.

5.4 Results and discussion of the hybridisation effects with the different washing buffers

This section shows the hybridisation experiment results for the probe 3 with the different hybridisation buffers and hybridisation times from which suitable conditions were determined.

The following results show the FI mean analysed using the Image J software described in 2.4.2.2 after the fluorescent images scanned by the GeneTAC LSIV fluorescent laser scanner described in 2.4.1.

5.4.1 Characterisation of the hybridisation effects on the hybridisation of the immobilised probe 3 on CCP with the different hybridisation duration

In this section, the hybridisation buffer which was used for probe 3 immobilized on CCP in conjunction with the target 1 has been explored and the appropriate hybridisation buffer determined. In this section, the PCR buffer was resourced externally (Promega) and diluted $\times 15$.

The hybridisation buffers described in 5.2.2 were tested following the procedure in 5.3.4. The hybridisation experiments with the different hybridisation buffers were tested to show the PCR buffer gave the better hybridisation signals after washing by the PCR buffer. The other buffers washed away the deposited DNA reflecting in no fluorescence signal. These results show that the PCR buffer is the suitable system for hybridisation.

One example of the results from these tests is shown as **Figure 5.3**. In this figure (and subsequent figures) the first histogram bars represent the hybridisation duration for 15 minutes. In this histogram bars, the dark blue bar shows the control probe (probe 1), the red bar shows the probe 1 deposited on the probe 3 in the PCR buffer, the green bar represents the FI mean signal following a single wash, the purple bar represents a two wash cycle and light blue bar represents a three wash cycle. The orange bar represents the basic substrate. The second, third, fourth, fifth, sixth and seventh histogram bars show the hybridisation durations for 30 minutes, 1 hour, 2 hours, 3 hours, overnight and 3 days respectively. The different FI mean signal levels from the control probe (probe 1) arise because of the small difference that is a consequence of using different control probe spots with the manual deposited techniques described in 3.3.3. The hybridisation leads to a consistent shift of approximately 5 FI units confirming success in this process stage after overnight hybridisation. After one washing cycle the FI mean decreases, the extent of which depends on the hybridisation duration.

Following this, the hybridisation duration was investigated using only the PCR buffer as the hybridisation buffer and this will be explored further as set out in the following section.

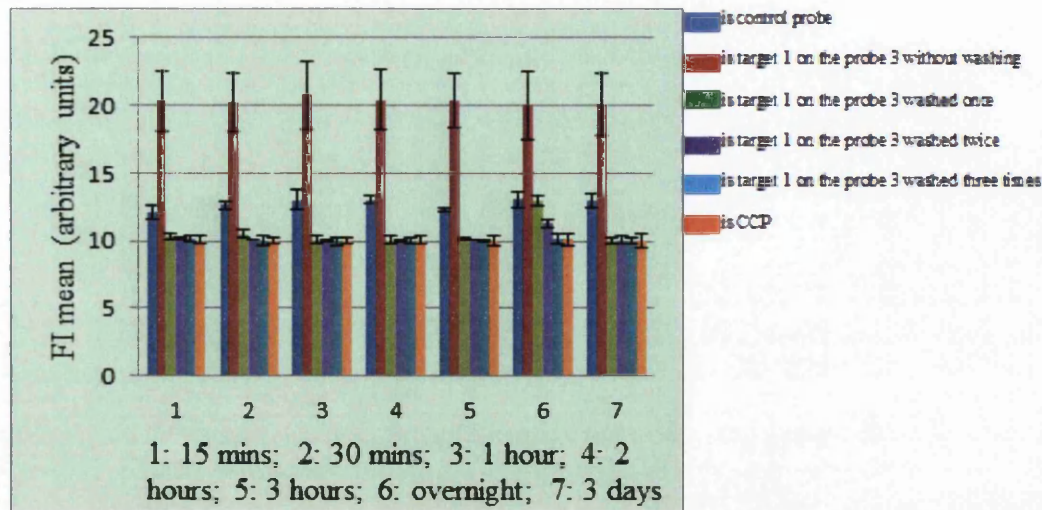


Figure 5.3 The hybridisation effects with the range of the hybridisation duration by washing with the PCR buffer

The series of the bars in **Figure 5.3** show the FI signals of the immobilized probe 3 on the different areas of the CCP for the hybridisation experiment. Because of the different deposition areas on the substrate, the bars between the series (for example: 1 and 2) could not be compared but the bars within each series are comparable.

From this graph, the sixth series of bars show the FI signals of the hybridisation of the immobilized probe 3 on the CCP after overnight hybridisation. The red bar (the deposited target 1 on the probe 3 without washing) comparing with the green bar (the deposited target 1 on the probe 3 after washing once with PCR buffer), the purple bar (the deposited target 1 on the probe 3 after washing twice) shows that there is still some target 1 hybridized on the immobilized probe 3 on the CCP after washing twice but the three times washing (the light blue bar) completely takes away the deposited target 1 on the probe 3. For the others, the FI signals decay to the background level after washing twice, so the overnight hybridisation gave the best results.

As mentioned in **5.4.1**, hybridisation duration can be an important parameter and this may be coupled with the washing process. Any linkage between an extended 3 days hybridisation duration and washing is explored in series 7 in **Figure 5.3**. But the

result shows that the 3 days hybridisation duration cannot give the good hybridisation effects in the PCR buffer.

5.4.2 Characterisation of the hybridisation effects with thermal preconditioning of the hybridisation of probe 3

When heat-denatured DNA is cooled slowly, the complementary strands re-associate to form a double-stranded molecule. This is a two-step process. First, the DNA strands collide randomly with each other and during the process may form imperfectly base-paired stretches. However, these will not be very stable and will quickly dissociate. More collisions will occur until eventually one successfully brings the bases of complementary strands into correct register. This event is known as nucleation. The second step is a rapid zippering up that produces a correctly base-paired duplex [Anderson 1999].

Incubation at a carefully determined temperature allows many initial base pairings to be sampled and broken until the most stable pairing is retained [Anderson 1999].

Instead the strands are trapped either in single-stranded or in imperfectly base-paired structures from the short hybridisation duration to give the bad hybridisation signals and easier to be washed off [Anderson 1999].

Previous work as above has highlighted the fact that the thermal environment will influence the hybridisation process and thus a preliminary experiment was carried out to explore this effect. The immobilized probe 3 was immersed into the optimal hybridisation buffer in a micro-centrifuge tube (200 μ l) which was then inserted in the Bio-Rad iCycler thermocycler (PCR) (see **Appendix C.2**). The temperature was then cycled from 90°C to 50°C. After this preconditioning, the probe 3 immobilized on the CCP was hybridized with the target 1 in the PCR buffer following the procedure described in 5.3.4. Three different washing buffers were used after the hybridisation experiment to test the hybridisation effects. The results from these experiments are shown in the following sub sections, notably PCR.

The PCR buffer has also been used as a washing buffer, but it is unknown whether this is the best buffer for this purpose following thermal preconditioning and whether it leads to some immobilised fluid being washed away due to poor adhesion.

The purpose of this section was to investigate the hybridisation effects of the pre-conditioning the probe 3 immobilized on the CCP by washing with the PCR buffer. These experiments were conducted using the procedure set out in Section 5.3.4.

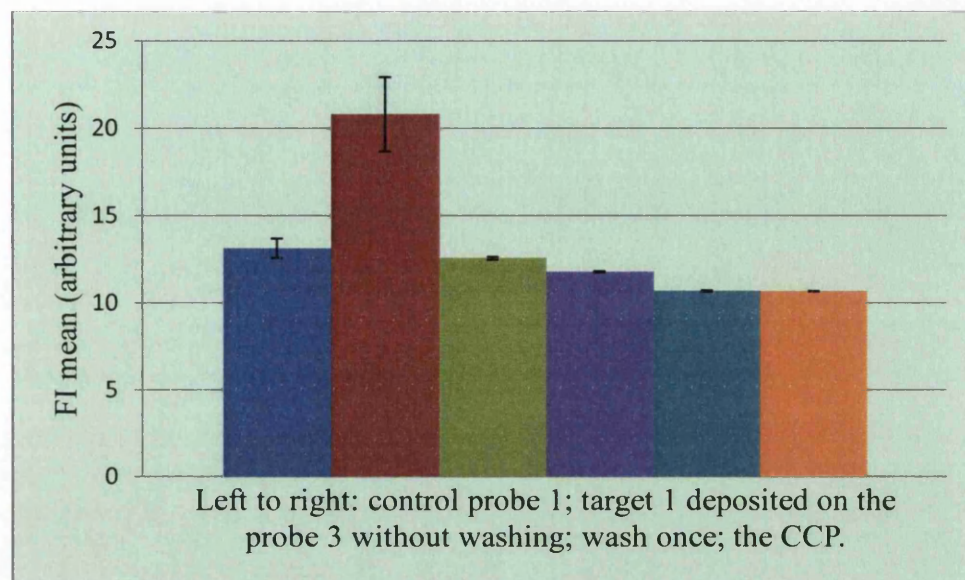


Figure 5.4 The hybridisation effects of the target 1 hybridizing experiments on the preconditioning probe 3 by washing with the PCR buffer

The results from this test are shown in **Figure 5.4**. They are similar to those displayed in **Figure 5.3** and therefore show that little benefit is gained by thermal preconditioning when using PCR as the washing buffer.

The following sections will investigate the washing effects of the hybridized target 1 on the probe 3 immobilized on the CCP by different buffer to choose the suitable washing buffer after hybridizing in the PCR buffer overnight. The washing buffer described in 5.2.3 will be investigated in next section.

5.5 Results and discussion of the characterisation of the washing effects of the hybridisation of the probe 3 immobilised on the CCP by washing with the different washing buffers

To discover the suitable washing buffer to the hybridisation of the target 1 on the probe 3 immobilized on the CCP is as follows.

The previous sections have confirmed that overnight hybridisation using a PCR buffer is the appropriate choice and this was adopted in this part of the study. In

completing this, thermal cycling was employed, but as confirmed in section 5.4.2 this had no effect. This had not been explored and analysed fully at the time of conducting the experiment within this section.

The washing buffers described in 5.2.3 were tested followed the procedure in 5.3.4.

The control probe 1 is the control for the hybridisation experiment comparison with the probe 3 and this was used as the proof that the immobilized ODN was not washed away by the washing buffers.

The target 1 in the PCR buffer ($90 \times 10^{-2} \mu\text{M}$) was used to do the overnight hybridisation following the procedure described in 5.3.4.

Within this part of the experimental programme, it is difficult to carry out a direct comparison between different washing buffers as it is necessary to deposit a series of drops on a series of substrates. As explained in Chapter 3 the manual nature of this work makes precise repetition difficult in a practical setting. However because the impact of washing is likely to be significant, the impact of such difficulties will be minimised.

The washing durations are not precisely identical. However, washing repetition time was explored. In repeating the washing cycle practically, this was achieved by repeated immersion and agitation within the washing buffer for typically 15 seconds.

5.5.1 Investigation of the washing effects by washing with the TNT buffer, Water, Tris Buffer, NaCl and SSC buffer

The purpose of this section was to investigate the washing effects of the hybridized target 1 on the immobilized probe 3 on the CCP by TNT buffer, water, Tris buffer, NaCl and SSC buffer as the washing buffers. These experiments were conducted using the procedure set out in Section 5.3.4.

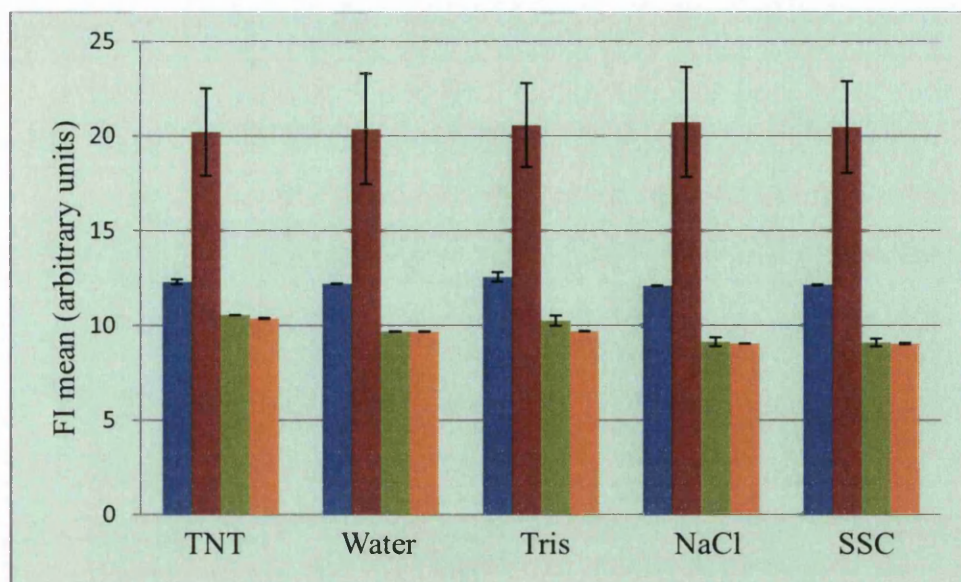


Figure 5.5 The washing effects of the target 1 by washing with the TNT buffer, Water, Tris buffer, NaCl and SSC buffer

This graph shows the washing effects by 5 different washing buffers. The blue bar in each series shows the control probe immobilized on the CCP. The red bar shows the deposited target 1 on the probe 3 immobilized on the CCP without washing. The green bar shows the deposited target 1 on the probe 3 immobilized on the CCP after washing once. The orange bar in each series show the FI mean signals of the CCP. The TNT buffer washing effects on the hybridisation experiment of the target1 and the probe 3 immobilized on the CCP showed the similar results as washing with the water, Tris buffer, NaCl and SSC buffer. They do not show the good washing effects because the deposited target 1 was washed away after once washing.

A very useful table detailing relative rates of DNA: DNA association at different ionic strengths has been drawn up [Britten et al, 1974]. For DNA: DNA hybridisations, the effect of salt concentration on the reaction rate has not been studied in such detail. However, the rate increases by 5-6 folds when ionic strength is increased from 0.2 to 1.5 M NaCl [Anderson 1999]. But here 500 mM NaCl cannot see good washing effects which stabilize the hybridized target 1 on the immobilized probe 3 on the CCP.

5.5.2 Investigation of the washing effects by washing with the Church buffer

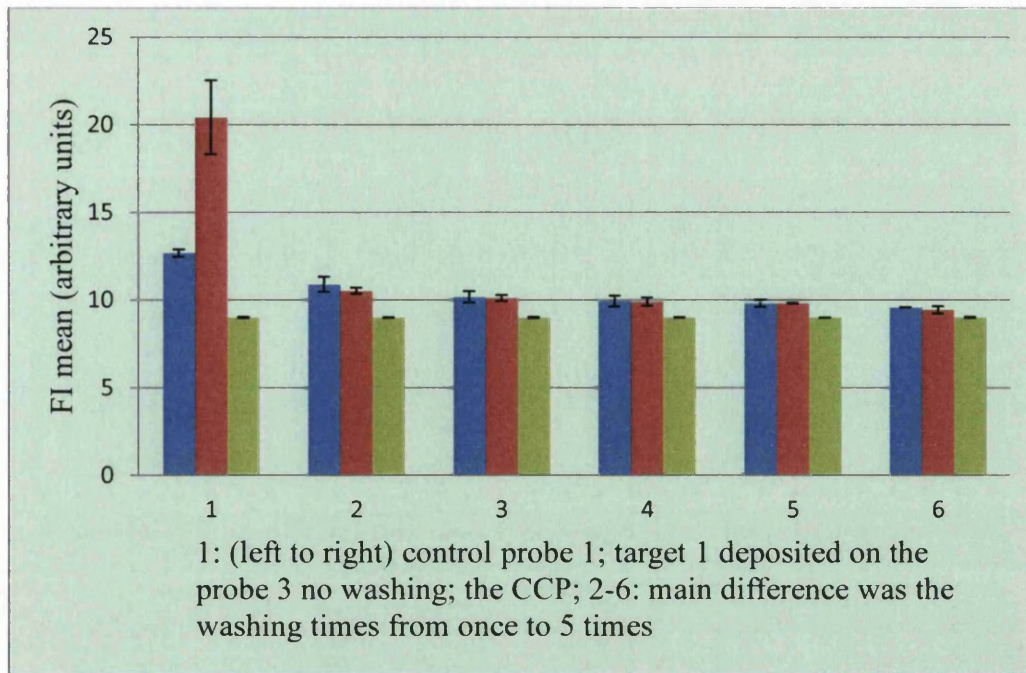


Figure 5.6 The washing effects of the target 1 by washing with the church buffer

Figure 5.6 shows the effect of washing using the church buffer. The green bars show some increasing trend after series washing cycles. This is caused by the contamination of the washing cycles on the CCP. It was not a good candidate to be as the washing buffer of the hybridization experiments because the blue bars show the decrease of control probe 1 by the church buffer washing.

5.5.3 Investigation of the washing effects by washing with the SDS (1%) aqueous solution

The purpose of this section was to investigate the washing effects of the hybridisation duration for overnight by SDS (1%) as the washing buffer. These experiments were conducted using the procedure set out in Section 5.3.4.

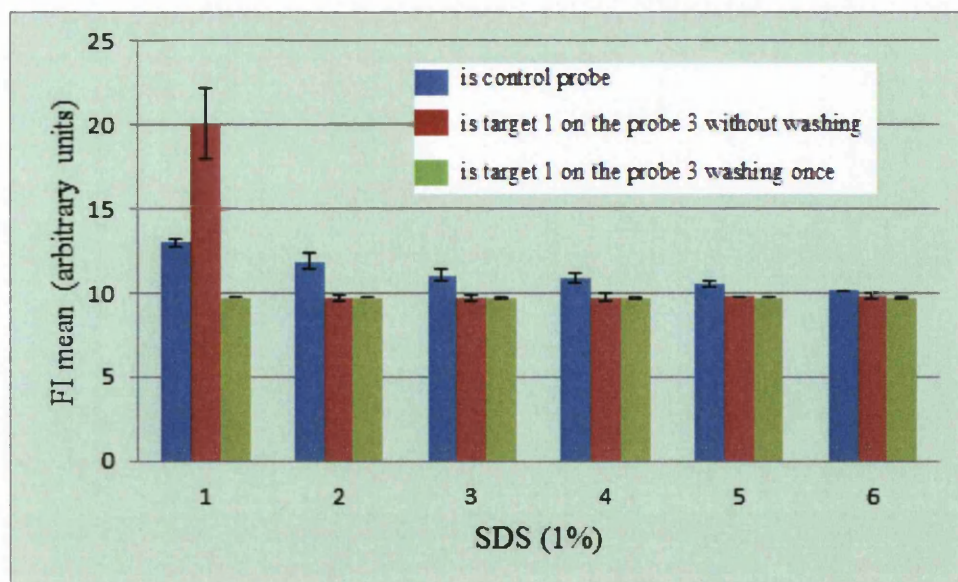


Figure 5.7 The washing effects of the target 1 by washing with the SDS (1%) buffer

This graph showed the 1% SDS washing the hybridisation of the probe 3 immobilized on the CCP. The bar arrangements are same as **Figure 5.6**. It is no good washing candidate with such results illustrated because 1% SDS has the same problems as the Church buffer which wash the immobilized control probe 1 away. This can be explained by the SDS which is anionic surfactant damaging the immobilisation of control probe 1 on the CCP. This mechanism is illustrated in **1.2.8**.

5.5.4 Investigation of the washing effects by washing with the sodium phosphate buffer

The purpose of this section was to investigate the washing effects of the hybridisation duration by sodium phosphate buffer as the washing buffer. These experiments were conducted using the procedure set out in Section **5.3.4**.

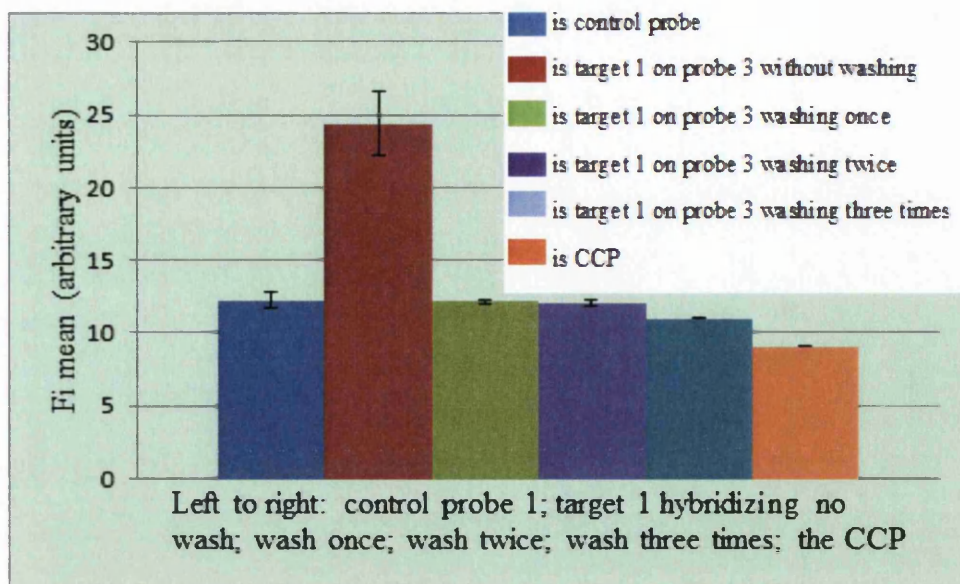


Figure 5.8 The washing effects of the target 1 by washing with the sodium phosphate buffer

This graph showed the sodium phosphate buffer washing the target 1 on the probe 3 immobilized on the CCP. This is the clear view about the better stable FI mean remained after washing three times with the sodium phosphate buffer.

In next section, the sodium phosphate buffer is used as the washing buffer to examine the hybridisation stringent effects of the target 1.

5.6 Results and discussion of the hybridisation stringent effects with the suitable hybridisation and washing buffers

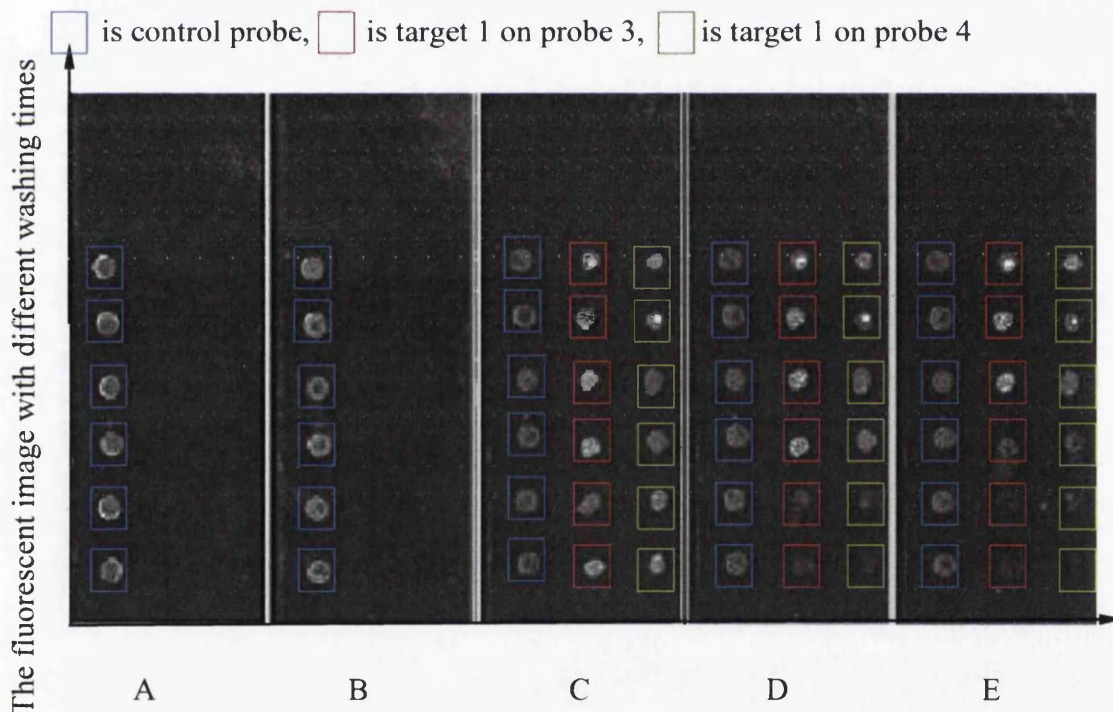
5.6.1 Characterisation of the hybridisation stringent effects on the hybridisation of the probe 3 immobilized on the CCP by washing with the sodium phosphate buffer

The purpose of this section was to investigate the hybridisation stringent effects of the hybridisation of the target 1 on the probe 3 immobilized on the CCP by washing with the sodium phosphate. These experiments were conducted using the procedure set out in Section 5.3.4. The target 1 in this section is in concentration equal to the probe 3 ($30 \times 10^{-2} \mu\text{M}$) to understand better the hybridisation stringent effects instead of the concentration priority on the hybridisation.

Figure 5.9 shows the process of washing to the target 1 hybridizing on the probe 3 and the probe 4 in the PCR buffer. On the slide A, the left column spots showed the

control probe 1 (blue) immobilizing on the CCP, the middle and right column showed the invisible probe 3 and probe 4 immobilizing on the CCP. All the immobilisation experiments were followed to the process in Chapter 3. On the slide B, the same spots as the slide A but washing once with the TNT buffer described in chapter 3. On the slide C, the slide was washed three times with the TNT buffer then doing the hybridisation experiments described in 5.3.4. In each image slide from C to J, these fluorescent slide images showed the visible signals of the washing process. The changing FI mean signals of the spots images showed the washing process in the same slide but different washing times described in 5.6.2. The more faded FI mean signals of the spots, the more washing times the spots are obtained.

This graph also showed the hybridisation stringent effects of the target 1 hybridized on the probe 3 immobilized on the CCP (red square spots on slides, C to J) by washing with the sodium phosphate buffer. It remains FI signals after washing seven times comparing the weaker signals on the target 1 hybridizing on the probe 4 immobilized on the CCP (green square spots on slide, C to J) described in 5.6.2.



Control probe, target 1 on probe 3, target 1 on probe 4 on the same slide with different washing times

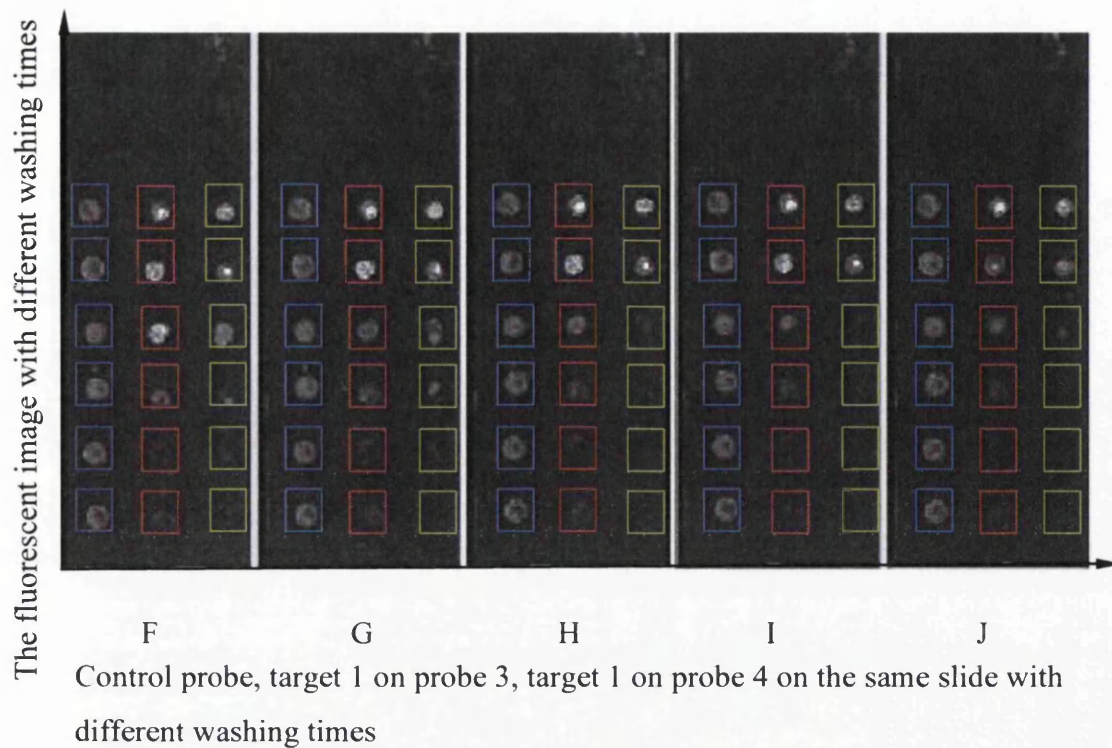


Figure 5.9. The fluorescent images analysis of the hybridisation effects of the target 1 by washing with the sodium phosphate buffer

Figure 5.10 is the typical graph that shows the experiment to check the sodium phosphate washing effects followed by the arrangement of control probe 1, probe 3 and probe 4 above but washing the whole slide instead the washing process described in 5.6.2.

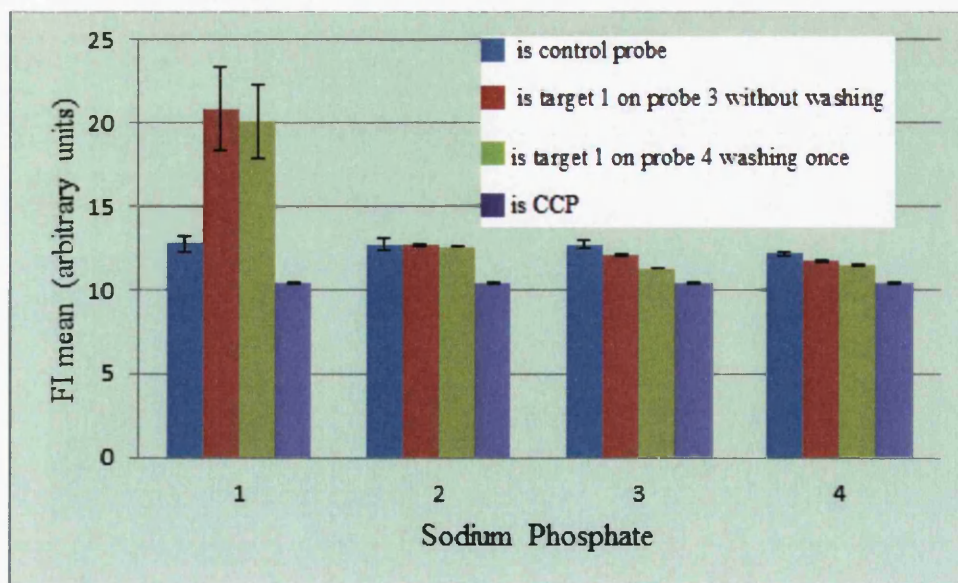
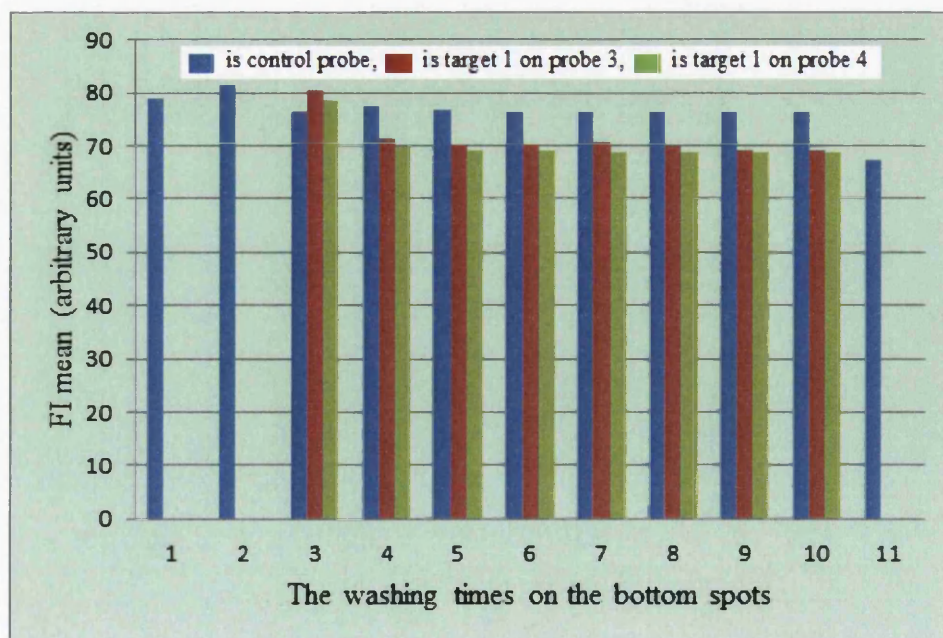


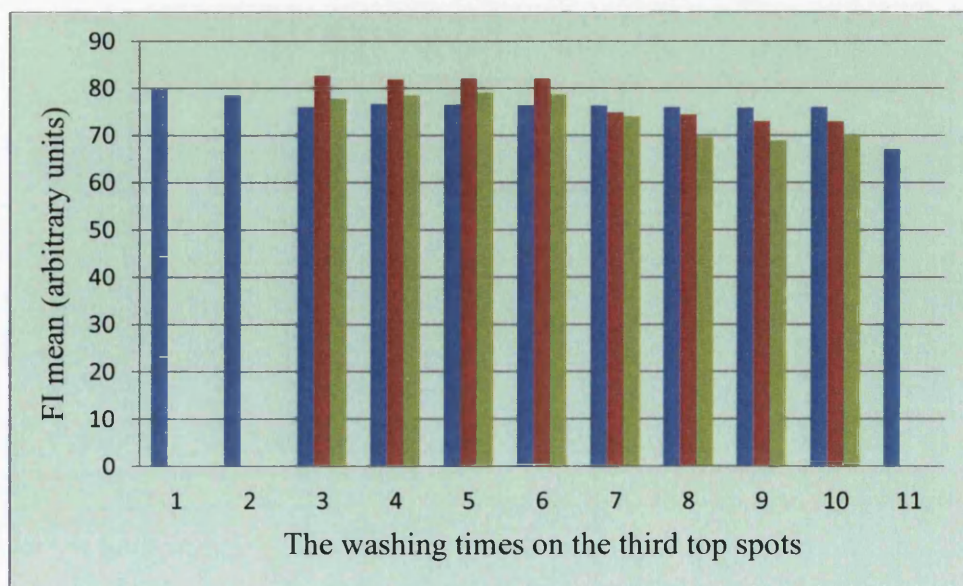
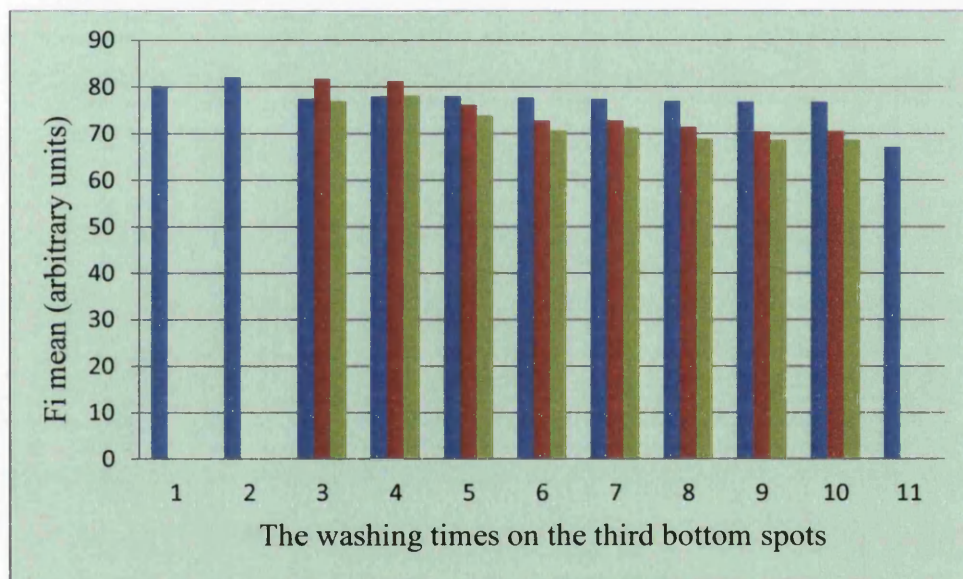
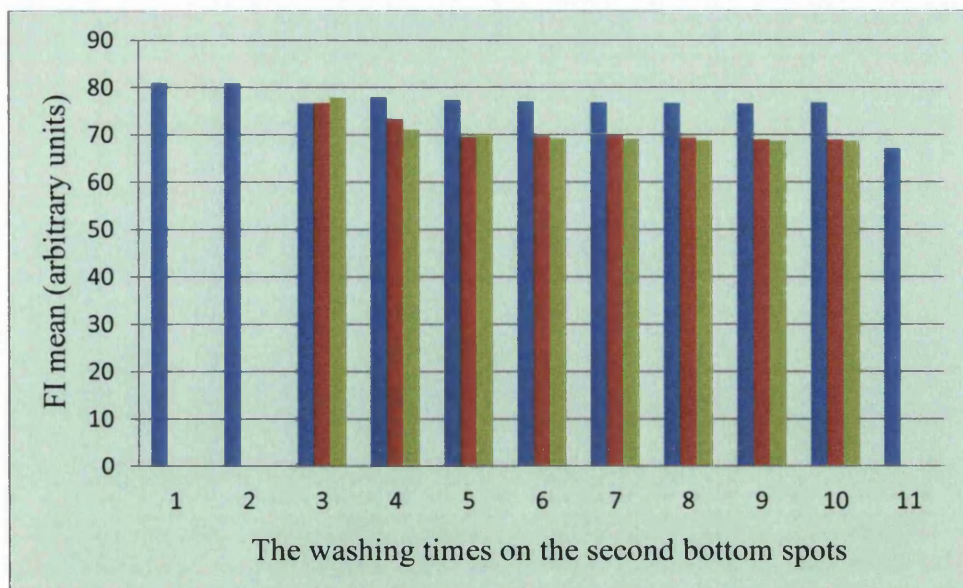
Figure 5.10 The hybridisation stringent effects of the target 1 hybridizing on probe 3 by washing with the sodium phosphate buffer

This graph showed the typical FI mean signals analysis of the sodium phosphate buffer washing the hybridisation experiments. The blue bars show the control probe 1, the red bars show the target 1 hybridizing on the probe 3 immobilized on the CCP, the green bars show the target 1 hybridizing on the probe 4 immobilized on the CCP and the purple bars show the CCP. The first series show the FI mean signal of these samples as above without washing. The second to fourth series show the FI mean signal of these samples as above washing once, twice and three times respectively. It showed some good signals to be the optimal candidates as the washing buffer with the FI signals left after several washing process. Further investigated was described in 5.6.2.

5.6.2 Characterisation of the hybridisation stringent effects of the probe 3 immobilised on the CCP by washing with the sodium phosphate buffer as the washing buffer in detailed analysis

The purpose of this section showed that the hybridisation stringent effects analysis by washing with the sodium phosphate buffer on the target 1 on the probe 3 immobilized on the CCP in the PCR buffer as the hybridisation buffer. The analysis process shows that the times of washing gave the insights into the hybridisation stringent effects by comparing the FI mean signals between the probe 3 and probe 4 after different times of washing with the sodium phosphate buffer. The meanings of bars colours are shown in **Figure 5.9** with the different columns of ODN spots.





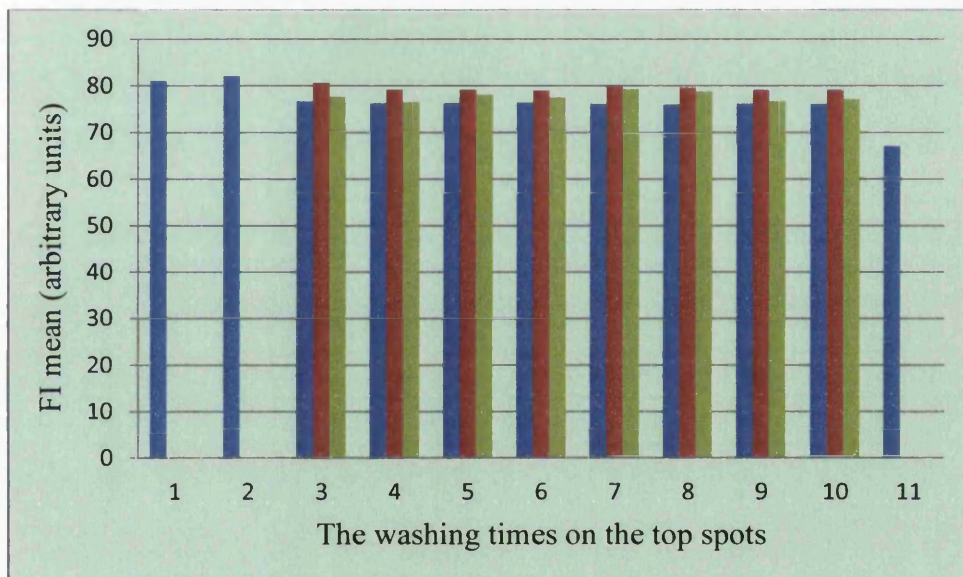
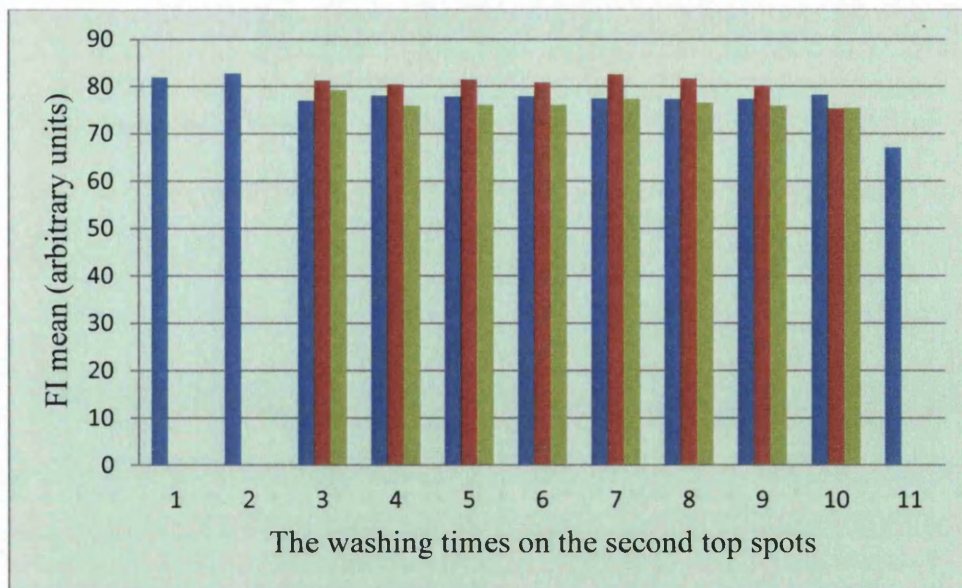


Figure 5.11 The hybridisation effects analysis of the target 1 by washing with the sodium phosphate buffer (area 304)

This graph showed the analysis process of the hybridisation stringent effects by washing with the sodium phosphate buffer. The details images were showed in **Figure 5.11**. The first two series bars (shown in A and B of **Figure 5.9**) showed the control probe 1 FI signals with the CCP background before the target 1 was hybridized on the probe 3 and probe 4. The third bar series (shown in C of **Figure 5.9**) showed that the hybridisation without washing of the control probe 1 (blue), target 1 hybridized on the probe 3 (red) and the probe 4 (green). From the fourth series bars (shown in D of **Figure 5.9**), it can be seen that the washing process began

with the washing once with the two bottom spots including the control probe 1, the target 1 hybridized on the probe 3 and the probe 4. The fifth and sixth series bars (shown in E and F of **Figure 5.9**) showed the starting to wash on the three bottoms spots including the control probe 1, the target 1 hybridized on the probe 3 and the probe 4. This was continued to start washing 4 bottoms spots in seventh and eighth series bars (shown in G and H of **Figure 5.9**). The ninth series bars (shown in I of **Figure 5.9**) showed the starting to wash on the fifth bottom spots. The final series bars (shown in J of **Figure 5.9**) showed the sixth bottom spots washed. The different spots have different washing times. For example, the bottom spots have 7 washing times because it starts to repeat immersing the washing buffer from fourth series bars (shown in D of **Figure 5.9**) until tenth series bars (shown in J of **Figure 5.9**). The spots numbers were the numbers of the spots on each column of the slide not the numbers of spots on each slide.

This graph showed that the control probe 1 was not affected by the washing buffer, sodium phosphate buffer. The FI mean signals of the target 1 hybridized on the probe 3 immobilized on the CCP could show some hybridisation effects. But comparing with the FI mean signals of the target 1 hybridized on the probe 4, this hybridisation did not so stringent to the complimentary ODN but in case the probe 4 obtained the shorter sequence of the ODN or the similar sequences.

The hybrids will be less stable (lower T_m) than the perfectly matched parental DNAs. This is because that in the mismatched hybrids there are fewer hydrogen bonds to be broken in order to dissociate the strands [Anderson 1999]. Nucleic acids containing mismatched bases are less stable thermally than perfectly matched duplexes [Anderson 1999]. The more mismatches there are, the less stable hybrids are. Every 1.7% base pair mismatching in DNA reduces the T_m by 1°C [Caccone, 1988]. Conditions which prevent formation of mismatched sequences are said to be stringent or of high stringency [Anderson 1999].

From **Figure 5.11**, it can be seen that the weak FI mean signal from the washed hybridizing target on the probe 4 immobilized on the CCP shows that the hybridisation stringent effects by washing with the sodium phosphate is low because the probe 4 gives the similar FI mean signals as the hybridized target 1 on the probe 3 immobilized on the CCP after washing many times on the different spots.

5.6.3 The reasons of the obscured hybridisation results

As in Chapter 3, the immobilisation mechanism between the ODN ink and the CCP has not been explored by other researchers. The hybridisation experiment influences the immobilisation bond by the hybridization and washing buffers with changing the electrostatic charges around the ODN immobilized on the CCP. Therefore, the amount of the ODN molecule stretching out of the CCP surface (effective hybridization ability ODN) is changing over the time and place to give no optimised hybridization and washing effects.

5.7 Closure

This Chapter shows the experiments on hybridization of the probe 3 immobilized on the CCP. The results show that the way of hybridization employed works, but establishing the optimal conditions requires further investigation. Ideally, the DNA needs to be immobilised so that the axis is normal to the substrate as this will facilitate exposure of links to bond during hybridisation. Optimisation will seek to establish the buffer as washing solutions that will facilitate this. This could include adding a series salts, changing pH or changing temperature. There are many combinations of parameters to explore and this will be considered as work to be done beyond this thesis.

Chapter 6 Conclusions and Future Work

The work in this project has focused on an experimental approach to exploring the feasibility of printing DNA on a flexible polymeric substrate by volume printing processes, which includes contact methods. This included exploration of wetting and adhesion, printing by inkjet (as a reference), flexography and rotogravure. The formulation of a DNA ink and its hybridisation was also explored. Each of these is a key requirement for the manufacture of low cost DNA devices based on printing technologies. From this work, the following conclusions and recommendations can be drawn.

6.1 Conclusions

A suitable polymer substrate was discovered to immobilise the ODN ink. The immobilisation mechanism was found to be through the combination of non-covalent bonds. One of the non-covalent bonds is made by the hydrophobic CTAB and the hydrophobic surface treated CCP. The CTAB is linked with the ODN by a polar charge between the negative charge of the phosphate group in the ODN and the polar charge of the hydrophilic head of CTAB. The other non-covalent bond is formed by the negative charge of the corona treated acrylic coated CCP with the positive partial charge of CTAB which is linked with the ODN by the phosphate. The CCP is the best found suitable substrate to print ODN ink. The washing time is decided. The concentration of ODN ink is decided by the washing experiments in $30 \times 10^{-2} \mu\text{M}$. The CCP chemical structure is analysed by FTIR to give the acrylic functional group. The Cy5 and ODN with amine are used to prove the immobilization mechanism. Temperature and humidity can affect the immobilization experiments.

The printability investigations were carried by inkjet, flexography and gravure printing technology. The inkjet gave acceptable good results with limited nozzle blocking by the ODN ink. The high volume printing by flexography and gravure shows some potential to print ODN ink in the faster ways than inkjet. However, the DNA did not survive this process, the reasons for which were unclear at this time and this requires further exploration. The surface energy and roughness of CCP prove the good adhesion favour to the ODN ink. The ODN ink viscosity and surface tension satisfy the inkjet printing but not to flexography and gravure printing. The viscosity

and immobilization of ODN ink are the factors to affect the viscosity modifier selection.

The hybridisation protocol of the ODN ink immobilised on the CCP was investigated by changing the different hybridisation and washing buffer combinations. The PCR buffer was suited to hybridisation and the phosphate buffer was suitable for washing. The stringency investigation was used to compare the non-complementary ODN with the complementary target ODN to prove the hybridisation protocol.

6.2 Recommended future work

The constraint of the ODN ink on these three printing technologies is due to the limited flexibility in formulating the ODN ink. This arises because of the viscosity that needs to be matched with the printing processes and the challenges of wetting and adhesion to the substrate. Consequently, following the initial study, further work is required in this area. This will focus on two areas.

The non-survival of the DNA may be attributed to the historical stress application in the contact printing processes. Stress is applied at different stages in the process (e.g. doctoring, splitting) and it will need to be explored independently, possibly through rheological tests under the shear rate decided by the experiments. This cannot be done by the limited project time.

Any new developments in printing technology that lead to lower contact pressures would subject the ink to lower stress levels and these should be evaluated for the printing of DNA

Optimisation of the hybridisation and washing buffers is also recommended for further work. A workable system has been demonstrated in this thesis, but there is significant scope for further work to explore a full range of combinations.

In this work, Cy5 has been used to demonstrate the function of DNA after deposition through fluorescence. Ethidium Bromide can be used to prove the DNA present on the CCP substrate. Further detailed information may be gained by adding dyes chosen for their absorption and emission spectra, the fluorescence Stoke-Shift, the extinction coefficient, pH-sensitivity, stability to photobleaching as well as the

quantum yield to the DNA and complementary DNA to gain a more detailed understanding of the hybridisation process.

Appendix A Supplement for Chapter 4

A.1 CTAB viscosity determination

The viscosity of CTAB is required to match with the requirements of the printing process. This section explains the procedure and results obtained from these experiments.

The experiments were conducted on a Bohlin Gemini 200 HR Nano Rheometer cone and plate rheometer fitted with a CP2/55 cone. Through software settings the tests were conducted at 25°C and the sequence of events was established as follows

Load a 1.3 ml sample, the gap size is 70 μm . The pre-shearing stress is 1 mPa for 10 seconds.

The results from these experiments were then transferred to Excel for further analysis and display.

The complete series graph of CTAB aqueous solution with the concentration series at 0.01, 0.05, 0.1, 0.15, 0.2, 0.4, 0.6, 0.8, 1 mM in **Figure 4.3** is as follows

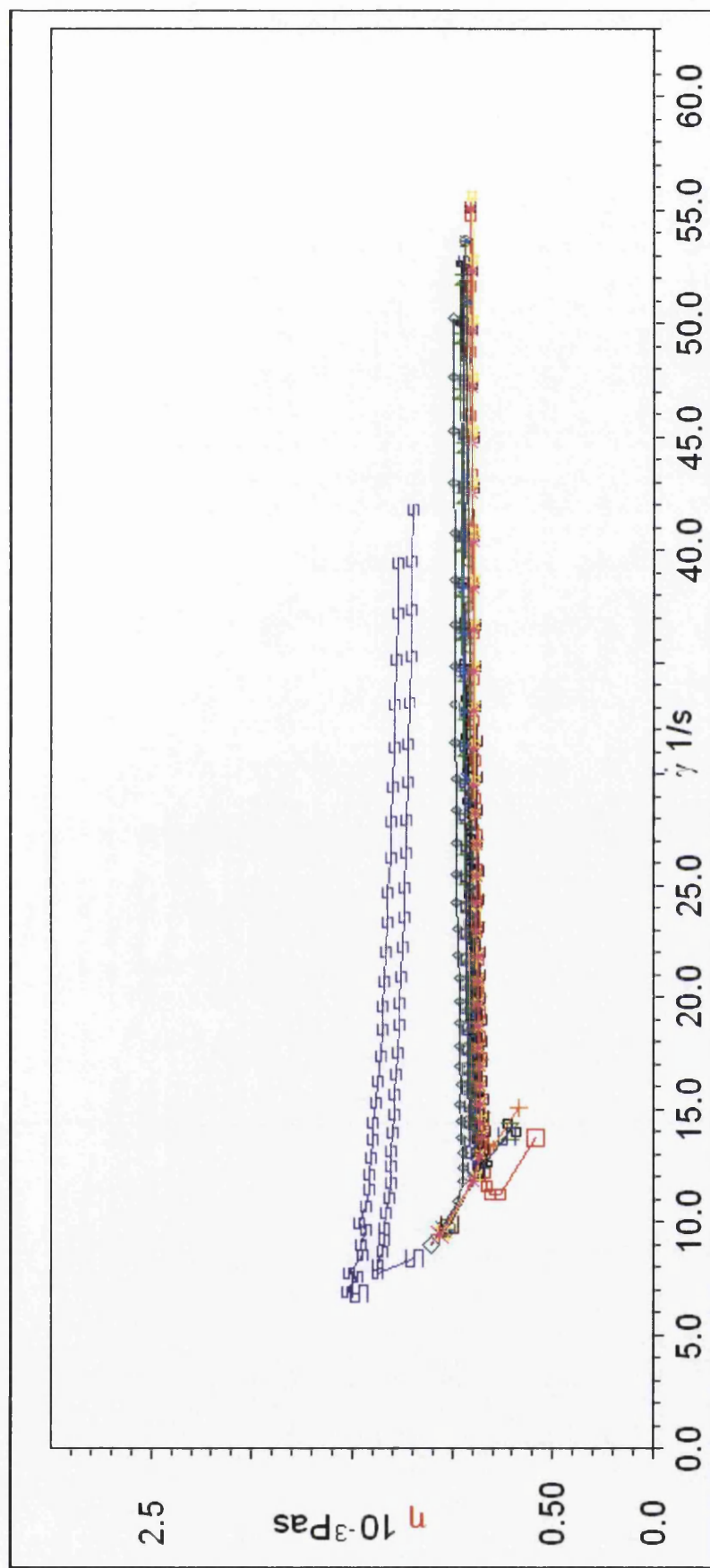


Figure A.1 Viscosity of the series concentration of CTAB

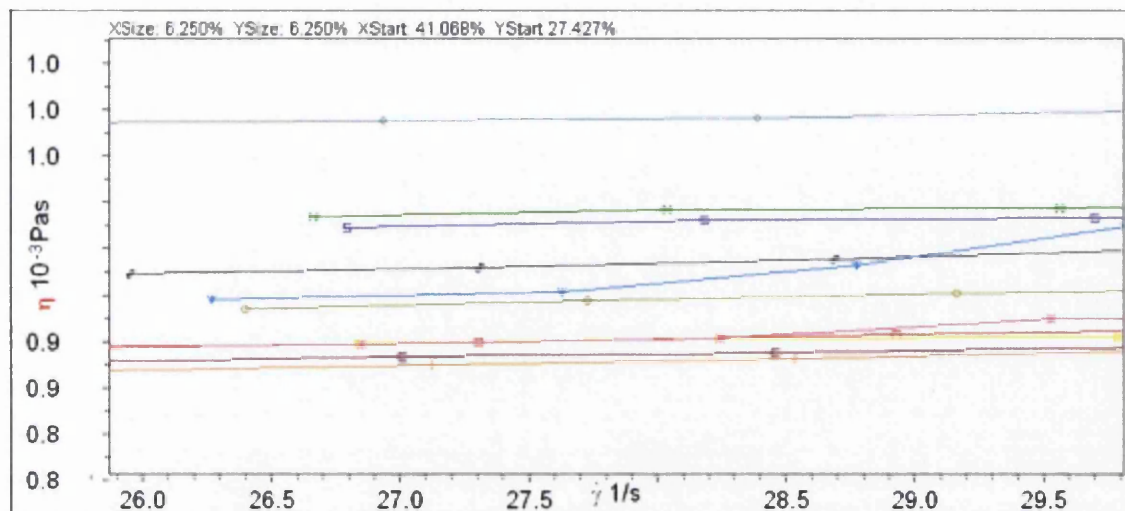




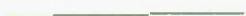

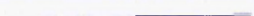



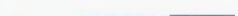





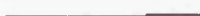



Figure A.2 Viscosity of the series concentration of CTAB in the large scale

Table A.1 viscosity symbols of different concentration CTAB

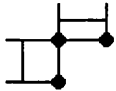
	colour of line	shape of mark
0.01		
0.05		
0.1		
0.15		
0.2		
0.4		
0.6		
0.8		
1		

The CTAB aqueous solution with the series of concentration shows that it is Newtonian solutions and the increasing concentration of CTAB aqueous solution varies the viscosity.

A.2 Dimatix printer settings for depositing the probe 1 ink

The basic settings for the Dimatix Materials Printer DMP-2800 Series include the following options. Tickle control: fluid evaporation, low amplitude pulse, frequency; Cartridge print height: 0.25-1.5mm and Drop spacing: it is the distance (in X and Y) between the drops that the DMP will deposit to create the pattern – this ranges from 5 to 254 μ m.

50 μ m



50 μ m

Drop spacing determines resolution or density. The drop spacing parameter is most useful for altering the fill density of lines and regulates the amount of jetted ink per unit area or creates rows of individual drops (spaced closer together than 254 μ m). An anti-blocking and cleaning cycle was employed before printing with settings as Purge 1, Blot 2, Split 500ms, Split 500ms.

Appendix B Survival Analysis of the Probe 1 Ink Sheared by Ink jetting

B.1 Introduction

The survival analysis of probe 1 ink sheared by ink jetting was done by gel electrophoresis.

B.1.1 Inkjet printing the DNA

The purpose of this section is to address the fact that during ink jet printing, the ink is subjected to a complex stress history that includes significant shear and extensional components. This work was conducted to confirm it as a successful way to transfer and immobilize the ODN onto the substrates. The inkjet was activated by a piezo device and thus applies a cyclic stress history to the working fluid within the ink jet head, nozzle, break away from the nozzle and its final impact on the substrate.

B.1.2 PAGE (Polyacrylamide Gel Electrophoresis)

Electrophoresis is the study of the movement of charged molecules in an electric field. Electrophoresis is a relatively inexpensive and convenient technique and capable of analysing and purifying several different types of biomolecules, but is especially applicable to the characterisation and analysis of charged biological polymers especially proteins and nucleic acids [Boyer 1993].

A Polyacrylamide Gel is a separation matrix used in electrophoresis of biomolecules, such as DNA fragments. Gels formed by polymerisation of acrylamide have several positive features in electrophoresis: (1) high resolving power for small and moderately sized proteins and nucleic acids (up to approximately 300 DNA bases), (2) acceptance of relatively large sample sizes, (3) minimal interactions of the migrating molecules with the matrix, and (4) physical stability of the matrix. Electrophoresis through polyacrylamide gels leads to enhanced resolution of sample components because the separation is based on both molecular sieving and electrophoretic mobility.

Polyacrylamide electrophoresis can be done using either of two arrangements, column or slab. A typical vertical slab gel apparatus is as follows. The

polyacrylamide slab is prepared between two glass plates that are separated by spacers. The spacers allow a uniform slab thickness of 0.5 to 2.0mm, which is appropriate for analytical procedures. Slab gels may be as large as 20 × 40 cm and can accommodate multiple samples. A plastic “comb” inserted into the top of the gel during polymerisation forms indentations in the gel that serve as sample wells. Up to 20 sample wells may be formed. After polymerisation, the tape and comb are carefully removed and the wells are rinsed thoroughly with buffer to remove salts and any unpolymerized acrylamide. The gel plate is clamped into place between two buffer reservoirs, a sample is loaded into each well, and voltage is applied. For visualization, the slab is removed and stained with an appropriate dye. The image is shown in **Figure B.1**.

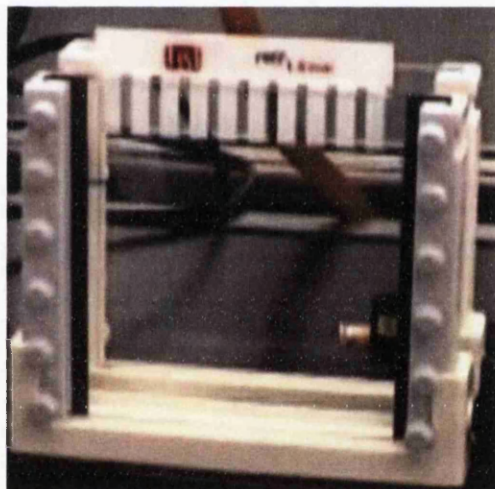


Figure B.1 PAGE cassette with comb and glass plates [Ualberta.ca, 2011]

B.2 Material

The materials to do the inkjet print in this section will be the probe 1 ink.

The probe 1 ink preparation is the same as that described in 3.4.2 and 3.3.2.

B.3 Methods

This section is to describe the inkjet printing process, electrophoresis process and analysis methods.

B.3.1 Inkjet printing shearing methods

The plasmid DNA (9 μ M) ink was inserted into the Dimatix inkjet cartridge. The cleaning process was operated before printing to get rid of the air bubbles in the bag inside the cartridge and the pathway between the nozzle head and liquid in the bag by using the cleaning cycle. During printing, the cleaning cycle was not needed. The inkjet cartridge nozzle tip was set up 1mm above a 96 well plate as the substrate. The printed DNA was collected in only one tube in the well plate. The printing cycle was set up to deposit about 2ml liquid. DNA in 0.1mM CTAB was filtered through a 0.2 μ m filter to remove large aggregates. The fluid was removed from its storage container, and a filter was put on the end of the syringe in front of the needle used to load the cartridge.

B.3.2 PAGE

This section describes the PAGE for analysis of the probe 1 ink. The gel was made by solidifying for 20 minutes after mixing autoclaved water (32ml), acrylamide (8ml) and 1 \times TBE (4.5ml) with APS (220 μ l) and TEMED (45 μ l). This was then exposed to the DNA samples on the comb slots. The electrophoresis process runs in TBE 1 \times under 50 V for 30 minutes. The gel was then taken out of the cassette and immersed in AgNO₃ (1g) in autoclaved water (1l) for 10 minutes and then developed in a solution which combined NaOH (13.5 g) in autoclaved H₂O (900 ml) with formaldehyde (3.6 ml).

B.3.3 Analysis methods by the gel electrophoresis

The ChemiDoc XRS+ system was used to analysis the results after PAGE.

The ChemiDoc XRS+ system can be used for imaging with a wide variety of applications that require high resolution and sensitivity. The system features a signal accumulation mode (SAM), which guides a user through determining optimum exposure time and capturing a desired image of a chemiluminescent sample. The ChemiDoc XRS+ system is based on CCD high-resolution, high-sensitivity detection technology and modular options to accommodate a wide range of samples and supports multiple detection methods including fluorescence, colorimetry, densitometry, chemiluminescence, and chemifluorescence. The system is controlled by Image Lab software to optimize imager performance for fast, integrated, and automated image capture and analysis of various samples. The system accommodates a wide array of samples, from large handcast polyacrylamide gels to small Ready

Agarose gels and various blots. The system enables image analysis and documentation of nucleic acids purification and characterisation.

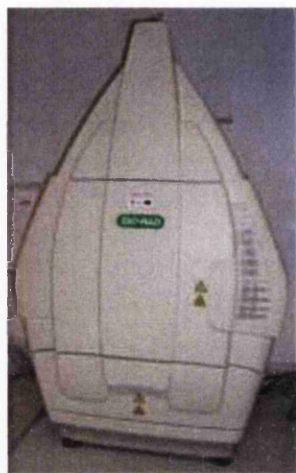


Figure B.2 UV ChemiDoc XRS+

B.4 Results and discussion in the PAGE analysis of the inkjet printed probe 1 Ink

The probe 1 ink was syringed into the inkjet cartridge with the filter Millex-GS (diameter; 33mm; por size: 0.22 μm ; membrane type: MF (Mixed cellulose esters)) and the ink deposited as set out in Sections B.3.1 and B.3.2 above. The images gained from the PAGE experiment are shown in Figure B.3.

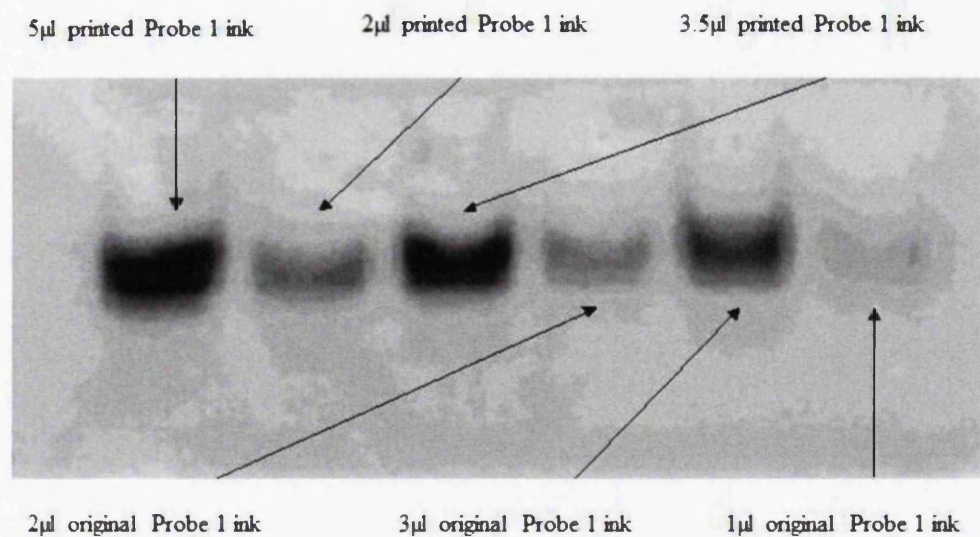


Figure B.3 The fluorescent images of the PAGE (polyacrylamide gel electrophoresis) with the inkjet printed probe 1 ink and the original probe 1 ink

There is no difference on the fluorescent images analysis by PAGE of the inkjet printed probe 1 ink and original probe 1 ink. Therefore the inkjet printing process does not affect the original Probe 1 ink through application of a stress history.

Appendix C Supplement for Chapter 5

C.1 Hybridisation experiments



Figure C.1 Hybridisation Oven

The Stovall Oven increases the speed of heating and cooling and provides a safer, seamless heating chamber. Hybridisations are carried out in leak proof bottles, rather than plastic bags or boxes. As many as 10 large bottles or 20 small bottles may be rotated at the same time. Dual LED's display both actual and set point temperatures continuously. Quick heating & recovery From room temperature to 65°C in 5 to 14 minutes. Seamless Stainless steel chamber for easy cleaning and safe containment of spills. Small footprint conserves counter space. A second oven can be stacked on top of first oven. Microprocessor, PID temperature controller with 2 digital readout for set point and actual oven temperature. Thermal fuse, controlled separately from the temperature controller, protecting incubator from thermal runaway. Large polycarbonate window for excellent visibility.

C.3 Bio-Rad iCycler PCR (Polymerase Chain Reaction) Machine



Figure C.2 Bio-Rad iCycler PCR

This device is for PCR experiment but in the pre conditioning experiment in Chapter. It is used for the temperature changing with the presetting function of software on the screen.

Glossary

Antisense oligonucleotides

Single strands of DNA or RNA that is complementary to a chosen sequence

Autoclave

A device that uses steam to sterilise equipment and other objects by high pressure saturated steam at 121 °C or more, typically for 15-20 minutes. This means that all bacteria, viruses, fungi, and spores are inactivated

Sterilisation

A term referring to any process that eliminates (removes) or kills all forms of life, including transmissible agents (such as fungi, bacteria, viruses, spore forms, etc.) present on a surface, contained in a fluid, in medication, or in a compound such as biological culture media

pH

An indication of how many hydrogen ions it forms in a certain volume of solution

Nuclease

An enzyme capable of cleaving the phosphodiester bonds between the nucleotide subunits of nucleic acids

Agarose

A linear polysaccharide extracted from seaweed

Reference

- Abramoff MD, Magelhaes PJ and Ram SJ, (2004) Image processing with Image J, *Biophotonics International*, 11 (7), 36-42.
- Allain LR, Askari M, Stokes DL and Vo-Dinh T, (2001) Microarray sampling-platform fabrication using bubble-jet technology for a biochip system, *Fresenius Journal of Analytical Chemistry*, 371(2), 146–150.
- Allain LR, Stratis-Cullum DN, and Vo-Dinh T, (2004) Investigation of microfabrication of biological sample arrays using piezoelectric and bubble-jet printing technologies, *Analytica Chimica Acta*, 518(1-2), 77–85.
- Anderson MLM, (1999) *Nucleic Acid Hybridizaion*, Springer-Verlag New York inc, New York, USA.
- Avseenko NV, Morozova TY, Ataullakhanov FI and Morozov VN, (2001) Immobilisation of proteins in immunochemical microarrays fabricated by electrospray deposition, *Analytical Chemistry*, 73(24), 6047–6052.
- Avseenko NV, Morozova TY, Ataullakhanov FI, and Morozov VN, (2002) Immunoassay with multicomponent protein microarrays fabricated by electrospray deposition, *Analytical Chemistry*, 74(5), 927–933.
- Bailey J, FE and Koleske JV, (1991) *Alkylene oxides and their polymers*, Marcel Dekker, New York.
- Balaguer P, Terouanne B, Allibert P, Cros P, Boussioux AM, Mandrand B and Nicolas JC, (1993) *Molecular and Cellular Probes*, 7, 155-159.
- Barbulovic-Nad I, Lucente M, Sun Y, Zhang M, Wheeler AR and Bussmann M, (2006) Bio-Microarray Fabrication Techniques-A Review, *Critical Reviews in Biotechnology*, 26, 237-259.
- Beier M and Hoheisel JD, (1999) Versatile derivatisation of solid support media for covalent bonding on DNA-microchips, *Nucleic Acids Research*, 27, 1970–1977
- Benters R, Niemeyer CM, Drutschmann D, Blohm D and Wohrle D, (2002) DNA microarrays with PAMAM dendritic linker systems, *Nucleic Acids Research*, 30, E10.
- Berre LV, Trevisiol E, Dagkessamanskaia A, Sokol S, Caminade AM, Majoral JP, et al, (2003) Dendrimeric coating of glass slides for sensitive DNA microarrays analysis, *Nucleic Acids Research*, 31, e88.
- Bernard A, Delamarche E, Schmid H, Michel B, Bosshard HR and Biebuyck H, (1998) Printing patterns of proteins, *Langmuir*, 14(9), 2225–2229.
- Bier FF, Kleinjung F and Fresen J, (2001) *Analytical Chemistry*, 371, 151.

Blake TD and Shikhmurzaev Y, (2002) Dynamic wetting by liquids of different viscosity, *Journal of Colloid and Interface Science*, 253, 196–202.

Blake TD and Shikhmurzaev YD, (2004) Comment on “Dynamic wetting by liquids of different viscosity,” by T.D. Blake and Y.D. Shikhmurzaev, *Journal of Colloid and Interface Science*, 280, 537–538.

Boddunan, (2009-10) Copyright, <http://www.boddunan.com/miscellaneous/51-General%20Reference/2209-structure-of-dna-primary-and-secondary-structure-tertiary-structure-double-helix-structure.html>.

Bowtell DD, (1999) Options available—from start to finish—for obtaining expression data by microarray, *Nature Genetics*, 21(Suppl 1), 25–32.

Boyer RF, (1993) *Modern Experimental Biochemistry*, 2nd edition, 115.

Briggs D, Brewis DM, Dahm RH and Fletcher IW, (2003) Analysis of the surface chemistry of oxidized polyethylene: comparison of XPS and ToF-SIMS, *Surface and Interface Analysis*, 35, 156–167.

Britten RJ, Graham DE and Neufeld BR, (1974) Analysis of Repeating DNA Sequences by Reassociation, *Methods Enzymol*, 29, 363-418.

Bromberg LE and Klibanov AM, (1994) Detergent-enabled transport of proteins and nucleic acids through hydrophobic solvents, *Applied Biological Sciences, Proceedings of the National Academy of Sciences, USA*, 91, 143-147.

Brown PO and Botstein D, (1999) Exploring the new world of the genome with DNA microarrays, *Nature Genetics Supplement*, 21, 33-37.

Brown TA, (2002) Chapter 1 The Human Genome, *Genomes*, Wiley-Liss, Oxford.

Bunemann T, (1982) Immobilisation of denatured DNA to macroporous supports: II. Steric and kinetic parameters of heterogeneous hybridization reactions, *Nucleic Acids Research*, 10, 7181-7196.

Butler JH, Cronin M, Anderson KM, Biddison GM, Chatelain F, Cummer M, Davi DJ, Fisher L, Frauendorf AW, Frueh FW, Gjerstad C, Harper TF, Kernahan SD, Long DQ, Pho M, Walker JA, and Brennan TM, (2001) In situ synthesis of oligonucleotide arrays by using surface tension, *Journal of the American Chemical Society*, 123(37), 8887–8894.

Caccone A, DeSalle R and Powell JR, (1988) Calibration of the change in thermal stability of DNA duplexes and degree of base pair mismatch, *Journal of Molecular Evolution*, 27, 212-216.

Call DR, Chandler DP and Brockman F, (2001) Fabrication of DNA microarrays using unmodified oligonucleotide probes, *Biotechniques*, 30(2), 368–372.

Catterall RW, (1997) Chemical Sensors, Oxford University Press, Oxford, UK.

Cen L, Neoh KG, Li YL and Kang ET, (2004) Assessment of in vitro bioactivity of hyaluronic acid and sulfated hyaluronic acid functionalized electroactive polymer, *Biomacromolecules*, 5, 2238–2246.

Chan CM, Ko TM and Hiraoka H, (1996) Polymer surface modification by plasmas and photons, *Surface Science Reports*, 24, 3–54.

Cheung VG, Morley M, Aguilar F, Massimi A, Kucherlapati R and Childs G, (1999) Making and reading microarrays, *Nature Genetics* 21(Suppl1), 15–19.

Chiu SK, Hsu M, Ku WC, Tu CY, Tseng YT, Lau WK, et al, (2003) Synergistic effects of epoxy- and amine-silanes on microarray DNA immobilisation and hybridisation, *Biochemical Journal*, 374, 625–632.

Chrisey LA, Lee GU and O’Ferrall CE, (1996) Covalent attachment of synthetic DNA to self-assembled monolayer films, *Nucleic Acids Research*, 24, 3031–3039.

Christopoulos TK, (1999) *Analytical Chemistry*, 71, 425R-438R.

Chu S, DeRisi J, Eisen M, Mulholland J, Botstein D, Brown PO, et al, (1998) The transcriptional program of sporulation in budding yeast, *Science*, 282, 699–705.

Church GM, Gilbert W, (1984) Genomic sequencing, *Biochemistry, Proceedings of the National Academy of Sciences*, 81, 1991-1995

Clark LC and Lyons C, (1962) Electrode system for continuous monitoring in cardiovascular surgery, *Annals of the New York Academy of Sciences*, 102, 174-180.

Collins TJ, (2007) ImageJ for microscopy, *BioTechniques* 43 (1 Suppl) 25–30

Correia NT, Moura Ramos JJ, Saramago BJV and Calado JCG, (1997) *Journal of Colloid and Interface Science*, 189, 361.

Covington AK, Bates RG, Durst RA, (1985) Definitions of pH scales, standard reference values, measurement of pH, and related terminology, *Pure and Applied Chemistry*, 57, 531–542.

Cros P, Kurfurst R, Allibert P, Battail N, Piga N, Roig V, Thuong NT, Mandrand B and Helene C, (1994) Monoclonal antibodies targeted to α -oligonucleotides- Characterisation and application in nucleic acid detection, *Nucleic Acids Research*, 22, 2951-2957.

Csaki A, Moller R, Straube W, Kohler JM and Fritzsche W, (2001) DNA monolayer on gold substrates characterized by nanoparticle labeling and scanning force microscopy, *Nucleic Acids Research*, 29, E81.

Czarnik AW, (1995) Desperately Seeking Sensors, *Chemistry and Biology*, 2, 423-428.

Dahm R, (2008) Discovering DNA: Friedrich Miescher and the early years of nucleic acid research, *Human Genetics*, 122(6), 565–81.

Thomas PS, (1980) Hybridisation of denatured RNA and small DNA fragments transferred to nitrocellulose, *Proceedings of the National Academy of Sciences of the United States of America*, 77(9), 5201-5205.

DeRisi JL, Iyer VR and Brown PO, (1997) Exploring the metabolic and genetic control of gene expression on a genomic scale, *Science*, 278(5338), 680–686.

DeRisi J, Penland L, Brown PO, Bittner ML, Meltzer PS, Ray M, Chen Y, Su YA and Trent JM, (1996) Use of a cDNA microarray to analyse gene expression patterns in human cancer, *Nature Genetics* 14 (4), 457–460.

Desai S and Singh RP, (2004) Surface modification of polyethylene, Long-term properties of polyolefins, Albertsson AC, Editor, New York, Springer, 231–293.

Dharmadi Y and Gonzalez R, (2004) DNA microarrays: experimental issues, data analysis, and application to bacterial systems, *Biotechnology Progress*, 20(5), 1309–1324.

Dinklage A, Klinger T, Marx G and Schweikhard L, (2005) Plasma physics, New York, Springer.

Dolan PL, Wu Y, Ista LK, Metzenberg RL, Nelson MA and Lopez GP, (2001) Robust and efficient synthetic method for forming DNA microarrays, *Nucleic Acids Research*, 29, E107–7.

Domínguez A, Fernández A, González N, Iglesias E and Montenegro L, (1997) Determination of Critical Micelle Concentration of Some Surfactants by Three Techniques, *Journal of Chemical Education*, 74 (10) 1227-1231.

Dufva M, (2005) Fabrication of high quality microarrays, *Biomolecular Engineering*, 22 173-184.

Dufva M, Petronis S, Bjerremann Jensen L, Krag C and Christensen C, (2004) Characterisation of an inexpensive, non-toxic and highly sensitive microarray substrate, *Biotechniques*, 37, 286–296.

Eberwine J, Kacharina JE, Andrews C, Miyashiro K, McIntosh T, Becker K, Barrett T, Hinkle D, Dent G and Marciano P, (2001) mRNA expression analysis of tissue sections and single cells, *The Journal of Neuroscience*, 21, 8310-8314.

Eggins BR, (1996) *Biosensors: An Introduction*, John Wiley & Sons limited.

Eggins BR, (2002) *Analytical Techniques in the Sciences (AnTS), Chemical Sensor and Biosensors*, David J Ando, John Wiley & Sons Ltd, West Sussex, England.

Eisen MB and Brown P, (1999) DNA microarrays for analysis of gene expression, *Method in Enzymology*, 303,179 – 205.

Fixe F, Dufva M, Telleman P and Christensen CB, (2004a) Functionalization of poly(methyl methacrylate) (PMMA) as a substrate for DNA microarrays, *Nucleic Acids Research*, 32 (1), e9, 1-8.

Fixe F, Dufva M, Telleman P and Christensen CB, (2004) One-step immobilisation of aminated and thiolated DNA onto poly(methylmethacrylate) (PMMA) substrates, *Lab on a Chip*, 4: 191–195.

Fowkes FM, (1962) Determination of interfacial tensions, contact angles and dispersion forces in surfaces by assuming additivity of intermolecular interactions in surfaces, *The journal of Physical Chemistry*, 66, 382.

Fuentes M, Mateo C, Garcia L, Tercero JC, Guisan JM and Fernandez-Lafuente R, (2004) Directed covalent immobilisation of aminated DNA probes on aminated plates, *Biomacromolecules*, 5, 883-888.

Furton, KG and Norelus, A, (1993) Determining the critical micelle concentration of aqueous surfactant solutions: Using a novel colorimetric method, *Journal of Chemical Education*, 70(3), 254.

George, RA, Woolley, JP and Spellman, PT, (2001) Ceramic capillaries for use in microarray fabrication, *Genome Research*, 11(10), 1780–1783.

Goddard JM and Hotchkiss J H, (2007) Polymer surface modification for the attachment of bioactive compounds, *Progress in Polymer Science*, 32, 698-725.

Granjeaud S, Bertucci F, Jordan BR, (1999) Expression profiling: DNA arrays in many guises, *BioEssays*, 21(9), 781–790.

Gut IG, (2001) Automation in genotyping of single nucleotide polymorphisms, *Human Mutation*, 17, 475-492.

Hames BD and Higgins SJ, (1985) *Nucleic Acid Hybridisation: A Practical Approach*, IRL press, Oxford.

Harasaki A, Schmit J and Wyant JC, (2000) Improved vertical-scanning interferometry, *Applied Optics*, 39 (13).

Hamblyn S, (1994) *The Role of the Plate in the Ink Transfer Process in Flexographic Printing*, WCPC, Swansea University.

Hengsakul M and Cass AEG, (1996) Protein patterning with a photoactivatable derivative of biotin, *Bioconjugate Chemistry*, 7(2), 249–254.

Hershey A, Chase M, (1952) Independent functions of viral protein and nucleic acid in growth of bacteriophage, *The Journal of General Physiology*, 36(1), 39–56.

Hong BJ, Sunkara V, Park JW, (2005) DNA microarrays on nanoscale-controlled Surface, *Nucleic Acids Research*, 33, e106.

Hsu C-PS, (1997) Chapter 15: infrared spectroscopy, In: Settle F, editor, *Handbook of instrumental techniques for analytical chemistry*, Upper Saddle River, New Jersey: Prentice-Hall, Inc, 247–283.

Iqbal SS, Mayo MW, Bruno JG, Bronk BV, Batt CA and Chambers JP, (2000) A review of molecular recognition technologies for detection of biological threat agents, *Biosensors and Bioelectron*, 15, 549.

Inagaki N, (1996) *Plasma surface modification and plasma polymerization*, Lancaster: Technomic Pub Co.

Ito S and Tachibana M, (2004) Spotting Pin, US Patent 6, 835–352 B2.

Ito S, Tachibana M and Yokokawa N, (2004). Spotting Pin, US Patent 6,726–883.

Kafatos FC, Jones CW and Efstratiadis A, (1979) Determination of nucleic acid sequence homologies and relative concentrations by a dot hybridisation procedure, *Nucleic Acids Research* 7(6), 1541–1552.

Kendrew A, (1994) *The Encyclopaedia of Molecular Biology*, Plate 1, Copyright, Blackwell Science.

Kim JW, 2002 http://www.signaling-gateway.org/data/cgi-bin/ProtocolFile.cgi/afcs_PS00000053.pdf?pid=PS00000053

Kim JW, Yamagata Y, Takasaki M, Lee BH, Ohmori H, and Higuchi T, (2005) A device for fabricating protein chips by using a surface acousticwave atomizer and electrostatic deposition, *Sensors and Actuators B-Chemical*, 107(2), 535–545.

Kipphan H, (2001) *Handbook of Print Media*, New York, Springer.

Kirby BJ, (2010) *Micro and Nanoscale Fluid Mechanics: Transport in Microfluidic Devices*, Cambridge University Press.

Kwok DY, (1999) The usefulness of the Lifshitz-van der Waals/acid-base approach for surface tension components and interfacial tensions, *Colloids and Surfaces A: Physicochemical and Engineering Aspects*, 156(1-3), 191-200.

Kumar A, Larsson O, Parodi D and Liang Z, (2000) Silanized nucleic acids: a general platform for DNA immobilisation, *Nucleic Acids Research*, 28(14), e71, 1-6.

Lane JM and Hourston DJ, (1993) Surface treatments of polyolefins, *Progress in Organic Coatings*, 21, 269–284.

Lashkari DA, DeRisi JL, McCusker JH, Namath AF, Gentile C, Hwang SY, Brown PO and Davis RW, (1997) Yeast microarrays for genome wide parallel genetic and

gene expression analysis, Proceedings of the National Academy of Sciences of the United States, 94(24), 13057–13062.

Lee LH, (2001) The Journal of Adhesion, 76(2), 163-183 (21).

Leichle T, Saya D, Belaubre P, Pourciel JB, Mathieu F, Laur JP, Nicu L, and Bergaud C, (2005) Liquid loading of silicon based cantilevers using electrowetting actuation for microspotting applications, 13th International Conference on Solid-State Sensors, Actuators and Microsystems, Seoul, Korea, 135–138.

Leitch AR, Schwarzaxher T, Jackson D and Leitch IJ, (1994) (eds) *in Situ* Hybridisation, BIOS Scientific Publishers, Oxford.

Levene P, (1919) The structure of yeast nucleic acid, The Journal of Biological Chemistry, 40(2), 415–424.

Ligler FS and Taitt RCA, (2002) Optical Biosensors: Present and Future, Elsevier Science BV, Amsterdam.

Liu J, Cao Z and Lu Y, (2009) Functional Nucleic Acid Sensors, Chemical Reviews, 109, 1948-1998.

Liu XH and Ma PX, (2004) Polymeric scaffolds for bone tissue engineering, Annals of Biomedical Engineering, 32, 477–86.

Liu Y and Rauch CB, (2003) DNA probe attachment on plastic surfaces and microfluidic hybridisation array channel devices with sample oscillation, Analytical Biochemistry, 317, 76-84.

Long TM, Prakash S, Shannon MA and Moore JS, (2006) Watervapor plasma-based surface activation for trichlorosilane modification of PMMA, Langmuir, 22, 4104–4109.

Mace J, ML, Montagu J, Rose SD and McGuinness GM, (2000) Novel microarray printing and detection technologies. In: Microarray Biochip Technology, Schena, M, Ed, Eaton Publishing, Natick, MA, 39–64.

Maniatis T, Fritsch EF and Sambrook J (1982), Molecular Cloning: A Laboratory Manual, Cold Spring Harbor University Press, Cold Spring Harbor.

Marie R, Schmid S, Johansson A, Ejlsing L, Nordstrom M, Hafliger D, Christensen C, Boisen A and Dufva M, Immobilisation of DNA to polymerised SU-8 photoresist, Biosensors and Bioelectronics, in press.

Martinsky T and Haje P, (2000) Microarray Tools, Kits, Reagents, and Services. In: Microarray Biochip Technology, Schena, M., Ed, Eaton Publishing, Natick, MA, 201–220.

McNaught D and Wilkinson A, (1997) IUPAC. Compendium of Chemical Terminology, 2nd ed. Blackwell Scientific Publications, Oxford

Meldrum D, (2000) Automation for genomics, part two: sequencers, microarrays, and future trends, *Genome Research*, 10, 1288-1303.

Mikkelsen SR, (1996) Electrochemical biosensors for DNA sequence detection, *Electroanalysis*, 8(1), 15-19.

Moerman R, Frank J, Marijnissen JCM, Schalkhammer, TGM, and van Dedem, GWK, (2001) Miniaturized electrospraying as a technique for the production of microarrays of reproducible micrometer-sized protein spots, *Analytical Chemistry*, 73(10), 2183-2189.

Morozov VN and Morozova TY, (1999) Electrospray deposition as a method for mass fabrication of mono- and multi- component microarrays of biological and biologically active substances, *Analytical Chemistry*, 71(15), 3110-3117.

Morozov V and Morozova TY, (2002) Electrospray apparatus for mass fabrication of chips and libraries, US Patent 6, 350-609.

Morozov VN, (2005) Protein microarrays: Principles and limitations. In: *Protein Microarrays*, Schena, M, Ed., Jones and Bartlett Publishers, Inc., Sudbury, MA. 71-106.

Murphy L, (2006) Biosensors and bioelectrochemistry, *Current Opinon in Chemistry Biology*, 10, 177-184.

Myers D, (1991) *Surfaces, Interfaces, and Colloids*; VCH, New York, 317.

Naorem H and Devi SD, (2006) *Journal of Surface Science and Technology*, 22(3-4), 89-100.

Naydenova I, Martin S and Toal V, (2009) Photopolymers: Beyond the Standard Approach to Photosensitisation, *Journal of the European Optical Society, Rapid Publications*, 4, 09042.

Neumann AW and Spelt, JK (1996) *Applied Surface Thermodynamics*, Dekker, New York.

Nguyen C, Rocha D, Granjeaud S, Baldit M, Bernard K, Naquet P and Jordan BR, (1995) Differential gene expression in the murine thymus assayed by quantitative hybridisation of arrayed cDNA clones, *Genomics*, 29(1), 207-216.

Nikiforov TT, Rendle RB, Goelet P, Rogers YH, Kotewicz ML, Anderson S, Trainor GL and Knapp MR, (1994a) Genetic Bit Analysis: a solid phase method for typing single nucleotide polymorphisms, *Nucleic Acids Research*, 22(20), 4167-4175.

Nikiforov TT, Rendle RB, Kotewicz ML and Rogers YH, (1994) The Use of Phosphorothioate Primers and Exonuclease Hydrolysis for the Preparation of

Single-stranded PCR Products and their Detection by Solid-phase Hybridisation, *Genome Research*, 3, 285-291.

Nikiforov TT and Rogers YH, (1995) The use of 96-well polystyrene plates for DNA hybridisation-based assays: an evaluation of different approaches to oligonucleotide immobilisation, *Analytical Biochemistry*, 227, 201-209.

Odom TW, Love JC, Wolfe DB, Paul KE, and George MWM, (2002) Improved pattern transfer in soft lithography using composite stamps, *Langmuir*, 18, 5314–5320.

Okamoto T, Suzuki T and Yamamoto N, (2000) Microarray fabrication with covalent attachment of DNA using Bubble Jet technology, *Nature Biotechnology*, 18(4), 438–441.

Owens DK and Wendt RC, (1969) Estimation of the surface free energy of polymers, *Journal of Applied Polymer Science*, 13, 1741-1747.

Oss VCJ, Good RJ, and Chaudhury MK, (1988) Interfacial Lifshitz-van der Waals and Polar Interactions in Macroscopic Systems, *Chemical Reviews*, 88, 927-941.

Ozdemir M, Yurteri CU and Sadikoglu H, (1999) Physical polymer surface modification methods and applications in food packaging polymers, *Critical Reviews in Food Science and Nutrition*, 39, 457–477.

Palecek E, Fojta M, Tomschick M and Wang J, (1998) Biosens Bioelectron, 13, 621-628.

Phimister B, (1999) Going global, *Nature Genetics* 21(Suppl 1), 1.

Plueddemann EP, (1991) Silane coupling agents, New York: Plenum Press.

Pontius BW and Berg P, (1991) Rapid renaturation of complementary DNA strands mediated by cationic detergents: A role for high-probability binding domains in enhancing the kinetics of molecular assembly processes, *Biochemistry Proceedings of the National Academy of Sciences of the United States of America*, 88, 8237-8241.

Preininger C, Bodrossy L, Sauer U, Pichler R and Weilharter A, (2004) ARChip epoxy and ARChip UV for covalent on-chip immobilisation of pmoA gene-specific oligonucleotides, *Analytical Biochemistry*, 330, 29–36.

Prissanaroon W, Brack N, Pigram PJ, Hale P, Kappen P and Liesegang J, (2005) Fabrication of patterned polypyrrole on fluoropolymers for pH sensing applications, *Synthetic Metals*, 154, 105–108.

Quick DJ and Anseth KS, (2003) *Pharmaceutical Research*, 20(11), 1730-1737.

Rao N M, (2006) Chapter 16, Nucleic Acids, *Medical Biochemistry*, revised second edition, New Age International (P) Limited, Publishers, 403-209.

Ramakrishna S, Mayer J, Wintermantel E and Leong KW, (2001) Biomedical applications of polymer-composite materials: a review, *Composition Science and Technology*, 61, 1189-1224.

Rasmussen JR, Stedronsky ER and Whitesides GM, (1977) Introduction, modification, and characterisation of functional groups on surface of low-density polyethylene film, *Journal of the American Chemical Society*, 99, 4736–4745.

Rastogi S and Dwivedi UN, (2007)
<http://nsdl.niscair.res.in/bitstream/123456789/763/1/NucleicAcids.pdf>

Renault JP, Bernard A, Bietsch A, Michel B, Bosshard HR, Delamarche E, Kreiter M, Hecht B, and Wild UP, (2003) Fabricating arrays of single protein molecules on glass using microcontact printing, *Journal of Physical Chemistry B*, 107, 703–711.

Review of the Universe, (2008) Nucleotides, Unicellular Organism in website: universe-review.ca

Roessler NJ, (1979) *Journal of Chemical Education*, 56, 675.

Rogers YH, Jiang-Baucom P, Huang ZJ, Bogdanov V, Anderson S and BoyceJacino MT, (1999) Immobilisation of oligonucleotides onto a glass support via disulfide bonds: a method for preparation of DNA microarrays, *Analytical Biochemistry*, 266, 23–30.

Rose D, (2000) Microfluidic technologies and instrumentation for printing DNA microarrays, In: *Microarray Biochip Technology*, Schena, M., Ed., Eaton Publishing, Natick, MA, 19-38.

Rujimethabhas M, Wilairat PJ, (1978) *Journal of Chemical Education*, 55, 342.

Sabanayagam CR, Smith CL and Cantor CR, (2000) Oligonucleotide immobilisation on micropatterned streptavidin surfaces, *Nucleic Acids Research*, 28(8), e33, 1-4

Saiki RK, Scharf S, Faloona F, Mullis KB, Horn GT, Elrich HA and Arnheim N, (1985) *Science*, 230(4732), 1350-1354.

Sambrook J, Fritsch EF and Maniatis T, (1989) In: *Molecular Cloning: A Laboratory manual*, 2nd Edn, Cold Spring Harbor laboratory Press, Cold Spring Harbor, NY.

Schena M, Shalon D, Davis RW and Brown PO, (1995) Quantitative monitoring of gene expression patterns with a complementary DNA microarray, *Science*, 270 (5235), 467-470.

Schena M, Shalon D, Heller R, Chai A, Brown PO and Davis RW, (1996) Parallel human genome analysis: microarray-based expression monitoring of 1000 genes, *Proceedings of the National Academy of Sciences of the United States of America*, 93, 10614–10619.

Schmid H and Michel B, (2000) Siloxane polymers for high resolution, high-accuracy soft lithography, *Macromolecules*, 33(8), 3042–3049.

Shalon D, Smith SJ and Brown PO, (1996) A DNA microarray system for analyzing complex DNA samples using two-colour fluorescent probe hybridisation, *Genome Research*, 6(7), 639–645.

Shchepinov MS, Case-Green SC and Southern EM, (1997) Steric factors influencing hybridisation of nucleic acids to oligonucleotide arrays, *Nucleic Acids Research*, 25, 1155–1161.

Sheehan PE, Edelstein RL, Tamanaha CR, and Whitman LJ, (2003) A simple pen-spotting method for arraying biomolecules on solid substrates, *Biosensors and Bioelectronics*, 18, 1455–1459.

Shenton MJ and Stevens GC, (2001) Surface modification of polymer surfaces: atmospheric plasma versus vacuum plasma treatments, *Journal of Physics D*, 34, 2761–2768.

Shikhmurzaev YD and Blake TD, (2004) Response to the comment on dynamic wetting by liquids of different viscosity by J. Eggers and R. Evans, *Journal of Colloid and Interface Science*, 280, 539–541.

Siboni S, Volpe CD, Maniglio D and Brugnara M, (2004) The solid surface free energy calculation: II The limits of the Zisman and of the "equation-of-state" approaches, *Journal of Colloid and Interface Science*, 271 (2) 454-472.

SMU, (2012) <http://train-srv.manipalu.com/wpress/?p=103072>

Snow ET., (1993) Second International Meeting on Molecular Mechanisms of Metal Toxicity and Carcinogenicity, Madonna di Campiglio, Italy.

Sosnowski RG, Tu E, Butler WF, O'Connell JP and Heller MJ, (1997) Rapid determination of single base mismatch mutations in DNA hybrids by direct electric field control, *Proceedings of the National Academy of Sciences of the United States of America*, 94, 1119–1123.

Sodium Phosphate buffer, Institute of Molecular Development LLC, (2001)

Southern EM, (1975) Detection of specific sequences among DNA fragments separated by gel electrophoresis, *Journal of Molecular Biology*, 98 (3), 503–517.

Steel AB, Herne TM and Tarlov MJ, (1998) Electrochemical quantitation of DNA immobilized on gold, *Analytical Chemistry*, 70, 4670–4677.

Stillman BA and Tonkinson JL, (2000) FAST slides: a novel surface for microarrays, *Biotechniques*, 29, 630–635.

Strachan T and Read AP, (1999) Human Molecular Genetics, 2nd edition, BIOS Scientific Publishers, Oxford.

Strother T, Cai W, Zhao X, Hamers RJ and Smith LM, (2000) Synthesis and characterisation of DNA-modified silicon (1 1 1) surfaces, Journal of the American Chemical Society, 122, 1205–1209.

Su, H, Williams, P and Thompson, M, (1995), Platinum anticancer drug binding to DNA detected by thickness-shear-mode acoustic wave sensor, Analytical Chemistry, 67, 1010-1013.

Svitova TF, Wetherbee MJ and Radk CJ, (2003) Journal of Colloid and Interface Science, 261, 170–179.

Syvanen AC, (2001) Accessing genetic variation: genotyping single nucleotide polymorphisms, Nature Reviews Genetics, 2, 930-942.

TeleChem International Inc, (2005) <http://arrayit.com>.

Tenover FC, (1988) Diagnostic deoxyribonucleic acid probes for infectious diseases, Clinical Microbiology Reviews, 1, 82-101.

Toda K and Shizuta Y, (1993) Molecular cloning of a cDNA showing alternative splicing of the 5'-untranslated sequence of mRNA for human aromatase P-450, European Journal of Biochemistry, 213 (1), 383–389.

Tran LD, Piro B, Pham MC, Ledoan T, Angiari C, Dao LH, et al, (2003) A polytyramine film for covalent immobilisation of oligonucleotides and hybridisation, Synthetic Metals, 139, 251-262.

Tseng FG, Kim CJ and Ho CM, (2002) A high-resolution high-frequency monolithic top-shooting micro-injector free of satellite drops, Part I: Concept, design, and model, Journal of Micro electromechanical Systems, 11(5), 427–436.

Tsien, RY, (1992) In Fluorescent Chemosensors for Ion and Molecule Recognition, Czarnik AW, Ed, ACS Symposium Series 538, American Chemical Society, Washington DC, 130-146.

Turner PC, McLennan AG, Bates AD and White MRH, (1997) Instant Notes in Molecular Biology, BIOS Scientific Publishers, Oxford.

Ualberta.ca, (2011) <http://www.wonderhowto.com/how-to/video/how-to-perform-polyacrylamide-gel-electrophoresis-in-the-lab-259920/>

University of Stanford, (2005) <http://cmgm.stanford.edu/pbrown/mguide/tips.html>.

Vadgama P and Grump PW, (1992), Biosensors: present trends, Analyst, 117, 1657-1670.

Volpe CD and Siboni S, (2000) Acid–Base Reactions:Relevance to Adhesion Science and Technology, KL Mittal (Ed.), VSP, New York, 2, 55–90.

Volpe CD and Siboni S, (2001) Encyclopedia of Surface and Colloid Science, A. Hubbard (Ed.), Dekker, New York, (Web version, 2002).

Wallace RB, Shaer J, Murphy RF, Bonner J, Hirose T and Itakura K, (1979) nucleic Acid Research, 6, 3543-3557.

Walker J and Dougan G (1989) DNA probes: a new role in diagnostic microbiology, Journal of Applied Bacteriology, 67, 229-238.

Wang DG, Fan JB, Siao CJ, Berno A, Young P, Sapolsky R, Ghandour G, Perkins N, Winchester E, Spencer J et al, (1998) Large-scale identification, mapping, and genotyping of single-nucleotide polymorphisms in the human genome, Science, 280, 1077-1082.

Wang J, (2000) Survey and Summary from DNA Biosensor to Gene Chips, Nucleic Acids Research, 28 (16), 3011-3016.

Wang J, Jiang M, Nilsen T and Getts R, (1998) Journal of the American Chemical Society, 120, 8281-8282.

Wasserman SR, Tao YT and Whitesides GM, (1989) Structure and reactivity of alkylsiloxane monolayers formed by reaction of alkyltrichlorosilanes on silicon substrates, Langmuir, 5, 1074–1087.

Watson JD and Crick FHC, (1953) Genetical implications of the structure of deoxyribonucleic acid, Nature, 171, 964-967.

Website 4 University of Stanford, (2005)
<http://cmgm.stanford.edu/pbrown/mguide/tips.html>.

Website 5 TeleChem International Inc, (2005) <http://arrayit.com>.

Website 6: Parallel Synthesis Technologies Inc, (2005) <http://www.parallel-synthesis.com/smt-info.htm>.

Weibel C, (2002) The Spotting Accelerator TM, customizable head assembly for advanced microarraying, Journal of the Association for Laboratory Automation, 7(3), 91–96.

Wetmur J and Davidson N, (1968) Journal of Molecular Biology, 31(3), 349-370.

Wexler A and Hasegawa S, (1954) Relative humidity-temperature relationships of some saturated salt solutions in the temperature range 0° to 50°, Journal of Research of the National Bureau of Standards, 53A, 19-25.

Whitesides GM and Laibinis PE, (1990) Wet chemical approaches to the characterisation of organic-surfaces—self-assembled monolayers, wetting, and the physical organic-chemistry of the solid liquid interface, *Langmuir*, 6, 87–96.

Wilson JS, (2005) *Sensor Technology Handbook*, Newnes, Oxford, UK

Wolcott, MJ, (1992) Advances in nucleic acid-based detection methods, *Clinical Microbiology Reviews* 5, 370-386.

Worley JD, (1992) Capillary radius and surface tensions, *Journal of Chemical Education*, 69 (8), 678-680.

Wu SH, Ramonell K, Gollub J and Somerville S, (2001) Plant gene expression profiling with DNA microarrays, *Plant Physiology and Biochemistry*, 39, 917-926.

WYKO Surface Profilers Technical Reference Manual, (1996) WYKO Corporation, 980-085.

Xia Y, Zhao X-M and Whitesides GM, (1996) Pattern transfer: selfassembled monolayers as ultrathin resists. *Microelectronic Engineering*, 32, 255–256.

Yan L, Huck WTS and Whitesides GM, (2004) Self-assembled monolayers (SAMS) and synthesis of planar micro- and nanostructures, *Journal of Macromolecular Science: Part C: Polymer Reviews*, 44(2), 175–206.

Yazdani SS and Gonzalez R, (2007) Anaerobic fermentation of glycerol: a path to economic viability for the biofuels industry, *Current Opinion in Biotechnology*, 18 (3), 213–219.

Yesille N, Hanso JL and Cohen DK, (2005) Characterisation of Surface Topography of SandProceedings of the 16th International Conference on Soil Mechanics and Geotechnical Engineering, Osaka, Japan, Millpress Science Publishers,1, 465-468.

Young T, (1805). An Essay on the Cohesion of Fluids, *Philosophical Transactions of the Royal Society London*, 95, 65–87.

Zammatteo N, Jeanmart L, Hamels S, Courtois S, Louette P, Hevesi L, et al, (2000) Comparison between different strategies of covalent attachment of DNA to glass surfaces to build DNA microarrays, *Analytical Biochemistry*, 280, 143–150.

Zhai J, Cui H and Yang R, (1997) DNA Based Biosensors, *Biotechnology Advances*, 15(1), 43-58.